

CONGRESS

JULY  
2024

# MINAR 12

Rimar Academy  
أكاديمية ريمار

Minar Journal  
مجلة مينار

المؤتمر العلمي الدولي الثاني عشر  
للعلوم الصرفة والتطبيقية والتكنولوجية

XII. INTERNATIONAL SCIENTIFIC CONGRESS OF  
PURE, APPLIED AND TECHNOLOGICAL SCIENCES

RIMAR ACADEMY  
Publishing House



**PROCEEDINGS  
BOOK**

**كتاب الوقائع**

CONGRESS

**MINAR 12**





**Publisher**

**Rimar Academy**

**Editor-in-Chief**

**Prof. Dr. Ghuson H. MOHAMMED**

**Design Coordinator**

**Ali HIJAZI**

**ISBN**

**978-625-98077-5-1**

**DOI**

**10.47832/MinarCongress12**

**Printing Date**

**August 2024**

**Conference Dates**

**24 - 25 - 26 July / 2024**

**Number of Pages**

**285**

**URL**

**[www.rimmaracademy.com](http://www.rimmaracademy.com)**

**Printing Certificate  
Number**

**47843**



# CO-SPONSORED BY

## الجهات الراعية





## الرؤساء الفخريون Honorary Committee



الأستاذ الدكتور مازن حسن جاسم الحسيني  
Prof. Dr. Mazin Hasan Jasim ALHASANY

رئيس جامعة واسط  
Rector of the University of Wasit

Iraq - العراق



الأستاذ الدكتور قصي كمال الدين الاحمدي  
Prof. Dr. Kossay K. Al-AHMADY

رئيس جامعة الموصل  
Rector of the University of Mosul

Iraq - العراق



الأستاذ الدكتور محمد حقي ألما  
Prof. Dr. Mehmet Hakkı ALMA

رئيس جامعة اغدير  
Rector of Iğdır University

Türkiye-تركيا



الأستاذ الدكتور وعد محمود رؤوف  
Prof. Dr. Waad Mahmood RAOOF

رئيس جامعة تكريت  
Rector of Tikrit University

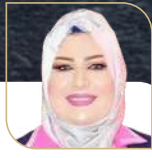
Iraq - العراق



الأستاذ الدكتور طارق حفطي الخياط  
Prof. Dr. Tariq Hafdhi Abbd Tawfeeq

رئيس جامعة الفراهيدي  
Rector of the University of Al-Farhidi

Iraq - العراق



الأستاذة الدكتور علياء عباس علي العطار  
Prof. Dr. Alyaa A. Ali Al-ATTAR

رئيس الجامعة التقنية الشمالية  
Rector of Northern Technical University

Iraq - العراق



الأستاذ الدكتور زكريا ظلام  
Prof. Dr. Zakaria ZALLAM

جامعة غازي عنتاب  
Gaziantep University

Türkiye-تركيا





الأستاذ الدكتور غصون حميد محمد  
Prof. Dr. Ghuson H. MOHAMMED

جامعة بغداد  
University of Baghdad

Iraq - العراق

رئيس المؤتمر  
Chair of Congress



الأستاذ الدكتور خميس عواد زيدان  
Prof. Dr. Khamis A. ZIDAN

نائب رئيس الجامعة العراقية  
للشؤون العلمية  
Vice Rector of Al-Iraqia  
University for Scientific Affairs

Iraq - العراق



الأستاذ الدكتور منير سالم طه  
Prof. Dr. Muneer salim TAHA

نائب رئيس جامعة الموصل  
للشؤون العلمية  
Vice-president for Scientific  
Affairs of the  
University of Mosul

Iraq - العراق



الأستاذ الدكتور عماد حسن رضا  
Prof. Dr. Emad Hasaan Ridha

جامعة البصرة للنفط والغاز / مساعد رئيس  
الجامعة للشؤون العلمية  
Vice - Chancellor for Scientific Affairs  
Basrah University for Oil and Gas

Iraq - العراق



أ. د. عبد الكريم دهش علي  
Prof. Dr. Abdulkareem Dash ALI

عميد كلية التربية للعلوم الصرفة -  
جامعة تكريت  
Dean of the College of Education Pure  
Science-Tikrit University

Iraq - العراق

رئيس الهيئة الإستشارية  
Chairman of Consultative Committee

رئيس الهيئة التحضيرية  
Chairman of Organizing Committee

رئيس الهيئة العلمية  
Chairman of scientific committee

الأمين العام للمؤتمر  
General Secretary



الهيئة الاستشارية  
Consultative Committee



**Prof. Dr. Kamal Hamid YASSER**  
University of Thi-Qar  
Iraq



**Prof. Dr. Khazaal Yaseen MUSTFA**  
University of AL-Hamdaniya  
Iraq



**Prof. Dr. Sattar Jaber KHALLAWY**  
Wasit University  
Iraq



**Prof. Dr. Hiyam Adil Ibrahim Ismail  
ALTAII**  
University of Mosul  
Iraq



**Prof. Dr. Derar ELEYAN**  
Palestine Technical University  
Palestine



**Lect. Dr. Bassim Kareem Mihsin**  
General Directorate of  
Education in karbala  
Iraq



**Assist. Prof. Dr. Najah Sobh Nayyef  
AL OMAR**  
University of Mosul  
Iraq



**Dr. Nabil Mohie Abdel-Hamid ALY**  
Kafrelsheikh University  
Egypt



**Dr. Osman TÜRK**  
Harran University  
Türkiye

الهيئة التحضيرية  
Organizing Committee



**Prof. Dr. Nihad Abdul-Lateef ALI**  
AL-Qasim Green University  
Iraq



**Prof. Dr. Nawras Abdelah Alwan**  
Basrah University  
Iraq



**Assist. Prof. Jalil Talab ABDULLA**  
Wasit University  
Iraq



**Assist. Prof. Dr. Farah Tariq SAEED**  
University of Mosul  
Iraq



**Assist. Prof. Iman radha JASIM**  
University of Mosul  
Iraq



**Assist. Prof. Dr. Zahraa Hussein  
KADHIM**  
AL-Qasim Green University  
Iraq



**Assist. Prof. Dr. Assma Ahmed  
Hatem Sultan**  
Middle technical university  
Iraq



**Lect. Dr. Ali Muhsen ALI**  
University of Kerbala  
Iraq



**Lect. Dr. Shaimaa muthana  
ABDULRAHMAN**  
University of Technology  
Iraq



**Lect. Dr. Inas Hasan Shukur  
AL- BAKRI**  
Baghdad University  
Iraq



**Dr. Amel D.HUSSEIN**  
Wasit University  
Iraq



**Dr. Dinara MAZHITOVNA**  
Rimar Academy  
Kazakhstan



## الهيئة العلمية



**Prof. Dr. Oruba Kuttof Hussein AL-BERMANI**  
Babylon University

Iraq



**Prof. Dr. Ebtahag .Z.SULYMAN**  
University of Mosul

Iraq



**Prof. Chèrif Fatima ZOHRA**  
Professor off Général Surgery and Oncology

Algeria



**Prof. Dr. Israa abdul razzaq ALDOBAISSI**  
University of Mosul

Iraq



**Prof. Dr. Sawsan Yousef KARA**  
Ministry of Education

Palestine



**Assist. prof. Dr. Muthik Abd Muslim GUDA**  
Kufa University

Iraq



**Assist. Prof. Dr. Nihad Taha Mohammed JADDOA**  
University of Baghdad

Iraq



**Assist. Prof. Dr. Sura Safi Obayes KHAFAJI**  
Al-Qasim Green University

Iraq



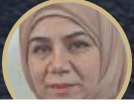
**Assist. Prof. Dr. Ekhlis Hmeyem SHALAL**  
University of Baghdad

Iraq



**Assist. Prof. Dr. Fatima Ramadan ABDUL Mustansiriyyah University**

Iraq



**Assist. prof. intisar ghanim TAHA**  
University of Mosul

Iraq



**Assist.Prof.. Hawraa Mahmood MURAD**  
Al-Qasim Green University

Iraq



**Assist. Prof. Dr. Wael Fahmi Abdulrahman ALSHAMARY**  
University of Kirkuk

Iraq



**Lect. Dr. Adil Hatem NAWAR**  
University of Anbar

Iraq



**Lect. Dr. Sabah Noori HAMMOODI**  
ASHur University Collage

Iraq



**Lect.Dr. Ammar AL-ZUBADE**  
University of Baghdad

Iraq



**Lect. Dr. Ikhlas Ali Hammoodi AL-HADEETHI**  
Wasit University

Iraq



**Dr. Husam R. ABED**  
Ministry of Education

Iraq



**Dr. Batool Abd Al Ameer Baqer ALSAFAR**  
Al Mustansiriyyah University

Iraq



**Dr. Rana Ramzi ABED**  
University of Mosul

Iraq



**Dr. Haleemah Jaber MOHAMMED**  
Al. Mustaqbal university

Iraq



**Dr. Mayson Thafir HADI**  
University of Baghdad

Iraq



**Dr. Amel ABBAS**  
Medicine faculty-University of Kasdi Merbah Ouarg

Algeria



**Dr. Mohammed Ali Hassan GHLEM**  
Aikarkh university

Iraq



**Dr. Ala HOUAM**  
Larbi Tebessi University

Algeria



**Dr. Fatiha HACHANI**  
KASDI Merbah University-Ouargla

Algeria



**Dr. Shatha Hizem SHAKER**  
Tikrit University

Iraq



**Dr. Jenan Atiyah GHAFIL**  
University of Baghdad

Iraq



**Dr. Mira Ausama AL-KATIB**  
University of Mosul

Iraq



**Dr. Mustafa M. Khalifa JABIRY**  
Management & Science University

Malaysia



**Dr. Zahraa Hasan RAHEEM**  
University of Baghdad

Iraq



**Dr. Mohamed RMAIDA**  
Libyan Iron and Steel Company(LISCO)

Libya



**Dr. Abdelaziz KEROUIM**  
EPH MOHAMMADIA, MASCARA

Algeria



**Dr. Abdelbaset Abdelsameaa Ahmed Alkharpotly**  
Aswan University

Egypt



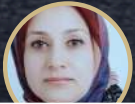
**Dr. Ielaf O. Abdul Majeed DAHL**  
University of Mosul

Iraq



**Dr. Naina DERAOUI**  
University of Kasdi Merbah Ouargla

Algeria



**Dr. Likaa Hamied MAHDI**  
Mustansiriyyah university

Iraq



**Dr. Symbat YESSIMKULOVA**  
ABAI University

Kazakhstan



**Dr. Riyam Adnan Hammudi AL INIZI**  
wasit university

Iraq



**Khalid EL BEKKAYE**  
University Mohammed I Oujda

Morocco





**Dr. Mutasim Ali Mohamed ELAGAB**  
Gezera University

Sudan



**Dr. Hanane ELANSARI**  
university of Cadi Ayyad

Morocco



**Dr. Naina DERAOU**  
University of Kasdi Merbah Ouargla

Algeria



**Dr. Ibrahem Rahem Jassim Al-AADILY**  
University of Sheffield

UK



**Dr. Morooj A. ABOOD**  
Ministry of Science and Technology

Iraq



**Dr. ZHAXYLYK ORALKANOVA**  
ABAI University

Kazakhstan



**Dr. FOUZIA Youcef**  
University of Kasdi Merbah Ouargla

Algeria



**Dr. Muslim Muhsin ALI**  
University of Missouri

USA



**Dr. Salar Karim Khalil**  
University of Duhok

Iraq



**Dr. Ali Abdulwahab RIDHA**  
University of Technology and Applied Sciences, Rustaq  
Sultanate of Oman

Sultanate of Oman



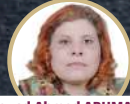
**Dr. Refag Suleiman Hamed MOHAMMED**  
University of Gezira

Sudan



**Dr. Rabee ALKHAYAT**  
Mosul University

Iraq



**Dr. Souad Ahmed ABUMARYAM**  
Sirte University

Libya



**Dr. Eman SHARAF**  
Animal Health Research Institute

Egypt



**Dr. Sanabel Abd Almonem Abd Almajeed AL THANOON**  
University of mosul

Iraq



**Dr. Saad M. Saleh AHMED**  
University of Baghdad

Iraq



**Dr. Baraa Ahmed Saeed**  
Ibn Sina University of Medical and Pharmaceutical Sciences

Iraq



**Dr. Ihab Qays Ali Aldalawi**  
Ibn Sina university for medical and pharmaceutical sciences

Iraq



**Dr. Nisreen SULAYMAN**  
Damascus University

Syrian Arab Republic



**Dr. Saeed Jebor Hemza**  
Wasit University

Iraq



**Assoc. Prof. Dr. Eda M. A. Alshailabi**  
Omar Almukhtar University

LIBYA



**Assist. Prof. Dr. Qusay Kamil Jasim**  
Northern technical unversity

Iraq



**Dr. Raja'a Al-Naimi**  
University of Petra

Jordan



**Dr. Ali farhan hashoosh**  
University of Misan

Iraq



**Dr. SUHAIR ABDELRAHMAN AHMED**  
Al Neelain University

Sudan



**Abdelhadi El haddaouy**  
the faculty of medicine and pharmacy-Rabat

Morocco



**Dr. Ahmed Kateb Jumaah**  
Al-Manara University

Iraq

## لجنة الاستقبال



**Ahmed Yossif EL-AGHA**  
Second Assalam School

Qatar



**Lect. Aseel Amer HASSAN**  
Baghdad University

Iraq



**Lect. Ali Khalaf Mousa**  
University of Misan

Iraq



# PREFACE

The 12th International Conference on Applied Sciences and Technology Research "MINAR CONGRESS", was organized by Istanbul Gedik University in collaboration with Remar Academy. The primary objective of this event was to compile and disseminate valuable scientific knowledge and make a meaningful contribution to the future.

Remarkably, a substantial number of researchers, both from local and international backgrounds, demonstrated their interest in this conference. The scientific committee meticulously reviewed the submissions and ultimately accepted a select group of individuals, totaling 84 applicants, 55 of them were accepted by the scientific committee.

The core of this conference was the presentation of 48 complete research papers, while the remaining articles and research findings are set to be featured in forthcoming issues of the MINAR Journal.

I would like to extend my sincere appreciation to all the contributors and scholars who played an essential role in making this conference a resounding success. Your dedication and valuable contributions are deeply respected and acknowledged.

Editor-in-Chief  
Prof. Dr. Ghuson H. MOHAMMED



# Table of Contents

**01**

**Hydrochemistry Assessment of the Ground Water Quality in Al-Najaf Province, Iraq**

- **Shahad Adil Al-Qaraghuli**
- **Fatima K. Khagoory**
- **Omnia K. Abd**

**11**

**The Effect of Cinnamon and Cardamom Oils On Some Virulence Factors of Pseudomonas aeruginosa**

- **Amina G.O. Al-Ani**
- **Aisha W. Al-Omari**
- **Najwa M. Al-Hadidi**

**24**

**Spaces of Lipschitz Functions on n-Modular Spaces**

- **Aamena Al - Qabani**
- **Iman A.Hussain**
- **Haneen A. Ameen**

**36**

**Dispersion Characterization of Poly (Vinyl Al Cohol) Doped with Iron Citrate Films**

- **Wasan A.Al-Taa'y**
- **Mohammed Ali H.Al-Beayaty**
- **Zainab A. Al-Taie**

**46**

**Novel Metal Oxide Nanoparticles Derived from Lactobacillus Isolated from Newborn Babies**

- **Kawther Hkeem Ibrahim**



# Table of Contents

**56**

**Effect of UV treatment on Hydrophilic SiO<sub>2</sub> thin film**

• **Hiba.M.Salman**

**65**

**Serum Profiles of Some Minerals, Vitamin D and Lipids in Heart Diseases in Mosul City**

• **Huda Y. Al-Attar**  
• **Tamara W. Jihad**

**79**

**Physiological Aspects of the Association Between Age, Gender, Vitamin D Levels and Obesity in The Iraqi Province of Al-Muthanna**

• **Hanaa Ali Aziz**  
• **Ibrahim A. abdulzahra**

**86**

**Effect The Inclusion of Different Polymer Types On Physical Properties of Heat Cure Acrylic Resins**

• **Marwah Hussein Abdulsattar**  
• **Alaa Hussein Jasim**

**92**

**Comparison of Cytomegalovirus Diagnosis Methods in Iraqi Aborted Women**

• **Tabarak Sabah Jassim**  
• **Noor A. Jihad**  
• **Rusul Waleed Ali**



# Table of Contents

**100**

**Modifications to Erdogan Method to Visualization of Skeletal System Using Dual Pigmentation with Red Alizarin and Alcian Blue**

- Nuha Hussam Abdulwahab
- Reem Saud Abed
- Lamyaa Khames Naif

**108**

**Estimation of Some Physiological Biomarkers Associated with Kidney Failure and Liver Damage in COVID Patients**

- Reem M. Obaid
- Aveen R. Mohsin
- Sama s. Salih
- Farah Tareq Yaseen

**121**

**Investigation of the Optical Properties and Spectroscopy Diagnostic of Magnesium Oxide Plasma by Nd: YAG Laser Method**

- Wassan D. Hussain
- Arkan K. Buraihi

**130**

**Design of Reconfigurable Antenna for UWB Operation and Dual-Band Rejection**

- Raad H. Thaher
- Lina M. Nori
- Adil S. Abduljabba

**144**

**Particle Pollution in University of Baghdad Campus**

- Nahla Shadeed Ajeel
- Hussein J. Khadim



# Table of Contents

**151**

**Date Palm Pollen (*Phoenix dactylifera* L.)**

**Supplementations: impact on the Fertility and Anti-cancer Properties**

- **Eslah S. rajab**
- **Mahmood A. Al-Azzawi**

**170**

**Study of the Runge-Kutta Scheme for Random Differential Equations**

- **Ali Sami Abdullah**
- **Esraa Habeeb Khaleel**

**178**

**Applying A Medium Developed from Some Chelating Elements to Grow Some Microalgae**

- **Maha Falah Al-Taie**
- **Mira Ausama Al-Katib**
- **Rana R. Abed**

**189**

**Evaluation of The Protective Effect of Propolis Extracts Against Atherosclerotic Lesions in Male Rats Exposed to Oxidative Stress Induced by Hydrogen Peroxide**

- **Sadoon Mohammed Abdullah**
- **Sahib Jummah Abdul Rahman**
- **Ass.Prof. Dr. Adil Ali Haider**

**203**

**A Review a Bout Educational of Students' Academic Performance Using Data Mining Algorithms**

- **Douaa Ibrahim Alwan Al Saadi**
- **Dr. Hind Abdul Razzaq Mohammed Ali**



# Table of Contents

214

In Vitro Activity of Spirulina Against Some Pathogenic Bacteria

- Zahraa khalid Al- kheroo
- Sura M.Y. Al-Taee
- Mahmood Abd Aljabbar Al Tobje

239

Preparing Titanium Dioxide Nanofibers for Bacterial & Fungal Selectivity

- Thamir Abdul Ameer Hassan
- Ali Q Tuama
- Ghaiath A. Fadhil

247

ST2 Concentration as Cardiac Biomarker in Cvd Patients with Hyperglycemia

- Maryam Kadhim Al-Shemery
- Fatema Ali AL kafhage

265

The Study of the Effect of Different Concentrations of Grape Seed Oil On Growth Rates and Some Biochemical Parameters of Common Carp Fish

- Israa Adel Fadhil
- Layla Abboud Aufy
- Khulood Abdul Ali
- Shaymaa AJ. Al-jumaiee

265

Effect of Hydrocortisone On Some Physiological and Morphological Changes in Mice Fetus

- Maha Khalaf Ali
- Amina jasem Mohamed
- Hassan I Mohamed







# Hydrochemistry Assessment of the Ground Water Quality in Al-Najaf Province, Iraq

Shahad Adil Al-Qaraghuli <sup>1</sup>

Fatima K. Khagoory <sup>2</sup>

Omnia K. Abd <sup>3</sup>



© 2024 The Author(s). This open access article is distributed under a Creative Commons Attribution (CC-BY) 4.0 license.


## Abstract


The hydrochemistry of groundwater was studied via 17 wells in Al-Najaf province to evaluate the groundwater quality by comparing the physiochemical characteristics and distribution of cations and anions in groundwater. Total dissolved solids (TDS), electrical conductivity (EC), PH, main cations ( $\text{Na}^+$ ,  $\text{K}^+$ ,  $\text{Mg}^{++}$ ,  $\text{Ca}^{++}$ ), and anions ( $\text{HCO}_3^-$ ,  $\text{Cl}^-$ ,  $\text{SO}_4^{--}$ ) were measured in the groundwater samples. The hydrochemical analysis findings indicate that the groundwater in the research region has low alkalinity with high TDS and EC values. TDS values ranged from 505 to 5112 mg/l. It is classified as brackish water except some samples are classified as Freshwater. The values of EC ranged from 715 to 7670  $\mu\text{s}/\text{cm}$ . Because of salinity, it is classified as excessively mineralized water.


Groundwater in the research region is characterized by hard to very hard water. The ratio of sodium concentration to chloride concentration ( $r \text{ Na}/r \text{ Cl}$ ) was calculated to determine the origin of water majority of the research region samples had a meteoric origin and marine water origin. Schoeller classifications showed that the majority of the studied region had a water type of  $\text{Na}_2\text{SO}_4$  which represents 53% whilst other samples have water types  $\text{NaCl}$  which represents 29%,  $\text{CaSO}_4$  which represents 12%, and  $\text{MgSO}_4$  which represents 6%. In the research area, the groundwater is unacceptable for drinking uses except samples (W16 and W17) are suitable for drinking uses.

**Keywords:** Hydrochemistry; Groundwater; Origin of Water; Water Type; Al-Najaf Area.

 <http://dx.doi.org/10.47832/MinarCongress12-01>

<sup>1</sup>  Department of Geophysics, College of Remote Sensing and Geophysics, Al-Karkh University for Science, Baghdad, Iraq [shahadadil889@gmail.com](mailto:shahadadil889@gmail.com)

<sup>2</sup>  Department of Geophysics, College of Remote Sensing and Geophysics, Al-Karkh University for Science, Baghdad, Iraq

<sup>3</sup>  Department of Studies and Planning, Al-Karkh University of Science, Baghdad, Iraq



## Introduction

In Iraq many regions, especially those that are far from the surface water supplies, groundwater is essential for human habitation and land development [1]. The water resources available for usage continuously decrease as a result of increased requests for these water resource rates, and the deteriorating of surface water quality, so the groundwater became necessary to supply water to use for different purposes [2]. The groundwater quality is near equal importance to quantity. The groundwater qualitative includes an explanation of the occurrence of its different components and their relationship between these components and the aquifer materials [3].

Chosen area is a part of Al-Najaf area which lies in Al-Najaf governorate, south-western part of Iraq (southern of the western desert) between latitudes ( $31^{\circ} 50' - 32^{\circ} 30'$ ) northern and longitudes ( $43^{\circ}45' - 44^{\circ} 25'$ ) eastern, (Figure 1). The studied region has an arid climate with a cold winter, dry hot summer, and an annual average rainfall of about 8.78 millimeters mostly from November to April, and an annual evaporation of 1329 millimeters [4].

The previous studies of hydrochemistry assessment of the groundwater quality were conducted in different world regions. One of the previous studies was conducted by [5] determining the evaluation of the hydrogeological and hydrochemical conditions for groundwater in Bahr Al-Najaf area. Another study of the region by [4] studied the groundwater quality by using the (WQI) for Al-Dammam formation in Al-Najaf governorate. While [6] studied the hydrogeochemical properties of the groundwater in Al-Najaf area. [7] Studied the hydrochemical assessment of groundwater by using statistical methods and calculated water quality index. The assessment of groundwater quality for human consumption in the Magdalena Valley, Colombia was studied by [8].

Geologically, the research region is situated within the boundaries of Al-Salman subzone, which is a component of the stable shelf zone [9]. The research region has two deep faults towards north west –south east , which extend in the research region, crucial in controlling the groundwater flow [10]. The spring's existence provides good evidence of these faults [11]. Stratigraphically, the formations in the studied region consist of Tertiary and Quaternary sediments started from the oldest to the recentest as follows; Umm ErRadhuma, Rus, Dammam, and Euphrates formations that are covered by Quaternary sediments [12]. These formations component the majority of the layers that carry and influence the chemistry of the groundwater, these layers differ from one another in terms of their hydraulic properties, which allow them to discharge, transport, and storage groundwater [6]. The geomorphology of the studied region is



characterized by a land elevation range of 8 and 65 meters above sea level. The land elevation of Al- Najaf region increases toward the western about 420 meters above sea level on the boundaries of Iraqi-Saudi. The slope of land progressively from the west and southwest in the direction of the north and northeast [13]. Study objectives include assessing the chemical and physical properties of the groundwater in the studied region, determining water quality and salinity, and determining possible uses.

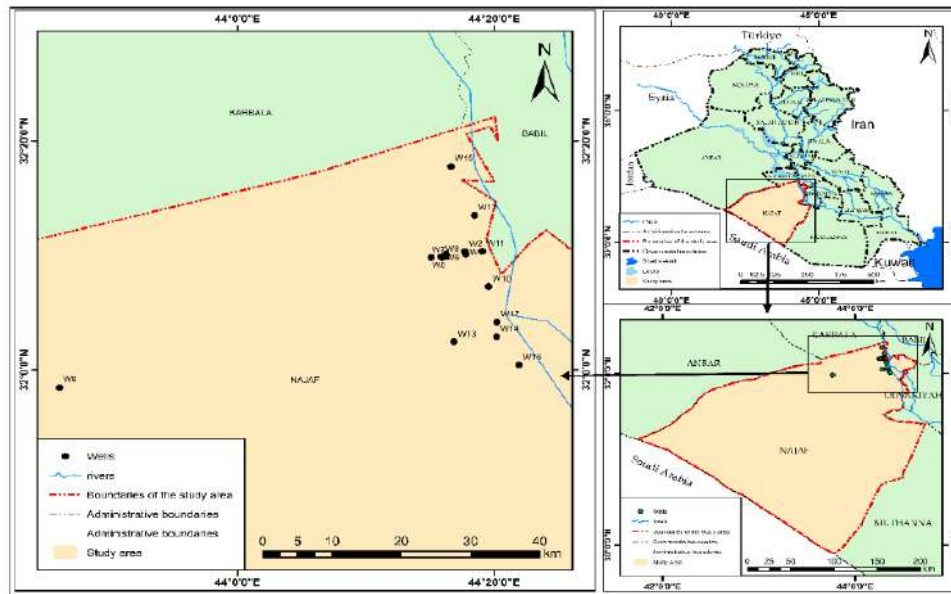


**Figure 1-** Show a map of the study region.

## Material and Method

Seventeen well samples were selected for the present study distributed in the region collected from selected groundwater wells in Al-Najaf area during September 2018 (Figure 1). Global Positioning System (GPS) was used to determining the locations (latitude, longitude and elevation) of each well. The pH was measured by pH meter while the total dissolved solids (TDS) and electrical conductivity (EC) of the water samples were measured directly by using HANA (HI 9811) meter. Each groundwater samples were analyzed for 12 parameters, these are EC, pH, TDS, total hardness (TH), sodium ( $\text{Na}^+$ ), magnesium ( $\text{Mg}^{+2}$ ), potassium ( $\text{K}^+$ ), calcium ( $\text{Ca}^{+2}$ ), bicarbonates ( $\text{HCO}_3^-$ ), chlorides ( $\text{Cl}^-$ ), sulfates ( $\text{SO}_4^{-2}$ ) and nitrates ( $\text{NO}_3^-$ ) by using the standard analytical method recommended by [14]. The results of the analysis of the concentration of major and minor ions, EC, TDS, TH, and pH are shown in Table 1.



**Table 1-** Physiochemical properties of groundwater wells in the studied region.

No. of Samp.	PH	EC ( $\mu\text{s}/\text{cm}$ )	TDS (mg/l)	TH (ppm)	Ca (ppm)	Mg (ppm)	Na (ppm)	K (ppm)	Cl (ppm)	SO <sub>4</sub> (ppm)	HCO <sub>3</sub> (ppm)	NO <sub>3</sub> (ppm)
W1	7.2	6420	4164	1555	351	165	581	113	685	1832	484	2.2
W2	7.2	4210	2765	1168	265	123	370	22	567	617	464	1.5
W3	7.15	2650	1760	803	165	95	165	18	250	740	70	1.2
W4	7.12	5700	3630	1333	300	142	560	100	670	1190	478	1.2
W5	7.17	3500	2770	1174	261	127	408	89	517	998	454	2.7
W6	7.13	5030	3600	1611	380	161	527	33	752	1393	327	2.1
W7	7.15	7670	4900	1756	359	209	754	121	1020	1655	470	2.1
W8	7.62	7300	5112	1607	360	172	620	12	732	1462	513	2.2
W9	7.15	3020	2140	829	187	88	322	4.6	330	681	446	1.7
W10	7.23	6980	4494	1168	270	120	480	8	554	1118	323	2.2
W11	7.22	5000	3600	1611	380	161	527	33	752	1393	327	1.2
W12	7.14	4750	3075	1262	283	135	392	28	600	635	473	1.4
W13	7.19	4800	3090	1103	287	94	135	9	247	565	67	2.1
W14	7.25	4400	2860	1143	260	120	360	20	560	610	460	2.1
W15	7.25	1394	950	495	88	67	89	5	185	380	50	1.3
W16	7.24	758	528	193	41	22	55	2	112	132	18	1.4
W17	7.3	715	505	175	37	20	53	1.7	98	117	17	1.6

## Results and Discussion

1. In this research, the physiochemical properties of groundwater samples are stated in Table 1. The PH values of samples range between (7.12 – 7.62), and average (7.22) which reflect high alkalinity. The EC values are ranging from (715 to 7670  $\mu\text{s}/\text{cm}$ ), average (4370  $\mu\text{s}/\text{cm}$ ). When comparing EC values of groundwater samples with [15] classification, it is concluded that the water kind in the region is as excessively mineralized water except samples W16 and W17 are highly mineralized water because of salinity.
2. The TDS values of groundwater samples are ranging from (505 to 5112 mg/l), average (2938 mg/l). Comparing TDS values of groundwater samples with [16] classification, it is concluded that the water kind in the region is brackish water, except for samples



(W15, W16, W17) which are freshwater. The values of TDS and EC for water samples are shown in Figure 2.

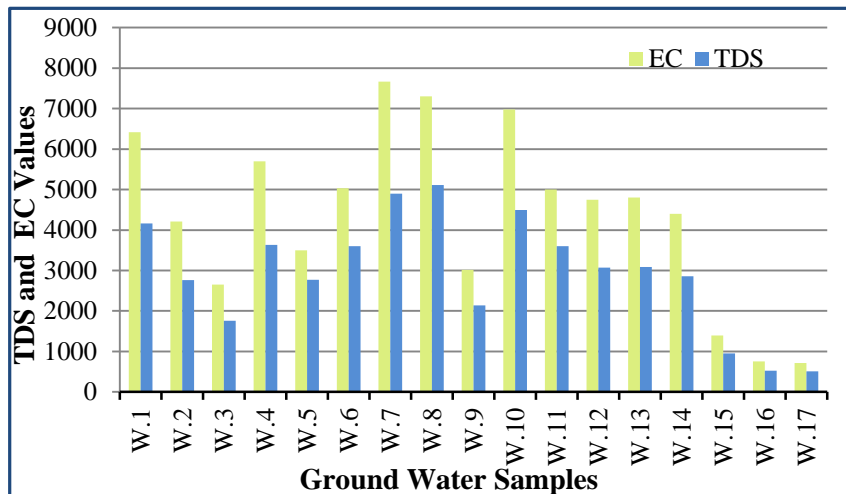


Figure 2- Values of TDS and EC for the samples.

The TH values of groundwater samples ranging from (175 to 1756 ppm) to, average (1117 ppm). TH values of groundwater samples are compared to the Todd classification [16], which indicates that the water type in the region is very hard water except for sample (W17), which is classified as hard water due to limestone exposures in recharge zone and the lithology includes carbonate rocks which are primarily wealthy in magnesium and calcium.

The main cations consist of (Ca, Na, Mg, and K) where the Calcium ion concentration in samples ranging from (37 to 380 ppm), average (251 ppm) and the magnesium ion concentration ranging from (20 to 209 ppm), average (119 ppm) and the sodium ion concentration ranging from (53 to 754 ppm), average (376 ppm) while the potassium ion concentration ranging from (1.7 to 121 ppm), average (36 ppm) (Figure 3).

The major anions consist of ( $\text{Cl}^-$ ,  $\text{SO}_4^{2-}$  and  $\text{HCO}_3^-$ ) where the concentration of Chloride ions in groundwater samples range between (98 to 1020 ppm), average (508 ppm) and the sulfate ion concentration ranging from (117 to 1832 ppm), average (913 ppm). Increasing concentrations of ( $\text{SO}_4^{2-}$ ) in the studied region can be a result of the dissolution of anhydrite and gypsum minerals in the aquifer rocks in the recharge region. The bicarbonate ion concentration ranges from (17 to 513 ppm), average (320 ppm) (Figure 4). The concentration of nitrate ions in groundwater samples ranges from (1.2 to 2.7 ppm), average (1.8 ppm). The chemical properties of groundwater are due to the long-term interactions with the adjacent environment rock [17].



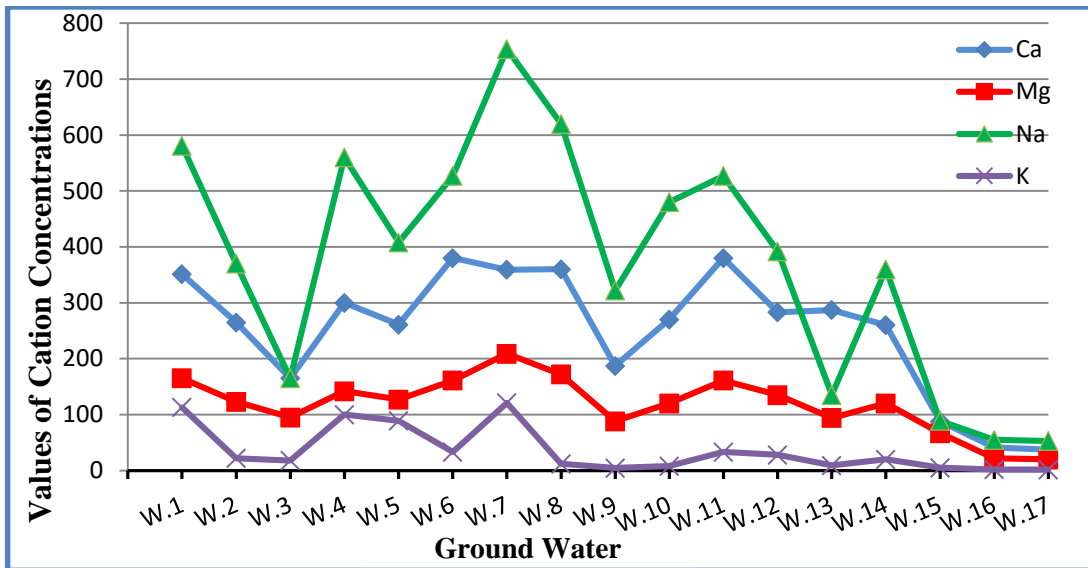


Figure 3- Values of Cation Concentrations for groundwater samples.

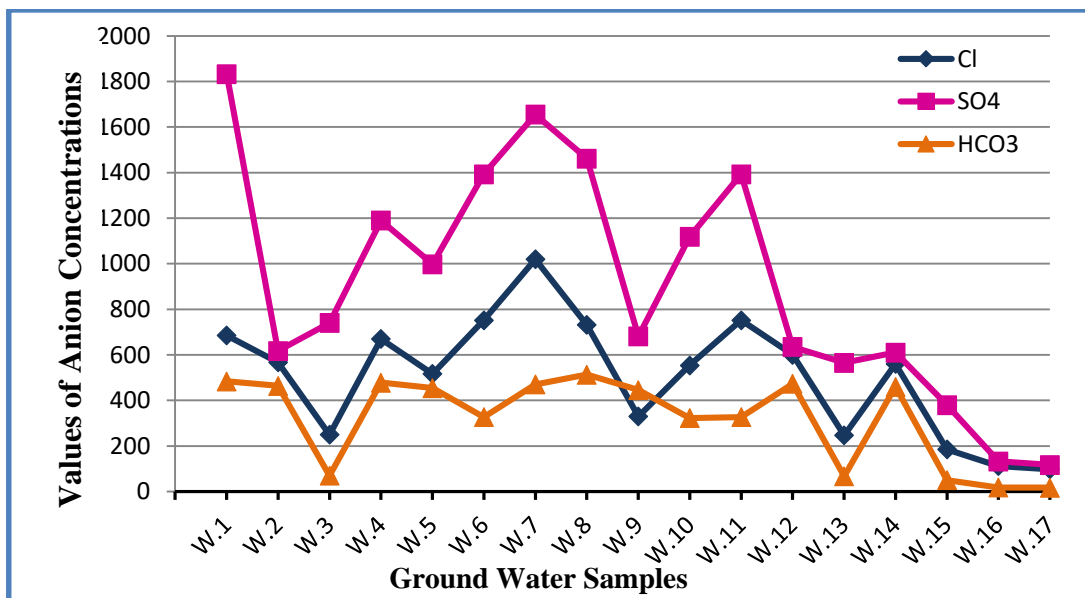


Figure 4- Values of Anion Concentrations for groundwater samples.

The ratio of sodium concentration to chloride concentration ( $r Na/r Cl$ ) in the (epm) unit was calculated to determine the origin of the water. [18] suggests that if the ratio of ( $r Na/r Cl$ ) is less than one, it means that the origin water is marine, and if it is more than one, it means that meteoric. The results from applying [18] classifications reflect all the groundwaters have a meteoric origin except samples (W13, W14, W15, W16, and W17) are marine origin (Table 3).



**Table 3-** The groundwater origin of water samples in the studied area

No. of Samples	r Na/r Cl	Water origin	No. of Samples	r Na/r Cl	Water origin
W1	1.3	Meteoric	W10	1.3	Meteoric
W2	1.0	Meteoric	W11	1.1	Meteoric
W3	1.0	Meteoric	W12	1.0	Meteoric
W4	1.3	Meteoric	W13	0.8	Marine
W5	1.2	Meteoric	W14	0.9	Marine
W6	1.1	Meteoric	W15	0.7	Marine
W7	1.1	Meteoric	W16	0.8	Marine
W8	1.3	Meteoric	W17	0.8	Marine
W9	1.5	Meteoric			

According to [19] classification the samples of groundwater in the studied region appears that the groups were SO<sub>4</sub> and Cl and their families were Mg-SO<sub>4</sub>, Na-SO<sub>4</sub>, Ca-SO<sub>4</sub> and Na-Cl (Table 4). The groundwater of Al-Najaf area has indicated that the sulfate group is dominated where the first family with one main type of water is Na<sub>2</sub>SO<sub>4</sub> which represents (53 %) of water samples, the second family water type is NaCl which represents (29 %), the third type is CaSO<sub>4</sub> which represents (12 %) and the fourth type is MgSO<sub>4</sub> which represents (6 %) from the samples (Figure 5). The availability of sulfate ions is attributed to the lithological and sulfate minerals that exist in sedimentary rocks like gypsum and anhydrite [16, 20].

**Table 4-** The water type in the studied region by [19] classification.

Samples No.	Type		Family	Group
	Anion	Cation		
W. (1, 4, 5, 6, 7, 8, 9, 10, 11)	r SO <sub>4</sub> - Cl - HCO <sub>3</sub>	r Na - Ca - Mg - K	Na - SO <sub>4</sub>	Sulfate
W. (2, 12, 14, 16, 17)	r Cl - SO <sub>4</sub> - HCO <sub>3</sub>	r Na - Ca - Mg - K	Na - Cl	Chlorides
W.3	r SO <sub>4</sub> - Cl - HCO <sub>3</sub>	r Ca - Mg - Na - K	Ca - SO <sub>4</sub>	Sulfate
W.13	r SO <sub>4</sub> - HCO <sub>3</sub> - Cl			
W.15	r SO <sub>4</sub> - Cl - HCO <sub>3</sub>	r Mg - Ca - Na - K	Mg - SO <sub>4</sub>	Sulfate



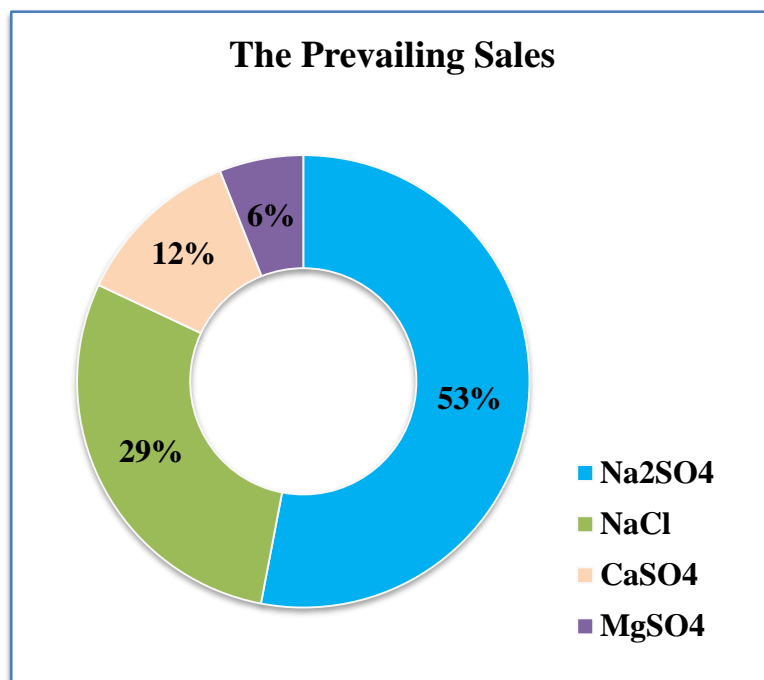


**Figure 5-** The percentage ratio of prevailing salts in the studied area.

To evaluate the groundwater suitability for drinking uses, the chemical analyses of water samples are compared with the Water Health Organization [21] and Iraqi standards [22]. As a result, it has been concluded that all groundwater samples are unsuitable for drinking, except samples W16 and W17, which are suitable.

It refers to the high salt concentration in addition to exceeding the permissible limits, in this case, the acceptable elements, the unacceptable element.

### Conclusions

The groundwater samples in Al-Najaf region are brackish water except some samples are Freshwater. The total hardness of ground water is hard to very hard water and the type of water is classified as excessively mineralized water. The origin of ground water is meteoric except some samples are marine origin. According to Schoeller classifications show that the mostly samples of water in the research region have a water type of Na<sub>2</sub>SO<sub>4</sub> which represents (53 %) of water samples, the second water type is NaCl which represents (29 %) and the third type is CaSO<sub>4</sub> which represents (12 %) while the fourth type is MgSO<sub>4</sub> which represents (6 %) from the samples. When comparing the groundwater samples with the Water Health Organization and Iraqi standards, the study region was not suitable for drinking uses except samples (W16 and W17) are acceptable.



## References

- Al-Qaraghuli, S. A., "Viability of the ground of Shithatha, western Iraqi plateau, for industrial and commercial uses via hydrochemistry analysis", IOP Conf. Ser.: Mater. Sci. Eng. 227, 2017.
- Al-Qaraghuli, S. A., Al-Khazrajia, O. N. A. and Idan, R. M., "Determination of hydrodynamic activity and the hydrocarbon accumulations effects of underground water in Khanaqin District, Northeastern Iraq", Vol. 62, Issue 09, 2020.
- Todd, D. K., "Groundwater hydrology" 2nd edit, John Wiley and Sons, Inc. Toppon Printing Company, Ltd, New York, and London, 535pp, 1980.
- Al-Hasnawi, S. S., Study the Ground Water Quality Using Water Quality Index for Al-Dammam Formation in the Western Desert: The Case Study in Najaf Governorate, Unpublished Ph.D. Thesis, college of sciences, University of Baghdad, 2009.
- Al-Azawi, A.A, (2009): Evaluation and management of groundwater in Bahr Al-Najaf basin, M.Sc. Thesis, College of Science, Baghdad University, (unpublished),p174.
- Al-Owaidi, M. R. A., Al-Enezy, A. W. A. and Hussein, M. L., "Hydrogeochemical properties and the exhaustion groundwater reserve from Dammam aquifer at Al-Najaf Governorate, middle Iraq", 2nd International Virtual Conference on Pure Science, Journal of Physics: Conference Series, 2021.
- Hamma, B., Alodah, A., Bouaicha, F. et al. "Hydrochemical assessment of groundwater using multivariate statistical methods and water quality indices (WQIs) ", Applied Water Science,14: 33., 2024. <https://doi.org/10.1007/s13201-023-02084-0>
- Lora-Ariza, B., Piña, A. & Donado, L.D., "Assessment of groundwater quality for human consumption and its health risks in the Middle Magdalena Valley, Colombia", Scientific Reports 14, 11346., 2024. <https://doi.org/10.1038/s41598-024-61259-0>
- Jassim, S.Z. and Goff, J.C., "Geology of Iraq ", Dolin Prague and Moravian Museum, Brno, 341, 2006.
- Thabit J. M., Al-Yasi A. I., and Al-Shemmari Al. N., " Estimation of hydraulic parameters and porosity from geoelectrical properties for fractured rock aquifer in middle Dammam Formation at Bahr Al-Najaf basin, Iraq", Iraqi Bulletin of Geology and Mining Vol.10, No.2, pp. 41-57, 2014.
- Ma'ala, K. A., "Tectonic and Structural Evolution", Geology of Iraqi Southern Desert, Special Issue of Iraqi Bulletin of Geology and Mining, pp. 35-52, 2009.
- Fouad S. F. A., "Tectonic and structural evolution", Special Issue of Iraqi Bulletin of Geology and Mining, pp. 29-50, 2007.



- Aqrawi A. A. M., Goff J. C., Horbury A. D., and Sadooni F. N., "The Petroleum Geology of Iraq", Scientific Press, Beacons field UK, 242 P, 2010.
- APHA, "Standard method for the examination of water and wastewater", 21st Ed. American Public Health Association, Washington, D.C, 2005.
- Detay M., "Water Wells- implementation, maintenance and restoration" John Wiley and Sons p. 379, 1997.
- Todd, D.K., "Ground water hydrology" third edition, Jhon Wiley and Sous, 3rd Ed., India, 535, 2007.
- Hou, Q., Pan, Y., Zeng, M. et al., "Assessment of groundwater hydrochemistry, water quality, and health risk in Hainan Island, China". Scientific Reports., 13, 12104,. 2023.  
<https://doi.org/10.1038/s41598-023-36621-3>
- BojaSrki, L., "Die anwendunge Hydrochemischen classification bei sucharbeiten auf Erdo 1- Z angew", Berlin, Geol. 16, 123- 125, 1970.
- Schoeller M., "Edute Geochemiique De La Nappe Des, Stables in fericurs Du Bassin D,aquitainse" Journal of Hydrology 15 (4) 317-328, 1972.
- Al-Dabbas M., Al-Kubaisi1 Q., Hussain T. A. and Al-Qaraghuli S., " Hydrochemical properties of groundwater of Rahaliya- Ekhedhur region, west Razzaza lake, Iraq", MATEC Web of Conferences 162, 05002, 2018.
- WHO Water Health Organization, "Guidelines for drinking water quality", 4th edit. WHO Press, Geneva. 564pp. ISBN: 978 92 4 154815 1, 2011.
- IQS Iraqi Quality Standard, "Drinking water Standard" No. 417, C. O. S. Q. C., Iraq, 2009.



# The Effect of Cinnamon and Cardamom Oils On Some Virulence Factors of *Pseudomonas aeruginosa*

Amina G.O. Al-Ani <sup>1</sup>

Aisha W. Al-Omari <sup>2</sup>

Najwa M. Al-Hadidi <sup>3</sup>



© 2024 The Author(s). This open access article is distributed under a Creative Commons Attribution (CC-BY) 4.0 license.

## Abstract

Globally, drug resistance by *Pseudomonas aeruginosa* is a major public health concern. It is important to look at different treatment methods and as a result, the approach taken in this work is to harness essential oils (EO) to combat the pathogenesis of bacterial diseases. Therefore, the aim of this study is to examine the effects of cardamom and cinnamon oils on *P. aeruginosa* biofilm formation, pyocyanin synthesis, and swarming motility. Each oil was used at four different concentrations (0.1, 0.2, 0.4, and 0.8)  $\mu\text{l/ml}$  to examine how it affects the formation of biofilms and the production of pyocyanin, while 0.2  $\mu\text{l/ml}$  has been used for swarming motility. Initially, the isolate showed the ability for forming strong biofilms. When studying the influence of cardamom and cinnamon oils on the formation of biofilms, cinnamon oil was more effective at a 0.8  $\mu\text{l/ml}$  concentration, while cardamom oil did not show any effect at all concentrations used. As for the effect of the oils used on the pyocyanin production, it showed that cinnamon oil had a greater effect at (0.4, 0.8)  $\mu\text{l/ml}$ , where the isolate under study lost its ability to produce the pigment pyocyanin. The cardamom oil had the lowest pigment production at concentration 0.8  $\mu\text{l/ml}$  compared to the control and other concentrations. Finally, the results of the effect of oils used at 0.2  $\mu\text{l/ml}$  concentration on the swarm movement showed that cinnamon oil was more effective in inhibiting movement compared to cardamom oil, as the diameter of the growing colony in the presence of cardamom and cinnamon oils was 15 mm and 10 mm, respectively, compared to the control 20 mm on Swarm agar medium.

**Key words:** *Pseudomonas Aeurogenosa*; Cinnamon Oil; Cardamom Oil; Biofilms.



<http://dx.doi.org/10.47832/MinarCongress12-02>



<sup>1</sup> Department of Biology, College of Sciences, University of Mosul, Mosul, Iraq  
[amesbio115@uomosul.edu.iq](mailto:amesbio115@uomosul.edu.iq)



<sup>2</sup> Department of Biology, College of Sciences, University of Mosul, Mosul, Iraq  
[Shsbio124@uomosul.edu.iq](mailto:Shsbio124@uomosul.edu.iq)



<sup>3</sup> Department of Biology, College of Sciences, University of Mosul, Mosul, Iraq  
[najsbio119@uomosul.edu.iq](mailto:najsbio119@uomosul.edu.iq)



## Introduction

*P. aeruginosa* is a rod-shaped, nonfermenting, motile, gram-negative bacteria that is a member of the Pseudomonadaceae family (1, 2, 3). widely dispersed across the environment, typically inhabiting water, soil, plants, and people. These microbes can thrive in a variety of temperatures ( 4 to 42°C), even in the absence of nutrients. *P. aeruginosa* has remarkable survivability and adaptability, enabling it to live for up to six months in hospitals on various dry surfaces (4,5).

*P. aeruginosa* can adjust to the unfavorable conditions of its hosts via producing a range of virulent factors, including hemolysin, pyocyanin pigment, biofilms, gelatinase, siderophores, lipases, lecithinase, DNase, and proteases, which all help to cause infection (6). These variables raise the possibility of emerging strains of multidrug-resistance causing a serious risk to medical facilities and generating a clinical issue on a worldwide scale. (7 ,8, 9). The opportunistic *P. aeruginosa* has been linked to a number of medical infections, such as pneumonia associated with ventilators and infections of the intensive care unit, bloodstream, urinary tract, burns, otitis media and keratitis (10,11).

One of the defining characteristics of *Pseudomonas* species' ability to survive in harsh environments and in vivo is its ability for biofilm formation. Biofilms are made of a matrix consisting of polysaccharides, extracellular DNA and proteins (12, 13). It is essential for horizontal transfer of genes, which makes it easier for virulence factors and resistance genes to spread, especially when antibiotic-selective stress is present (14, 15).

Another significant virulence factor that *P. aeruginosa* produces as a secondary metabolic product is called pyocyanin, a pigment that is secreted extracellularly formed from phenazine (16). It can also change the cycle of glutathione redox, induce apoptosis of neutrophils, inactivate catalase and impede cellular respiration. Strains of *P. aeruginosa* that produce pyocyanin show more virulence and resistance to several medications than non- producing strains (17, 18).

*P. aeruginosa*'s ability to swarm is another tool that boosts its pathogenicity and efficacy. The quick and well-organized movement of certain bacterial species' flagella during multicellular activity along semi-solid media is known as swarming motility. The antibiotic resistance is closely linked to this significant aspect (19, 20). Different essential oils have been discovered to limit biofilm generation in addition to other *P. aeruginosa* virulence factors (21, 22).



Cinnamon is phytochemical that has antimicrobial characteristics which is reliable and frequently utilized in daily life. Due to its traditional use as a remedy for digestive issues like nausea, diarrhea and vomiting, cinnamon oil is included in toothpastes as a common antibacterial alternative (23, 21).

Cardamom oil is utilized as an "organic product" to cure a variety of illnesses, such as asthma, bronchitis, colds, jaundice, and indigestion. It has also been used as a stimulating agent for patients with anorexia (24). Researchs on cardamom's health benefits have shown that it has antimicrobial, antioxidant and potentially anticancerogenic features (25).

As a result of the increasing resistance to antibiotics in recent decades, which led to the urgent demand to develop efficient ways to solve these issues., the focus was on strategies that target the virulence factors of bacteria instead of the survival of bacteria, because altering virulent factors may inhibit bacteria from growing and developing drug resistance in them. Therefore, the aim of the research is to examine the natural oils' (cinnamon and cardamom) effects on a few *P. aeruginosa* virulence factors, which included : biofilm formation, pyocyanin production and swarming motility .

## **Materials and Methods:**

The *P. aeruginosa* isolate was obtained from the Biology Department /College of Science /University of Mosul .

### **1. Biofilms Formation**

#### **A. Investigating the ability of *P. aeruginosa* to form biofilms:**

The ability of *P. aeruginosa* to form biofilms was investigated using the microtiter plate method.

The sterile Tryptic Soy Broth (TSB) medium was inoculated with pre-activated *P. aeruginosa* and the incubation period extended to 24 hours in 37°C, bacterial growth was compared with a standard 0.5 McFarland tube. 200 µL of sterile TSB medium were placed in the first column wells and considered a control for comparison, where three replicates were made. 200 µL of bacterial inoculum were placed in the first three wells of the second column. The plate was covered with its own lid and incubated at 37°C for 18–24 hours.

Non-adherent bacterial cells were eliminated by washing the wells with normal saline, produced by 0.9 grams of sodium chloride dissolved in 100 cm<sup>3</sup> of D.W. (26). 200 µL of the prepared crystal violet at a concentration of (1%) were added to each well and left for 45



minutes, then removed with sterile distilled water. The plate was left to dry at room temperature for 45 minutes. Then, add 200  $\mu$ L of (99 %) ethanol to each well and mix.

The absorbance was obtained at (630) nm utilizing an ELIZA reader device (American-made). The efficiency of bacterial isolate in biofilms formation was determined by comparing the readings according to certain equations(27,28,29).

### **B. Cinnamon and cardamom oils effects on the formation of biofilms:**

Both cinnamon and cardamom oils produced by (AL\_EMAD Company) were used to study their effect on biofilms formation by the *P. aeruginosa* isolate under study, as they were purchased from a herbal shop.

Different concentrations of cinnamon and cardamom oils were prepared with TSB as follows: (0.1, 0.2, 0.4, 0.8)  $\mu$ l/ml.

By using the microtiter plate method, 300  $\mu$ L of the first concentration of cinnamon oil were added in the first column of the microtiter plates (for control) in three replicates, then 290  $\mu$ L of the first concentration of cinnamon oil were added in the second column, with the addition of 10  $\mu$ L of bacterial inoculum (0.5 McFarland) in three replicates. The process was repeated for the remaining concentrations sequentially in subsequent columns.

Follow the same steps regarding cardamom oil concentrations, starting from the fourth row of the first column and sequentially. The microtiter plates have been kept at 37°C for 24 hours of incubation. After the incubation, the concentration effects of cinnamon and cardamom oils were studied by following the steps mentioned previously in paragraph (A). (27,28,29).

## **2. Pyocyanin Production**

To know the effect of oils on the production of pyocyanin, we prepared Nutrient Broth Medium (N.B.) with concentrations (0.1, 0.2, 0.4, and 0.8)  $\mu$ l/ml of the cinnamon and cardamom oils separately and without oils for control, then inoculated with *P. aeruginosa* (0.5 McFarland) with incubation for 24 hours at 37°C (30).

## **3. Assays for swarming motility**

Assays for motility were conducted using a previously published protocol (31). Point-inoculation of *P. aeruginosa* cultures was done onto swarm agar plates (prepared by dissolving each of the following: 1 g of glucose, 0.5 g of bactoagar, 0.6 g of bactopectone, and 0.2 g of yeast extract in 100 ml of distilled water) with 0.2  $\mu$ l/ml cinnamon and cardamom oils and



without the latter for the control plates. Incubation was carried out by placing the plates in a straight-up position for 24 hours at 37 °C .

## Results and Discussion:

### 1. Biofilms formation

Biofilms have been linked to higher mortality and morbidity rates as well as major medical problems.

The ability of the *P. aeruginosa* isolate to form biofilms was evaluated using the microtiter plate method, and after reading the results in the ELIZA reader device and applying them to the equation, the result showed the isolate's ability to create strong biofilms with comparison to the control ,as shown in figure (1).

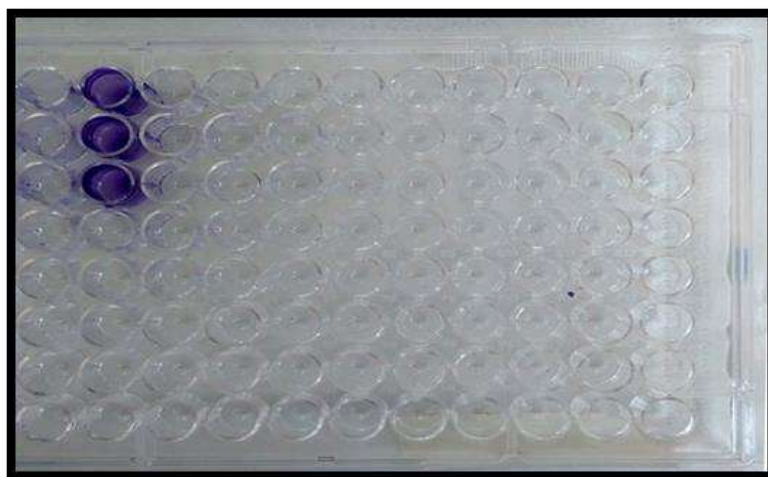


**Figure 1-** Biofilm formation by *P. aeruginosa*

This is consistent with Kunwar *et al.* (32), they indicated the ability of some *P. aeruginosa* isolated from burn patients to form strong biofilms. Abdelraheem *et al.* (33), stated that 14% of their isolates of *P. aeruginosa* were strong at forming biofilms. As well as Tuon *et al.* (34), pointed to the vital role of *P. aeruginosa* for biofilm formation.

*P. aeruginosa* forms biofilms through a complex mechanism in which a floating bacterium first adheres reversibly to a surface. Adhesins of the surface then permanently attach the bacteria to the surface, and extracellular matrix formation results in the production of a mature biofilm. Ultimately, bacteria spread out of the matrix to settle on other surfaces (35).



## 2. Cinnamon and cardamom oils effects on the formation of biofilms:

The results showed that 0.8  $\mu\text{l/ml}$  concentration of cinnamon oil was more effective than other concentrations in converting the isolate from strong biofilm formation to weak biofilm formation after comparing it with the control. As for cardamom oil, it did not show any effect on biofilm formation for all concentrations, which indicates that the isolate remained strong in biofilms formation compared to the control, as shown in figure (2).

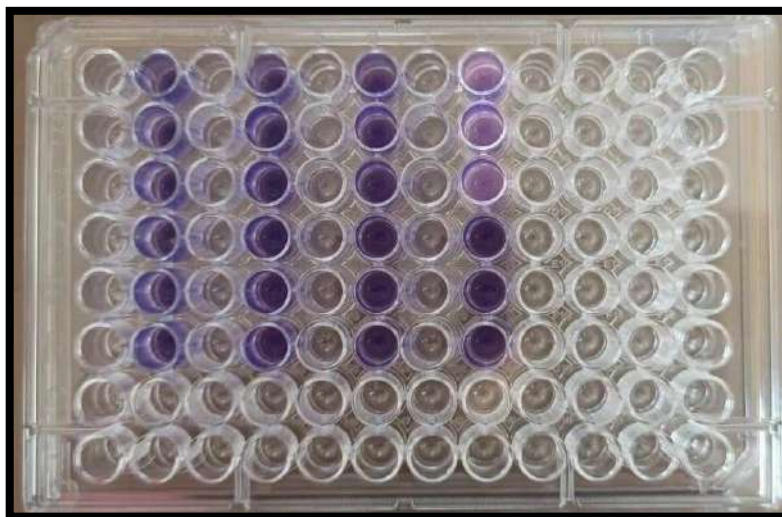


**Figure 2-** The effect cinnamon and cardamom oils on biofilms formation

Kalia *et al.* (21), reported that 0.8  $\mu\text{l/ml}$  concentration of cinnamon oil had a high inhibition on biofilms formation by *P. aeruginosa* because it reduced the content of bound extracellular DNA and extracellular polymeric substances (EPS), the well-established elements of biofilms. As well as Wijesinghe *et al.* (36), they pointed out the cinnamon oil's effects on biofilms formation by *P. aeruginosa*, *Staphylococcus aureus*, and *Klebsiella pneumoniae*.

In this regard, the authors reported that cinnamaldehyde which is the essential ingredient of cinnamon, inhibited quorum sensing, interference with bacterial motility and alginate production which is an essential extracellular component that leads to biofilms structure integrity; therefore, the inhibition of alginate had an effect on biofilms maturation (37,21,38)

## 3. Pyocyanin Production

The results of the effect of both cinnamon and cardamom oils on pyocyanin production showed that cinnamon oil was more effective than cardamom oil. Cinnamon oil showed inhibition of pigment production at concentrations of 0.4–0.8  $\mu\text{l/ml}$  in terms of the absence of color compared to the control, while at 0.2  $\mu\text{l/ml}$ , the pigment production was reduced compared



to the control, as shown in figure ( 3). The cardamom oil had the lowest pigment production at a concentration of 0.8  $\mu\text{l/ml}$  comparison with control and other concentrations, as in the figure (4 ).

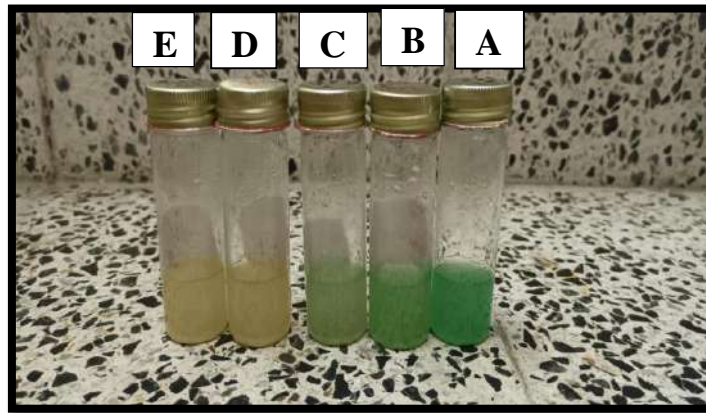


**Figure 3-** Cinnamon oil effect ( $\mu\text{l/ml}$  ) on Pyocyanin Production

**A- control , B- 0.1 , C- 0.2 , D- 0.4 , E- 0.8**

**B-**

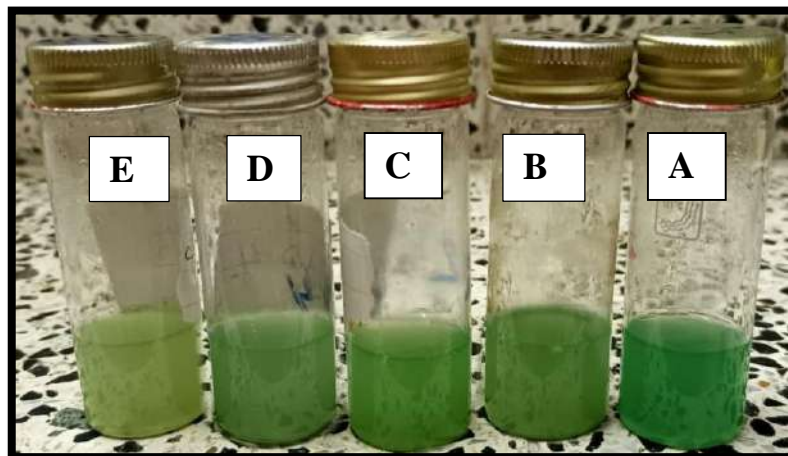


**Figure 4-** Cardamom oil effect ( $\mu\text{l/ml}$ ) on Pyocyanin Production

**A- control , B- 0.1 , C- 0.2 , D- 0.4 , E- 0.8**

Regarding cinnamon oil, this is consistent with what Kalia *et al.* (21), indicated; they used cinnamon oil with various concentrations. It decreased the production of pigment at 0.2  $\mu\text{l/ml}$  concentration by 22% . Farisa Banu *et al.* (39), also mentioned the cinnamon oil ability to inhibit pyocyanin production via *P. aeruginosa*. They indicated that the *rhl* or LasR inhibitor in essential oil presence could inhibit the production of pyocyanin whereas *P. aeruginosa* has *rhl*, which plays a role in gene expression to produce pigment.



As for cardamom oil, many researchers have mentioned the biological effectiveness of the oil. Alam *et al.* (40), demonstrated cardamom oil's role in inhibiting the growth of *P. aeruginosa*.

#### 4. Assays for swarming motility

Motility has been recognized as a key virulent feature for pathogens, permitting these organisms to spread into favorable environments as nutrients become limited as well as competing with other species.

Results of the effect of both cinnamon and cardamom oils at 0.2  $\mu\text{l/ml}$  concentration on the motility of *P. aeruginosa* showed that cinnamon oil had a greater effect than cardamom oil when compared to the control.

The diameter of the colony for the control was equal to 20 mm, while the diameter of the colony with cardamom and cinnamon oil was equal to 15 and 10 mm, respectively on Swarm Agar Medium, as shown in the figure. (5).

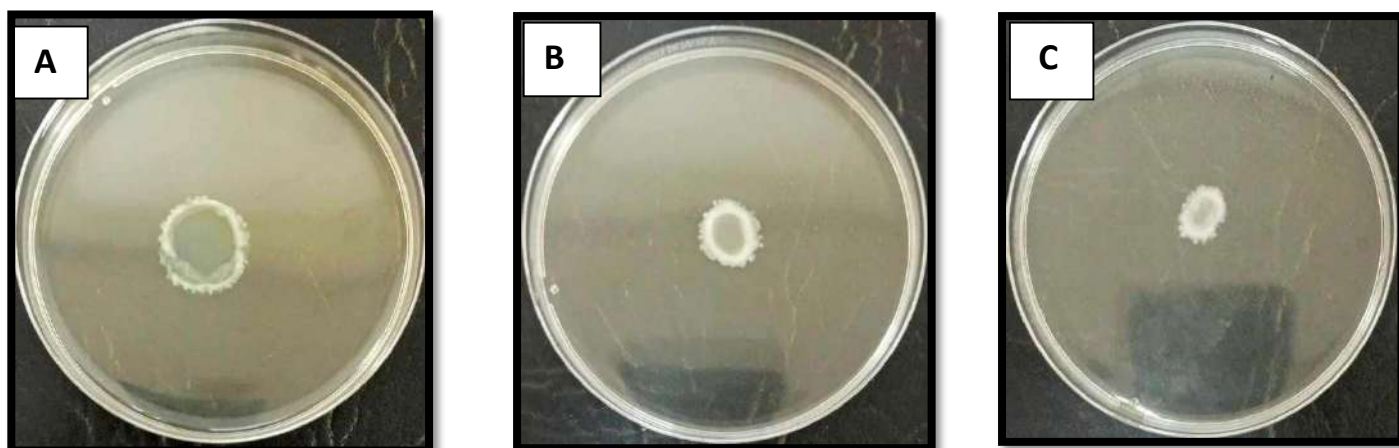


**Figure 5-** Effects of cinnamon and cardamom oils at concentration (0.2  $\mu\text{l/ml}$ ) on Swarm Agar Medium.

**A: Control    B: Cardamom oil    C: Cinnamon oil**

Agha (41), pointed out the role of cinnamon oil in the anti-swarming motility of *Pseudomonas*, as she stated that cinnamon and eucalyptus tree oils are more effective than other oils used. Also, Kalia1 *et al.* indicated the swarming motility inhibition via cinnamon oil. Cinnamon oils decrease the *rhlA* and *fliC* expression related with the rhamnolipid and flagella protein flagellin synthesis (42). In addition, Tuba *et al.* reported that Cinnamaldehyde (CAD) reduced *P. aeruginosa* swarming motility, which has a role in reducing movement and disrupting biofilms through the modulation of intracellular signaling processes (43).

Noumi *et al.* (44), mentioned the role of cardamom oil in inhibiting the swarming motility, as indicated by the decrease in the diameter of the colony compared to the control.

Akrayi (45), mentioned that the reason for the effect of oil on movement, may be due to the presence of phenolic groups that bind to the phospholipids and proteins in the cell wall's outer membrane and this will stop the cells from becoming swimmers.

### **Conclusions:**

In the current study, it was found that cinnamon oil had a greater effect than cardamom oil, as cinnamon oil had an effect on the ability of the isolate under study to form a biofilm, while cardamom oil had no effect. In addition, cinnamon oil was more effective on pyocyanin production and swarming motility than cardamom oil. Hence, this study showed evidence that essential oils can be used to influence the virulence factors of *P. aeruginosa* thus reducing many of the infections that can occur due to this bacterial species and the possibility of reducing the use of antibiotics, which has become a problem today due to the known resistance to antibiotics.



## References

- Wu W., Jin Y., Bai F., et al. In: *Molecular Medical Microbiology*. 2nd ed. Tang T.W., Sussman M., Liu D., Poxton I., Schwartzman J., editors. Academic Press; Cambridge, MA, USA: 2015. Chapter 41—*Pseudomonas aeruginosa*; pp. 753–767. [CrossRef] [Google Scholar]
- El-Fouly M.Z., Sharaf A.M., Shahin A.A.M, et al. Biosynthesis of pyocyanin pigment by *Pseudomonas aeruginosa*. *J. Radiat. Res. Appl. Sci.* 2015;8(1):36–48. doi: 10.1016/j.jrras.2014.10.007. [CrossRef] [Google Scholar]
- Brady M.T., Leber A. *Principles and Practice of Pediatric Infectious Diseases*. Elsevier; 2018. Less Commonly Encountered Nonenteric Gram-Negative bacilli; pp. 855–859. [CrossRef] [Google Scholar]
- Wu, M., & Li, X. (2015). *Klebsiella pneumoniae* and *Pseudomonas aeruginosa*. In *Molecular medical microbiology* (pp. 1547-1564). Academic Press
- Diggle, S. P., Whiteley, M. (2020). Microbe Profile: *Pseudomonas Aeruginosa*: Opportunistic Pathogen and Lab Rat. *Microbiol. (Reading England)* 166 (1), 30–33. doi: 10.1099/mic.0.000860
- Vidaillac, C., & Chotirmall, S. H. (2021). *Pseudomonas aeruginosa* in bronchiectasis: infection, inflammation, and therapies. *Expert review of respiratory medicine*, 15(5), 649-662
- Ghanem, S. M., Abd El-Baky, R. M., Abourehab, M. A., Fadl, G. F., & Gamil, N. G. (2023). Prevalence of Quorum Sensing and Virulence Factor Genes Among *Pseudomonas aeruginosa* Isolated from Patients Suffering from Different Infections and Their Association with Antimicrobial Resistance. *Infection and Drug Resistance*, 2371-2385
- Ozer, E., Yaniv, K., Chetrit, E., Boyarski, A., Meijler, M. M., Berkovich, R., ... & Alfonta, L. (2021). An inside look at a biofilm: *Pseudomonas aeruginosa* flagella biotracking. *Science advances*, 7(24), eabg8581.
- Newman, J. W., Floyd, R. V., & Fothergill, J. L. (2017). The contribution of *Pseudomonas aeruginosa* virulence factors and host factors in the establishment of urinary tract infections. *FEMS microbiology letters*, 364(15), fnx124.
- Ito, C. A. S., Bail, L., Arend, L. N. V. S., Nogueira, K. D. S., & Tuon, F. F. (2021). The activity of ceftazidime/avibactam against carbapenem-resistant *Pseudomonas aeruginosa*. *Infectious Diseases*, 53(5), 386-389.
- Kalluf, K. O., Arend, L. N., Wuicik, T. E., Pilonetto, M., & Tuon, F. F. (2017). Molecular epidemiology of SPM-1-producing *Pseudomonas aeruginosa* by rep-PCR in hospitals in Parana, Brazil. *Infection, Genetics and Evolution*, 49, 130-133
- Bai, X., Nakatsu, C. H., & Bhunia, A. K. (2021). Bacterial biofilms and their implications in pathogenesis and food safety. *Foods*, 10(9), 2117.
- Cepas, V., López, Y., Muñoz, E., Rolo, D., Ardanuy, C., Martí, S., ... & Soto, S. M. (2019). Relationship between biofilm formation and antimicrobial resistance in gram-negative bacteria. *Microbial Drug Resistance*, 25(1), 72-79.

- Tajbakhsh, E., Ahmadi, P., Abedpour-Dehkordi, E., Arbab-Soleimani, N., & Khamesipour, F. (2016). Biofilm formation, antimicrobial susceptibility, serogroups and virulence genes of uropathogenic *E. coli* isolated from clinical samples in Iran. *Antimicrobial Resistance & Infection Control*, 5(1), 1-8.
- Mittal, S., Sharma, M., & Chaudhary, U. (2015). Biofilm and multidrug resistance in uropathogenic *Escherichia coli*. *Pathogens and global health*, 109(1), 26-29.
- Wamik, A. (2018). Production and antimicrobial, antioxidant and anticancer applications of pyocyanin from isolated *Pseudomonas aeruginosa*. *SF J Ferm Micro Technol*, 1(2), 2.
- Noto, M. J., Burns, W. J., Beavers, W. N., & Skaar, E. P. (2017). Mechanisms of pyocyanin toxicity and genetic determinants of resistance in *Staphylococcus aureus*. *Journal of bacteriology*, 199(17), 10-1128.
- Abdelaziz, A. A., Kamer, A. M. A., Al-Monofy, K. B., & Al-Madboly, L. A. (2023). *Pseudomonas aeruginosa*'s greenish-blue pigment pyocyanin: its production and biological activities. *Microbial Cell Factories*, 22(1), 110.
- Gazel, D., Zer, Y., Manay, A. B., & Akdoğan, H. (2021). Inhibition of swarming motility using in vitro hyperthermia. *Journal of Thermal Biology*, 100, 102955..
- Rütschlin, S., & Böttcher, T. (2020). Inhibitors of bacterial swarming behavior. *Chemistry—A European Journal*, 26(5), 964-979.
- Kalia, M., Yadav, V. K., Singh, P. K., Sharma, D., Pandey, H., Narvi, S. S., & Agarwal, V. (2015). Effect of cinnamon oil on quorum sensing-controlled virulence factors and biofilm formation in *Pseudomonas aeruginosa*. *PLoS one*, 10(8), e0135495.
- Pejčić, M., Stojanović-Radić, Z., Genčić, M., Dimitrijević, M., & Radulović, N. (2020). Anti-virulence potential of basil and sage essential oils: Inhibition of biofilm formation, motility and pyocyanin production of *Pseudomonas aeruginosa* isolates. *Food and chemical toxicology*, 141, 111431.
- Rao, P. V., & Gan, S. H. (2014). Cinnamon: a multifaceted medicinal plant. *Evidence-Based Complementary and Alternative Medicine*, 2014.
- Ashokkumar, K., Murugan, M., Dhanya, M. K., & Warkentin, T. D. (2020). Botany, traditional uses, phytochemistry and biological activities of cardamom [*Elettaria cardamomum* (L.) Maton]—A critical review. *Journal of ethnopharmacology*, 246, 112244.
- Cheikhoussef, A., Cheikhoussef, N., Sharma, R., & Hussein, A. A. (2023). Health-Promoting Effects of Cardamom (*Elettaria cardamomum*). In *Cardamom (Elettaria cardamomum): Production, Processing and Properties* (pp. 133-156). Cham: Springer International Publishing.
- Christensen, G. D., Simpson, W. A., Younger, J. J., Baddour, L. M., Barrett, F. F., Melton, D. M., & Beachey, E. H. (1985). Adherence of coagulase-negative staphylococci to plastic tissue culture plates: a quantitative model for the adherence of staphylococci to medical devices. *Journal of clinical microbiology*, 22(6), 996-1006.
- Cruz-Soto, A. S., Toro-Castillo, V., Munguía-Magdaleno, C. O., Torres-Flores, J. E., Flores-Pantoja, L. E., Loeza-Lara, P. D., & Jiménez-Mejía, R. (2020). Genetic relationships, biofilm formation,



- motility and virulence of *Escherichia coli* isolated from bovine mastitis. *Revista mexicana de ciencias pecuarias*, 11(1), 167-182.
- H Ghellai, L., Hassaine, H., Klouche, N., Khadir, A., Aissaoui, N., Nas, F., & Zingg, W. (2014). Detection of biofilm formation of a collection of fifty strains of *Staphylococcus aureus* isolated in Algeria at the University Hospital of Tlemcen. *Journal of bacteriology research*, 6(1), 1-6.
- Nassar, H. M., Li, M., & Gregory, R. L. (2012). Effect of honey on *Streptococcus mutans* growth and biofilm formation. *Applied and environmental microbiology*, 78(2), 536-540.
- Abdelaziz, A. A., Kamer, A. M. A., Al-Monofy, K. B., & Al-Madboly, L. A. (2023). *Pseudomonas aeruginosa*'s greenish-blue pigment pyocyanin: its production and biological activities. *Microbial Cell Factories*, 22(1), 110.
- Krishnan, T., Yin, W. F., & Chan, K. G. (2012). Inhibition of quorum sensing-controlled virulence factor production in *Pseudomonas aeruginosa* PAO1 by ayurveda spice clove (*Syzygium Aromaticum*) bud extract. *Sensors*, 12(4), 4016-4030.
- Kunwar, A., Shrestha, P., Shrestha, S., Thapa, S., Shrestha, S., & Amatya, N. M. (2021). Detection of biofilm formation among *Pseudomonas aeruginosa* isolated from burn patients. *Burns Open*, 5(3), 125-129.
- Abdelraheem, W. M., Abdelkader, A. E., Mohamed, E. S., & Mohammed, M. S. (2020). Detection of biofilm formation and assessment of biofilm genes expression in different *Pseudomonas aeruginosa* clinical isolates. *Meta Gene*, 23, 100646.
- Tuon, F. F., Dantas, L. R., Suss, P. H., & Tasca Ribeiro, V. S. (2022). Pathogenesis of the *Pseudomonas aeruginosa* biofilm: a review. *Pathogens* 11: 300.
- Ghafoor, A., Hay, I. D., & Rehm, B. H. (2011). Role of exopolysaccharides in *Pseudomonas aeruginosa* biofilm formation and architecture. *Applied and environmental microbiology*, 77(15), 5238-5246.
- Wijesinghe, G. K., Feiria, S. B., Maia, F. C., Oliveira, T. R., Joia, F., Barbosa, J. P., ... & Höfling, J. F. (2021). In-vitro antibacterial and antibiofilm activity of *Cinnamomum verum* leaf oil against *Pseudomonas aeruginosa*, *Staphylococcus aureus* and *Klebsiella pneumoniae*. *Anais da Academia Brasileira de Ciências*, 93, e20201507.
- Rafeeq, H. F., & Sharba, Z. A. (2022). Study the effect of cinnamon and tea tree oils on biofilm formation of *Klebsiella pneumoniae*. *Journal of Applied Sciences and Nanotechnology*, 2(2), 16-26.
- Didehdar, M., Chegini, Z., Tabaeian, S. P., Razavi, S., & Shariati, A. (2022). *Cinnamomum*: The new therapeutic agents for inhibition of bacterial and fungal biofilm-associated infection. *Frontiers in Cellular and Infection Microbiology*, 12, 930624.
- Farisa Banu, S., Murugan, R., Wilson, A., Gowrishankar, S., Pandian, S. K., & Nithyanand, P. (2017). Antivirulent properties of underexplored *Cinnamomum tamala* essential oil and its synergistic effects with DNase against *Pseudomonas aeruginosa* Biofilms—an in vitro study. *Frontiers in microbiology*, 8, 256779.

- Alam, A., Rehman, N. U., Ansari, M. N., & Palla, A. H. (2021). Effects of essential oils of *Elettaria cardamomum* grown in India and Guatemala on gram-negative bacteria and gastrointestinal disorders. *Molecules*, 26(9), 2546.
- Agha, Y. Y. (2020). Effect of some plant oils on swarming motility and Biofilm formation in *Proteus*, *Aeromonas*, and *Pseudomonas*. *Journal of Advanced Pharmacy Education and Research*, 10(4-2020), 64-71.
- Lakshmanan, D., Harikrishnan, A., Vishnupriya, S., & Jeevaratnam, K. (2019). Swarming inhibitory potential of cinnamtannin B1 from *Cinnamomum tamala* T. Nees and Eberm on *Pseudomonas aeruginosa*. *ACS omega*, 4(16), 16994-16998.
- Topa, S. H., Subramoni, S., Palombo, E. A., Kingshott, P., Rice, S. A., & Blackall, L. L. (2018). Cinnamaldehyde disrupts biofilm formation and swarming motility of *Pseudomonas aeruginosa*. *Microbiology*, 164(9), 1087-1097.
- Noumi, E., Snoussi, M., Alreshidi, M. M., Rekha, P. D., Saptami, K., Caputo, L., ... & De Feo, V. (2018). Chemical and biological evaluation of essential oils from cardamom species. *Molecules*, 23(11), 2818.
- Akrai, H. F. S. (2012). Antibacterial effect of seed extracts of cardamom (*Elettaria cardamomum*) against *staphylococcus aureus* and *proteus mirabilis*. *Tikrit Journal of Pure Science*, 17(2), 1813-1662.



## Spaces of Lipschitz Functions on $n$ -Modular Spaces

Aamena Al - Qabani <sup>1</sup>

Iman A.Hussain <sup>2</sup>

Haneen A. Ameen <sup>3</sup>




© 2024 The Author(s). This open access article is distributed under a Creative Commons Attribution (CC-BY) 4.0 license.

### Abstract

*The intent of this article is to explore some properties of the set of all bounded linear operators and the set of all Lipschitz functions that are defined on  $n$ -modular spaces. We introduce the definition of  $n$ -modular bounded linear operator and then we describe the set of all  $n$ -modular bounded linear operator. One of our main results shows that this set is Banach space. Moreover, we give the definition of  $n$ -modular Lipschitz functions and then we characterize the set of all  $n$ -modular Lipschitz function. For a specific norm one of our main results shows that this set is Banach space.*

**Keywords:** Lipschitz;  $n$ -Modular; Spaces.

---

 <http://dx.doi.org/10.47832/MinarCongress12-03>

<sup>1</sup>  Department of Mathematics and Computer Applications, College of Sciences, Al-Nahrain University, Baghdad, Iraq [amena.raimmohammed@nahraiuniv.edu.iq](mailto:amena.raimmohammed@nahraiuniv.edu.iq)

<sup>2</sup>  Department of Mathematics and Computer Applications, College of Sciences, Al-Nahrain University, Baghdad, Iraq [imana.hussain@nahraiuniv.edu.iq](mailto:imana.hussain@nahraiuniv.edu.iq)

<sup>3</sup>  Department of Mathematics and Computer Applications, College of Sciences, Al-Nahrain University, Baghdad, Iraq [haneen.abdulkareem@nahraiuniv.edu.iq](mailto:haneen.abdulkareem@nahraiuniv.edu.iq)

## Introduction

The study of properties of the concept of modular spaces has received great attention from researchers since it was first known by Nakano in 1950, [9]. Owing to the significance of modular space numerous researches and studies appeared to develop these space and generalize its' theory. For example see [1],[3],[11]. In general, the modular space can be defined as follows, [12]

### Definition

Hypothesize that  $\mathcal{E}$  is a vector space over  $\mathbb{C}$  or  $\mathbb{R}$ . Then the real non-negative function

$\psi_m: \mathcal{E} \rightarrow [0, \infty)$  is called modular if:

- For  $\mu \in \mathcal{E}$ ,  $\psi_m(\mu) = 0$  if and only if  $\mu = \theta$ , (where  $\theta$  is the zero vector in  $\mathcal{E}$ ).
- For every  $\mu \in \mathcal{E}$ ,  $\psi_m(-\mu) = \psi_m(\mu)$ .
- For every  $\mu, \xi \in \mathcal{E}$ ,  $\psi_m(\check{\alpha}\mu + \check{b}\xi) \leq \psi_m(\mu) + \psi_m(\xi)$ , where  $\check{\alpha}, \check{b}$  are real numbers such that  $\check{\alpha}, \check{b} \geq 0$  and  $\check{\alpha} + \check{b} = 1$ .

With this modular function  $\psi_m$ , the pair  $(\mathcal{E}, \psi_m)$  is called a modular space.

An interesting development to the theory of modular spaces is to study the properties of modular function spaces, when the vector spaces  $\mathcal{E}$  is regarded as space of measurable functions, see for example, [8], [5],[7], [6].

Recently, a significant study appeared to extended the operator theory on modular spaces. In [4], the Hudzik, Musielak and Urban'ski studied some properties of the bounded linear operators between two modular spaces, moreover, they investigated the adjoint linear operators on conjugate modular spaces. Nurnugroho, Supama and Zulijanto in [2], investigated some topological properties of 2-modular spaces. They also characterized a bounded linear operator on 2-modular spaces. The work in [10] is sacrificed to study bounded linear operators on  $n$ -modular spaces. The authors generalized the modular spaces to  $n$ -modular spaces depending on the notion of the  $n$ - normed spaces. They defined the continuous and compact operators on  $n$ -normed spaces. Furthermore, they gave some applications to  $n$ -modular fixed point.

In this article our work is dedicated to study some properties of the set of all bounded linear operators and the set of all Lipschitz functions that are defined on  $n$ -modular spaces. With an appropriate norm on the set of all bounded linear operators that are defined on  $n$ -modular spaces, we proved that this set is a Banach space. In section three we introduce the definition of a Lipschitz function on  $n$ -modular spaces. Moreover, we characterize the set of all of all



Lipschitz functions that are defined on  $n$ -modular spaces. One of our significant results shows that this set, with suitable norm, is a Banach space.

Before we mention our results let us recall the definition of  $n$ -modular spaces, [10].

**Definition**

Hypothesize that  $\mathcal{E}$  is a vector space over  $R$  with dimension  $v$ , where  $v \geq n$ . Then the non-negative real function  $\varphi_n: \mathcal{E}^n \rightarrow [0, \infty)$  is called  $n$ -modular if:

- For  $\mu = (\mu_1, \mu_2, \dots, \mu_n) \in \mathcal{E}^n$ ,  $\varphi_n(\mu) = 0$  if and only if  $\mu_1, \mu_2, \dots, \mu_n$  are linearly independent.
- For every  $\mu = (\mu_1, \mu_2, \dots, \mu_n) \in \mathcal{E}^n$ ,  $\varphi_n(\mu_1, \mu_2, \dots, -\mu_n) = \varphi_n(\mu_1, \mu_2, \dots, \mu_n)$ .
- $\varphi_n(\mu_1, \mu_2, \dots, \mu_n)$  is invariant under permutation, where  $\mu_1, \mu_2, \dots, \mu_n \in \mathcal{E}$ .
- $\varphi_n(\check{a}\mu_0 + \check{b}\mu_1, \mu_2, \dots, \mu_n) \leq \varphi_n(\mu_0, \mu_2, \dots, \mu_n) + \varphi_n(\mu_1, \mu_2, \dots, \mu_n)$ , for any real numbers  $\check{a}, \check{b}$

where  $\check{a}, \check{b} \geq 0$  and  $\check{a} + \check{b} = 1$ .

With this  $n$ -modular function  $\varphi_n$ , the pair  $(\mathcal{E}^n, \varphi_n)$ , or  $\mathcal{E}_{\varphi_n}^n$  in short, is called an  $n$ -modular space. An interesting examples about these spaces can be found in [10].

**Bounded Linear Operators On N-Modular Space**

This section is devoted to investigate the properties of the set of all bounded linear operators defined on  $n$ -modular space.

**Definition**

Hypothesize that  $(\mathcal{E}^n, \varphi_n)$  is  $n$ -modular space and  $(\Gamma, \|\cdot\|_\Gamma)$  is a normed space. A linear operator

$\bar{T}: \mathcal{E}^n \rightarrow \Gamma$  is called  $n$ -modular bounded operator if there exists a constant  $M > 0$  such that

$$\|\bar{T}(\mu_1, \mu_2, \dots, \mu_n)\|_\Gamma \leq M\varphi_n(\mu_1, \mu_2, \dots, \mu_n), \text{ for each, } \mu = (\mu_1, \mu_2, \dots, \mu_n) \in \mathcal{E}^n.$$

**Definition**

Hypothesize that  $(\mathcal{E}^n, \varphi_n)$  is  $n$ -modular space and  $(\Gamma, \|\cdot\|_\Gamma)$  is a normed space. Then the set of all  $n$ -modular bounded linear operators on  $\mathcal{E}^n$ , will denoted by

$$BO_{mod_n}(\mathcal{E}_{\varphi_n}^n, \Gamma) = \{\bar{T}: \mathcal{E}_{\varphi_n}^n \rightarrow \Gamma, \bar{T} \text{ is } n - \text{modulr bounded linear operator}\}.$$

Obviously,  $BO_{mod_n}(\mathcal{E}_{\varphi_n}^n, \Gamma)$  is a linear space.

The theorem below shows that  $BO_{mod_n}(\mathcal{E}_{\varphi_n}^n, \Gamma)$  is a Banach space.

**Theorem**

Hypothesize that  $(\mathcal{E}^n, \varphi_n)$  is  $n$ -modular space and  $(\Gamma, \|\cdot\|_\Gamma)$  is a normed space. Then the vector space is  $BO_{mod_n}(\mathcal{E}^n_{\varphi_n}, \Gamma)$  is a normed space with the norm defined by:

$$\|\bar{T}\| = \sup \left\{ \frac{\|\bar{T}(\mu_1, \mu_2, \dots, \mu_n)\|_\Gamma}{\varphi_n(\mu_1, \mu_2, \dots, \mu_n)} : \varphi_n(\mu_1, \mu_2, \dots, \mu_n) \neq 0 \right\} \quad (1)$$

Where,  $\mu_1, \mu_2, \dots, \mu_n \in \mathcal{E}$ . Furthermore, if  $(\Gamma, \|\cdot\|_\Gamma)$  is complete, then  $BO_{mod_n}(\mathcal{E}^n_{\varphi_n}, \Gamma)$  is Banach space.

*Proof.*

Take  $\bar{T}, \bar{S}$  in  $BO_{mod_n}(\mathcal{E}^n_{\varphi_n}, \Gamma)$  and  $\alpha$  is a scalar, then:

(1) It is obvious that  $\|\bar{T}\|$  is well defined and  $\|\bar{T}\| \geq 0$ .

(2) If  $\bar{T} = 0$ , then it is clear that  $\|\bar{T}\| = 0$ . Conversely, if  $\|\bar{T}\| = 0$ , then  $\|\bar{T}(\mu_1, \mu_2, \dots, \mu_n)\|_\Gamma = 0$ ,

(3) for any  $\mu_1, \mu_2, \dots, \mu_n \in \mathcal{E}$  This means that  $\bar{T} = 0$ .

(4) Let  $\mu_1, \mu_2, \dots, \mu_n \in \mathcal{E}$ , then

$$\begin{aligned} \|\bar{T}\| &= \sup \left\{ \frac{\|\bar{T}(\mu_1, \mu_2, \dots, \mu_n)\|_\Gamma}{\varphi_n(\mu_1, \mu_2, \dots, \mu_n)} : \varphi_n(\mu_1, \mu_2, \dots, \mu_n) \neq 0 \right\} \\ \|\bar{T}\| &= |\alpha| \sup \left\{ \frac{\|\bar{T}(\mu_1, \mu_2, \dots, \mu_n)\|_\Gamma}{\varphi_n(\mu_1, \mu_2, \dots, \mu_n)} : \varphi_n(\mu_1, \mu_2, \dots, \mu_n) \neq 0 \right\} \\ &= |\alpha| \|\bar{T}\|. \end{aligned}$$

(5) Take  $\mu_1, \mu_2, \dots, \mu_n \in \mathcal{E}$ , then

$$\begin{aligned} \|\bar{T} + \bar{S}\| &= \sup \left\{ \frac{\|(\bar{T} + \bar{S})(\mu_1, \mu_2, \dots, \mu_n)\|_\Gamma}{\varphi_n(\mu_1, \mu_2, \dots, \mu_n)} : \varphi_n(\mu_1, \mu_2, \dots, \mu_n) \neq 0 \right\} \\ &\leq \sup \left\{ \frac{\|\bar{T}(\mu_1, \mu_2, \dots, \mu_n)\|_\Gamma}{\varphi_n(\mu_1, \mu_2, \dots, \mu_n)} : \varphi_n(\mu_1, \mu_2, \dots, \mu_n) \neq 0 \right\} \\ &\quad + \sup \left\{ \frac{\|\bar{S}(\mu_1, \mu_2, \dots, \mu_n)\|_\Gamma}{\varphi_n(\mu_1, \mu_2, \dots, \mu_n)} : \varphi_n(\mu_1, \mu_2, \dots, \mu_n) \neq 0 \right\} \\ &= \|\bar{T}\| + \|\bar{S}\|. \end{aligned}$$



Therefore,  $BO_{mod_n}(\mathcal{E}_{\varphi_n}^n, \Gamma)$  is a normed space.

To prove that  $BO_{mod_n}(\mathcal{E}_{\varphi_n}^n, \Gamma)$  is a Banach space, suppose that  $(\Gamma, \|\cdot\|_\Gamma)$  is complete normed space and let  $\{\bar{T}_k\}_{k=1}^\infty$  be a Cauchy sequence in  $BO_{mod_n}(\mathcal{E}_{\varphi_n}^n, \Gamma)$  then  $\|\bar{T}_n - \bar{T}_m\| \rightarrow 0$  as  $n, m \rightarrow \infty$ . But for each  $n, m \in N$ , Equation (1) gives:

$$\|(\bar{T}_n - \bar{T}_m)(\mu_1, \mu_2, \dots, \mu_n)\|_\Gamma \leq \|\bar{T}_n - \bar{T}_m\| \varphi_n(\mu_1, \mu_2, \dots, \mu_n), \text{ for any } \mu_1, \mu_2, \dots, \mu_n \in \mathcal{E}.$$

Hence,  $\{\bar{T}_k(\mu)\}_{k=1}^\infty$  is a Cauchy sequence in  $\Gamma$  for every  $\mu = (\mu_1, \mu_2, \dots, \mu_n) \in \mathcal{E}^n$ . That is there exists  $\eta_\mu \in \Gamma$ , such that  $\bar{T}_k(\mu) \rightarrow \eta_\mu$  as  $k \rightarrow \infty$ , for each  $\mu = (\mu_1, \mu_2, \dots, \mu_n) \in \mathcal{E}^n$ .

**From now, and for more convenient we will use  $\mu \in \mathcal{E}^n$  instead of  $\mu_1, \mu_2, \dots, \mu_n \in \mathcal{E}$ .**

Define  $\bar{T}_0: \mathcal{E}_{\varphi_n}^n \rightarrow \Gamma$  as follows  $\bar{T}_0(\mu) = \eta_\mu$  for all  $\mu \in \mathcal{E}^n$  we will show that  $\bar{T}_0 \in BO_{mod_n}(\mathcal{E}_{\varphi_n}^n, \Gamma)$ .

- For the linearity of  $\bar{T}_0$ . Take  $\mu = (\mu_1, \mu_2, \dots, \mu_n)$ ,  $\xi = (\xi_1, \xi_2, \dots, \xi_n) \in \mathcal{E}^n$  and  $\alpha$  is a scalar, then

$$\bar{T}_0(\mu + \xi) = \eta_{(\mu+\xi)} = \bar{T}_k(\mu + \xi) = \bar{T}_k(\mu) + \bar{T}_k(\xi) = \eta_\mu + \eta_\xi = \bar{T}_0(\mu) + \bar{T}_0(\xi),$$

and

$$\bar{T}_0(\alpha\mu) = \eta_{(\alpha\mu)} = \bar{T}_k(\alpha\mu) = \bar{T}_k(\mu) = \alpha\eta_\mu = \alpha\bar{T}_0(\mu).$$

This confirms that  $\bar{T}_0$  is linear.

- For the boundedness of  $\bar{T}_0$ . Let  $\mu = (\mu_1, \mu_2, \dots, \mu_n) \in \mathcal{E}^n$  and for each  $k$  we have

$$\|\bar{T}_k(\mu)\|_\Gamma \leq \|\bar{T}_k\| \varphi_n(\mu),$$

and since  $\{\bar{T}_k\}_{k=1}^\infty$  is a Cauchy sequence in  $BO_{mod_n}(\mathcal{E}_{\varphi_n}^n, \Gamma)$  then it is bounded. That is there exists  $M > 0$  such that

$$\|\bar{T}_k\| \leq M \text{ for all } k,$$

so

$$\|\bar{T}_k(\mu)\|_\Gamma \leq M \varphi_n(\mu),$$

thus

$$\|\bar{T}_0(\mu)\|_\Gamma \leq \|\bar{T}_0(\mu) - \bar{T}_k(\mu)\|_\Gamma + \|\bar{T}_k(\mu)\|_\Gamma \leq \|\bar{T}_0(\mu) - \bar{T}_k(\mu)\|_\Gamma + M \varphi_n(\mu),$$

as  $k \rightarrow \infty$  we get,

$$\|\bar{T}_0(\mu)\|_\Gamma \leq M \varphi_n(\mu),$$

this shows that  $\bar{T}_0$  is bounded and therefore,  $\bar{T}_0 \in BO_{mod_n}(\mathcal{E}_{\varphi_n}^n, \Gamma)$ .

The following steps are shown that  $\bar{T}_k$  converges to  $\bar{T}_0$  in  $BO_{mod_n}(\mathcal{E}_{\varphi_n}^n, \Gamma)$ .

Let  $\varepsilon > 0$ , then there exists  $N \in \mathbb{N}$  such that

$$\|\bar{T}_n - \bar{T}_m\| < \varepsilon \quad \text{for all } n, m > N \quad (\{\bar{T}_k\}_{k=1}^{\infty} \text{ is a Cauchy sequence}).$$

Therefore for any  $\mu = (\mu_1, \mu_2, \dots, \mu_n) \in \mathcal{E}^n$ ,

$$\|\bar{T}_n(\mu) - \bar{T}_m(\mu)\|_{\Gamma} < \varepsilon \varphi_n, \quad \text{for all } n, m > N.$$

Now, as  $m \rightarrow \infty$ ,

$$\|\bar{T}_n(\mu) - \bar{T}_0(\mu)\|_{\Gamma} < \varepsilon \varphi_n, \quad \text{for all } n, m > N.$$

Hence,

$$\|\bar{T}_n - \bar{T}_0\| = \sup \left\{ \frac{\|(\bar{T}_n - \bar{T}_0)(\mu_1, \mu_2, \dots, \mu_n)\|_{\Gamma}}{\varphi_n(\mu_1, \mu_2, \dots, \mu_n)} : \varphi_n(\mu_1, \mu_2, \dots, \mu_n) \neq 0 \right\} < \varepsilon \quad \text{for all } n > N.$$

This confirms that  $\bar{T}_k \rightarrow \bar{T}_0$  as  $k \rightarrow \infty$ .

The next two corollary follows immediately from the previous theorem.

### 1.1. Corollary

*Hypothesize that  $(\mathcal{E}^n, \varphi_n)$  is  $n$ -modular space and  $(\Gamma, \|\cdot\|_{\Gamma})$  is a normed space. Then the vector*

*Space of all  $n$ -modular bounded linear operators on  $\mathcal{E}^n$ ,*

$$BO_{mod_n}(\mathcal{E}_{\varphi_n}^n, \Gamma) = \{\bar{T}: \mathcal{E}_{\varphi_n}^n \rightarrow \Gamma, \bar{T} \text{ is } n\text{-modular bounded linear operator}\}$$

*is modular space with the following modular function:*

$$\psi(\bar{T}) = \sup \left\{ \frac{\|\bar{T}(\mu_1, \mu_2, \dots, \mu_n)\|_{\Gamma}}{\varphi_n(\mu_1, \mu_2, \dots, \mu_n)} : \varphi_n(\mu_1, \mu_2, \dots, \mu_n) \neq 0 \right\},$$

*where,  $\mu = (\mu_1, \mu_2, \dots, \mu_n) \in \mathcal{E}^n$ .*

### Corollary

*Hypothesize that  $(\mathcal{E}^n, \varphi_n)$  is  $n$ -modular space and  $K$  is the field of complex or real numbers.*

*Then*

*the vectors spaces of all  $n$ -modular bounded functional on  $\mathcal{E}^n$ ,*



$$BF_{mod_n}(\mathcal{E}_{\varphi_n}^n, K) = \{\bar{F}: \mathcal{E}_{\varphi_n}^n \rightarrow K, \bar{F} \text{ is } n\text{-modular bounded linear functional}\}$$

is a Banach space with the following norm:

$$\|\bar{F}\| = \sup \left\{ \frac{|\bar{F}(\mu_1, \mu_2, \dots, \mu_n)|}{\varphi_n(\mu_1, \mu_2, \dots, \mu_n)} : \varphi_n(\mu_1, \mu_2, \dots, \mu_n) \neq 0 \right\},$$

where,  $\mu = (\mu_1, \mu_2, \dots, \mu_n) \in \mathcal{E}^n$ .

The next interesting result considers that the n-modular bounded linear operator between two modular spaces.

**Theorem**

Let  $(\mathcal{E}^n, \varphi_n)$  be an n-modular space and  $(\Gamma, \psi)$  be a modular space. Then the set of all n-modular bounded linear operators on  $\mathcal{E}^n$ ,

$$B_{mod_n}(\mathcal{E}_{\varphi_n}^n, \Gamma_{\psi}) = \{\mathcal{T}: \mathcal{E}_{\varphi_n}^n \rightarrow \Gamma_{\psi}, \mathcal{T} \text{ is } n\text{-modular bounded linear operator}\}$$

is a vector space. Furthermore, this space is modular space with the following modular function:

$$\theta(\mathcal{T}) = \sup \left\{ \frac{\psi(\mathcal{T}(\mu))}{\varphi_n(\mu)} : \mu \in \mathcal{E}^n \text{ with } \varphi_n(\mu) \neq 0 \right\}, \tag{2}$$

where,  $\mu = (\mu_1, \mu_2, \dots, \mu_n)$  and  $\mu_1, \mu_2, \dots, \mu_n \in \mathcal{E}$  are linearly independent

*Proof.*

(1) It is clear that  $\theta(\mathcal{T}) = 0$  if and only if  $\mathcal{T} = 0$ .

(2) For  $\mathcal{T} \in B_{mod_n}(\mathcal{E}_{\varphi_n}^n, \Gamma_{\psi})$ , it is obvious that  $\theta(-\mathcal{T}) = \theta(\mathcal{T})$ .

(3) Let  $\mathcal{T}, \mathcal{S} \in B_{mod_n}(\mathcal{E}_{\varphi_n}^n, \Gamma_{\psi})$  and  $\check{\alpha}, \check{b} \geq 0$  with  $\check{\alpha} + \check{b} = 1$ , then

$$\begin{aligned} \theta(\check{\alpha}\mathcal{T} + \check{b}\mathcal{S}) &= \sup \left\{ \frac{\psi((\check{\alpha}\mathcal{T} + \check{b}\mathcal{S})(\mu))}{\varphi_n(\mu)} : \mu \in \mathcal{E}^n \text{ with } \varphi_n(\mu) \neq 0 \right\} \\ &= \sup \left\{ \frac{\psi(\check{\alpha}\mathcal{T}(\mu) + \check{b}\mathcal{S}(\mu))}{\varphi_n(\mu)} : \mu \in \mathcal{E}^n \text{ with } \varphi_n(\mu) \neq 0 \right\}, \end{aligned}$$

since  $\psi$  is modular, then

$$\begin{aligned} \theta(\check{\mathcal{T}} + \check{\mathcal{S}}) &= \sup \left\{ \frac{\psi(\mathcal{T}(\mu))}{\varphi_n(\mu)} : \mu \in \mathcal{E}^n \text{ with } \varphi_n(\mu) \neq 0 \right\} \\ &+ \sup \left\{ \frac{\psi(\mathcal{S}(\mu))}{\varphi_n(\mu)} : \mu \in \mathcal{E}^n \text{ with } \varphi_n(\mu) \neq 0 \right\}. \end{aligned}$$

Hence,

$$\theta(\check{\mathcal{T}} + \check{\mathcal{S}}) = \theta(\mathcal{T}) + \theta(\mathcal{S})$$

### Lipschitz Functions on n-modular space

This section is dedicated to study the properties of the set of all Lipschitz functions that are defined on  $n$ -modular space. We begin with the following definition:

#### Definition

Hypothesize that  $(\mathcal{E}^n, \varphi_n)$  is  $n$ -modular space and  $(\Gamma, \|\cdot\|_\Gamma)$  is a normed space. A function  $\bar{F}_{Lip}: \mathcal{E}^n \rightarrow \Gamma$

is called  $n$ -modular Lipschitz function if there exists a constant  $M_L > \mathbf{0}$  such that

$$\|\bar{F}_{Lip}(\mu) - \bar{F}_{Lip}(\xi)\|_\Gamma \leq M_L \varphi_n(\mu - \xi),$$

for each  $\mu, \xi \in \mathcal{E}^n$ . Furthermore, we suppose that there exists a fixed point  $\mathbf{a}_\mu \in \mathcal{E}^n$  such that  $\bar{F}_{Lip}(\mathbf{a}_\mu) = \mathbf{0}$ .

The set of all  $n$ -modular Lipschitz functions on  $\mathcal{E}^n$ , will denoted by

$$LF_{mod_n}(\mathcal{E}_{\varphi_n}^n, \Gamma) = \{\bar{F}_{Lip}: \mathcal{E}_{\varphi_n}^n \rightarrow \Gamma, \bar{F}_{Lip} \text{ is } n\text{-modular Lipschitz function}\}.$$

It is not difficult to prove the following result.

#### Lemma

For the  $n$ -modular space  $(\mathcal{E}^n, \varphi_n)$  and the normed space  $(\Gamma, \|\cdot\|_\Gamma)$ , the set

$$LF_{mod_n}(\mathcal{E}_{\varphi_n}^n, \Gamma) = \{\bar{F}_{Lip}: \mathcal{E}_{\varphi_n}^n \rightarrow \Gamma, \bar{F}_{Lip} \text{ is } n\text{-modular Lipschitz function}\}.$$

is a vector space.

The result below shows that  $LF_{mod_n}(\mathcal{E}_{\varphi_n}^n, \Gamma)$  is a Banach space.



**Theorem**

Hypothesize that  $(\mathcal{E}^n, \varphi_n)$  is  $n$ -modular space and  $(\Gamma, \|\cdot\|_\Gamma)$  is a normed space. Then the vector space

$LF_{mod_n}(\mathcal{E}_{\varphi_n}^n, \Gamma)$  is a normed space with the norm defined by:

$$\|\bar{F}_{Lip}\| = \sup \left\{ \frac{\|\bar{F}_{Lip}(\mu) - \bar{F}_{Lip}(\xi)\|_\Gamma}{\varphi_n(\mu - \xi)} : \mu, \xi \in \mathcal{E}^n, \text{ with } \mu \neq \xi \right\} \quad (3)$$

Moreover, if  $(\Gamma, \|\cdot\|_\Gamma)$  is complete, then  $LF_{mod_n}(\mathcal{E}_{\varphi_n}^n, \Gamma)$  is Banach space.

*Proof.*

(1) It is obvious that  $\|\cdot\|$  is well defined and for any  $\bar{F}_{Lip} \in LF_{mod_n}(\mathcal{E}_{\varphi_n}^n, \Gamma)$ ,  $\|\bar{F}_{Lip}\| \geq 0$ .

(2) If  $\bar{F}_{Lip} = 0$  then it is clear that  $\|\bar{F}_{Lip}\| = 0$ . Conversely, if  $\|\bar{F}_{Lip}\| = 0$ ,  $\|\bar{F}_{Lip}(\mu) - \bar{F}_{Lip}(\xi)\|_\Gamma = 0$ . This

implies that  $\bar{F}_{Lip}(\mu) = \bar{F}_{Lip}(\xi)$  with  $\mu \neq \xi$ , then if we put  $\xi = a_\mu$ , we get  $\bar{F}_{Lip}(\mu) = \bar{F}_{Lip}(a_\mu) = 0$  for

$\mu \neq a_\mu$ . In case  $\mu = a_\mu$ , then  $\bar{F}_{Lip}(a_\mu) = 0$ . Therefore,  $\bar{F}_{Lip}(\mu) = 0$  for any  $\mu \in \mathcal{E}^n$ .

(3) Let  $\bar{F}_{Lip} \in LF_{mod_n}(\mathcal{E}_{\varphi_n}^n, \Gamma)$  and  $\alpha$  be a scalar, then

$$\begin{aligned} \|\alpha \bar{F}_{Lip}\| &= \sup \left\{ \frac{\|(\alpha \bar{F}_{Lip})(\mu) - (\alpha \bar{F}_{Lip})(\xi)\|_\Gamma}{\varphi_n(\mu - \xi)} : \mu, \xi \in \mathcal{E}^n, \text{ with } (\mu - \xi) \neq 0 \right\} \\ &= |\alpha| \sup \left\{ \frac{\|\bar{F}_{Lip}(\mu) - \bar{F}_{Lip}(\xi)\|_\Gamma}{\varphi_n(\mu - \xi)} : \mu, \xi \in \mathcal{E}^n, \text{ with } (\mu - \xi) \neq 0 \right\} \\ &= |\alpha| \|\bar{F}_{Lip}\|. \end{aligned}$$

(4) Let  $\bar{F}_{Lip}, \bar{G}_{Lip} \in LF_{mod_n}(\mathcal{E}_{\varphi_n}^n, \Gamma)$ , then

$$\begin{aligned} \|\bar{F}_{Lip} + \bar{G}_{Lip}\| &= \sup \left\{ \frac{\|(\bar{F}_{Lip} + \bar{G}_{Lip})(\mu) - (\bar{F}_{Lip} + \bar{G}_{Lip})(\xi)\|_\Gamma}{\varphi_n(\mu - \xi)} : \mu, \xi \in \mathcal{E}^n, \text{ with } (\mu - \xi) \neq 0 \right\} \\ &\leq \sup \left\{ \frac{\|\bar{F}_{Lip}(\mu) - \bar{F}_{Lip}(\xi)\|_\Gamma}{\varphi_n(\mu - \xi)} : \mu, \xi \in \mathcal{E}^n, \text{ with } (\mu - \xi) \neq 0 \right\} \end{aligned}$$

$$+ \sup \left\{ \frac{\|\bar{G}_{Lip}(\mu) - \bar{G}_{Lip}(\xi)\|_{\Gamma}}{\varphi_n(\mu - \xi)} : \mu, \xi \in \mathcal{E}^n, \text{ with } (\mu - \xi) \neq 0 \right\}$$

$$= \|\bar{F}_{Lip}\| + \|\bar{G}_{Lip}\|.$$

Therefore, we infer that  $LF_{mod_n}(\mathcal{E}_{\varphi_n}^n, \Gamma)$  is a normed space.

To prove  $LF_{mod_n}(\mathcal{E}_{\varphi_n}^n, \Gamma)$  is a Banach space, suppose that  $\Gamma$  is complete normed space and let  $\{\bar{F}_{Lip_k}\}_{k=1}^{\infty}$  be a Cauchy sequence in  $LF_{mod_n}(\mathcal{E}_{\varphi_n}^n, \Gamma)$ , then

$$\|\bar{F}_{Lip_n} - \bar{F}_{Lip_m}\| \rightarrow 0 \text{ as } n, m \rightarrow \infty.$$

Now for every  $\mu \in \mathcal{E}^n$ ,

$$\|(\bar{F}_{Lip_n} - \bar{F}_{Lip_m})(\mu)\|_{\Gamma} = \|(\bar{F}_{Lip_n} - \bar{F}_{Lip_m})(\mu) - (\bar{F}_{Lip_n} - \bar{F}_{Lip_m})(a_{\mu})\|_{\Gamma}$$

and from Equation (3) we get

$$\|(\bar{F}_{Lip_n} - \bar{F}_{Lip_m})(\mu)\|_{\Gamma} \leq \|\bar{F}_{Lip_n} - \bar{F}_{Lip_m}\| \varphi_n(\mu - a_{\mu}),$$

hence,  $\|(\bar{F}_{Lip_n} - \bar{F}_{Lip_m})(\mu)\|_{\Gamma} \rightarrow 0$  as  $n, m \rightarrow \infty$ , where  $\mu \neq a_{\mu}$ .

If  $\mu = a_{\mu}$ , then  $\|(\bar{F}_{Lip_n} - \bar{F}_{Lip_m})(\mu)\|_{\Gamma} = 0$ . Thus  $\{\bar{F}_{Lip_k}(\mu)\}_{k=1}^{\infty}$  is a Cauchy sequence in  $\Gamma$ .

Since  $\Gamma$

is complete, then there exists  $\zeta_{\mu} \in \Gamma$ , such that  $\bar{F}_{Lip_k}(\mu) \rightarrow \zeta_{\mu}$  as  $k \rightarrow \infty$ , for all  $\mu \in \mathcal{E}^n$ .

Moreover,

$$\bar{F}_{Lip_k}(a_{\mu}) \rightarrow 0 \text{ as } k \rightarrow \infty, \text{ so } \zeta_{a_{\mu}} = 0.$$

Define  $\bar{F}_{Lip_0}: \mathcal{E}_{\varphi_n}^n \rightarrow \Gamma$  as follows,  $\bar{F}_{Lip_0}(\mu) = \zeta_{\mu}$  for all  $\mu \in \mathcal{E}^n$ . It obvious that  $\bar{F}_{Lip_0}(a_{\mu}) = 0$ .

We will show that  $\bar{F}_{Lip_0} \in LF_{mod_n}(\mathcal{E}_{\varphi_n}^n, \Gamma)$ :

For any  $\mu, \xi \in \mathcal{E}^n$  and for each  $k$  we have

$$\|\bar{F}_{Lip_k}(\mu) - \bar{F}_{Lip_k}(\xi)\|_{\Gamma} \leq \|\bar{F}_{Lip_k}\| \varphi_n(\mu - \xi),$$

and since  $\{\bar{F}_{Lip_k}\}_{k=1}^{\infty}$  is a Cauchy sequence in  $LF_{mod_n}(\mathcal{E}_{\varphi_n}^n, \Gamma)$  then it is bounded. That is there exists  $M_L > 0$  such that  $\|\bar{F}_{Lip_k}\| \leq M_L$  for all  $k$ , so



$$\|\bar{F}_{Lip_k}(\mu) - \bar{F}_{Lip_k}(\xi)\|_{\Gamma} \leq M_L \varphi_n(\mu - \xi),$$

and as  $k \rightarrow \infty$  we get,

$$\|\bar{F}_{Lip_0}(\mu) - \bar{F}_{Lip_0}(\xi)\|_{\Gamma} \leq M_L \varphi_n(\mu - \xi),$$

this shows that  $\bar{F}_{Lip_0} \in LF_{mod_n}(\mathcal{E}_{\varphi_n}^n, \Gamma)$ .

The following steps are shown that  $\bar{F}_{Lip_k}$  converges to  $\bar{F}_{Lip_0}$  in the space  $LF_{mod_n}(\mathcal{E}_{\varphi_n}^n, \Gamma)$ .

Let  $\varepsilon > 0$ , then there exists  $N \in \mathbb{N}$  such that

$$\|\bar{F}_{Lip_n} - \bar{F}_{Lip_m}\| < \varepsilon \quad \text{for all } n, m > N \quad (\{\bar{F}_{Lip_k}\}_{k=1}^{\infty} \text{ is a Cauchy sequence})$$

therefore for any  $\mu \in \mathcal{E}^n$

$$\|(\bar{F}_{Lip_n} - \bar{F}_{Lip_m})(\mu) - (\bar{F}_{Lip_n} - \bar{F}_{Lip_m})(\xi)\|_{\Gamma} < \varepsilon \varphi_n(\mu - \xi) \quad \text{for all } n, m > N.$$

Now, as  $m \rightarrow \infty$

$$\|(\bar{F}_{Lip_n} - \bar{F}_{Lip_0})(\mu) - (\bar{F}_{Lip_n} - \bar{F}_{Lip_0})(\xi)\|_{\Gamma} < \varepsilon \varphi_n(\mu - \xi) \quad \text{for all } n > N,$$

Hence,

$$\|\bar{F}_{Lip_n} - \bar{F}_{Lip_0}\| = \sup \left\{ \frac{\|(\bar{F}_{Lip_n} - \bar{F}_{Lip_0})(\mu) - (\bar{F}_{Lip_n} - \bar{F}_{Lip_0})(\xi)\|_{\Gamma}}{\varphi_n(\mu - \xi)} : \mu, \xi \in \mathcal{E}^n, \text{ with } \mu \neq \xi \right\}$$

$$< \varepsilon \quad \text{for all } n > N.$$

This confirm that  $\bar{F}_{Lip_n} \rightarrow \bar{F}_{Lip_0}$  as  $n \rightarrow \infty$  in  $LF_{mod_n}(\mathcal{E}_{\varphi_n}^n, \Gamma)$ .

Consider the following corollary which can easily deduce from the previous theorem.

**Corollary**

*Hypothesize that that  $(\mathcal{E}^n, \varphi_n)$  is  $n$ -modular space and  $(\Gamma, \|\cdot\|_{\Gamma})$  is a normed space. Then the set of all  $n$ -modular Lipschitz functions on  $\mathcal{E}^n$ ,*

$$LF_{mod_n}(\mathcal{E}_{\varphi_n}^n, \Gamma) = \{\bar{F}_{Lip}: \mathcal{E}_{\varphi_n}^n \rightarrow \Gamma, \bar{F}_{Lip} \text{ is } n\text{-modular Lipschitz function}\}$$

is a modular space with the following modular function

$$\psi_L(\bar{F}_{Lip}) = \sup \left\{ \frac{\|\bar{F}_{Lip}(\mu) - \bar{F}_{Lip}(\xi)\|_{\Gamma}}{\varphi_n(\mu - \xi)} : \mu, \xi \in \mathcal{E}^n, \text{ with } \mu \neq \xi \right\}.$$

## Bibliography

- HANA Abobaker and Raymond A Ryan. Modular metric spaces. *arXiv preprint arXiv:2203.12359*, 2022.
- Supama Burhanudin Arif Nurnugroho and Atok Zulijanto. 2-linear operators on 2-modular spaces. *Far East Journal of Mathematical Sciences (FJMS)*, 102(12), 2017.
- Somaye Grailoo, Abasalt Bodaghi, and Abolfazl Niazi Motlagh. Some results in metric modular spaces. *International Journal of Nonlinear Analysis and Applications*, 13(2):983–988, 2022.
- H Hudzik, J Musielak, and R Urban´ski. Linear operators in modular spaces. *Commentationes Mathematicae*, 23(1), 1983.
- Maria A Jap´on. Some geometric properties in modular spaces and application to fixed point theory. *Journal of mathematical analysis and applications*, 295(2):576–594, 2004.
- Mohamed A Khamsi and Wojciech M Kozłowski. *Fixed point theory in modular function spaces*. Birkh´auser, 2015.
- WM Kozłowski. Notes on modular function spaces. ii. *Commentationes Mathematicae*, 28(1), 1988.
- Julian Musielak. *Orlicz spaces and modular spaces*, volume 1034. Springer, 2006.
- Hidegorō Nakano. *Modulated semi-ordered linear spaces*. Maruzen Company, 1950.
- Kourosh Nourouzi and Samira Shabanian. Operators defined on n-modular spaces. *Mediterranean Journal of Mathematics*, 6(431), 2009.
- Tayebe Lal Shateri. New generalizations of modular spaces. *Hacettepe Journal of Mathematics and Statistics*, 49(3):1076–1083, 2020.
- Supama. On fixed point theorems in modular spaces characterized by  $c^*$ -class functions. *Hilbert Journal of Mathematical Analysis*, 1(1):14–21, 2022.



# Dispersion Characterization of Poly (Vinyl Al Cohol) Doped with Iron Citrate Films

Wasan A.Al-Taa'y <sup>1</sup>

Mohammed Ali H.Al-Beayaty <sup>2</sup>

Zainab A. Al-Taie <sup>3</sup>



© 2024 The Author(s). This open access article is distributed under a Creative Commons Attribution (CC-BY) 4.0 license.


## Abstract


*In this article, the optical characteristics as well as the dispersion parameter of pure and doped poly (vinyl alcohol) (PVA) with iron citrate (Fe) films have been studied. The deposited films were attained through casting approach considering a variety of concentrations (0, 0.5, 1.5, 2 and 2.5) wt%. In detail, absorbance, transmittance, reflectance, skin depth, single-oscillator energy, static refractive index, dispersion energy, average oscillator position, high frequency dielectric constant, moments of the imaginary part, and average oscillator strength of the optical spectrum were investigated within the spectrum range (200-800) nm. All outcomes of these parameters showed a clear change where the absorbance and reflectance spectrums increase after adding of Fe to PVA but the transmittance and skin depth decrease. Single-oscillator energy, moments of the imaginary part, static refractive index, dispersion energy, high frequency average oscillator strength, dielectric constant of the optical spectrum appeared to increase for all samples after adding of Fe to PVA but average oscillator position showed opposite behavior.*

**Key words:** PVA; Fe Citrate; Dispersion Properties.

---

 <http://dx.doi.org/10.47832/MinarCongress12-04>

<sup>1</sup>  Department of Physics, College of science, AL-Nahrain University, Jadriya, Baghdad, Iraq  
[wassan.ali.mousa@nahrainuniv.edu.iq](mailto:wassan.ali.mousa@nahrainuniv.edu.iq)

<sup>2</sup>  College of energy and environmental sciences, Al-karkh University of science, Baghdad, Iraq,  
[albeaty33@kus.edu.iq](mailto:albeaty33@kus.edu.iq)

## Introduction

There is a renewed support in the properties of modified polymer/s, wherein the optical properties are of crucial importance for uses in new technology as well as for academic knowledge [1-3]. Polymer matrix composites are of tremendous interest since they play an important part in many facets of our daily lives. Their abundance, inexpensive, and flexibility are some of their appealing qualities. Most polymers are thought to be non-toxic, they could easily serve as host matrices for various fillers [4, 5]. Mineral particles (metallic powder, glass fibers, carbon black, etc.) are frequently employed as fillers. Recently, a novel class of polymers called "nanocomposites" that contain nanoparticles was created [6, 7]. Previous research has shown the viability of using synthetic polymer-based materials in electrical and optical systems [4, 8]. Implanting fillers in small quantities to fit desired applications can improve the optical, electrical, and physical features of polymers. Further, capacitors, sensors, solar cells, and other optical devices are some of these uses [4, 9-11]. PVA polymer was utilized in this study because of its exceptional qualities, including stability, solubility, reactivity, and affordability. It also delivers outstanding biological features such as including tasteless, odorless, biodegradability, and nontoxicity.

A range of metals and organometals may interact well with PVA due to its linear synthetic and/or semi-crystalline polymer composition as well as the interactions within its functional group [12]. To change the properties of the final film blend, polymer blending along different metal and/or metal oxide could be a useful technique. Combining conductive materials with a desired polymer, PVA in particular, the targeted applications can be expanded [13]. T.S. Soliman et al, demonstrated a systematic work through which the properties of PVA were enhanced via solution cast method with iron (Fe) nanoparticles; in detail, the optical profile of the attained nano-composite was compared to that obtained in pure PVA [14]. Another study conducted by Qayssar M. Jebur et al revealed that using iron oxide nanoparticles (2, 4, and 6 wt%) within PVA matrix along with polyethylene oxide, and polyethylene (PVA-PEO-Fe<sub>2</sub>O<sub>3</sub>) can significantly enhance the optical, electrical, dielectric characteristics of pure PVA [15]. Herein, the present work demonstrates a comprehensive analysis concerning the optical and dispersion parameters of pure and iron citrate doped PVA nanocomposite.

## Experimental

Polyvinyl alcohol films (PVA, BDH chemicals) with molecular weight of 10000 (*g/mol*) was prepared through solution mixture of PVA with different percentage of Fe ions (0.5, 1.5, 2 and 2.5) wt% under constant stirring rate of 700 rpm for 30 minutes at 80°C in distilled water



until a complete dissolvment was attained. The resultant mixture was then poured into pre-cleaned glass plate at room temperature for four days, where the obtained sheet thickness was found to be  $\sim 100 \mu\text{m}$ . Hereinafter, an in-depth optical characteristic such as absorbance, reflectance, and transmittance, was carried out via UV-Vis spectrophotometer (shimadzu UV-1601). Other optical parameters (skin depth, single- oscillator energy, average oscillator position and strength, high frequency dielectric constant, and the imaginary part of moments) were investigated within a spectral rage of 200 to 800 nm.

## Results and discussion

The optical features of the prepared samples were considered to evaluate the influence of Fe particles addition within the PVC matrix at different percentages (0.5, 2.5, 2, and 2.5); these include reflection, transmission, and absorption within the range of 200 to 800 nm, the attained results are elucidated in Figure 1. Generally, pristine PVC exhibited a decreasing trend as the wavelength increased wherein a clear cut-off phenomenon was observed at around 250 nm. Continuously, Batho-chromic (Blue) shift was acquired as the Fe particles were introduced to the PVC matrix; higher Fe percentage resulted in a significant change in the cut-off phenomenon which indicate the alteration occurred in the molecular structure of the PVC matrix such as free radicals, polymer fragments, and degradation) [16].

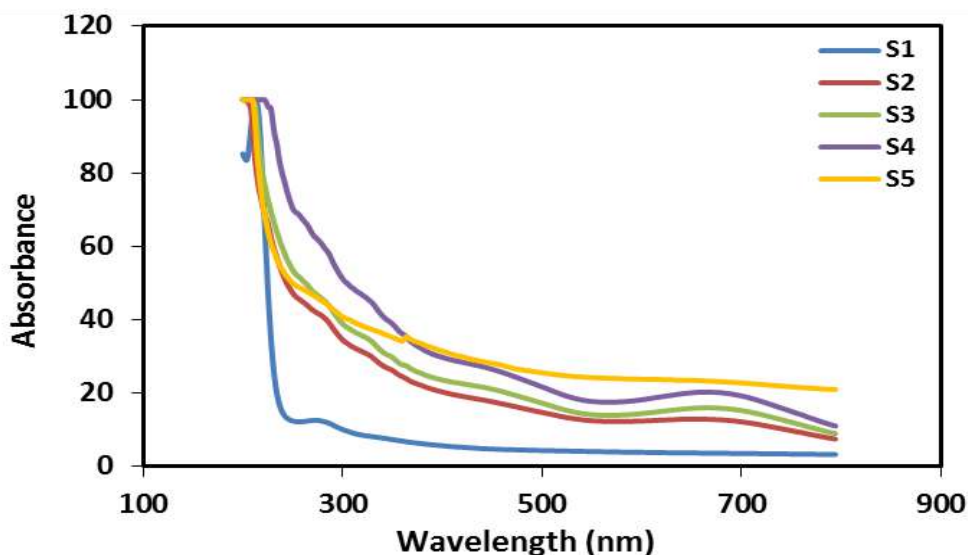
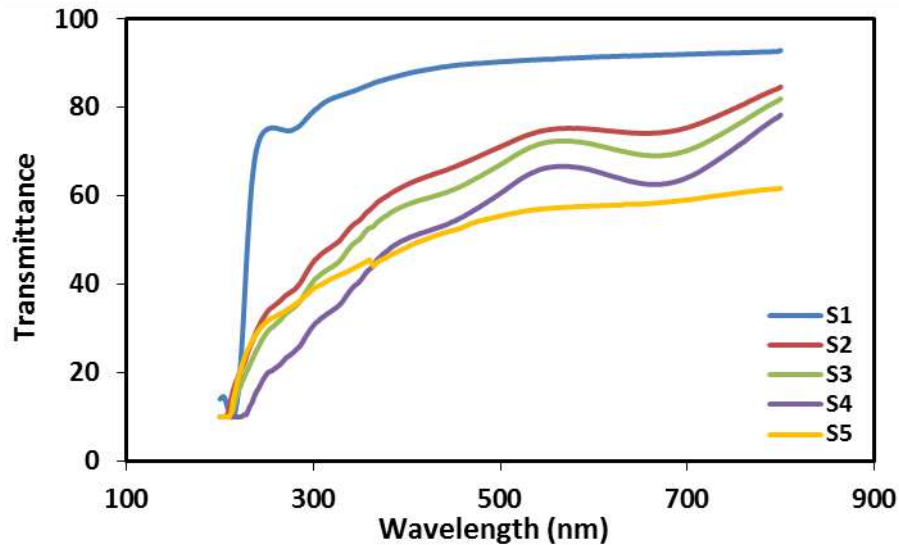


Figure 1- Absorbance variation of as a function of wavelength.

The transmittance curves of the fabricated samples (200-800 nm) are illustrated in Figure 2. In general observation, an increase in the transmission spectra can be noticed as a function of wavelengths' range. Further, PVC curve revealed a transmission of 90% at the UVA and visible range. However, as the addressed matrix was doped with Fe particles, a pronounced

decrease in the aforementioned spectra was perceived. In detail, almost  $\geq 15\%$  reduction of the transmission was attained with addition of 0.5% of Fe particles, after which the intended decreasing percentage was further augmented at higher concentration of Fe particles.



**Figure 2-** The transmittance of skin depth as a function of wavelength.

Figure 3 demonstrates the evaluated reflectance of the fabricated samples as function of wavelengths' range (200-800 nm). A gradual decrease in the reflectance spectrum of PVC was attained along the scanned wavelength. This behavior indicates the low absorption of pristine PVC sample in the visible region. After the Fe doping, the resultant film/s exhibited an increased reflectance which confirms the attained shift in the based Fe particles doping-absorption curves. New peaks were acquired at higher wavelength range for samples with higher Fe concentrations (S3, S4, and S5) due to the molecular structure alteration as stated earlier.

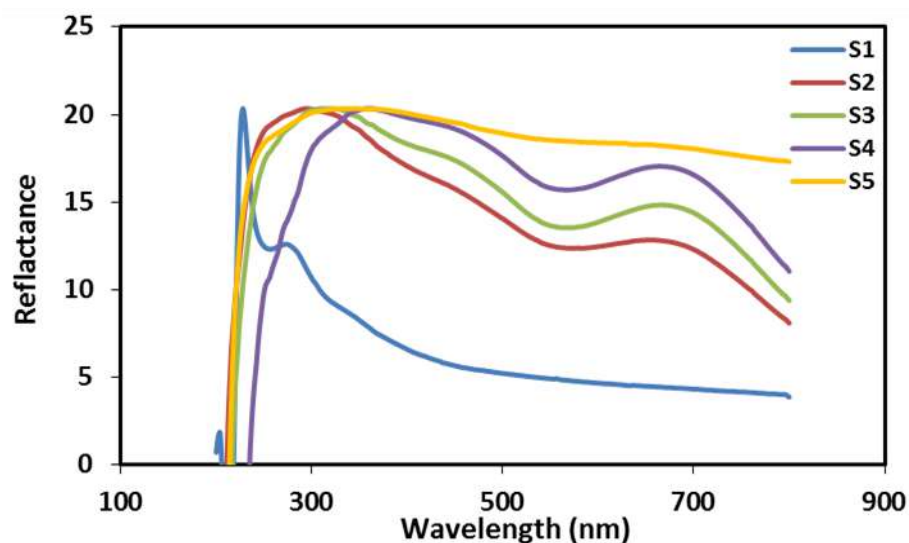


**Figure 3-** The variation of reflectance spectra of the prepared samples.



Investigations on the optical characteristics of films using optical absorbance within the UV-Vis range (200-800 nm) are conducted. Figure (4) depicts the relationship between skin depth and wavelength in all films both before and after they have been doped with Fe citrate at several ratios of metal (0, 0.5, 1.5, 2, and 2.5) wt%.

The electromagnetic wave's amplitude will decrease after crossing a thickness, and skin depth ( $\chi$ ) are computed using equation (1) [17]:

$$\chi = \frac{\lambda}{2\pi k} \dots \dots \dots (1)$$

herein,  $\lambda$  represent the wavelength, k is extinction coefficient.

From Fig (4), It can be shown that the evaluated skin depth increased as a function of wavelength, and decreases with adding of Fe citrate concentrations of all films. After doping, it is seen that all films have very poor transparency in the visible region, and that skin depth then rapidly decreases as Fe concentrations increase. This behavior may be due to the films' accuracy and stoichiometry [17].

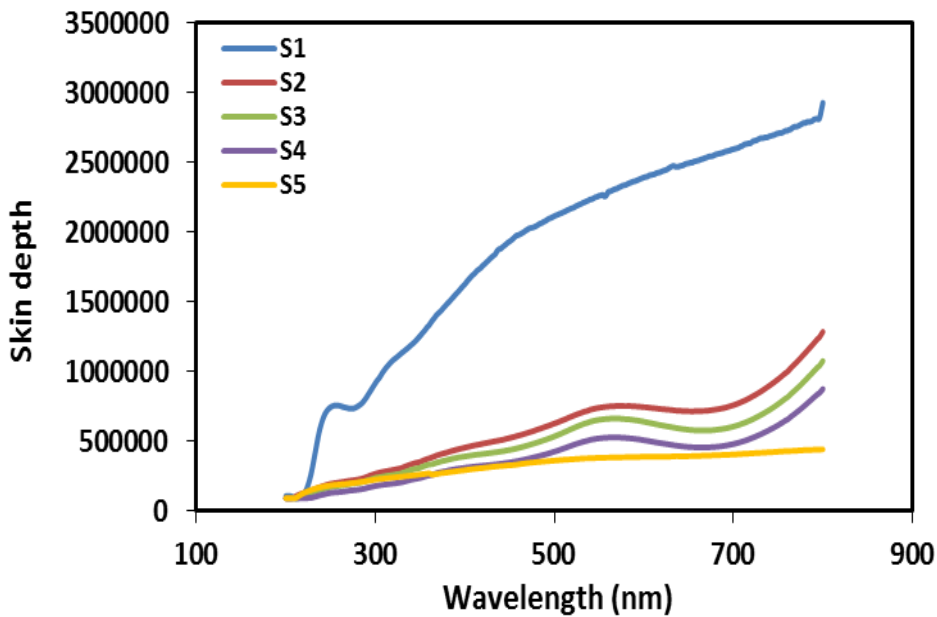


**Figure 4-** Skin depth variation as a function of the scanned wavelength's range.

The dispersion gap within the refractive index (n) of the fabricated samples was proposed by Wemple and Didomenico via single oscillator model. Herein, the occurred dispersion-based refractive index data were utilized through the following equation [18, 19].

$$n^2 - 1 = \frac{E_o E_d}{E_o^2 - (h\nu)^2} \dots \dots \dots (2)$$

herein, the single oscillator energy parameter is represented by the symbol  $E_o$ , while the dispersion energy is denoted as  $E_d$ ; the latter is considered as a measure of the interband transitions strength. The addressed parameters,  $E_o$  and  $E_d$ , could be estimated through a plot of  $E^2$  versus  $(n^2-1)^{-1}$  as presented in Figure 5. Equation (2) was employed to evaluate the static refractive index  $n(0)$ , where parameters including  $E_o$ ,  $E_d$  and  $n(0)$  are tabulated in Table (1). The stated values demonstrated an increased profile as the Fe particle concentration augmented within the PVC matrix.

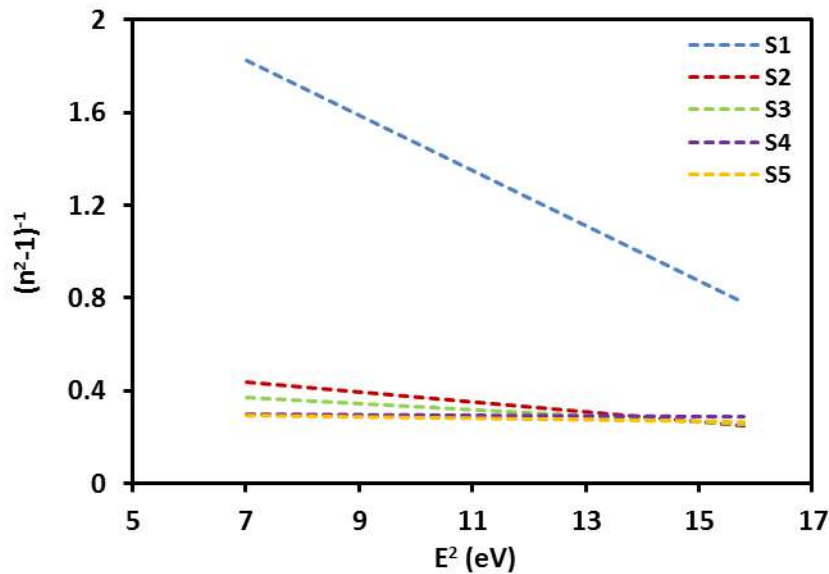


Figure 5- The variation of  $(n^2-1)^{-1}$  as function of  $E^2$ .

Table 1- PVA as well as samples S1 - S5 optical characteristics.

Sample	Wt %	$\lambda_o$ (nm)	$E_d$ (eV)	$M_{-1}$	$E_o$ (eV)	$M_{-3}$ (eV) <sup>-2</sup>	$S_o * 10^{-5}$ (m <sup>-2</sup> )	$n(0)$	$\epsilon'_{\infty}$
S1	0	262.47	1.77	0.37	4.72	0.016	0.54	1.17	<b>1.53</b>
S2	0.5	236.48	8.88	1.69	5.23	0.061	3.03	1.64	<b>3.79</b>
S3	1.5	209.92	12.73	2.15	5.90	0.061	4.89	1.77	<b>4.36</b>
S4	2	86.65	46.43	3.23	14.35	0.015	43.07	2.05	<b>5.25</b>
S5	2.5	120.73	32.51	3.17	10.25	0.030	21.76	2.04	<b>4.47</b>

The following equation is used to determine how refractive index ( $n$ ) depends on the wavelength of light [18, 20]:

$$n^2(\lambda)-1 = \frac{S_o \lambda_o^2}{1 - (\lambda_o/\lambda)^2} \dots\dots\dots(3)$$

Where  $\lambda_o$  is the average oscillator position and  $S_o$  is the average oscillator strength. The parameters  $S_o$  and  $\lambda_o$  is calculated by the draw plotting  $(n^2-1)^{-1}$  versus  $\lambda^{-2}$ , show is Fig (6). The  $S_o$ ,  $\lambda_o$  values as mentioned in Table (1) where  $S_o$  values appeared increases for all samples after adding of Fe to PVA but  $\lambda_o$  showed opposite behavior.



According to the single oscillator model, the single oscillator parameters  $E_o$  and  $E_d$  are related to the moments of the imaginary part of the optical spectrum. The  $M_{-1}$  and  $M_{-3}$  moments can be derived from the relations (4) and (5) [21, 22].  $M_{-1}$  and  $M_{-3}$  values appeared increases for all samples after adding of Fe to PVA and are given in Table (1).

$$E_o^2 = \frac{M_{-1}}{M_{-3}} \dots\dots\dots(4)$$

$$E_d^2 = \frac{M_{-1}^3}{M_{-3}} \dots\dots\dots(5)$$

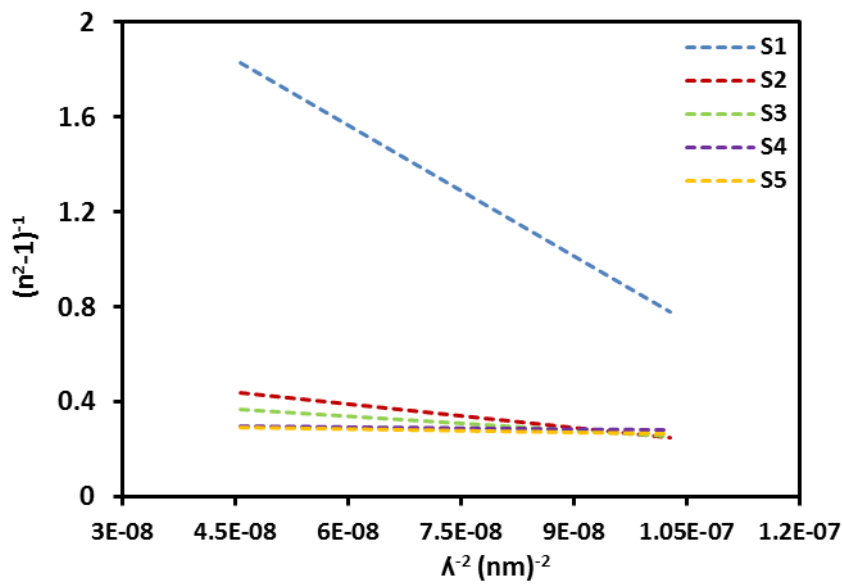


**Figure 6-** The variation of  $(n^2-1)^{-1}$  as a function of  $\lambda^{-2}$ .

The infinitely high frequency dielectric constant  $\epsilon'_{\infty}$  can be attained through refractive index data analysis. The  $\lambda^2$  versus  $\epsilon'$  curve presented in Fig (7), where the results of infinitely high frequency dielectric constant estimated from the extrapolation of these plots to  $\lambda^2 = 0$  and were tabulated in Table (1) as a function of the films compositions. The non-linear dielectric constant and refractive index were perceived to be compositionally dependent in a manner similar to amorphous materials. Average refractive index values are computed using optical constants for all scanned wavelengths. This figure demonstrates that following Fe citrate doping, the infinitely high frequency dielectric constants increase for all samples [23].

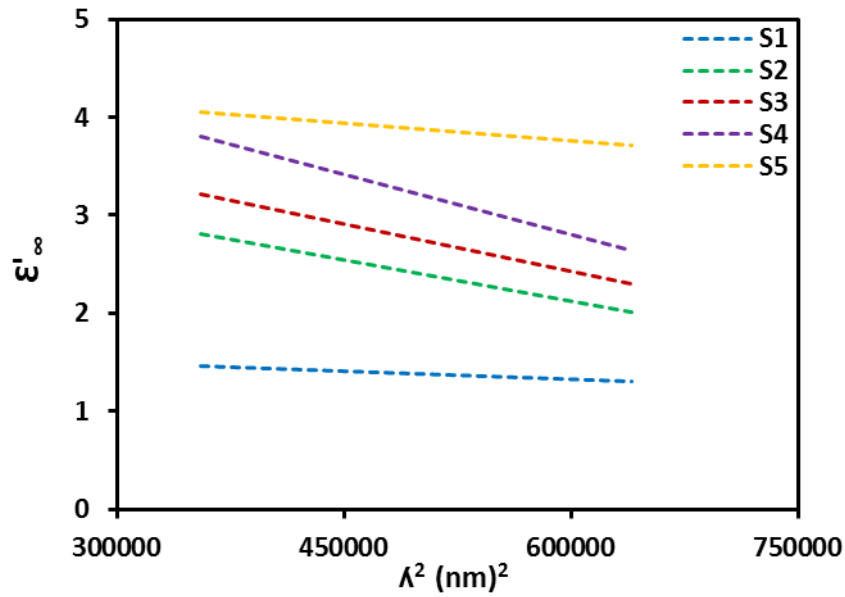


**Figure 7-** The variation of  $\epsilon'_{\infty}$  as a function of  $\lambda^2$ .

## Conclusion

The outcomes showed that Fe could efficiently dope PVA and improve its optical characteristics. While the absorption and reflection increase when Fe is present, the transmission decreases as Fe concentrations increases. Skin depth and dispersion characterization, for instance average oscillator strength, dispersion energy, single- oscillator energy, moment of the imaginary part  $M_{-1}$ , static refractive index and infinitely high frequency dielectric constant was increases after doping with Fe citrate for all concentrations. The average oscillator position showed a significant decrease with concentration while moment of the imaginary part  $M_{-3}$  it showed a fluctuation in the results between increase and decrease with the change of concentration.



## References

- Zageer, D., et al., Optical Properties and Morphological Study of New Films Derived From Poly (Vinyl Chloride)-Phenyl Phrine HCl Acid Complexes. *Al-Nahrain Journal of Science*, 2016. 19(2): p. 51-57.
- Salih, E.Y., et al., Dielectric Behaviour of Zn/Al-NO<sub>3</sub> LDHs Filled with Polyvinyl Chloride Composite at Low Microwave Frequencies. *Advances in Materials Science and Engineering*, 2014. 2014.
- Al-Taa'y, W.A., et al., Optical Properties and AFM Study of New Polymers Derived From Poly (Vinyl Chloride)-2-Acetoxy Benzoic Acid Complexes. *RESEARCH JOURNAL OF PHARMACEUTICAL BIOLOGICAL AND CHEMICAL SCIENCES*, 2016. 7(4): p. 1079-1086.
- Badawi, A., et al., Exploring the structural and optical properties of FeS filled graphene/PVA blend for environmental-friendly applications. *Journal of Polymer Research*, 2021. 28: p. 1-12.
- Al-Beayaty, M.A.H., Structural, optical and morphological characterization of Cdse/Cds Core/shell quantum dots synthesized via chemical bath. *Iraqi Journal of Science*, 2021: p. 4323-4332.
- Assekouri, A., et al., Improvement of optical, dielectric and mechanical properties of a new nanocomposite based on polyvinyl alcohol and layered double hydroxide. *Journal of Composite Materials*, 2022. 56(19): p. 3049-3061.
- Mohammed, S.A., et al., Optical properties study of new films derived from poly (vinyl chloride)-N-(4-hydroxy-phenyl)-acetamide. *RESEARCH JOURNAL OF PHARMACEUTICAL BIOLOGICAL AND CHEMICAL SCIENCES*, 2016. 7(4): p. 1064-1071.
- Al-Beayaty, M.A.H., L.K. Abbas, and R.K. Mohammed. Effect of L-cysteine capping the CdSe, CdSe: CdS on structural and morphological properties. in *AIP Conference Proceedings*. 2023. AIP Publishing.
- Abdulghani, S.O., E.Y. Salih, and A.S. Mohammed, Fabrication and photo-responsive characteristics of GeO<sub>2</sub> doped SnO<sub>2</sub>/porous Si film for ultraviolet photodetector application. *Materials Chemistry and Physics*, 2023. 303: p. 127859.
- Salih, E.Y., Characterization and performance evaluation of nanostructured rod-like CdTe/Si fast-response visible light photodetector. *Physica B: Condensed Matter*, 2024. 685: p. 416056.
- Aldaghri, O., et al., Rapid fabrication of fast response CdS/Si visible light photodetector: Influence of laser energy. *Results in Physics*, 2023. 54: p. 107112.

- Ahmed, B.Y. and S.O. Rashid, Synthesis, characterization, and application of metal-free sulfonamide-vitamin C adduct to improve the optical properties of PVA polymer. *Arabian Journal of Chemistry*, 2022. 15(10): p. 104096.
- Susilawati, S., et al., Optical Properties and Conductivity of PVA–H<sub>3</sub>PO<sub>4</sub> (Polyvinyl Alcohol–Phosphoric Acid) Film Blend Irradiated by  $\gamma$ -Rays. *Polymers*, 2021. 13(7): p. 1065.
- Soliman, T. and S. Vshivkov, Effect of Fe nanoparticles on the structure and optical properties of polyvinyl alcohol nanocomposite films. *Journal of Non-Crystalline Solids*, 2019. 519: p. 119452.
- Jebur, Q., A. Hashim, and M. Habeeb, Fabrication, structural and optical properties for (polyvinyl alcohol–polyethylene oxide–iron oxide) nanocomposites. *Egyptian Journal of Chemistry*, 2020. 63(2): p. 611-623.
- El-Deen, H.Z. and A. Hafez, PHYSICO-CHEMICAL STABILITY OF PVA FILMS DOPED WITH Mn 2+ IONS AGAINST WEATHERING CONDITIONS. *Arabian Journal for Science & Engineering (Springer Science & Business Media BV)*, 2009. 34.
- Al-Taa'y, W.A., et al., Fabrication and characterization of nickel chloride doped PMMA films. *Advances in Materials Science and Engineering*, 2015. 2015(1): p. 913260.
- Raj, A.M.E., et al., Growth mechanism and optoelectronic properties of nanocrystalline In<sub>2</sub>O<sub>3</sub> films prepared by chemical spray pyrolysis of metal-organic precursor. *Physica B: Condensed Matter*, 2008. 403(4): p. 544-554.
- Salih, E.Y., et al., In-depth optical analysis of Zn (Al) O mixed metal oxide film-based Zn/Al-layered double hydroxide for TCO application. *Crystals*, 2022. 12(1): p. 79.
- Salih, E.Y., et al., Thermal, structural, textural and optical properties of ZnO/ZnAl<sub>2</sub>O<sub>4</sub> mixed metal oxide-based Zn/Al layered double hydroxide. *Materials Research Express*, 2018. 5(11): p. 116202.
- Kurt, A., Influence of AlCl<sub>3</sub> on the optical properties of new synthesized 3-armed poly (methyl methacrylate) films. *Turkish Journal of Chemistry*, 2010. 34(1): p. 67-80.
- Bashir, M.B.A., et al., In-depth thermal, microstructural and photoluminescence analysis of mesoporous ZnO/ZnAl<sub>2</sub>O<sub>4</sub>-MMO: the effect of molar ratio. *ECS Journal of Solid State Science and Technology*, 2021. 10(10): p. 106006.
- Bakry, A. and S. Mahmoud. Effect of substrate temperature on the optical dispersion of sprayed nickel oxide thin films. in 2011 Saudi International Electronics, Communications and Photonics Conference (SIECPC). 2011. IEEE.

# Novel Metal Oxide Nanoparticles Derived from *Lactobacillus* Isolated from Newborn Babies

Kawther Hkeem Ibrahim <sup>1</sup>



© 2024 The Author(s). This open access article is distributed under a Creative Commons Attribution (CC-BY) 4.0 license.

## Abstract

*Lactobacillus* has received much attention from researchers as one of the important probiotics in the baby's gut, the average abundance of *Lactobacillus* cells in the baby's stomach is 14.34%. *Lactobacillus* is the most common bacteria in the intestines of babies, and the coliform bacteria are important in children, especially because of their increased ability to prevent intestinal bacteria from the immune system. prevent viral diseases, which made them stronger. Studies found that the antibacterial activity of titanium nanoparticles that produce by some bacteria are attractive and can be considered as a new agent against the bacteria. In the current study, it has been used 20 probiotic bacteria isolated from 33 fecal samples of healthy newborns. According to the biochemical characteristics, the newborns are classified as (11) each of *L.gasseri*, *L.fermentum*, (6) *L.crispatus* (2) and *L.rhamnosus* ( 1) developed  $TiO_2$  nanoparticles and studied nanoparticles that are used biologically. different ways. Atomic force microscopy (AFM), scanning electron microscopy (SEM) and AFM showed the average size. of  $TiO_2$  nanoparticles (71, 70, 96) nm of *L. gasseri* (L4), *L. rhamnosus* (L19), *L. fermentum* (L14) The smallest size of the nanoparticles (70.) nm appeared from *L. rhamnosus* (L19) 70nm was smallest size from *L. rhamnosus* (L19) was analyzed by electron microscope and was observed as an oval shape with anatase.

**Keywords:** Biosynthesis; Infant Feces;  $TiO_2$  Nanoparticles; Metal Oxide Nanoparticles.



<http://dx.doi.org/10.47832/MinarCongress12-05>



<sup>1</sup> Department of Water Source and Soil, College of Agriculture, Kirkuk University, Kirkuk, Iraq  
[microbiology\\_1975@uokirkuk.edu.iq](mailto:microbiology_1975@uokirkuk.edu.iq)



## INTRODUCTION

Recently, researches the field of intestinal microbiota has been increased with the advance and commercialization of microbial cell preparations that, when applied, effect the composition of the intestinal microflora (1) and are beneficial to the consumer. everyone. These preparations are called "probiotics (2)".

Generally, lactobacilli are used as probiotic bacteria. There are a large number of anaerobic bacteria in the intestine, but lactic acid bacteria are often found in the feces. In other humans, lactic acid bacteria are not detected or the composition of Lactobacillus species changes over time (3) Due to the important chemical and physical characteristics of nanomaterials, nanomaterials such as TiO<sub>2</sub> nanoparticles (TiO<sub>2</sub> - NPs), of smaller diameter. over 100 nm, they have developed to a new generation of high-quality materials because they are bright, as well as exciting optical, dielectric and photocatalytic properties with quantifiable, drug-resistant and unopened form, if the nanoparticle formulas contain what they ask for. (4). Microorganisms are used as a nanoindustry that can be used to create an environmentally friendly, non-toxic and clean way to produce nanoparticles. Nanoparticles can be biosynthesized as soon as microorganisms capture target ions from their environment and convert them into elemental metals using enzymes produced by cell activity (5,6) .This can be both intracellular and extracellular connections, depending on where the nanoparticles are made. Biosynthetic nanoparticles are used in many applications including drug delivery for targeted drug delivery, cancer therapy, gene therapy and DNA detection, bacterial drugs, biosensors, separation science and resonance imaging. Magnet (7,8). The current study aimed to use Lactobacillus spp. isolated from healthy newborn babies feces for TiO<sub>2</sub> NPs biosynthesis as a bioactive agent and then to validate this product by characterization. It is a very different method, safe and cheap, in addition to being environmentally friendly for the microbiology of nanoparticles (non-pathogenic bacteria)

## MATERIALS AND METHODS

**Isolation of Lactobacillus in the feces of infants:** Thirty samples were taken only from newborn infants, less than 2 days old and in good health. Samples are collected at the DIK hospital and transported under refrigerated conditions to the laboratory for culture and identification. A fresh sample (1 mg) was suspended and serially dissolved in 9 ml of distilled water. 100 µl aliquots of the mixed samples were positioned on MRS agar plates, and incubated at 37 °C for 48 hours (9)

**Identification of Lactobacillus isolates:** Check the macroscopic appearance of all colonies for cultivation on MRS agar and morphological examination. The properties of different types of bacteria were examined, and the final identification was performed by standard microbiological tests; such as, catalase, morphological Gram stain and oxidase tests, motility, indole production, growth at 15 °C, and carbohydrate fermentation (mannitol, arabinose, galactose, lactose, fructose, salicin, trehalose, and sucrose)(10)

**Detection for production** Generally, three tubes were used to isolate and each one was filled with 40ml of MRS liquid. After this, 20 ml of TiO<sub>2</sub> (0.025 m) was added to the first and second tubes where made to stir for duration of 30 min while the third tube contained only MRS broth. The last visit will end up being even. Each isolate was opened in the first and third container in a CO<sub>2</sub> incubator at 37C° after 24, 48, 72 hours. The second glass used as a space for the first, the color changes from light brown to dark brown and the production of sediment were visible from the first discovery of the product. (11)

### **Characterization of biosynthesized TiO<sub>2</sub>nanoparticles**

A sample of nanoparticles was synthesized after a period of 72 hours of incubation. The structure of TiO<sub>2</sub> metal oxide nanoparticles were studied by atomic force microscopy (AFM), X-ray diffraction (XRD), and scanning electron microscopy (SEM).

### **Characterization of titanium nanoparticles by Atomic Force Microscopy**

Park XE 100 AFM system was used to obtain atomic force images. Liquid titanium nanoparticles are placed on top of freshly poured mica grains. At the deigning, the aliquot sample was left for 1 min; then, washed with deionized water; and finally, allowed to dry for 15 min. These images were acquired by scanning mica in air under non-contact conditions (12). The size, shape and size of TiO<sub>2</sub> nanoparticles were found using atomic force microscopy.

### **Characterization of titanium nanoparticles by Scanning Electron Microscope**

To determine the composition, the shape, powder of a thin film of titanium nanoparticle is made on a suitable aluminum plate through placing a small amount of the sample on the plate, the other solution is removed by paper in the movie. and let it dry overnight. SEM analysis was performed with an instrument operating at an operating voltage of 15.00 kV (13)

## RESULTS AND DISCUSSION

The appearance of the area and solid structure was studied in terms of shape, color, size, opacity and size as described by Kandler and Wiess (1986) (14). Colonies are examined for culture properties on MRS agar comprising calcium carbonate (dissolved in acid produced by bacteria). The results show that all *Lactobacillus* isolates can grow on MRS agar media, producing yellow or white, large, soft and round. Visual examination showed that *Lactobacillus* cells are positively reacted to gram stain. When checked under a light compound microscope, long or short rods appear alone, in pairs, or in short but irregular chains. (Hames and Vogel, 1995) (15). The biochemical properties of the isolated *Lactobacillus* are shown in (Table1).

**Table 1-** Biochemical tests of lactobacillus isolates

test	<i>L.gasseri</i>	<i>L.crispatus</i>	<i>L.rhamnosus</i>	<i>L.fermentum</i>
<b>catalase</b>	-	-	-	-
<b>oxidase</b>	-	-	-	-
<b>gelatinase</b>	-	-	-	-
<b>Growth45</b>	+	+	+	+
<b>Growth15</b>	-	-	+	-
<b>glucose</b>	+	+	+	+
<b>mannitol</b>	-	-	+	-
<b>maltose</b>	V	+	-	+
<b>Mannose</b>	+	+	+	+
<b>Sucrose</b>	+	+	+	+
<b>Salicin</b>	V	+	+	-
<b>Lactose</b>	+	+	-	+
<b>Raffinose</b>	V	-	-	+
<b>Trehalose</b>	V	-	+	+
<b>Xylose</b>	-	-	-	-
<b>Fructose</b>	+	+	+	+
<b>Arabinose</b>	-	-	+	+
<b>Cellobiose</b>	+	+	+	-

The results showed that these characteristics were very similar to those described by Carr et al. (2002) (16) for 20 *Lactobacillus* isolates. Results showed that all isolates were catalase, oxidase and gelatinase negative. The carbohydrate fermentation examination is the most important one for identifying *Lactobacillus* species (15,16). Separated by the type of stool of infant as shown in table2



**Table 2-** Lactobacillus isolates from infant feces

Isolate No.	<i>Lactobacillus</i> Sp	Isolate No.	<i>Lactobacillus</i> Species
L <sub>1</sub>	<i>L.fermentum</i>	L11	<i>L.fermentum</i>
L <sub>2</sub>	<i>L.fermentum</i>	L12	<i>L.gasseri</i>
L <sub>3</sub>	<i>L.gasseri</i>	L13	<i>L.gasseri</i>
L <sub>4</sub>	<i>L.gasseri</i>	L14	<i>L.fermentum</i>
L <sub>5</sub>	<i>L.gasseri</i>	L15	<i>L.gasseri</i>
L <sub>6</sub>	<i>L.fermentumi</i>	L16	<i>L.fermentum</i>
L <sub>7</sub>	<i>L.gasseri</i>	L17	<i>L.gasseri</i>
L <sub>8</sub>	<i>L.gasseri</i>	L18	<i>L.gasseri</i>
L <sub>9</sub>	<i>L.gasseri</i>	L19	<i>L. rhamnosus</i>
L <sub>10</sub>	<i>L.crispatus</i>	L20	<i>L.crispatus</i>

As (11) each between *L.gasseri* and *L.fermentum*, (6) *L.crispatus* (2) and *L.rhamnosus* (1) as shown in (table2). *fermentum* is the main heterofermentative species of *Lactobacillus* in the human intestine (17). Bello et al. (2003) (18) reported that *L.fermentum* species, *L.gasseri* can be isolated from healthy animal waste.

All 20 isolates were checked for TINP making. Titanium dioxide exposed to bacteria degrades and produces titanium nanoparticles. The solution color changed from brown to brown in the behavior of three producers, including *L. gasseri* (L4), *L. rhamnosus* (L19), *L. fermentum* (L14). The ability of eukaryotic and prokaryotic microorganisms and plant systems to produce nanoparticles is important in the development of nanobiotechnology. *Lactobacilli* have a negatively charged cell wall that attracts the electrostatically positive charge of metal ions (cations), and then cell wall enzymes convert the metal ions into nanoparticles (19). Microorganisms' enzymes have a major role in the process of bio-reduction. Biosynthesis of Nanoparticles occurred when microorganisms capture targeted ions from their environment and convert metal ions into elemental metals by enzymes produced by the cell's activity. It can be extracellular and intracellular connection (20) depending on where the nanoparticles are produced (21). Nanoparticles of different sizes are produced by a series of morphologies, dimensions and surface charges. To ensure that the products produced by *Lactobacillus* are nanomaterials, these materials are analyzed using an atomic force microscope (AFM) to measure the nanoparticles' average diameter and define their shape. and parts (regions and three examples). According to the results appeared in figures(1,2,3)

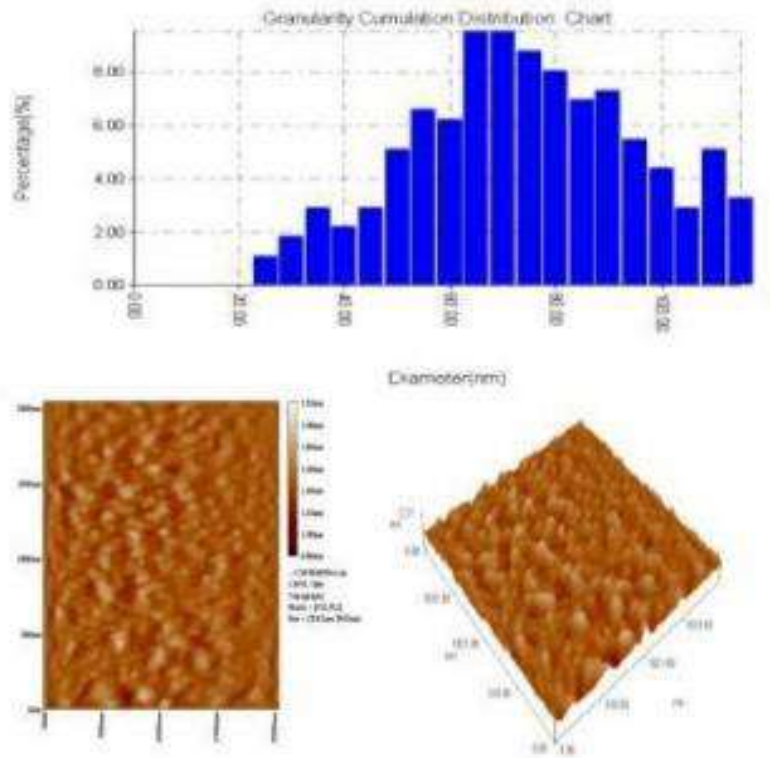


**Figure 1-** Atomic Force Microscopy image of TiO<sub>2</sub> nanoparticles synthesized *Lactobacillus gasseri* (L4)

The average size of TiO<sub>2</sub> nanoparticles are 71, 70, and 96 nm formed by the isolate of *Lactobacillus* L. *gasseri* (L4), L. *rhamnosus* (L19), L. *fermentum* . The smallest nanoparticle size (70.) nm of L. *rhamnosus* (L19) (fig2).

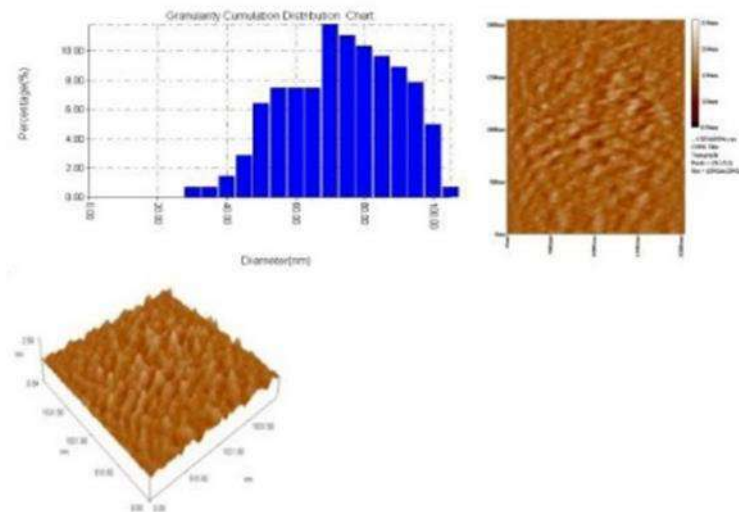


**Figure 2-** Atomic Force Microscopy image of TiO<sub>2</sub> nanoparticles synthesized by *Lactobacillus rhamnosus* (L19)

While greater size with average 96 nm produced by lactobacillus fermentum (14)(fig3)

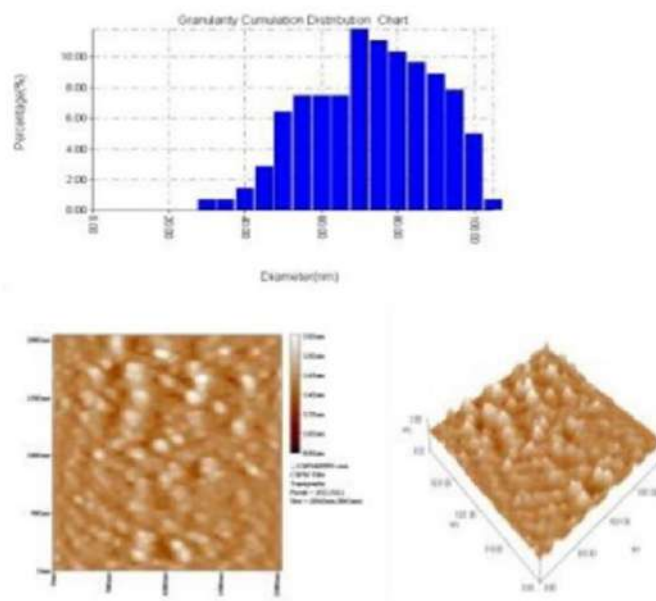


**Figure 3-** Atomic Force Microscopy image of TiO<sub>2</sub> nanoparticles synthesized by Lactobacillus fermentum(L14).

Bacteria have been widely studied for nanoparticle synthesis because of their rapid growth and easy genetic manipulation (22). On the other hand, TiO<sub>2</sub> NPs can change the structure and composition of the human gut microbiota, represented by probiotics (23). Images of synthesized TiO<sub>2</sub> nanoparticles produced by Scanning electron microscope (SEM) showed round and oval shape (Fig4)

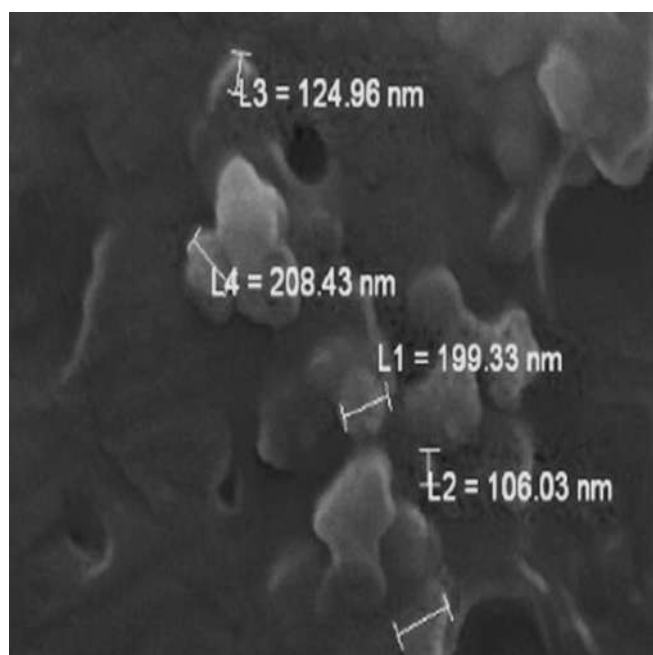


**Figure 4-** images obtained from scanning electron microscopic for TiO<sub>2</sub> nanoparticles synthesized by Lactobacillus rhamnosus



Which was confirmed by other studies (Jha et al., 2009; 11) using *Lactobacillus* spp. It has been observed that the Nanoparticles created by biological means have different shapes and sizes, the difference in size can be explained due to the fact that TiO<sub>2</sub> nanoparticles are shaped at different times (19). Synthesis of NP observed is affected by Two important factors; (1) the microorganisms' type; (2) and their source. Studies showed that, in the food industry, some of the most commonly used microorganisms are *Lactobacillus*; a bacterium used in products of dairy and as a probiotic supplement (24) .

## **CONCLUSION**

In the past decades, titanium dioxide metal oxide (TiO<sub>2</sub>) nanoparticles have been widely applied because of their unique physicochemical characteristics and biological usages. In this study, a simple, low-cost, cost-effective, non-toxic and non-toxic method of bioproduced titanium nanoparticles has been studied using lactobacilli as newborn probiotics. which provides a unique opportunity for the development of medical devices. AFM and SEM were used to characterize the formed titanium nanoparticles. The smallest 70 nm material obtained from *L.rhamnosus* has anatase crystal structure.

## **ACKNOWLEDGEMENT**

We would like to present our grateful to DiK Hospital staff, for their cooperation and contribution and the staff of Alrazi Research Center, Iran, for their help in taking images of NPs in a Scanning and Atomic electron microscope.

## REFERENCES

- Hemarajata, P., & Versalovic, J. (2013). Effects of probiotics on gut microbiota: Mechanisms of intestinal immunomodulation and neuromodulation. *Therapeutic Advances in Gastroenterology*, 6, 39–51.
- 2-Kechagia M, Basoulis D, Konstantopoulou S, Dimitriadi D, Gyftopoulou K, Skarmoutsou N, Fakiri EM.(2013) Health benefits of probiotics: a review. *ISRN Nutr.* 2;2013:481651. doi: 10.5402/2013/481651.
- Bermudez-Brito M, Plaza-Díaz J, Muñoz-Quezada S, Gómez-Llorrente C, Gil A.(2012) Probiotic mechanisms of action. *Ann Nutr Metab.*;61(2):160-74. doi: 10.1159/000342079.
- Ozioma, U. A., Kakuru, A., Iqbal, M. Z., & Wu, A. (2020). TiO<sub>2</sub> Nanoparticles: Applications in Nanobiotechnology and Nanomedicine. In A. Wu & W. Ren (Eds.), *TiO<sub>2</sub> Nanoparticles: Properties and Applications* (1st ed.). Wiley-VCH Verlag GmbH & Co. KGaA
- Xiangqian, L., Huizhong, X., Zhe-Sheng, C., & Guofang, C. (2011). Biosynthesis of Nanoparticles by Microorganisms and Their Applications. *Journal of Nanomaterials*, 2011, Article ID 270974, 16 pages. <https://doi.org/10.1155/2011/270974>
- 23-Obaid, H. M. (2022). In vitro assessment of biosynthesized silver nanoparticles effect on some intestinal protozoan cystic stages. *International Journal of Biology Research*, 7(3), 22–27. <https://doi.org/10.2455/ijbr.2022.7.3.4>
- Li, S., Zhao, Y., Zhang, L., Zhang, X., Huang, L., Li, D., Niu, C., Yang, Z., & Wang, Q. (2012). Antioxidant activity of *Lactobacillus plantarum* strains isolated from traditional Chinese fermented foods. *Food Chemistry*, 135, 1914-1919
- Obaid, H. M., & Shareef, H. A. (2022). Evaluation of the inhibitory impact of biosynthesized silver nanoparticles using *Bacillus cereus* and *Chromobacterium violaceum* bacteria on some intestinal protozoa. *Annals of Parasitology*, 68(4), 767–777. <https://doi.org/10.17420/ap6804.484>
- Tannock, G. W., Munro, K., Harmsen, H. J. M., Welling, G. W., Smart, J., & Gopal, P. K. (2000). Analysis of the Fecal Microflora of Human Subjects Consuming a Probiotic Product Containing *Lactobacillus rhamnosus* DR20. *Applied and Environmental Microbiology*, 66(6), 2578–2588.
- Savino, F. L., Cordisco, L., Tarasco, V., Locatelli, E., Di Gioia, D., & Oggero, R. (2011). Antagonistic effect of \**Lactobacillus*\* strains against gas-producing coliforms isolated from colicky infants. *BMC Microbiology*, 11\*(2), 157.
- Azhar, A., Behtas, L., Ladan, S., Ajabadi Ebrahimi, M. T., & Heydari, M. (2011). Lactobacillus-mediated biosynthesis of titanium nanoparticles in MRS broth medium. *Brno, Czech Republic; EU*, 9, 21–23.
- Daniel, K. S., Nehru, K., & Sivakumar, M. (2012). Rapid biosynthesis of silver nanoparticles using *Eichhornia crassipes* and its antibacterial activity. *Current Nanoscience*, 8(1), 1-5.

- Sarvamangala, D., Kondala, K., Sivakumar Babu, M. S., & Manga, S. (2013). Synthesis, characterization and antimicrobial studies of AgNP using probiotics. *International Research Journal of Pharmacy*, 4(3), 240-243.
- Kandler, O., & Weiss, N. (1986). Genus *Lactobacillus*. In P. H. A. Sneath, N. S. Mair, & J. G. Hold (Eds.), *Bergey's Manual of Systematic Bacteriology* (Vol. 2). Baltimore, MD, USA: William and Wilkins Co.
- Hammes, W. P., & Vogel, R. F. (1995). The Genus *Lactobacillus*. In B. J. B. Wood & W. H. Holzapfel (Eds.), *The Genera of Lactic Acid Bacteria* (pp. 19-54). Glasgow, UK: Blackie Academic and Professional.
- Carr, F. J., Chill, D., & Maida, N. (2002). The lactic acid bacteria: a literature survey. *Critical Reviews in Microbiology*, 28(4), 281-370.
- Dickson, E. M., Riggio, M. P., & Macpherson, L. A. (2005). A novel species-specific PCR assay for identifying *Lactobacillus fermentum*. *Journal of Medical Microbiology*, 54(3), 299-303.
- Bello, F. D., Walter, J., Hammes, W. P., & Hertel, C. (2003). Increased complexity of the species composition of lactic acid bacteria in human feces.
- Jha, A., & Prasad, K. (2010). Biosynthesis of metal and oxide nanoparticles using *Lactobacilli* from yoghurt and probiotic spore tablets. *Microbial Biotechnology Journal*, 5(3), 285-291.
- Abbas, A. Z., Abdulrahman, R. B., & Mustafa, T. A. (2024). Preparation and characterization of silver nanoparticles and its medical application against pathogenic bacteria. *Baghdad Science Journal*, 21(1), 204–216.
- Li, S., Zhao, Y., Zhang, L., Zhang, X., Huang, L., Li, D., Niu, C., Yang, Z., & Wang, Q. (2012). Antioxidant activity of *Lactobacillus plantarum* strains isolated from traditional Chinese fermented foods. *Food Chemistry*, 135, 1914-1919.
- Vithiya, K., & Sen, S. (2011). Biosynthesis of nanoparticles. *International Journal of Pharmaceutical Sciences and Research*, 2(11), 2781-2785.
- Han, S., Chen, Z. J., Zhou, D., Zheng, P., Zhang, J. H., & Jia, G. (2020). Effects of titanium dioxide nanoparticles on fecal metabolome in rats after oral administration for 90 days. *Journal of Peking University (Health Sciences)*, 52(18), 457-463.
- López de Dicastillo, C., Guerrero Correa, M., B. Martínez, F., Streitt, C., & José Galotto, M. (2021). Antimicrobial Effect of Titanium Dioxide Nanoparticles. IntechOpen. doi: 10.5772/intechopen.90891.



## Effect of UV treatment on Hydrophilic SiO<sub>2</sub> thin film

Hiba.M.Salman <sup>1</sup>



© 2024 The Author(s). This open access article is distributed under a Creative Commons Attribution (CC-BY) 4.0 license.

### Abstract

*This study explores the effect of UV treatment on the wettability of SiO<sub>2</sub> films. A method of sol-gel was used to produce pure silica oxide SiO<sub>2</sub>. It was dried, converted into powder, and pressed and the pulsed laser deposition method produced thin films. A group of samples were exposed to ultraviolet radiation for different periods (15, 30, and 60) minutes. After comparing the samples treated with ultraviolet rays with the untreated samples, it was found that the adhesion angle decreased from 46.05 to 23.47, which indicates that they became more hydrophilic. In addition to the above, the energy gap was measured and was equal to 5.65 eV. Investigations were conducted on structural, surface morphology, and optical properties for 500°C annealing temperature. SiO<sub>2</sub> is amorphous silica, as indicated by the X-ray diffraction pattern. Energy dispersive X-ray analysis (EDX) has been used to determine the elements' concentration and purity in SiO<sub>2</sub>.*

**Keywords:** Sol-Gel; Pulse Laser Deposition; Silicon Dioxide (SiO<sub>2</sub>); Thin Film; Hydrophilic.



<http://dx.doi.org/10.47832/MinarCongress12-06>



<sup>1</sup> Ministry of Education, General Directorate of Education Baghdad Karkh II, Iraq, Baghdad  
[Hibamohammedsalman4@gmail.com](mailto:Hibamohammedsalman4@gmail.com)

## Introduction

SiO<sub>2</sub> thin film has outstanding electrical and optical properties, making it a valuable material utilized in the semiconductor [1], optical [2], and electro-optical [3] industries. It is nearly absorption-free between 200 and 2000 nm and has a low refractive index "n 1.46 at 550 nm wavelength", which makes it a promising material for anti-reflective applications in optics [4,5]. Because these materials can be used as protective, photocatalytic, or self-cleaning coatings in a variety of industrial applications, there has been a lot of interest in them recently [6]. These days, hydrophobic surface treatments are highly prevalent and include corrosion prevention [8,9] and widely utilized self-cleaning [7]. Hydrophobic surface can generally be produced by reducing surface energy and forming a rough texture. It is therefore challenging to create a sufficient hydrophobic surface on a smooth surface [11] Properly built active photocatalysts with a suitable coating of hydrophobic material on their surface can interact significantly with hydrophobic moieties. Water droplets may be repelled by the surface [12].

Recently, researchers have become interested in self-cleaning surfaces that exhibit both hydrophobicity and photocatalytic activity [13]. It seems that a surface that has been roughened up can be made to be much more well-built and exceptionally water-resistant. Furthermore, a variety of techniques have been employed to create rough surfaces for hydrophobic surfaces, including etching, bundling, electro-spinning, PLD[10], curing chemical vapor deposition, electro-deposition, and so on [14]. these hydrophobic surfaces showed remarkable corrosion resistance and displayed distinctive behaviour throughout the self-cleaning process, allowing water molecules to. The contact angle with water is analyzed to determine the degree of hydrophobicity. This entails using the sessile drop technique [17] to measure the angle after putting a liquid drop on a level surface. In this work, a thin layer was created using pulsed laser deposition (PLD) technology, and pure silicon dioxide (SiO<sub>2</sub>) was generated using the sol-gel process. X-ray diffraction (XRD) analysis and UV-visible (UV-VIS) spectroscopy were then used to determine the material's bandgap energy.

## Experiment

Material produces:

They employed the sol-gel method to synthesize the required components and nanoparticles. Tetraethyl orthosilicate (TEOS) Si (OC<sub>2</sub>H<sub>5</sub>)<sub>4</sub> (99% pure) from Sigma-Aldrich. Isopropanol alcohol (CH<sub>3</sub>)<sub>2</sub>CHOH assay: 99.8% (GCC). Chromic nitrate (Cr(NO<sub>3</sub>)<sub>3</sub>), deionized water (bought from Al-Tabieaa Company to create colors), and GPS were used to

obtain a 97% pure sample. Using the sol-gel process, 4.4 ml of tetraethyl orthosilicate (TEOS) and 15.6 ml of isopropanol alcohol are mixed, and nitric acid (HNO<sub>3</sub>) is added to correct the pH. This yields SiO<sub>2</sub> nanoparticles. After 30 minutes of mixing, the mixture is known as (Sol 1). Following that, 15.4 ml of alcohol isopropanol and 1 ml of deionized water are combined, and after mixing for 30 minutes, the mixture is known as Sol 2. After progressively adding a solution (Sol 2) by distillation to a room-temperature solution (Sol 1), the mixture is stirred for two hours using a magnetic stirrer. The resultant solution was aged for 24 h at 56°C to produce the translucent sol that is depicted in Figure 1(A). To create the powder, the sol is first dried at 85 degrees Celsius. The material was then crushed after being ground into a powder and calcined at 500 °C. Thin films were deposited onto glass slides using the pulsed laser deposition method as shown in Figure 1(B).

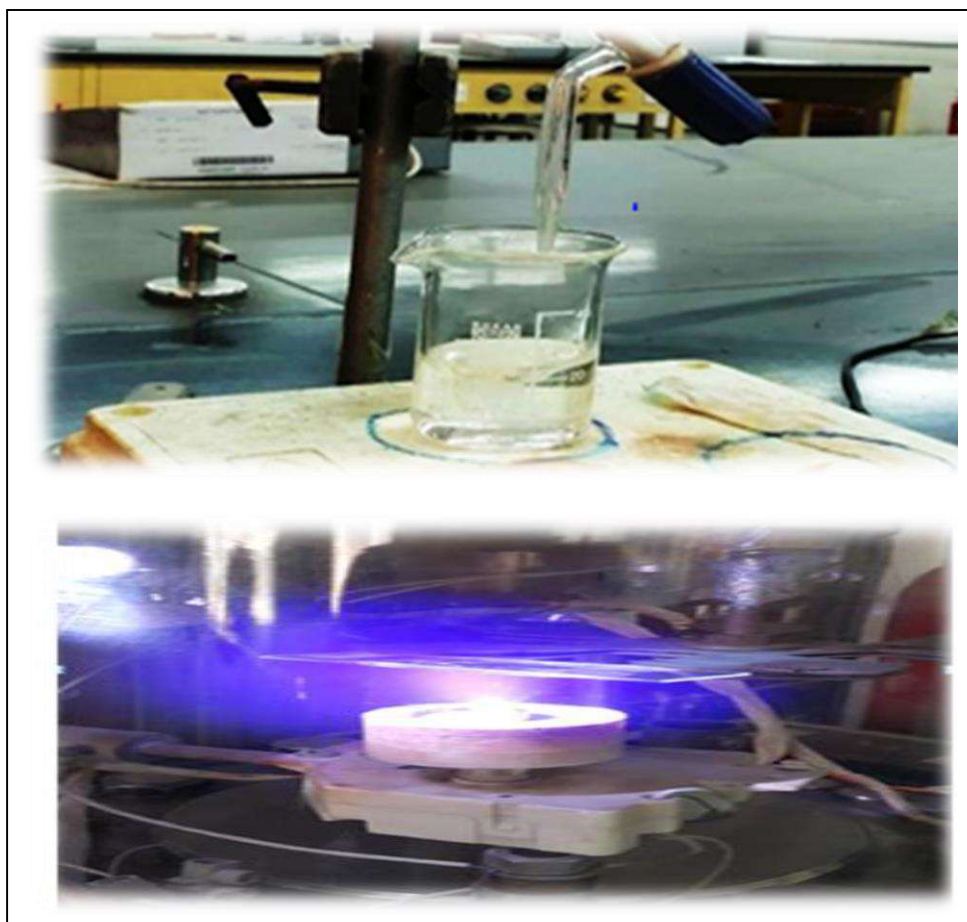


**Figure 1-** (A) SiO<sub>2</sub> sample preparation (B) Film deposition by pulsed laser

### **Result and dissection**

Figure 2 displays the X-ray diffraction data of a SiO<sub>2</sub> film that was created using the pulse laser deposition method on a glass substrate. It mentions that the film is pure amorphous SiO<sub>2</sub>. The resulting material is amorphous silica, as shown by the wide band in the spectra and the



equivalent Bragg angle of  $2\theta = 22.6^\circ$  [18]. There is no impurity peak for  $\text{SiO}_2$  when the results are compared to the JCPDS data (card No. 01-086-1561) for  $\text{SiO}_2$  [19, 20].

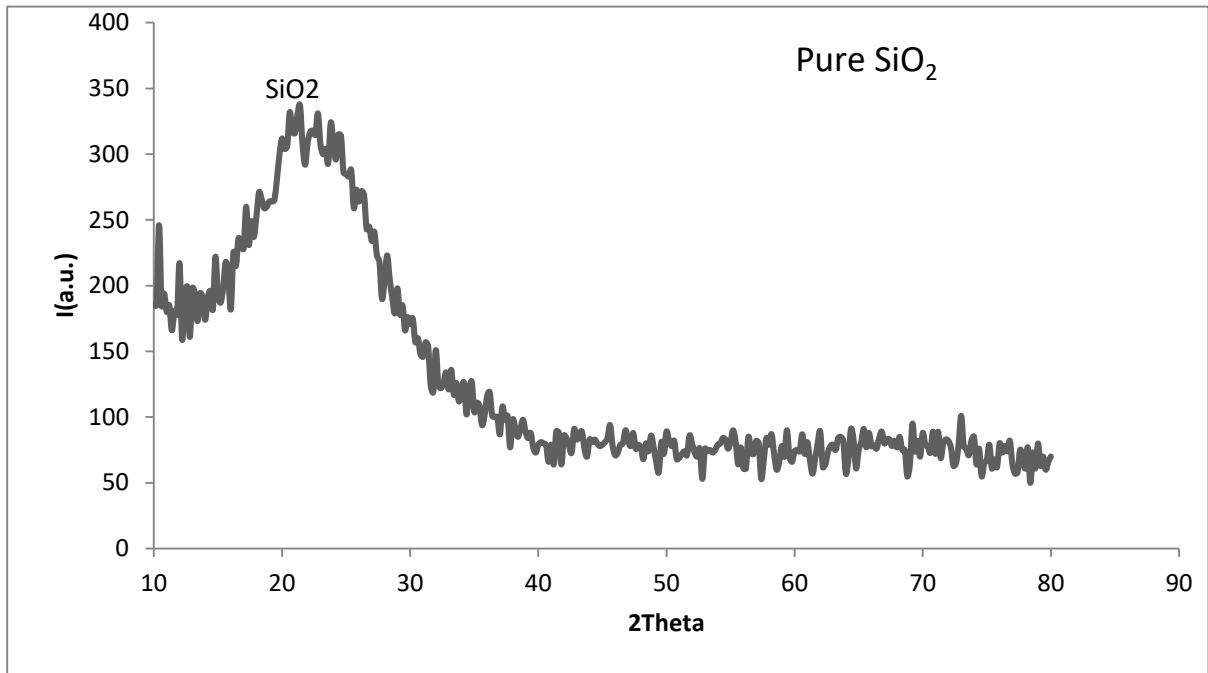


Figure 2- X-RAY for  $\text{SiO}_2$

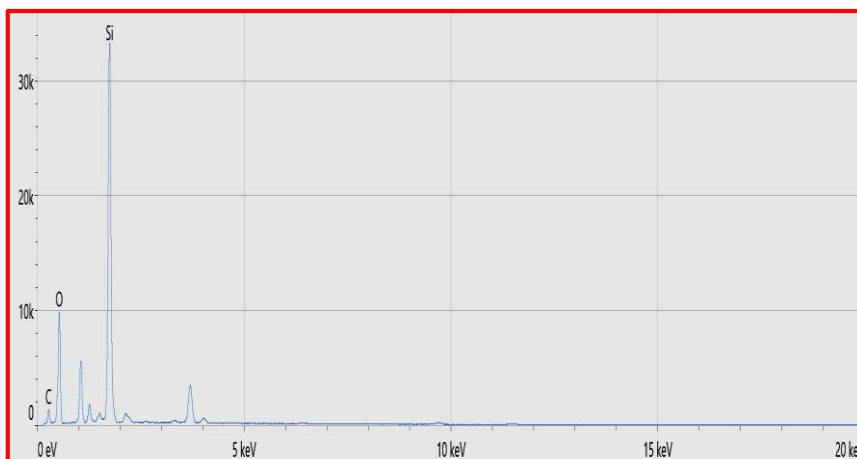
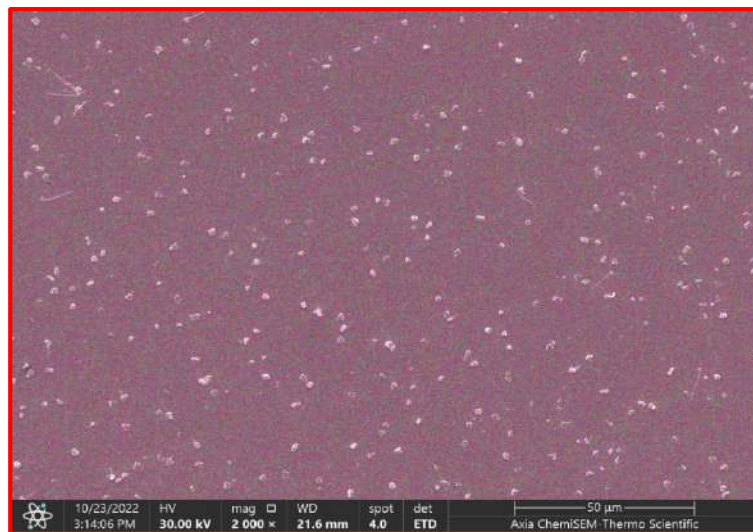
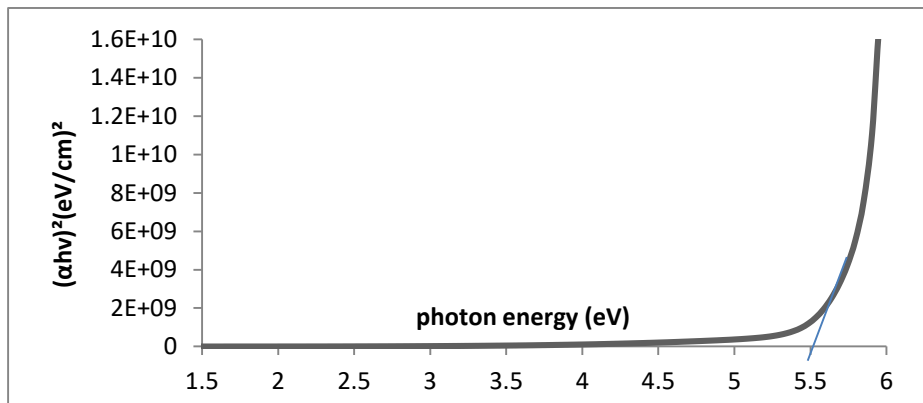


Figure 3- EDX OF  $\text{SiO}_2$  PURE THIN FILM

**Table 1-** EDX of SiO<sub>2</sub> thin film

Element	Atomic %	Atomic % Error	Weight %	Weight % Error
C	20.0	0.3	13.3	0.2
O	56.0	0.3	49.5	0.3
Si	24.0	0.1	37.2	0.1

The elements' concentration and purity in SiO<sub>2</sub> have been ascertained through the use of energy-dispersive X-ray analysis (EDX). The SiO<sub>2</sub> EDX spectra are displayed in Figure 3. Only the elements C, O, Si, and Cr are present in these spectra, indicating that the produced composite is highly pure and that the presence of C is due to the substrate. Table 1 shows the final concentrations.



**Figure 4-**  $(\alpha h\nu)^2$  about  $(h\nu)$  pure SiO<sub>2</sub>

Silicon dioxide (SiO<sub>2</sub>) has a wide energy gap, which is a key property that makes it so useful in electronics. The most fundamental absorption edge of a semiconductor follows the exponential law.

$$\alpha h\nu = A(h\nu - E_g)^n$$

A and E<sub>g</sub> represent the constant and the optical band gap energy, respectively,

The SiO<sub>2</sub> pure figure 4 shows the relationship between photon energy (hν) and (αhν)<sup>2</sup>, with an energy band gap of 5.65 eV. [20,21]. Figure 5 and Table 2 show the contact angle of the water drop significantly decreases after UV treatment from 46.05 to 23.47 because UV breaks down organic contaminants on the surface of a material causing the surface of a material to become more oxidized, making it more hydrophilic.

**Table 2-** The alteration in the water's contact angle upon UV treatment

	contact angle
Without processing	46.06°
after UV treatment for 15 min	44.95°
after UV treatment for 30 min	25.38°
after UV treatment for 60 min	23.47°

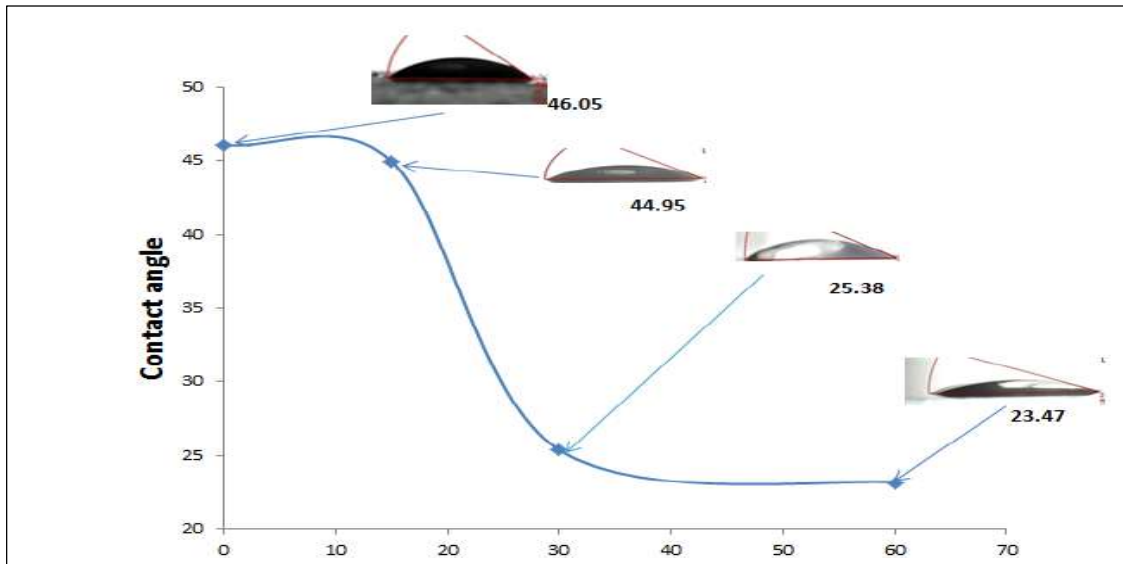


**Figure 5-** Contact angle according to the UV irradiation treatment

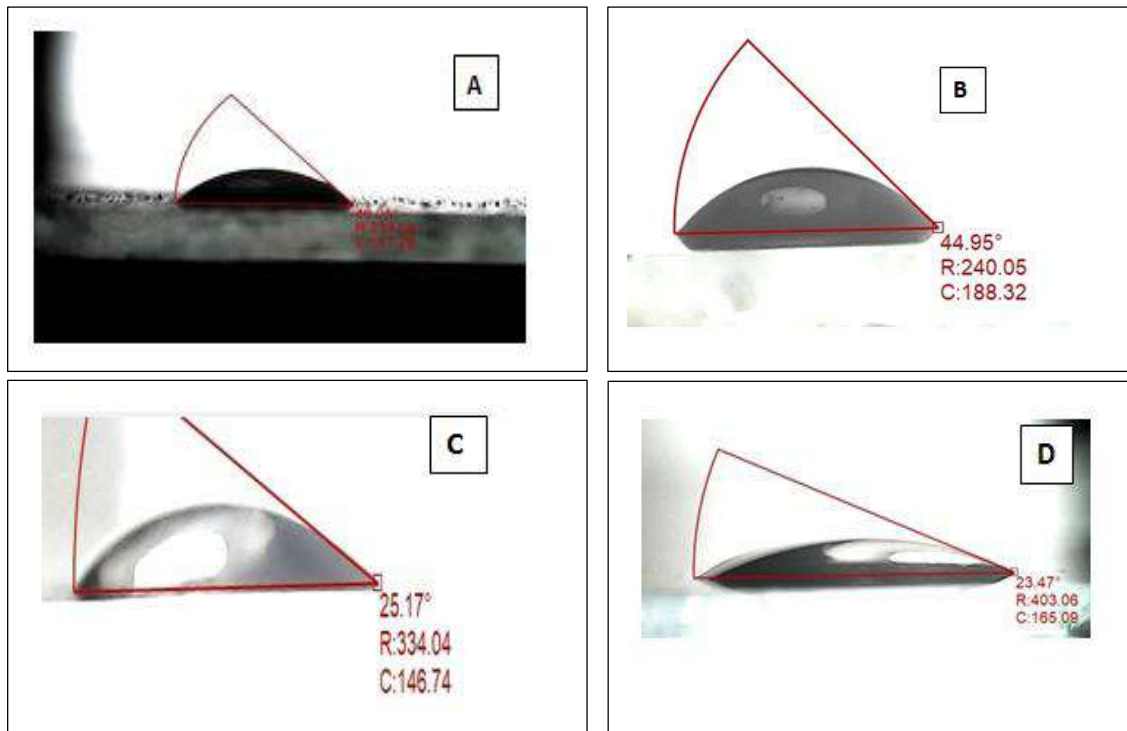


**Figure 6-** Water drop images on the surface of SiO<sub>2</sub> films (A) Without processing (B) after UV treatment for 15 min (C) after UV treatment for 30 min (D) after UV treatment for 60 min



## Conclusion

This work focuses on the preparation in away sol-gel and deposition thin-film by pulsed laser deposition (PLD). SiO<sub>2</sub> thin-film characterization is achieved through the use of an easy-to-use and reasonably priced. On a glass substrate, the deposition was done at ambient temperature, and it was then annealed at 500°C. This study displays properties related to structure and optical. According to the X-ray diffraction pattern, the thin films formed at 500°C for annealing the X-ray of a pure SiO<sub>2</sub> thin film It states that pure amorphous SiO<sub>2</sub> makes up the film. The wide band in the spectra and the analogous Bragg angle of  $2\theta = 22.6^\circ$ , which indicates the creation of the brookite phase present, indicate that the resultant material is amorphous silica. The purity and concentration of the elements

have been determined by energy dispersive X-ray analysis (EDX) in SiO<sub>2</sub> pure. These spectra only show the elements C, O, Si, and Cr, suggesting that the generated composite is extremely pure and that the substrate is responsible for the presence of C. An energy band gap of 5.65 eV was determined. the contact angle of the water drop significantly decreases after UV treatment from 46.05 to 23.47 because UV breaks down organic contaminants on the surface of a material causing the surface of a material to become more oxidized, making it more hydrophilic.

## Acknowledgment

The author thanks the Ministry of Education, the University of Baghdad's Department of Physics, and the plasma laboratory in particular for facilitating the creation of To prepare samples and make the required measurements. I also want to express my gratitude to Dr. Falah for her notes and advice, which made the work go more smoothly.

## References

- D. Niemann, N. Gunther, C. Kwong, M. Barycza, M. Rahman, *Solid-State Electron* 50 , 2006, 1097.
- M.C. Bautista, A. Morales, *Sol. Energy Mater. Sol. Cells* 80 ,2003, 217.
- D.-G. Sun, Z. Liu, J.M.S.-T. Hob, *Opt. Laser Technol.* 39 ,2007 285.
- E.-C. Cho, J. Xia, A.G. Aberle, M.A. Green, *Sol. Energy Mater. Sol. Cells* 74 ,2002, 147.
- F. Richter, H. Kupfer, P. Schlott, T. Gessner, C. Kaufmann, *Thin Solid Films* 389 ,2001, 278.
- Shokuhfar A., Alzamani M., Eghdam E., Karimi M., Mastali S., SiO<sub>2</sub>-TiO<sub>2</sub> nanostructure films on windshields prepared by sol-gel dip-coating technique for self-cleaning and photocatalytic applications, *Nanosci. Nanotechnol.*, 2012, 2:16.
- Zhou X., Yu S., Jiao S., Lv Z., Liu E., Zhao Y., Cao N., Fabrication of superhydrophobic TiO<sub>2</sub> quadrangular nanorod film with self-cleaning, anti-icing properties, *Ceramics International*, 2019, 45:11508
- Xue Y., Wang S., Zhao G., Taleb A., Jin Y., Fabrication of NiCo coating by electrochemical deposition with high super-hydrophobic properties for corrosion protection, *Surface and Coatings Technology*, 2019, 363:352
- Liang J., Wu X.W., Ling Y., Yu S., Zhang Z., Trilaminar structure hydrophobic graphene oxide decorated organosilane composite coatings for corrosion protection, *Surface and Coatings Technology*, 2018, 339:65
- Kumar D., Wu X., Fu Q., Ho J.W.C., Kanhere P.D., Li L., Chen Z., Hydrophobic sol-gel coatings based on polydimethylsiloxane for self-cleaning applications, *Materials and Design*, 2015, 86:855
- Wang Y., Nie L., Liu J., Preparation of hydrophobic SiO<sub>2</sub> film with high transmittance by sol mixing method, *Chemical Physics Letters*, 2020, 747:137331
- Lee J.H., Park E.J., Kim D.H., Jeong M.G., Kim Y.D., Superhydrophobic surfaces with photocatalytic activity under UV and visible light irradiation, *Catalysis Today*, 2016, 260:32
- Ding X., Pan S., Lu C., Guan H., Yu X., Tong Y., Hydrophobic photocatalytic composite coatings based on nano-TiO<sub>2</sub> hydrosol and aminopropyl terminated polydimethylsiloxane prepared by a facile approach, *Materials Letters*, 2018, 228:5
- Hu Y.W., He H.R., Ma Y.M., Preparation of Superhydrophobic SiO<sub>2</sub> Coating on Stainless Steel Substrate, *Key Engineering Materials*, 2012, 512-515:1028

- Wu W., Cheng L., Yuan M., Bai S., Wei Z., Jing T., Qin Y., Surface Engineering Method to Fabricate a Bendable Self-Cleaning Surface with High Robustness, *Science of Advanced Materials*, 2013, 5:933
- Roach P., Shirtcliffe N., Newton M., "Progress in superhydrophobic surface Development", *Soft Matter*, 2008, 4:224
- Ahmad D., Van Den Boogaert I., Miller J., Presswell R., Jouhara H., Hydrophilic and hydrophobic materials and their applications, *Energy Sources, Part A: Recovery, Utilization, and Environmental Effects*, 2018, 40:2686
- M. F. Abdel Messih , Ahmed E. Shalan ,Mohamed F. Sanad ,M. A. Ahmed" Facile approach to prepare ZnO@SiO<sub>2</sub> nanomaterials for photocatalytic degradation of some organic pollutant models", *Journal of Materials Science: Materials in Electronics*, 2019 , pages14291:14299.
- Tabatabaei, S., Shukohfar, A., Aghababazadeh, R., Mirhabibi, A. Experimental study of the synthesis and characterization of silica nanoparticles via the sol-gel method. EMAG–NANO 05: Imaging, Analysis and Fabrication on the Nanoscale. *Journal of Physics: Conference Series* 2006,26. 371:374
- Bajpai, N., Tiwari, A., Khan, S. A., Kher, R. S., Bramhe, N., Dhoble, S. J., Effects of rare earth ions (Tb, Ce, Eu, Dy) on the thermoluminescence characteristics of sol–gel derived and  $\gamma$ -irradiated SiO<sub>2</sub> nanoparticles. *Luminescence*. 2013, 29, 669:673.
- M. F. Abdel Messih, Ahmed E. Shalan, Mohamed F. Sanad, M. A. Ahmed" Facile approach to prepare ZnO:SiO<sub>2</sub> nanomaterials for photocatalytic degradation of some organic pollutant models", *Journal of Materials Science: Materials in Electronics*, 2019, 14291:14299
- Hamid Darabi, Mehdi Adelifard and Yasser Rajab,"Characterization of nonlinear optical refractive index for graphene oxide–Silicon oxide nanohybrid composite", *Journal of Nonlinear Optical Physics & Materials*, 2019, 28, 1.



## Serum Profiles of Some Minerals, Vitamin D and Lipids in Heart Diseases in Mosul City

Huda Y. Al-Attar <sup>1</sup>

Tamara W. Jihad <sup>2</sup>



© 2024 The Author(s). This open access article is distributed under a Creative Commons Attribution (CC-BY) 4.0 license.

### Abstract

*Vitamin D, a lipid-soluble vitamin that acts as a steroid hormone, can be acquired from dietary sources or manufactured in the skin upon exposure to ultraviolet (UV). It is related to the presence of cardiovascular risk factors in adults which contributes to the high global prevalence of cardiovascular illnesses. For three months, 60 blood samples were collected from healthy people and patients with cardiovascular diseases, ranging in age from 25- 65 years, after which the lipid profile was analyzed, and found remarkable associations between the aforementioned minerals and total cholesterol levels (TC), Triglyceride (TG), High-Density Lipoprotein (HDL), Low-Density Lipoprotein (LDL), Very- Low-Density Lipoprotein (VLDL) and Atherogenic Index (A.I). The results showed the existence of a significantly increased concentration of calcium, phosphorus, and potassium in the patient's serum compared to the control group, observed an adverse moral association of calcium with vitamin D and a direct moral association of potassium with vitamin in the control group were observed in comparison to the patients at the level ( $P \leq 0.05$ ). When compared to the control group, the vitamin D readings showed a significant drop at the level ( $P \leq 0.05$ ). In the patient population, analytical statistics revealed a substantial rise in TC, TG, LDL, VLDL, and Atherogenic Index (A.I) when contrasted with the control condition. About for High- high-density lipoprotein (HDL), no significant difference was observed between the patients and control groups at a significant level ( $P \leq 0.05$ ).*

**Keywords:** Vitamin 25 (OH)D; Lipid Profile; Calcium; Phosphorus; Potassium; Cardiovascular Disease.



<http://dx.doi.org/10.47832/MinarCongress12-07>



<sup>1</sup> Department of Biology, College of Science, University of Mosul, Iraq  
[waleed.tamara@yahoo.com](mailto:waleed.tamara@yahoo.com)



<sup>2</sup> Department of Biology, College of Education of Pure Sciences, University of Mosul, Iraq  
[tamara.jihad@uomosul.edu.iq](mailto:tamara.jihad@uomosul.edu.iq)

## INTRODUCTION

Vitamin D is an active part involved in multiple metabolic pathways and plays an essential part in muscle and bone health it is a fat-soluble vitamin, but the evidence also points to its crucial role in regulating Blood Pressure (BP) and vascular health (Schwetz *et al.*, 2018). Studies have suggested a connection between inadequate vitamin D intake with cardiovascular conditions such as myocardial injury, heart failure (HF), coronary artery disease, and stroke plus atherosclerosis, which is evidence strong sign among levels of vitamin D and atherosclerosis, were correlated with low levels among the population, including mostly healthy and elderly people (Jeong *et al.*, 2017).

However, studies have demonstrated a considerable correlation between elevated 25(OH)D levels and blood lipid levels, without considering the effects of vitamin D supplements on blood lipid levels. studies have yielded mixed results, some of which have had a positive impact and some have had a negative impact (Alanouti *et al.*, 2020; Qi *et al.*, 2022). There has been evidence that vitamin D has a significant role in regulating skeleton physiology. for its crucial role in regulating calcium metabolism and phosphorus through its influence on the intestines, bones, and renal, Vitamin D levels must be enough for levels of phosphorus and calcium to stay at normal levels to prevent hyperactivity of Parathyroid Hormone (PTH) (Anderson, 2017).

In this case, Vitamin D is essential for promoting increased calcium absorption in the intestines, it has significant effects on the bones by maintaining the mineral balance (; Caykara *et al.*, 2020; Voulgaridou *et al.*, 2023). According to accumulated epidemiological data, Health issues are connected to the potential link between calcium supplementation and an increased risk of cardiovascular disease, as circulating calcium content is directly tied to the pathophysiology of most persons. (Maddaloni *et al.*, 2018; Kobylecki *et al.*, 2021) Potassium has a crucial function in keeping cellular polarization and is necessary to transmit electrical impulses through the heart muscle, adjustments in the natural balance between potassium concentrations inside and outside the cell lead to arrhythmias, low potassium levels in the blood lead to ventricular tachycardia or fibrillation (Depret *et al.*, 2019). Lipid metabolism is influenced by many nutrients, namely potassium, phosphor, calcium, and sodium, which alter cellular function, many studies have confirmed that the usage of important metals can affect changes in fatty acid metabolism in some cases. (Caykara *et al.*, 2020; Kaur *et al.*, 2021).

Low calcium levels in the blood have been shown to inhibit intestinal fat absorption and the release of fatty acids in fat cells (Caykara *et al.*, 2020; Yamagata, 2023); high calcium levels

in the blood also contribute to the risk of cardiovascular disease, leading to alterations in the artery walls' structure and functionality, to cause atherosclerosis (Park and Iee, 2019). The research aims to estimate Vitamin D concentration being an indicator of cardiovascular disease and investigate whether there was a relation among the concentrations of Vitamin D and lipid layers through the occurrence of atherosclerosis in these conditions, as well as the appointment of concentrations of certain minerals such as calcium, phosphorus, and potassium in the serum of these patients.

## **MATERIALS AND METHODS**

Throughout the research period, 60 blood samples were collected, including 30 samples from patients with cardiovascular a cardiovascular illness, samples were collected from reviews of several community laboratories in Nineveh governorate for the period from 1/3 to 30/6, aged (25-65) years, additionally, 30 serum samples from healthy individuals were collected as a control group. 5 ml of each patient's blood was drawn from the vein. Separate the blood in test containers without preservatives. and obtain serum using a centrifuge at a speed of 300 cycles/minutes for five minutes (Tietz, 1994).

Vitamin D level has been measured using a proprietary measurement Kit equipped by the Korean AFIAS company, Fluorescence Immuno Assay (FIA) (Holick, 2006).

As for the estimate of the calcium, phosphorus, and potassium levels in the serum, a special measurement Kit was equipped by the Spanish BIOLABO company (Tietz, 1999; Tietz, 2006). Blood lipid levels have also been calculated with the aid of a specialized measurement kit furnished by the Spanish BIOLABO company. (Tietz, 1999).

### ***Statistical evaluation***

Data analysis was done to investigate the standard rate as well as the error using a test (t-test), and the correlation factor test between biochemical and vitamin D indicators and lipid levels, serum concentration was also used as a test (person), and statistical analysis was considered statistically significant at a level of ( $P \leq 0.05$ ) (Williams, 2017).

## **RESULTS AND DISCUSSION**

The findings shown in Table (1) are significantly different in vitamin D, where there is a significant decrease in its value in the patient's serum in contrast to a command group at a level of ( $P \leq 0.05$ ). This decrease may be due to its role in high blood pressure and Parathyroid



Hormone metabolism (PTH) and calcium resulting in a decrease in vitamin concentration which increases the secretion of Parathyroid Hormone (PTH) (Oberoi *et al.*, 2019).

Initially, the pressure on the blood vessels increases, ultimately causing a rise in Blood pressure. (BP) and the incidence of heart disease in general people, and metabolic height of several other pathways such as the system of Renin- Angiotensin Aldosterone (RAAS). This results from vitamin D function in the cardiac muscle, which in turn is involved in various cardiovascular issues, the strategy of vitamin D insufficiency leads to atherosclerosis because of the rise in Parathyroid Hormone (PTH), thus the increase in the levels of activity of the system (RAAS) (Muscogiuri *et al.*, 2017). Physiologically, this all occurs because of high levels of calcium within the cells, leading to dysfunction in the growth of the lining of the blood vessels (Park and Iee, 2019).

While (Wu *et al.*, 2023) pointed out in their study that obesity might play a big role in the level decline of 25(OH)D in the plasma which may be the result of several hypotheses, one suggests that a high concentration of lipids in the body serves as a source of low-saturated vitamin D it leads to a decrease in its percentage and, as another hypothesis has indicated, the high levels of leptin, which is released by most fatty tissue so that it may be for (Interleukin-6) (IL-6) inhibitory effects on 25(OH) D synthesis through its receptors.

The results of blood lipids concentration showed a significant difference for each variable in comparison with a control group if there is a significantly high ( $P \leq 0.05$ ) for each of the total cholesterol (TC), Triglycerides (TG), protein fatty low density (LDL), very low-density lipoprotein (VLDL) and Atherogenic Index (A.I) in the group of patients in comparison with the control group when ( $P \leq 0.05$ ) as shown in the table (1) and that in turn is the same as what he's referring to (Surdu *et al.*, 2021; Bekibele *et al.*, 2023)

As for High-Density Lipoprotein (HDL), the results shown in Table (1) do not imply that the patient group differs substantially from the level's control group ( $P \leq 0.0134$ ), it has been demonstrated that individuals with vitamin D deficiency had a high percentage of (HDL-C) and had higher values than (TG) in comparison with the control group which might have been linked to the danger of injury to a lipid disorder in the blood (Elmi *et al.*, 2021).

Obesity and blood lipid metabolism as indicators of cardiovascular disease leading to excessively high lipid levels, and that's what Schwetz also confirmed in his study (Schwetz *et al.*, 2018), so that vitamin D may hurt lipid levels such as TC, TG, LDL, and A.I, this disorder, in turn of, causes a considerably increased risk of cardiac illness (Surdu *et al.*, 2021).

As shown in Table (1), a significant difference in the concentrations of phosphorus, calcium, and potassium in the patient's serum was observed. At the level of ( $P \leq 0.05$ ), a significantly higher level was observed for each patient group component in comparison to the control group. This could be because calcium levels in the blood are associated with phosphate levels in the serum at a low glomerular filtration rate (GFR), when phosphate levels in the blood rise, calcium levels in the blood drop, and the infected kidney can't revitalize Vitamin D. Also, reduced vitamin D levels cause decreased uptake of calcium, where the body attempts to raise low calcium levels in the blood via secreting Thyroid Hormone (TH) to increase the calcium level in the blood (Nista *et al.*, 2018).

The current findings are in agreement with those of (Wang *et al.*, 2012; McIntosh, 2022), who explored a positive relationship between calcium levels in the blood and the estimated risk of cardiovascular disease over ten years. Various biological strategies may show blood calcium's association with atherosclerosis and the danger of heart attacks due to a blood clot, which leads to an imbalance in the lining, connects to calcium receptors, or interacts with pyrophosphate, an important inhibitor of tissue hardening. A high calcium level also causes lower concentrations of serum pyrophosphate and increases the classification of the vessels.

Moreover, Vitamin D and parathyroid hormone levels contribute to calculating the serum calcium level and cardiovascular disease (CVD) (He *et al.*, 2022).

As for the high levels of significant potassium ( $P \leq 0.05$ ) in the cohort of patients compared to the control group shown in Table (1), it is caused by an increased potassium concentration or difference in the distribution between outside and within cells in individuals with cardiac failure as well as a decrease of kidney secretion due to physiological disease or as a result of the effects of treatment (Yamada and Lnaba, 2021).

Where people who are experiencing Heart Failure (HF) potassium balance is influenced by the neuroendocrine mechanism associated with the disease as well as by the drugs used to treat (HF), the significant reduction in mortality rates is associated with neurohormone inhibition by multiple levels of enzyme inhibitors-converting angiotensin however, these treatments can increase blood potassium concentrations (Clephas *et al.*, 2023).

**Table 1-** Vitamin D concentrations, lipids and minerals in serum patients with cardiovascular disease.

Biochemical parameters	Mean $\pm$ SD		P. value
	Age 25-65 years		
	Controls N=30	Patients N=30	
TC mg/dl	136.25 $\pm$ 28.87	300.04 $\pm$ 60.70	0.000*
TG mg/dl	112.50 $\pm$ 22.86	206.93 $\pm$ 49.40	0.000*
VLDL-C mg/dl	28.55 $\pm$ 24.05	42.15 $\pm$ 9.10	0.010*
LDL-C mg/dl	67.15 $\pm$ 24.6	22.19 $\pm$ 52.42	0.000*
HDL-C mg/dl	40.45 $\pm$ 4.86	38.56 $\pm$ 3.65	0.0134
AI	3.42 $\pm$ 0.77	7.81 $\pm$ 1.25	0.000*
Vit.D3 ng/ml	49.71 $\pm$ 12.47	16.78 $\pm$ 84.89	0.000*
Calcium mg/dl	9.56 $\pm$ 0.68	10.05 $\pm$ 0.71	0.021*
Potassium mg/dl	4.57 $\pm$ 0.57	5.31 $\pm$ 0.35	0.000*
Phosphorous mg/dl	3.53 $\pm$ 0.64	4.74 $\pm$ 0.27	0.000*

TC= Total cholesterol

TG=Triglycerides

VLDL-C= very low-density lipoprotein

LDL-C= low-density lipoprotein

HDL-C= High-density lipoprotein

AI= Atherogenic Index

SD= Standard Deviation

\*= Statistically significant ( $p \leq 0.05$ )

Vitamin D deficiency is linked with increased risk factors for heart disease. indicators, there is also a relationship between decreased levels of vitamin D in the blood elevated serum levels of TC and LDL-C, and low HDL-C levels in the blood (Faridi *et al.*, 2017). The relationship reverses a significant correlation relationship between lipids like cholesterol level and low-density lipoprotein and the level of vitamin D, which is also shown in Table (2) it was identical to what it came up with (Setayesh *et al.*, 2021). Both confirmed (Mohammad *et al.*, 2019; Han *et al.*, 2021) that the level of 25(OH)D positively pertains to the level of (HDL-C) and has a negative correlation with the level of TC, TG, LDL-C, increased absorption of intestinal calcium can reduce the manufacture of secretions TG, this converts hepatic cholesterol into bile acids and thus reduces cholesterol level in the blood.

A different study confirmed that the analysis of statistical correlation proved to be a positive significant relationship with serum vitamin D levels (HDL-C), the rise in vitamin D levels leads to an increase in (HDL-C), thus the likelihood of developing heart disease is reduced (Mohammad *et al.*, 2019). Obesity is a contributing factor in confusion or imbalance in the level of blood lipids, which encompass low HDL and high TG values, in addition, obesity



has affected vitamin D metabolism because fatty tissue in obese people prefers to take vitamin D (Barman *et al.*, 2022).

And was observed that there was an adverse significant association of calcium with vitamin D in the patient cohort in comparison to the control group at a level of ( $P \leq 0.05$ ) in Table (2), and this is consistent with what he indicated (Mohammed *et al.*, 2019) in that an elevated blood calcium level was linked to a decreased danger of cardiovascular disease (Kong *et al.*, 2017).

Table (2), also showed a direct and significant association between potassium and vitamin D when comparing the sick group to the control group, which may be because potassium secretion during the administration is not associated with cardiovascular disease risks based on the World Health Organization (Ferreira *et al.*, 2020).

In contrast, the introduction of potassium in the dour has also been linked to significantly lower mortality and cardiovascular disease danger (Strohm *et al.*, 2017).

Research of potassium's direct effects on the risk of heart disease showed high potassium levels may greatly lower the risk of heart disease through their positive effect on blood pressure because blood pressure constitutes one the main reasons for heart failure, that's consistent with what they found (Lin *et al.*, 2023).

**Table 2-** Testing the correlation coefficient among vitamin D level and biochemical variables in sick persons compared to the control group

Biochemical parameters	(r)	
	Vit. D3	
	Controls	Patients
TC mg/dl	-0.513*	-0.452*
TG mg/dl	-0.406	-0.230
VLDL-C mg/dl	-0.369	-0.328
LDL-C mg/dl	-0.563**	-0.462*
HDL-C mg/dl	-0.221	-0.316
AI	-0.380	-0.338
Vit.D3 mg/ml	0.1	0.1
Calcium mg/dl	0.555*	-0.593**
Potassium mg/dl	0.484*	-0.176
Phosphorous mg/dl	0.270	-0.187

Vit.D3: Vitamin D3

r: correlation coefficient

\* Statistically significant ( $P \leq 0.05$ )

\*\* Statistically significant ( $P \leq 0.001$ )

Recent research demonstrates that a calcium or phosphorus metabolic change could directly affect the vascular system and cardiac. Analysis shows the correlation factor between calcium concentration and blood lipid levels, table (3) showed an adversely significant association with the level of each Atherogenic Index (AI), low-density protein (LDL), and Total cholesterol (TC), while there is a positive significant attachment between the patient group's lipoprotein-very low level and the control group at the level of significant ( $P \leq 0.05$ ), and that's contrary to what he's referred to (Caykar *et al.*, 2020; Alkhtib *et al.*, 2023) The blood calcium content is positively associated with the fatty layers, it has been observed that calcium levels have the highest serum value in LDL, TC which has a major effect on the metabolism of lipids in the blood where there are many mechanisms to explain a relationship between lipids and calcium, it may be due to the high concentration of calcium that hampers the oxidative processes in mitochondria and the production of ATP and increase the calcium inside it (Weaver *et al.*, 2016; Alkhatib *et al.*, 2023). Increased calcium in cellular membranes is to blame for the disruption of fatty acid metabolism and the development of hyperlipid blood (Ticinesi *et al.*, 2016; Poitelon *et al.*, 2020).

As the high level of Para Thyroid Hormone (PTH) in the blood, affects the activity of lipase, low activity of this enzyme can increase triglycerides, total cholesterol and low-density lipoprotein clarifies the link between calcium and lipid in the blood (Higashioka *et al.*, 2020). As for phosphorus and its relation to blood lipid levels, it was observed that there was a significant negative correlation between it and the levels of A.I, HDL, and TC, in the patient cohort, compared with the control when ( $P \leq 0.05$ ) and as in the table (3), this may be due to the effect of phosphates on the metabolism of phospholipid in the liver, or because of the reduction of lipoprotein activity caused by the high concentration of thyroid hormones leading to fat metabolic (Caykara *et al.*, 2020).

**Table 3-** Test the correlation coefficient between lipid levels and mineral concentration in the sick serum comparison to the control group

Biochemical parameters mg/dl	minerals concentration					
	controls			patients		
	Calcium (r)	Phospho r (r)	Potassiu m (r)	Calcium m (r)	Phospho r (r)	Potassiu m (r)
TC	-0.543*	-0.187	-0.383	0.560**	0.590**	0.523**
TG	-0.267	-0.233	-0.268	0.372	0.295	0.390*
VLDL-C	-0.379	0.210	-0.229	0.477*	0.369	0.477*
LDL-C	-0.611**	0.025	-0.174	0.561**	0.537**	0.427*
HDL-C	0.068	-0.469*	-0.272	0.361	0.476*	0.395*
AI	-0.523*	0.034	-0.217	0.423*	0.384*	0.3556

r: correlation coefficient

\* Statistically significant ( $p \leq 0.05$ )

\*\* Statistically significant ( $p \leq 0.01$ )

## **Conclusion**

This study concludes the significance of getting adequate vitamin D levels in the serum to decrease the incidence of atherosclerosis with other cardiac conditions, Increased lipid levels have been associated with vitamin D deficiency, as well as have played an important factor to happen of heart disease, mineral consumption also contributes in part to the disturbance of serum lipid levels. Changes in lipid levels can partially affect mineral concentration levels in a patient's serum.

## **ACKNOWLEDGMENTS**

We are grateful to acknowledge the University of Mosul.



## REFERENCES

- Alan HB, & Wu (2006). Tietz Clinical Guide to Laboratory Test (4th Ed). W.B. Saunders Company: 852-855. Available from: [https://www.google.co.uk/books/edition/Tietz\\_Clinical\\_Guide\\_to\\_Laboratory\\_Tests/aQqjBQA-AQBAJ?hl=en&gbpv=1&dq=Clinical+Guide+to+Laboratory+Test&pg=PP1&printsec=frontcover](https://www.google.co.uk/books/edition/Tietz_Clinical_Guide_to_Laboratory_Tests/aQqjBQA-AQBAJ?hl=en&gbpv=1&dq=Clinical+Guide+to+Laboratory+Test&pg=PP1&printsec=frontcover)
- Alanouti F, Abboud M, Papandreou D, Mahboub N, Haidar S, Rizk R (2020). Effect of vitamin D supplementation on lipid profile in adults with the metabolic syndrome: A systematic review and meta-analysis of randomized controlled trials. *Nutrients*. 12(11): 3352. <https://doi.org/10.3390/nu12113352>
- Alkhatib B, Agraib LM, Al-Dalaeen A, Al-Shami I (2023). Are There Any Correlations between Vitamin D, Calcium, and Magnesium Intake and Coronary and Obesity Indices?. *Journal of the American Nutrition Association*. 4: 1-8. <https://doi.org/10.1080/27697061.2023.2203225>
- Anderson PH (2017). Vitamin D activity and metabolism in bone. *Current Osteoporosis Reports*.15:443-449. <https://doi.org/10.1007/s11914-017-0394-8>
- Barman P, Jahan N, Pondit PK, Hoque MA, Roy M, Akhter A (2022). Relationship between Obesity and Serum Vitamin D Levels in Young Women. *Scholars Journal of Applied Medical Sciences*. 10(11):1990-1994. <https://doi.org/10.36347/sjams.2022.v10i11.031>
- Bekibele GE, Anacletus FC, Patrick-Iwuanyanwu KC, Nwaogazie I L (2023). The protective effect of red cabbage on water-soluble fractions of spent crankcase oil-induced alterations in lipid function biomarkers and atherogenic indices in male Albino rats. *Toxicology Research*. 12(1): 39-48. <https://doi.org/10.1093/toxres/tfac079>
- Caykara B, Ozturk G, Mutlu HH, Arslan E (2020). Relationship between vitamin D, calcium, and phosphorus levels. *Journal of Academic Research in Medicine*. 10(3):252-257. <https://doi.org/10.4274/jarem.galenos.2020.3351>
- Clephas PR, Radhoe SP, Linssen GC, Langerveld J, Plomp J, Smits JP (2023). Serum potassium level and mineralocorticoid receptor antagonist dose in a large cohort of chronic heart failure patients. *ESC heart Failure*. 10(2): 1481-1487. <https://doi.org/10.1002/ehf2.14285>
- Depret F, Peacock WF, Liu KD, Ravigue Z, Rossignol P, Legrand M (2019). Management of hyperkalemia in the acutely ill patient. *Annals of Intensive Care*. 9(32): 1-16. <https://doi.org/10.1186/s13613-019-0509-8>

- Elmi C, Fan MM, Le M, Cheng G, Khalighi K (2021). Association of serum 25-Hydroxy Vitamin D level with lipid, lipoprotein, and apolipoprotein level. *Journal of Community Hospital Internal Medicine Perspectives*.11(6): 812-816. <https://doi.org/10.1080/20009666.2021.1968571>
- Faridi KF, Lupton JR, Martin SS, Banach M, Quispe R, Kulkarni K (2017). Vitamin D deficiency and non-lipid biomarkers of cardiovascular risk. *Archives of Medical Science*.13(4): 732-737. <https://doi.org/10.5114/aoms.2017.68237>
- Ferreira JP, Butler J, Rossignol P, Pitt B, Anker SD, Kosiborod M (2020). Abnormalities of potassium in heart failure: JACC state-of-the-art review. *Journal of the American College of Cardiology*.75(22):2836-2850. <https://doi.org/10.1016/j.jacc.2020.04.021>
- Han YY, Hsu SHJ, Su TC (2021). Association between vitamin D deficiency and high serum levels of small dense LDL in middle-aged adults. *Biomedicines*. 9(5):464. <https://doi.org/10.3390/biomedicines9050464>
- He J, Sun X, Nie R, Zhao L (2022). Relationship between serum parathyroid hormone levels and abdominal aortic calcification in patients starting hemodialysis who have never taken calcium tablets, calcitriol, or vitamin D analogs. *Renal Failure*. 44(1):1409-1416. <https://doi.org/10.1080/0886022X.2022.2114369>
- Higashioka M, Sakata S, Honda T, Hata J, Shibata M, Yoshida D, Hiraoka Y, Shibata M, Goto K, Kitazono T, Osawa H, Ninomiya T (2020). Small dense low-density lipoprotein cholesterol and the risk of coronary heart disease in Japanese community. *Journal of atherosclerosis and thrombosis*. 27(7): 669-682. <https://doi.org/10.5551/jat.51961>
- Holick MF (2006). High prevalence of Vitamin D inadequacy and implications for health. *Mayo Clin Proc*. 81(3): 353-373. <https://doi.org/10.4065/81.3.353>
- Jeong HY, Park KM, Lee MJ, Yang DH, Kim SH, Lee SY (2017). Vitamin D and hypertension. *Electrolytes & Blood Pressure*. 15(1): 1-11. <https://doi.org/10.5049/EBP.2017.15.1.1>
- Kaur S, Héroult J, Caruso A, Pencreac'h G, Come M, Gauvry L (2021). Proteomics and expression studies on lipids and fatty acids metabolic genes in *Isochrysis galbana* under the combined influence of nitrogen starvation and sodium acetate supplementation. *Bioresource Technology Reports*. 15: 100714. <https://doi.org/10.1016/j.biteb.2021.100714>

- Kobylecki CJ, Nordestgaard BG, Afzal S (2021). Plasma ionized calcium and risk of cardiovascular disease: 106 774 individuals from the Copenhagen General Population Study. *Clinical Chemistry*. 67(1): 265-275. <https://doi.org/10.1093/clinchem/hvaa245>
- Kong SH, Kim JH, Hong AR, Cho NH, Shin CS (2017). Dietary calcium intake and risk of cardiovascular disease, stroke, and fracture in a population with low calcium intake. *The American journal of clinical nutrition*. 106(1):27-34. <https://doi.org/10.3945/ajcn.116.148171>
- Lin Z, Zheng J, Liu X, Hu X, Fuxian R, Gao D (2023). Assessing potassium levels in critically ill patients with heart failure: application of a group-based trajectory model. *ESC Heart Failure*.10(1): 57-65. <https://doi.org/10.1002/ehf2.14161>
- Maddaloni E, Cavallari L, Napoli N, Conte C (2018). Vitamin D and Diabetes Mellitus. *Front Horm Res*. 50:161-176.  
<https://doi.org/10.1159/000486083>
- McIntosh J (2022). Mechanistic Insights Into Changes in Blood Flow Following Application of Intermittent Negative Pressure. UK, University of Dundee. Available from:  
[https://discovery.dundee.ac.uk/ws/portalfiles/portal/72719639/JMcIntosh\\_Thesis\\_Final\\_Mar\\_2022.pdf](https://discovery.dundee.ac.uk/ws/portalfiles/portal/72719639/JMcIntosh_Thesis_Final_Mar_2022.pdf)
- Muscogiuri G, Annweiler C, Duval G, Karras S, Tirbassi G, Salvio G (2017). Vitamin D and cardiovascular disease: from atherosclerosis to myocardial infarction and stroke. *International journal of cardiology*. 230:1-9. <https://doi.org/10.1016/j.ijcard.2016.12.053>
- Mohammad AJ, Noor AA, Khalid K, Razzak A (2019). Association of 25-hydroxy Vitamin D with HDL- cholesterol and other cardiovascular risk biomarkers in subjects with non-cardiac chest pain. *Lipids in health and disease*. 18(27): 1-10. <https://doi.org/10.1186/s12944-019-0961-3>
- Nista A, Toutouza M, Machairas N, Mariolis A, Philippou A, Koutsilieris M (2018). Vitamin D in cardiovascular disease. *In Vivo*.32(5): 977-981. <https://doi.org/10.21873/invivo.11338>
- Oberoi D, Mehrotra V, Rawat A (2019). Vitamin D as a profile marker for cardiovascular diseases. *Annals of cardiac anaesthesia*.22(1): 47-50. [https://doi.org/10.4103/aca.ACA\\_66\\_18](https://doi.org/10.4103/aca.ACA_66_18)
- Park B, lee YJ (2019). Borderline high serum calcium levels are associated with arterial stiffness and 10-year cardiovascular disease risk determined by Framingham risk score. *The Journal of Clinical Hypertension*. 21(5):668-673. <https://doi.org/10.1111/jch.13532>
- Poitelon Y, Kopec AM, Belin S (2020). Myelin fat facts: an overview of lipids and fatty acid metabolism. *Cells*.9(4): 812. <https://doi.org/10.3390/cells9040812>



- Qi KJ, Zhao ZT, Zhang W, Yang F (2022). The impacts of vitamin D supplementation in adults with metabolic syndrome: A systematic review and meta-analysis of randomized controlled trials. *Frontiers in Pharmacology*. 13: 1033026. <https://doi.org/10.3389/fphar.2022.1033026>
- Schwetz V, Scharnagl H, Trummer C, Stojakovic T, Pandis M, Grubler MR (2018) Vitamin D supplementation and lipoprotein metabolism: a randomized controlled trial. *Journal of clinical lipidology*. 12(3): 588-596. <https://doi.org/10.1016/j.jacl.2018.03.079>
- Setayesh L, Amini A ,Bagheri R, Moradi N ,Yarizadeh H, Asbaghi O (2021). Elevated plasma concentrations of vitamin D-binding protein are associated with lower high-density lipoprotein and higher fat mass index in overweight and obese women. *Nutrients*. 13(9):3223. <https://doi.org/10.3390/nu13093223>
- Strohm D, Ellingers S, Leschik-Bonnet E, Maretzke F, Hesecker H (2017). Revised reference values for potassium intake. *Annals of Nutrition and Metabolism*.71(1-2): 118- 124. <https://doi.org/10.1159/000479705>
- Surdu A M, Pinzariu O, Ciobanu DM, Negru AG, Cainap SS, Lazea C (2021). Vitamin D and its role in the lipid metabolism and the development of atherosclerosis. *Biomedicines*.9(2):172. <https://doi.org/10.3390/biomedicines9020172>
- Ticinesi A, Nouvenne A, Ferraro PM, Folesani G, Lauretani F, Allegri F (2016). Idiopathic calcium nephrolithiasis and hypovitaminosis D A case control study. *Urology*. 87: 40-45. <https://doi.org/10.1016/j.urology.2015.10.009>
- Tietz NW, Ashwood ER, Burtis CA (1994). Tietz Textbook of Clinical Chemistry (2nd ed). W.B. Saunders Company, U.S.A: 13211-13216. Available from: <https://Icn.Ioc.gov/93022596>
- Tietz NW, Ashwood ER, Burtis CA (1999). Tietz Textbook of Clinical Chemistry (3rd ed). W.B. Saunders Company, U.S.A: 809-857. Available from: <https://cir.nii.ac.jp/crid/1130282272007514112>
- Voulgaridou G, Papadopoulou SK, Detopoulou P, Tsoumana D, Giaginis C, Kondyli FS (2023). Vitamin D and calcium in osteoporosis, and the role of bone turnover markers. A narrative review of recent data from RCTs. *Diseases*. 11(1): 29. <https://doi.org/10.3390/diseases11010029>
- Wang LU, Manson JE, Sesso HD (2012). Calcium intake and risk of Cardiovascular disease: a review of prospective studies and randomized clinical trials. *American Journal of Cardiovascular Drugs*.12(2): 105-116.
- <https://doi.org/10.2165/11595400-000000000-00000>

- Weaver CM, Alexander DD, Boushey CJ, Dawson- Hughes B, Lappe JM, Leboff MS, Liu S (2016). Calcium plus vitamin D supplementation and risk of fractures: an updated meta-analysis from the national osteoporosis foundation. *Osteoporosis International*. 27:367-376. <https://doi.org/10.1007/s00198-015-3386-5>
- Williams B (2017). *Biostatistics: Concepts and Applications for Biologists* (2nd ed.). CRC Press, Chapman and Hall: p 213. Available from: <https://doi.org/10.1201/9781315150314>
- Wu O, Yuan C, Leng J, Zhang X, Liu W, Yang F (2023). Colorable role of interleukin (IL)-6 in obesity hypertension: A hint from a Chinese adult case-control study. *Cytokine*. 168:156226. <https://doi.org/10.1016/j.cyto.2023.156226>
- Yamada S, Inaba M (2021). Potassium metabolism and management in patients with CKD. *Nutrients*.13(6):1751. <https://doi.org/10.3390/nu13061751>
- Yamagata K (2023). Fatty acids act on vascular endothelial cells and influence the development of cardiovascular disease. *Prostaglandins & Other Lipid Mediators*: 106704. <https://doi.org/10.1016/j.prostaglandins.2023.106704>

## Physiological Aspects of the Association Between Age, Gender, Vitamin D Levels and Obesity in The Iraqi Province of Al-Muthanna

Hanaa Ali Aziz <sup>1</sup>

Ibrahem A. abdulzahra <sup>2</sup>



© 2024 The Author(s). This open access article is distributed under a Creative Commons Attribution (CC-BY) 4.0 license.

### Abstract

*Background: Obesity is an excessive accumulation of body fat that poses significant health risks. The study aimed to evaluate the impact of obesity on gender, age, vitamin D deficiency, and other factors. The current investigation analyzed sixty samples. Twenty men and forty women, weighing between 70 and 100 kg, were included in the sample. They were between the ages of 25 and 55. According to the research, there is a statistically significant ( $P<0.05$ ) rise in females compared to males and in the 35–45 age range when compared to other age groups. Eventually, the study found that the amount of vitamin D had significantly decreased at ( $P<0.05$ ).*

**Keywords:** Obesity; Age; Gender; Vitamin D; Iraq.



<http://dx.doi.org/10.47832/MinarCongress12-08>



<sup>1</sup> College of Science, Al-Muthanna University, Iraq [hanabio-1983@mu.edu.iq](mailto:hanabio-1983@mu.edu.iq)



<sup>2</sup> College of Science, Al-Muthanna University, Iraq



## Introduction

Obesity can be defined as having too much body fat. A cut-off point for the excess fatness in adolescents and children who are obese or overweight isn't widely agreed upon (Sahoo *et al.*, 2015). The social, economic, and technological advancements made during the past few decades have unintentionally contributed to the obesity pandemic in the US. Food is abundant and reasonably priced, and fast-food restaurants and prepackaged items with a high calorie density are easy to find. Because of labor-saving technologies, physical activity that was formerly a component of daily life has substantially decreased. Finally, A sedentary lifestyle is encouraged by the constant presence of electronic gadgets in homes, particularly for young people (Pi-Sunyer, 2002). Body Mass Index (BMI), which is calculated by dividing weight in kg by height in square meters, is applied for defining obesity. Adults with a BMI of (25–29.90) kg/m<sup>2</sup> are considered overweight, and those with a BMI of 30kg/m<sup>2</sup> or higher are considered obese Jensen *et al.* (2014).

For teenagers and children between the ages of two and eighteen, a percentile system depending on the child's age and gender is advised rather than using BMI Fitch et al. (2013). It is well accepted that an imbalance between the expenditure and consumption of energy is causes a rise in obesity, and that the lifestyle choices and food preferences are highly connected with increases in the positive energy balance. Nevertheless, Accumulating data suggests that an individual's genetic profile is a key factor in obesity (Birch and Davis, 2001). On chromosome 16q12.2, FTO (fat mass and obesity-related) gene was discovered. This gene is linked to severe obesity in both children and adults, as well as early onset. (Dina *et al.*, 2007). Even though the exact origins of obesity are not known, a complicated interaction appears to exist between psychological, biological, and behavioral factors like the genetics, socioeconomic status , and cultural influences, Skelton *et al.*, (2011). Obesity was connected to epigenetics, microorganisms, increased fecundity, maternal age, endocrine disruptors, sleep deprivation, intrauterine and intergenerational effects, pharmacological pathogenesis, and more (McAllister et al, 2009). Excessive weight is linked to several medical conditions, which include high blood pressure, hypothyroidism, polycystic ovarian syndrome (PCOS), type 2 diabetes, gallbladder disease, Cushing's syndrome, and a few neurological problems (Apovian, 2016).

## Materials and method

In this experiment, a total of 60 blood samples from people weighing between 70 and 100 kg were taken. Every individual had data recorded, including blood group, gender, and age. Everybody's weight has been measured as well. A biochemical test was performed on each sample for the determination of the levels of vitamin D. They were between the ages of 25 and 55. The study was carried out in 2020 between March and October. Each subject had two milliliters of venous blood drawn and placed in plain tubes. The obtained blood was centrifuged, and the serum was taken out and stored in a plastic tube labeled for vitamin D measurement.

## Vitamin D concentration test

The Bio-Autolyzer, a comprehensive system comprising calibrator and control reagents, was utilized to measure the vitamin D concentration, a biochemical parameter.

## Results and Discussion

In comparison to other age groups, Figure 1 indicates a significant ( $P < 0.05$ ) increase in the 35–45 age range. These results may be due to decrease in the metabolic activity of people, as with age, Metabolism significantly decreases due to reduced physical activity of the internal organs and limited movement from people staying at home (Heo *et al.*, 2006). Accompanied by an unhealthy diet and eating various types of foods and thus a decrease in caloric burning, all of which leads to weight gain With age. (Blüher *et al.*, 2011).

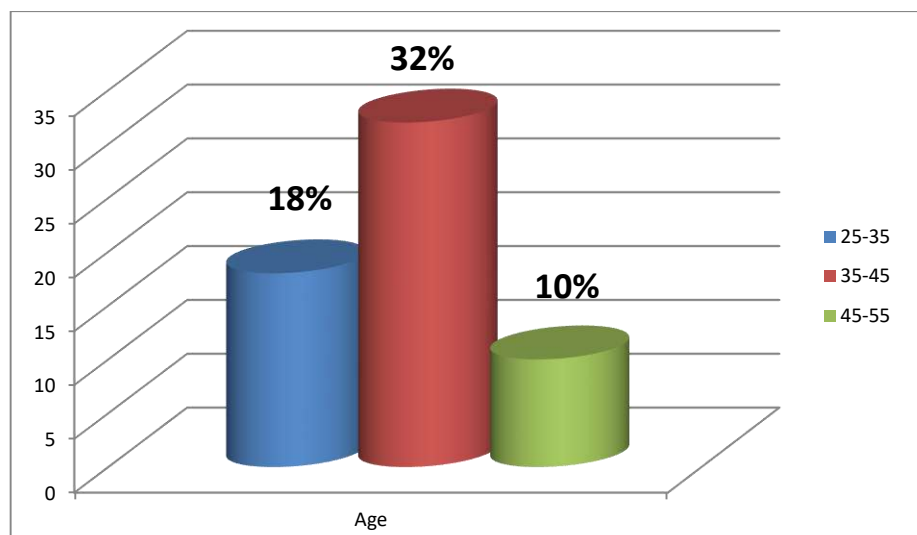


**Figure 1-** The relative of the obesity infection with age.

The study noted a significant increase at ( $P < 0.05$ ) in females compared with males Figure (2). These results may be due to several reasons, the most important of which are the samples collected, the numbers of females were more than males and because the stress that women

suffer, which results in an increase in body fat because of the increase in the secretion of the hormone cortisone (Sakurai *et al.*, 2006). Also due to aging and the entry of females into the menopause stage, which leads to a series of physiological changes In the body, such as a decrease in the rate of metabolism, which causes the accumulation of fat, in addition, the amount of fat in female body is more than in the male(Simoncig Netjasov *et al.*, 2016) and (Shah, 2009). So, any imbalance that leads to obesity as pregnancy that occurs in females, especially pregnancy at later ages. It will be difficult to lose weight as a result of pregnancy(Shah, 2009).Also, lack of exercise, sitting for long hours, eating food and taking medication, as all of these are helpful factors that increase the chance of obesity(Menegoni *et al.*, 2009).

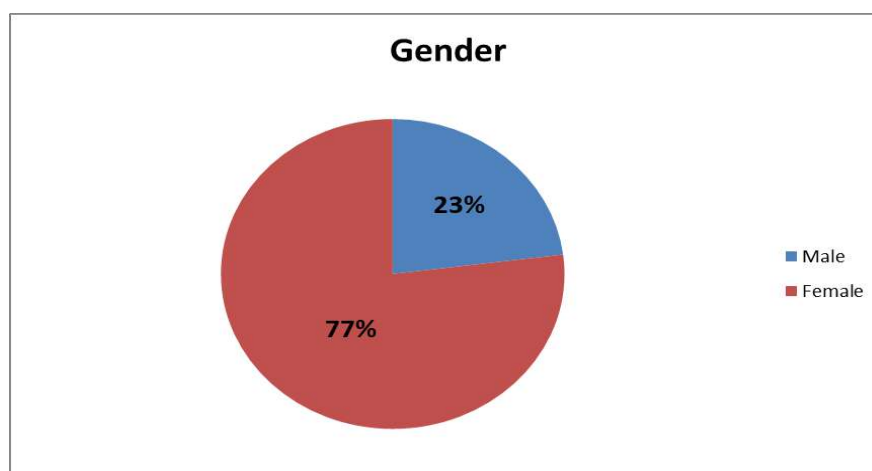


**Figure 2-** The percentage of males and females with obesity.

Also, the current study noted a significant decreased at ( $P < 0.05$ ) in vitamin D figure (3). There are a several of obesity causes that cause a deficiency in vitamin D, and most significant of these causes is the lack of food entering the body, which has a role in increasing the amounts of vitamin D in the body or increasing the consumption of ready-made food, which causes an increase in the amount of fat in the body and thus reduces the absorption of the vitamin D (Himbert *et al.*, 2017). The sun is one of the natural sources of vitamin D, so the lack of sunlight exposure will impede the formation and building of vitamin D in the skin, noting that people who suffer from obesity are exposed to equal amounts of sun compared to people of moderate weight, but the difference is in the response to this vitamin to manufacture it. And its composition, in addition, tablets and medicines that are taken by some people by way may also be a cause of a decrease in the level of vitamin in the serum.(Gallagher *et al.*, 2014).

Also changes in metabolism rates results in increasing obesity, and thus decreasing the amount of vitamin D in the serum, as well as changes related to the manufacture of proteins or

an increase in the size of cells and body tissues, all of which are factors that ultimately lead to a decrease in the level of vitamin in the body (Botella-Carretero *et al.*, 2007). Low vitamin levels in obese individuals are thought to reduce the amount of calcium absorbed by their bones compared to ordinary weight individuals, resulting in an increase in metals and a thickening of the bone cortex (Evans *et al.*, 2015). It is necessary to know the relationship of obesity in children, the lack of calcium in the bones, the increase in rickets, and thus a decrease in the amount of vitamin D absorbed by the bone.. (Dimitri *et al.*, 2012).

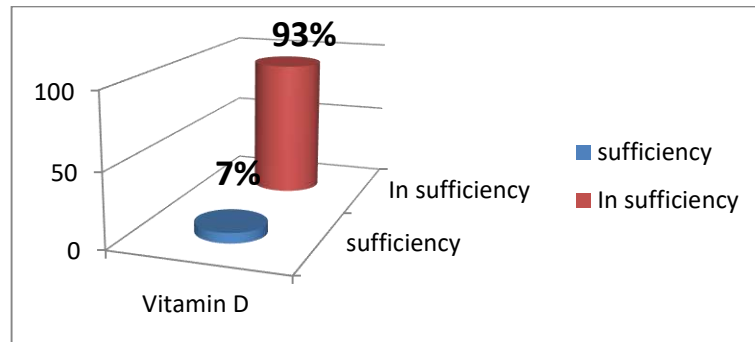


**Figure 3-** The percentage of vitamin D deficiency with obesity.



## REFERENCES

- Apovian, C. M. (2016). Obesity: definition, comorbidities, causes, and burden. *Am J Manag Care*, 22(7 Suppl), s176-85.
- Blüher, S., Meigen, C., Gausche, R., Keller, berhard, Pfäffle, R., Sabin, M., Werther, G., Odeh, R., & Kiess, W. (2011). Age-specific stabilization in obesity prevalence in German children: a cross-sectional study from 1999 to 2008. *International Journal of Pediatric Obesity*, 6(sup3), e199-206.
- Botella-Carretero, J. I., Alvarez-Blasco, F., Villafruela, J. J., Balsa, J. A., Vázquez, C., & Escobar-Morreale, H. F. (2007). Vitamin D deficiency is associated with the metabolic syndrome in morbid obesity. *Clinical Nutrition*, 26(5), 573–580.
- Davison, K. K., & Birch, L. L. (2001). Childhood overweight: a contextual model and recommendations for future research. *Obesity Reviews*, 2(3), 159–171.
- Dimitri, P., Bishop, N., Walsh, J. S., & Eastell, R. (2012). Obesity is a risk factor for fracture in children but is protective against fracture in adults: a paradox. *Bone*, 50(2), 457–466.
- Dina, C., Meyre, D., Gallina, S., Durand, E., Körner, A., Jacobson, P., Carlsson, L. M. S., Kiess, W., Vatin, V., & Lecoœur, C. (2007). Variation in FTO contributes to childhood obesity and severe adult obesity. *Nature Genetics*, 39(6), 724–726.
- Evans, A. L., Paggiosi, M. A., Eastell, R., & Walsh, J. S. (2015). Bone density, microstructure and strength in obese and normal weight men and women in younger and older adulthood. *Journal of Bone and Mineral Research*, 30(5), 920–928.
- Fitch, A., Fox, C., Bauerly, K., Gross, A., Heim, C., Judge-Dietz, J., & Webb, B. (2013). Prevention and management of obesity for children and adolescents. *Institute for Clinical Systems Improvement*. ([Http://Bit. Ly/2DrvBVv](http://bit.ly/2DrvBVv)).
- Gallagher, J. C., Smith, L. M., & Yalamanchilia, V. (2014). Incidence of hypercalciuria and hypercalcemia during vitamin D and calcium supplementation in older women. *Menopause (New York, NY)*, 21(11), 1173.
- Heo, M., Pietrobelli, A., Fontaine, K. R., Sirey, J. A., & Faith, M. S. (2006). Depressive mood and obesity in US adults: comparison and moderation by sex, age, and race. *International Journal of Obesity*, 30(3), 513–519.
- Himbert, C., Ose, a J., Delphan, M., & Ulrich, C. M. (2017). A systematic review of the interrelation between diet-and surgery-induced weight loss and vitamin D status. *Nutrition Research*, 38, 13–26.

- Jensen, M. D., Ryan, D. H., Apovian, C. M., Ard, J. D., Comuzzie, A. G., Donato, K. A., Hu, F. B., Hubbard, V. S., Jakicic, J. M., & Kushner, R. F. (2014). AHA/ACC/TOS guideline for the management of overweight and obesity in adults: a report of the American College of Cardiology/American Heart Association Task Force on Practice Guidelines and The Obesity Society. *Journal of the American College of Cardiology*, *63*(25 Part B), 2985–3023.
- McAllister, E. J., Dhurandhar, N. V., Keith, S. W., Aronne, L. J., Barger, J., Baskin, M., Benca, R. M., Biggio, J., Boggiano, M. M., & Eisenmann, J. C. (2009). Ten putative contributors to the obesity epidemic. *Critical Reviews in Food Science and Nutrition*, *49*(10), 868–913.
- Menegoni, F., Galli, M., Tacchini, E., Vismara, L., Caviglioli, M., & Capodaglio, P. (2009). Gender-specific effect of obesity on balance. *Obesity*, *17*(10), 1951–1956. <https://doi.org/10.1038/oby.2009.82>
- Pi-Sunyer, F. X. (2002). The obesity epidemic: pathophysiology and consequences of obesity. *Obesity Research*, *10*(S12), 97S-104S.
- Sahoo, K., Sahoo, B., Choudhury, A. K., Sofi, N. Y., Kumar, R., & Bhadoria, A. S. (2015). Childhood obesity: causes and consequences. *Journal of Family Medicine and Primary Care*, *4*(2), 187.
- Sakurai, M., Miura, K., Takamura, T., Ota, T., Ishizaki, M., Morikawa, Y., Kido, T., Naruse, Y., & Nakagawa, H. (2006). Gender differences in the association between anthropometric indices of obesity and blood pressure in Japanese. *Hypertension Research*, *29*(2), 75–80. <https://doi.org/10.1291/hypres.29.75>
- Simoncig Netjasov, A., Tančić-Gajić, M., Ivočić, M., Marina, L., Arizanović, Z., & Vujović, S. (2016). Influence of obesity and hormone disturbances on sexuality of women in the menopause. *Gynecological Endocrinology*, *32*(9), 762–766.
- Skelton, J. A., Irby, M. B., Grzywacz, J. G., & Miller, G. (2011). Etiologies of obesity in children: nature and nurture. *Pediatric Clinics*, *58*(6), 1333–1354.

## Effect The Inclusion of Different Polymer Types On Physical Properties of Heat Cure Acrylic Resins

Marwah Hussein Abdulsattar <sup>1</sup>

Alaa Hussein Jasim <sup>2</sup>



© 2024 The Author(s). This open access article is distributed under a Creative Commons Attribution (CC-BY) 4.0 license.

### Abstract:

**Background:** Poly methyl methacrylate is still utilized as a foundation material for dentures because of the many beneficial properties it has, including its simplicity of processing, stability in the oral environment, convenience in terms of repair, and better aesthetics. However, the content is not excellent in every respect. Thus, the present study aimed to evaluate incorporation of different types of polymers on heat cure acrylic resins.

**Materials and methods:** In this study, 20 disc-shaped samples of heat cure acrylic resins reinforced with chitosan and corn starch powder have designed with dimensions of  $(12\pm 0.1)$  mm diameter and  $(2\pm 0.1)$  mm thickness. Then, they were divided into two major groups according to type of material included. 1% of chitosan and corn starch powder were added. The surface roughness test was measured by using the profilometer digital device.

**Results:** Descriptive statistic results showed that there was a significant difference between the two major groups. Chitosan group revealed the highest mean value of surface roughness which was (1.57), while corn starch group showed the lowest mean value which was (0.62).

**Conclusion:** 1% of chitosan powder had a negative effect on surface texture of acrylic resin in comparison with corn starch powder.

**Keywords:** Heat Cure Acrylic Resin; Chitosan; Corn Starch; Roughness.

---

 <http://dx.doi.org/10.47832/MinarCongress12-09>

<sup>1</sup>  College of Health and Medical Techniques, Middle Technical University, Iraq  
[marwahhusseinlazzawi87@gmail.com](mailto:marwahhusseinlazzawi87@gmail.com)

<sup>2</sup>  College of dentistry, Al Mustansiriya University, Iraq

## Introduction

Since older populations develop, there is a need for dentures to return their stomatognathic functions and enhance their lives' quality <sup>(1)</sup>. Dentures bases which are made by polymethylmethacrylate have many advantages such as acceptable esthetic value, low cost and ease of manipulation. However, it does have certain drawbacks, such as inadequate surface hardness. Increased water sorption, and low impact resistance, the latter of which is the major reason denture base resins break <sup>(2)</sup>. Thus, this material has been strengthened with materials including metal oxide, clay minerals, and carbon graphite fibers to improve their properties <sup>(3)</sup>.

The biodegradable polymers, such as chitosan and starch come from renewable sources which are used for overcoming severe environmental problems resulting from incorrect synthetic plastic material disposals, while the non-biodegradable polymers are derivatives of petroleum sources <sup>(4)</sup>. The manufactured starch–chitosan based films help to improve the properties of each one, thereby they add their good properties and compensate for some restrictions <sup>(5)</sup>.

In the denture bases, irregularities and porosities are regarded undesirable characteristic since they affect their mechanical, physical and aesthetic characteristics. Denture bases are usually in contact with different oral microorganism like *Candida albicans* <sup>(6)</sup>.

The present study aimed to assess the impact of addition of chitosan and corn starch powders on surface texture of acrylic resin denture base material and investigate newly developed denture's base resins.

## Materials and methods

Twenty-disc-shaped of heat cure acrylic resin specimens with  $(12\pm 0.1)$  mm dimension and  $(2\pm 0.1)$  mm thickness have been designed <sup>(7)</sup> as shown in fig:(1). Then, they were divided into two major groups according to types of materials incorporated. Firstly, 1% of each Chitosan, corn starch powder and 21g of acrylic resin were weighed by using an electrical balance as shown in table (1) , fig (2). Then, they were diluted with a  $\text{CH}_3\text{COOH}$  acid and distilled water in a glass container as shown in fig (3). After that, they were mixed by using magnetic stirrer for thirty minutes. To decrease the risk of phase separation and particle agglomeration, acrylic powder was blended really quick with the suspension of monomer and filler by using a clean spatula. The mixing was done in a dry



and clean mixing bowl for 30 seconds according to the guidelines of the manufacturer, then, the mixture was covered and allowed to stand for around 20 minutes at 23°C. The traditional method (flasking method) have been used, and when acrylic resin reached the dough stage, it was taken out of the jar, rolled, and then put into the molds. Metal to metal contact was established by sealing the two halves of the flask together under pressure (hydraulic press) and held at 20 bar for five minutes, as seen in figure (4).

Then, they were clamped and transferred to the water bath for approximately one and a half hour at 74°C. Then, the acrylic specimens were deflasked and removed from the die stone molds. Finally, all the specimens were finished by using burs to remove any excess of acrylic resin. Then, they were put in distilled water containers for 48 hrs. at 37°C before the specimens have been tested. Finally, all the samples subjected to surface roughness test by using the profilometer device to determine chitosan and corn starch powder impact on acrylic resin's surface texture <sup>(8)</sup>. The sharp stylus of the apparatus comes in contact with the sample surface to record all the peaks and recesses of their surface by its scale as shown in fig (5).

## Results

**Table 1-** Descriptive Statistics of roughness between groups

	<b>Gropus</b>	<b>N</b>	<b>Mean</b>	<b>SD</b>	<b>Max-Min</b>	<b>T-test</b>	<b>P-value</b>
Roughness	A- Chitosan	10	1.57	0.82	2.46-.11	2.60	0.02
	B- Starch	10	0.62	0.503	1.36-.25		

Table (2) showed that the highest mean value of roughness was (1,57) for chitosan group, while the lowest value was for corn starch group which was (0.62).

**Table 2-** Mixing ratio of acrylic resin with 1% of chitosan and corn starch powder

<b>Amount of reinforcement (addition)</b>	<b>Amount of chitosan</b>	<b>Amount of corn starch</b>	<b>Amount of polymer</b>	<b>Amount of Monomer</b>
0%	0%	0%	22 g	10ml
1% of chitosan	1%	—	21g	10ml
1% of corn starch	—	1%	21g	10ml

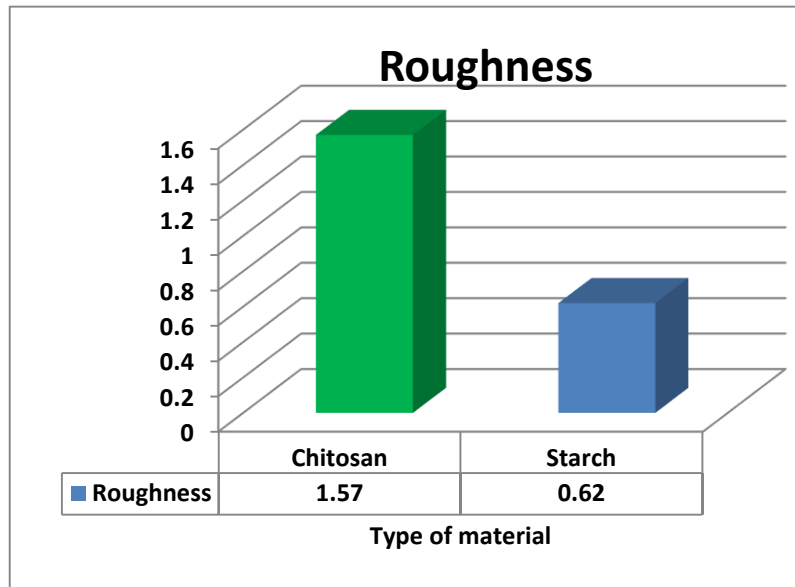


**Figure 1-** Bar chart showing the surface roughness between groups

## Discussion

Acrylic resin denture base is widely use due to a combination of benefits rather than a single outstanding feature, including its popularity in meeting aesthetic criteria and having a clearly defined processing technique in dental applications<sup>(9)</sup>. However, this material is not perfect in every way, especially when it comes to fulfilling the mechanical and physical needs of a prosthesis <sup>(10)</sup>.

For more improvement of the PMMA characteristics like (impact strength, hardness strength surface roughness), many methods of mechanical reinforcements and chemical modifications that use different fiber and micro-nanoparticle types were documently recently <sup>(11)</sup>.

Surface roughness of denture materials is of clinical relevance because it may impact the buildup of plaque and discoloration of the prosthesis <sup>(12)</sup>. Although plays a role in the trapping of microorganisms on acrylic surfaces, considerably larger numbers of microbes were discovered on roughened surfaces in comparison to smooth surface <sup>(13)</sup>.

According to statistical analysis results in the table (2) and fig (6), the addition of (1%) of chitosan powder to a heat cure acrylic resin in order to improve their properties so that it could withstand the load when the prosthesis were used. It had a negative effect on their surface roughness in comparison with corn starch powder that can be explained by the fact that the surface roughness formation may be resulted from the deficient homogeneity of mixture during

mixing, as well as various parameters of monomer and polymer mixing e.g. pressing pressures and mixing temperatures and their effect on the formation of pores up on acrylic resin surface (1), (14) .

In contrast, the results of corn starch powder addition appeared to have positive effect on surface roughness of acrylic resin by decreasing surface roughness that may be due to starch is not truly thermoplastic polymer, and it can be melted and flown at high temperatures under pressure and shear <sup>(5)</sup> (15). The main limitations of our study included unavailability of more previous researchers that have used chitosan and corn starch powder with any types of acrylic resin in their studies.



Figure 2- Disc-shaped wax specimens

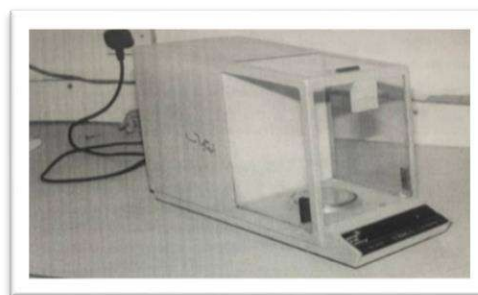


Figure 3- Sensitive Balance high accuracy



Figure 4- Heating plate and magnetic stirrer



Figure 5- Packing of the crylic resin by hydraulic press

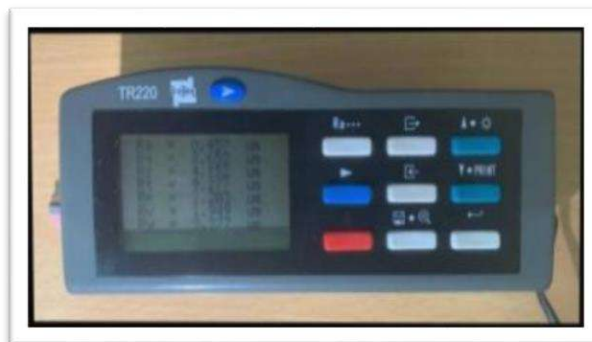


Figure 6- TR220 Portable Roughness

## References

- Ismiyati T, Alhasyimi AA, Siswomihardjo W. The Effect of Chitosan and Acrylate Acid Complex into Acrylic Resin as Denture Material Against Fibroblast and Inflammatory Cells. *Journal of International Dental & Medical Research*. 2021;14(4).
- AlFuraiji N, Atallah W, Qasim SSB. Evaluation of Flexure Strength of Heat Cure Acrylic Resin Reinforcement with Nano Al<sub>2</sub>O<sub>3</sub> After Polishing with Different Abrasive Materials. *Journal of Techniques*. 2023;5(2):134-40.
- Jaber MA-R. Evaluation of the effect of different surface treatment on the transverse strength of the repaired acrylic denture base resin cured by two different techniques. *Mustansiria Dental Journal*. 2010;7(2):204-13.
- Luchese CL, Pavoni JMF, Dos Santos NZ, Quines LK, Pollo LD, Spada JC, et al. Effect of chitosan addition on the properties of films prepared with corn and cassava starches. *Journal of food science and technology*. 2018;55:2963-73.
- Ali Abdul Amir AM. Preparation and Characterization of Biodegradable Films From Sago Starch and Chitosan Blends: *Universiti Putra Malaysia*; 2004; 15(1):72-79..
- Ismiyati T, Alhasyimi AA. Effect of Chitosan and Acrylic Acid Addition to Acrylic Resin on Porosity and *Streptococcus mutans* Growth in Denture Base. *European Journal of Dentistry*. 2023;17(03):693-8.
- Abdulsattar MH. Assessment of the surface roughness and hardness of acrylic resin after incorporation of sodium fluoride salts (An In-vitro Study). *Mustansiria Dental*
- Olewi JK, Hamad QA. Studying the mechanical properties of denture base materials fabricated from polymer composite materials. *Al-Khwarizmi Engineering Journal*. 2018;14(3):100-11.
- Al-Jorani LE, Al-Azzawi SI, Yaseen IN. Comparing & Evaluating the Effect of Air-Powder Polishing System on the Hot Cure Acrylic Denture Base Material Cured by Different Methods. *Al Mustansiriyah Journal of Pharmaceutical Sciences*. 2015;15(2):1-12.
- Hardita A, Ismiyati T, Wahyuningtyas E. Effect of addition titanium dioxide nanoparticles as acrylic resin denture base filler on cytotoxicity. *Majalah Kedokteran Gigi Indonesia*. 2019;5(2):86-91
- Alraziqi ZNR. Water temperature effect on hardness and flexural strength of (PMMA/TiO<sub>2</sub> NPs) for dental applications. *Baghdad Science Journal*. 2022;19(4):0922.
- Zissis AJ, Polyzois GL, Yannikakis SA, Harrison A. Roughness of denture materials: a comparative study. *International Journal of Prosthodontics*. 2000;13(2)).
- Ansarifard E, Zahed M, Azarpira N, Jooyandeh S. Investigating the biocompatibility, flexural strength, and surface roughness of denture base resin containing copper oxide nanoparticles: An in vitro study. *Heliyon*. 2023;9(9).
- Nejatian T, Nathwani N, Taylor L, Sefat F. Denture base composites: Effect of surface modified nano- and micro-particulates on mechanical properties of polymethyl methacrylate. *Materials*. 2020;13(2):307.
- Rasan DS, Farhan FA. Influence of Zirconia and Polymerized Microfiller on Some Properties of Polymethyl Methacrylate Denture Base. *Al-Khwarizmi Engineering Journal*. 2024;20(1):42-50.



## Comparison of Cytomegalovirus Diagnosis Methods in Iraqi Aborted Women

Tabarak Sabah Jassim <sup>1</sup>

Noor A. Jihad <sup>2</sup>

Rusul Waleed Ali <sup>3</sup>



© 2024 The Author(s). This open access article is distributed under a Creative Commons Attribution (CC-BY) 4.0 license.

### Abstract:

*Cytomegalovirus (CMV) is a ubiquitous member of the Herpes viridian family, subfamily Beta herpes. CMV is the major infectious cause of congenital infection and hearing loss in children as well as an important pathogen in immune compromised patients.*

**Aim of Study:** *The current research aims to compare between Enzyme Immunoassay and Chemi-Luminescence assay in CMV infected aborted women.*

**Materials and Methods:** *This study was conducted during the period from August 2023 to April 2024. Sixty blood serum were collected and divided into two groups, thirty blood serum were collected from aborted women, and thirty healthy women as a control group. Ethical approval has been warranted by the Ministry of Health (No. 4790 dated 27\11\2023).*

**Results:** *The results revealed that anti-CMV IgG was high in both Chemi-Luminescence assay and Enzyme Immunoassay test, but the Chemi-Luminescence assay percent was increased by 23% and anti-CMV IgM percent was 10%, ages 20-30 years old represented the largest percentage (66.5%) of observed abortions by Enzyme Immunoassay test and 63.7% for Chemi-Luminescence assay, and single abortion had ratio by both assay.*

**Conclusion:** *Chemi-Luminescence assay could be used for ideal detection of CMV associated abortion in Iraqi women.*

**Keywords:** *Chemi-Luminescence; Cytomegalovirus.*



<http://dx.doi.org/10.47832/MinarCongress12-10>

<sup>1</sup> Department of Plant Biotechnology, College of Biotechnology, Al-Nahrain University, Baghdad, Iraq

<sup>2</sup> Department of Plant Biotechnology, College of Biotechnology, Al-Nahrain University, Baghdad, Iraq

<sup>3</sup> Medical Genetic, Iraqi center for cancer research and medical genetics, Mustansiriyah University, Baghdad- Iraq

## Introduction

Abortion is describing as defined as pregnancy loss during the first trimester of pregnancy (less than Twelve weeks of gestation). It is among the most common unfavorable pregnancy outcomes (1). The placenta is a critical barrier between fetal and maternal blood circulation (2). The integrity of this barrier could be affected by trans placental transmission of some viruses such as human CMV (3) Out of the more than a hundred known Herpes viruses, eight routinely infect humans: herpes simplex virus types 1 and 2 (HSV-1 and 2), cytomegalovirus (CMV), Epstein-Barr virus (EBV), varicella-zoster virus (VZV), human herpes virus 6 (HSV-6), human herpes virus 7 (HSV-7), and Kaposi's sarcoma virus or human herpes viruses 8 (HSV-8)(4). Every herpes virus has the ability to cause latent infection in particular human tissues, which sets them apart from one another (5). Human CMV is the most frequent cause of congenital infection in humans. Globally, HCMV infection is quite prevailing, with sero-positive rates variable from 40% in wealthy nations to 99% in poor nations (6). The current research aims to compare between rapid test, TORCH and immunological test COBAS e41, in CMV infected aborted women.

## Materials and Methods:

This study was conducted during the period from August 2023 to April 2024. Sixty blood serum were collected and divided into two groups, thirty blood serum were collected from aborted women, and thirty healthy women as a control group. The age of patients and healthy females ranged between (17-40) years. The test was performed by using 5 ml of blood sample, transported to plain tubes, and allowed to clot at room temperature for 30 minutes. Sera were parted by centrifugation until used in recognition of Cytomegalovirus by serological examination. Enzyme Immunoassay test kit was used for detection of IgM and IgG percent (Bio check/USA).

## Results and Discussions

Thirty serum samples of aborted and healthy women were examined using Enzyme Immunoassay test. The results showed that fifteen samples were positive for anti- CMV IgG (50%), five tested positives for the IgM (16.6%), and ten samples were negative for CMV (33.4%).

**Table 1-** Detection of CMV in aborted women using Enzyme Immunoassay test

Enzyme Immunoassay test	Patients (30) samples		Control (30) samples	
	No.	Percentage %	No.	Percentage %
<b>IgG</b>	15	50%	0	00%
<b>IgM</b>	5	16.6%	0	00 %
<b>CMV (-ve)</b>	10	33.4%	0	00%

Negative: -ve

Thirty serum samples from healthy and aborted women were observed using Chemi-Luminescence assay for detection of anti-CMV IgG and IgM antibodies and the results revealed that 22 samples tested positive for IgG (73.3%) and 2 samples that tested positive for IgM (26.6%), with the control group containing of healthy women.

**Table 2-** Detection of CMV in aborted women using by Chemi-Luminescence assay

Chemi-Luminescence assay	Patients (30) samples		Control (30)samples	
	No.	Percentage %	No.	Percentage %
<b>IgG</b>	22	73.3%	0	00%
<b>IgM</b>	8	26.6%	0	00 %

Anti-CMV IgG tested positive in 50% of cases using Enzyme Immunoassay test, while the Chemi-Luminescence assay showed a higher prevalence of 73.3% (Table 3). And 26.6% of tested samples tested were positive for IgM by chemi-Luminescence assay compared to 16.6% of by Enzyme Immunoassay Test.

**Table 3-**Comparing detection of CMV by Enzyme Immunoassay test and chemi-Luminescence assay

Category	Enzyme Immunoassay test		Chemi-Luminescence assay	
	No.	Percentage (%)	No.	Percentage (%)
<b>IgG</b>	15	50%	22	73.3%
<b>IgM</b>	5	16.6%	8	26.6%

The results revealed that ages of 20 and 30 had highest abortion rates, with 66.6% for Enzyme Immunoassay test and 63.7% for chemi-Luminescence assay, Whereas age group of

31 to 40 years old had the lowest abortion percentage of 13.4% for Enzyme Immunoassay test and 13.6% for the Chemi-Luminescence assay (Table -4).

**Table 4-** Distribution of aborted women by age group

Variables	Category	Enzyme Immunoassay test		Chemi-Luminescence assay	
		No.	Percentage (%)	No.	Percentage (%)
Age Groups	<20	3	20%	5	22.7%
	20-30	10	66.6%	14	63.7%
	31-40	2	13.4%	3	13.6%
	Total	15	100%	22	100%

The results showed that cases resulting from a single abortion were more likely to have an abortion, with 53.3% of cases tested by the Enzyme Immunoassay test and 59% observed by the Chemi-Luminescence assay. In contrast, cases including four abortions were less likely to have an abortion, with the lowest percentage (6.7% for the Enzyme Immunoassay test and 9.3% for Chemi-Luminescence assay (Table 5).

**Table 5-** Distribution of patients according to their recurrent abortion

Variables	Category	Enzyme Immunoassay		Chemi-Luminescence assay	
		No.	Percentage (%)	No.	Percentage (%)
Abortion number	Once	8	53.3%	13	59%
	Twice	4	26.7%	4	18.1%
	Thrice	2	13.3%	3	13.6%
	Four times	1	6.7%	2	9.3%
	Total	15	100%	22	100%

Primary pregnancy, which disturbs 14% to 16% of naturally conceived pregnancies, is a general time for abortions (7). An irregular uterine cavity, parental karyotypes, endocrine variables, infection, and/or autoimmune are all potential reasons of abortions (8). The high rate of CMV detection through pregnancy is a suitable tool for analyzing the relationship between first-trimester spontaneous abortion and infections, even though causal relationships between the two are hard to establish. This relationship aims to lower maternal and fetal morbidity and mortality (9).

Simultaneously, TORCH showing is presently frequently and widely used in clinical gynecology to display for suspected cases of congenital and perinatal infections (10). However, it has been discovered that this screening method is limited to a small number of infectious agents (Toxoplasma, Rubella, CMV, and HSV) and lacks specificity and sensitivity because it



depends on antibody testing (11). It is also requested at a late stage of signs (12). It should be noted that, utilizing identical abortion cases, this study was the first to directly compare the serological enzyme Immunoassay and Chemi-Luminescence assay (13).

But both assays detected a significant amount of IgG, the Chemi-Luminescence assay outperformed the enzyme Immunoassay by 23%, but the IgM CMV virus was only slightly higher by 10% (14). Higher ratios were perceived in that report, mostly for the IgG CMV virus, for unclear reasons (15). Other potential contributing factors contain technical difficulties, specimen handling and sampling, sources of pathogen-specific antibodies, and the accuracy of antibody titer analyses. 11.1% of spontaneous abortion samples had CMV detected (16). This recommends a link between abortion and infection and an increase in seropositive CMV IgG (17). This could be due to CMV affects cellular metabolism and activates other viruses that co-infect the cells, producing subclinical inflammation (18).

As a result, Enzyme immunoassay results varied greatly between researches, whether conducted in the region or in Iraq (19). This suggests an absence of consistency and trustworthiness. Such diversity may be recognized to various stages of infection, disparities in the hosts' immune response to various pathogens, technological efficiency and/or accuracy of collecting various sample types, or data analysis methodology (20).

All of the samples of aborted women were between 17 and 40 years old. Ages of 20–30 years old had the highest ratio (66.6%) for the immunoassay test ( ) and (63.7%) for the TORCH test. These results were consistent with a research in Kurdistan, Iraq (21, 22) which showed that 94% of positive results for ages 25–34. This is because younger ages (20–30) have a larger probability of becoming pregnant than older ages (31–40) (23). The frequency of testing four abortions was lower, with the lowest percentage being 6.7% for enzyme immunoassay and 9.3% for the chemi-luminescence test. These results were similar to those reported 67% and 54% of the samples had one abortion (24). In case series data analysis from several countries, 30–40% of newborns with BA had serological evidence of CMV infection (25). An immunoglobulin M (IgM) response was first seen on the hepatocyte canaliculi membranes of the newborns with BA in a Swedish investigation that discovered CMV DNA in half of the infants (26). It has been proposed that CMV IgM-positive BA is a distinct clinical entity that makes poorer than CMV IgM-negative BA (27). Serological analyses are highly sensitive and specific, and while antibody levels can decline with aging and severe immunosuppression, IgG seropositive is typically permanent (28).

These tests are used in recognition (29). Because the human cytomegalovirus can reactivate often during gestation and can still transmit to the fetus despite maternal immunity, pregnancy-related infections involving the virus are significantly more complicated than other diseases (30). Although the small sample size and short length of our study have limitations, it does detention the realities of a state. Supplementary research is requisite with bigger and more evenly distributed populations to confirm our results.

### **Conclusions:**

The Chemi-Luminescence assay might be used for ideal detection of CMV-associated abortion in Iraqi women. Compared to women in good health, there is a higher frequency of anti-CMV antibodies (IgG and IgM) among women who have had abortions.

### **Ethical Approval:**

The study was ethically approved by the Ministry of Health (decree order 4790 on 27/11/2023).

## References:

- Akunaeziri, U. A, Anyaka. C, Magaji. F.A, Ocheke. A. N. (2021). Cytomegalovirus Infection among Women with Recurrent Miscarriages. Tropical Journal of Obstetrics & Gynaecology Published by Journal Gurus; Vol. 38 No. 2.
- Arski, E.; Shenk, T. and Pass, R. (2007). Cytomegaloviruses. In: Fields of virology (Knipe, D. and Howley, p. ed.) 5 th ed., Lippincott. Philadelphia. 2701-2772.
- Arora N, Sadovsky Y, Dermody TS, Coyne CB. (2017). Microbial vertical transmission during human pregnancy. Cell Host Microbe. 21: 561-567.
- Casjens, S.; Mahy, B.W.J. and Regenmortel, v .(2010). MHV. Desk Encyclopedia of General Virology. Academic Press. Boston: p. 167.
- Giakoumelou S, Wheelhouse N, Cuschieri K, Entrican G, Howie SE, Horne AW. (2016). the role of infection in miscarriage. Hum Reprod Update. 22: 116-133.
- Gibson, W. (2008). Structure and formation of the *Cytomegalovirus* Virion. Curr. Top. Microbiol. Immunol. 325: 187- 204.
- Griffiths, P. D. (2002). The treatment of *Cytomegalovirus* infection. J. Antimicrob. Chemother. 49 (2): 243-253.
- Kenneson, A. and Cannon, M.J. (2007). Review and meta-analysis of the epidemiology of congenital *Cytomegalovirus* (CMV) infection. Rev. Med. Virol. 17(4): 253-276.
- Kheirandish F, Nazari H, Mahmoudvand H, Yaseri Y, Tarahi MJ, Fallahi Sh. (2016). Possible link between toxoplasma gondii infection and mood disorders in lorestan province, Western Iran. Arch Clin Infect 11(4):e36602–e36602.).
- Koonin, E.V.; Senkevich ,T.G. and Dolja ,V.V.(2006). The ancient Virus World and evolution of cells. Biol. Direct;1: 29.
- Koonin, E.V.; Senkevich ,T.G. and Dolja ,V.V.(2006). The ancient Virus World and evolution of cells. Biol. Direct;1: 29.
- La Scola B.; Desnues, C.; Pagnier, I.; Robert, C.; Barrassi, L.; Fournous, G.; Merchat, M; Suzan-Monti, M.; Forterre, P.; Koonin, E. and Raoult, D.(2008). The virophage as a unique parasite of the giant. Marseille Cedex, Nature .; 455(7209): 100–104.
- Lamichhane, S.; Malla, S. and Basnyat, S. (2007). Seroprevalence of IgM antibodies against the agents of TORCH infections among the patients visiting National Public Health Laboratory. Teku. Kathamndu. J. Nep. Health. Res. Council. 2: 21-25.
- Li YH, Marren A. (2018). Recurrent prgnanacy loss. Austraiian J General Pract . 47(7):432-436)
- Mahdi, B.; Saour, M.; and Salih, W. (2011). *Cytomegalovirus* infection in infertile women. J. ExpInteg. Med. 14: 273-276
- Murphy, E., Rigoutsos, I., Shibuya, T. and Shenk, T. E. (2003). Reevaluation of human *Cytomegalovirus* coding potential. Proc. Natl. Acad. Sci. U.S.A. 100: 13585-13590.
- Nishat. A. H, Satpathy. G, Chawla. R, Tandon. R. (2021). Multiplex PCR for Detection of Herpes Simplex Viruses Type-1 and Type-2, Cytomegalovirus, Varicella-zoster Virus, and Adenovirus in Ocular Viral Infections. Journal of ophthalmic and vision research; 16(1). 3-11.

- Paquet C, Yudin MH. (2013). Society of Obstetricians and Gynaecologists of Canada. Toxoplasmosis in pregnancy: prevention, screening, and treatment. *J Obstet Gynaecol Can.* 35(1):78–81.)
- Pass, R. F. and Boppana, S. (1999). Cytomegalovirus. In: *Viral Infections in Obstetrics and Gynaecology.* (Jeffries, D. J. and Hudson, C. N. Ed.). New York, U.S.A. 35-56.
- Azo, F. M, Akbay, C. (2016). Prevalence and risk factors of abortion among a sample of married women in Kurdistan Region of Iraq. *Zanco J. Med. Sci.*, Vol. 20, No. (3).
- Riley HD, J. R. (1997). History of the *Cytomegalovirus*. *South Med. J.* 90(2): 184-190.
- Sinclair, J. and Sissons, P. (2006). Latency and reactivation of human *Cytomegalovirus*. *J. Gen. Virol.* 87: 1763-1779.
- Sotoodeh, A.; Jahromil, J. and Jahrom, M. (2009). Seropositivity for cytomegalovirus in women with spontaneous abortion. PhD Thesis. University of Medical Science, Bander Abbas, Iran.
- Straface G, Selmin A, Zanardo V, De Santis M, Ercoli A, Scambia G. (2012). Herpes simplex virus infection in pregnancy. *Infectious Diseases in Obstetrics and Gynecology*: 1–6.
- Sugiura-Ogasawara, M, Suzumori. N. (2010). Genetic factors as a cause of miscarriage. *Curr Med Chem*; 17(29):3431-7.
- Umeh, E. U., Onoja, T. O., Aguru, C. U., & Umeh, J. C. (2015). Seroprevalence of cytomegalovirus antibodies in pregnant women, Benue State, Nigeria. *Journal of Infectious Diseases & Therapy* y.
- Varada, S. (2014). Mother to child transmission of CMV during pregnancy. *New Eng. J. Med.* 370:1316-1326.
- Yiska Weisblum 1, Amos Panet, Ronit Haimov-Kochman, Dana G Wolf. (2014). Models of vertical cytomegalovirus (CMV) transmission and pathogenesis. *Semin Immunopathology*; 10.1007/s00281-014- 0449.
- Akter, S., Karim, A. B., Mazumder, M. W., Rukunuzzaman, M., Nahid, K. L., Dey, B. P. & Khadga, M. (2022). A Comparative Study between Cytomegalovirus Immunoglobulin M-Positive and CMV Immunoglobulin M-Negative Biliary Atresia in Infants Attending a Tertiary Care Hospital in Bangladesh. *Pediatric Gastroenterology, Hepatology & Nutrition*, 25(5), 413.
- John, O. C., & Awopeju, A. T. (2024). Seroprevalence of cytomegalovirus (CMV) among pregnant women at a tertiary facility in southern Nigeria. *International Journal of Science and Research Archive*, 11(2), 455-464.
- Iijima, S. (2022). Pitfalls in the serological evaluation of maternal cytomegalovirus infection as a potential cause of fetal and neonatal involvements: a narrative literature review. *Journal of Clinical Medicine*, 11(17), 5006.
- Liu, M., He, H., Zhang, J., Xin, S., Lu, Q., Zhang, L., & Ren, W. (2024). Retinitis after haematopoietic stem cell transplantation with multiple intraocular viral infections (cytomegalovirus, Epstein–Barr virus and herpes simplex virus)-a case report. *BMC ophthalmology*, 24(1), 38.



## Modifications to Erdogan Method to Visualization of Skeletal System Using Dual Pigmentation with Red Alizarin and Alcian Blue

Nuha Hussam Abdulwahab <sup>1</sup>

Reem Saud Abed <sup>2</sup>

Lamyaa Khames Naif <sup>3</sup>



© 2024 The Author(s). This open access article is distributed under a Creative Commons Attribution (CC-BY) 4.0 license.



### Abstract

*Skeletal system dyeing is critical mode in anatomy to diagnose skeletal impairments. The point of this paper was to modernization dyeing and clearing mode of mice employing Alcian Blue- Alizarin Red S. The fetuses were, fixed, dyed, cleared, and preserved in glycerine with thymol crystals to prevent mold growth. This modulation stained the bone and the cartilage without harming the skeleton.*

**Keywords:** *Mice; Skeleton; Alizarin Red S; Alician Blue; Double Staining.*



<http://dx.doi.org/10.47832/MinarCongress12-11>

<sup>1</sup>  Faculty of Education for Pure science Tikrit University, Iraq [noha.h.Abdelwahhab@tu.edu.iq](mailto:noha.h.Abdelwahhab@tu.edu.iq)

<sup>2</sup>  Faculty of Physical Education Tikrit University, Iraq [reem.saud@st.tu.edu.iq](mailto:reem.saud@st.tu.edu.iq)

<sup>3</sup>  Faculty of Sciences Tikrit University, Iraq [lmyaa.m.khames@tu.edu.iq](mailto:lmyaa.m.khames@tu.edu.iq)

## Introduction

Teratology, is the science that specializes in studying the environment-induced impairments, this science began in the 1930s.(1). This science has recently begun in the early twentieth century, and developed greatly during recent years especially with the progress taking place in genetic, molecular biology, animal laboratory science, and toxicology.(2). Teratogenesis, is devastation of a critical number of cells oncoming of which the fetus is able to return by late proliferation. It is critical to remember the effects of drugs on pregnancy, and the 6 principles of teratology: Development stage, end points, genetic susceptibility, mechanisms, dose response and access(3). This mode of dyeing is too successful to stain skeleton of young rodent and fetal(4). Many researches registered methods to dyeing skeletons and clarification of mice bone and cartilage. Inouye developed Double staining mode in 1976(5). The bone genesis gets through two processes: Endochondral bone genesis gets after cells in mesenchymal condensations discriminate into chondrocytes. A cartilaginous extracellular matrix rich in collagen(II & X), glycosaminoglycans, and proteoglycans excreted by these cells. Chondrocytes submit to changes of stratified differentiation and programmed eath, enablment the substitution of cartilage by bone. Conversely, mesenchymal cells mean while intramembranous ossification, distinction straightly into bone-formation osteoblasts (6). Alcian blue dyeing cartilage linked robustly to sulfated GAGs and glycoproteins as a cationic dye and Alizarin red dyeing bone, linked to cationic metals like calcium as an anionic dye, (7). however, This research will expose to view modified double staining method for effective dyeing in mice fetuses skeleton

## Materials and Methods

Mice that were used in the experiment are *A Mus Musculus* fetuses. The fetuses were not skinned The method Consisted of three steps:

**1. Fixation:** Fetuses fixation was performed in 95% ethanol for 10 days to harding it, after the hardening the fetuses placed into pure acetone 24 hours to remove fats. The volume of ethanol and acetone should be more than fetus volume 10 times.

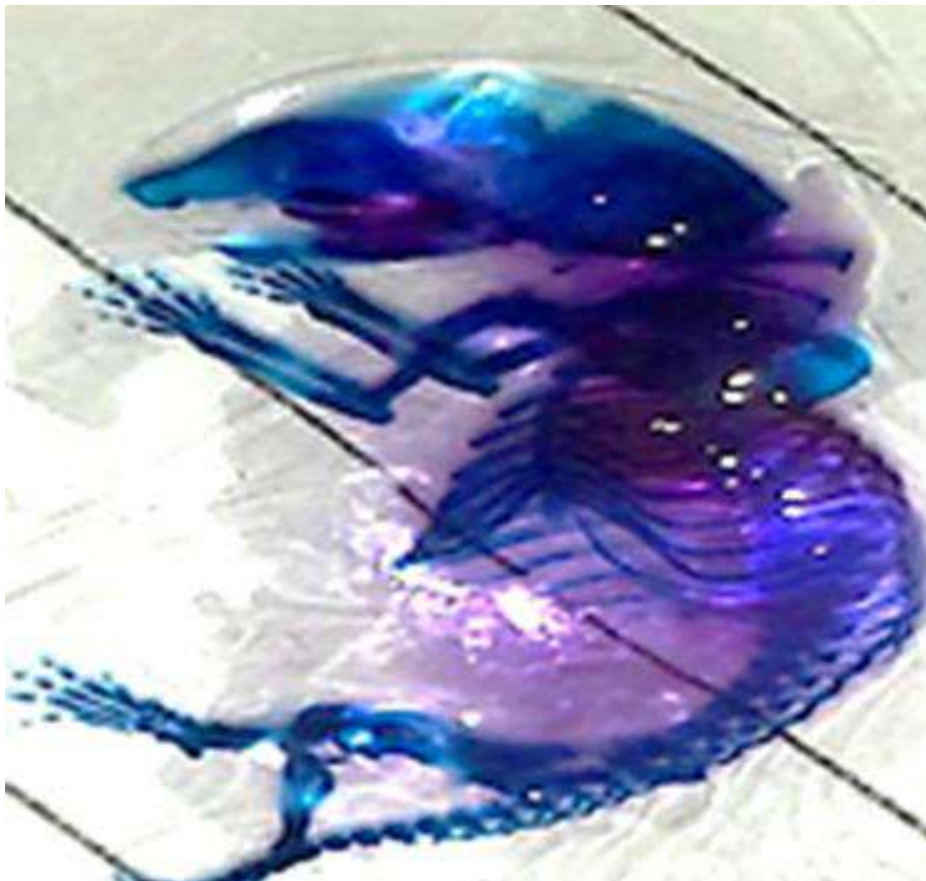
**2. Staining:** Staining was performed at a temperature of 40 °C for 4 days. Staining solution was prepared by dissolving Alcian blue 300 mg in 70% ethanol 100 ml, Alizarin red-s 100 mg dissolved in ethanol 95% 100 ml mixed together then 100 ml Glacial acetic acid added to the mixture and mixed with it; 1700 ml ethanol 70% was added to the solution of the

stain. The staining solution was used in 100 ml for each mouse fetus, the specimen were washed for 2 hours in tap water.

**3. Clearing :** Fetuses were Placed in aqueous KOH 2% solution for two days and 6 hours instead of 3 in Erdogan method, and then in aqueous solution consist of glycerine 20% and KOH 1% until the skeletons become visible palpably. The specimen were placed in 50%, 80% and 100% for five days instead of 7 days in Erdogan method and preserved in 100% glycerine with thymol crystals to prevent mold growth.

### Results and Discussion

This research considered a development of Erdogan method to staining skeleton. The cartilage dyeing with blue staining and the bone with red staining. Thus, we can distinguished deformities, without skinning and harming the skeleton. Fetuses placed in KOH 2% two days and 6 hours instead of 3 days in Erdogan method because 3 days cause softness and harming the skeleton as in the figure(E), as we note. Potassium hydroxid was used as a degradation agent to influence bone tissue(8). These modifications reduce the researcher's time, because the time too expensive for researchers and efforts especially for new researchers that may be harm skeleton during skinning.



A- Lateral view for *Mus Musculus* mice fetus dye employing Alizarin red- S & Alcian blue 8X

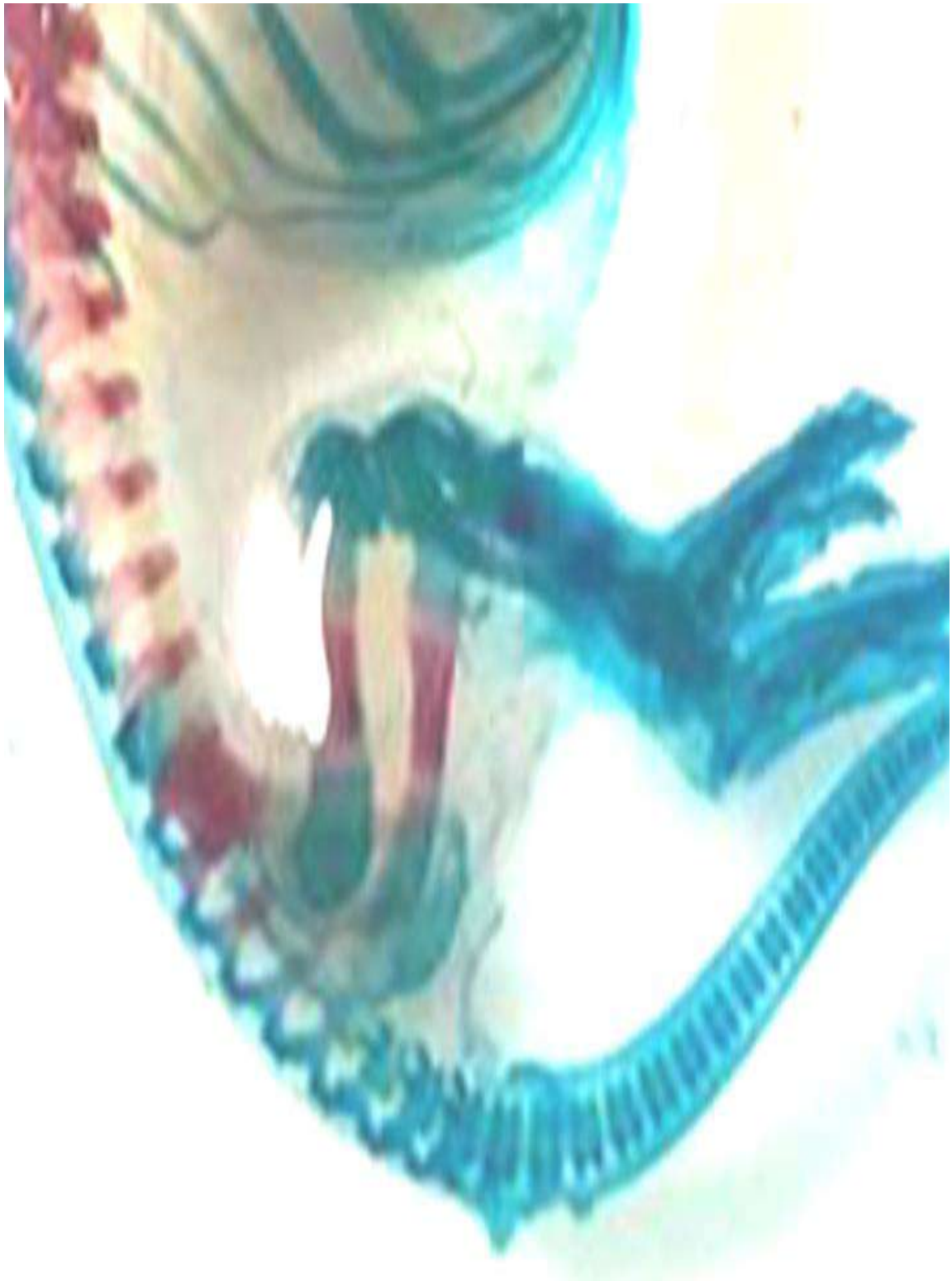


**B-** Lateral view of ribs for *Mus Musculus* mice fetus dye employing Alizarin red- S & Alcian Blue 8X





C- Lateral view for the skull and upper extremity of *Mus Musculus* mice fetus dye employing Alizarin red-S & Alcian blue 8X



**D-** Lateral view for low extremity and tail of *Mus Musculus* mice fetus dye employing Alizarin red-S & Alcian blue 8X



**E-** Lateral view for low extremity and tail of *Mus Musculus* mice fetus dye employing Alizarin Red-S & Alcian blue according to Erdogan method 8X

## References

Hale F.(1933).Pigs Born Without Eye Ball. J. Hered. Vol 24,Iss:3, pp 105-106.

Maria dos Anjos Pire and Ana M.Calado.(2018). An Overview of Teratology. Methods Mol Biol. :1797:3-32.

doi: 10.1007/978-1-4939-7883-0\_1.

Part of the book series: Methods in Molecular Biology ((MIMB,volume 1797).

Richard H. Finnell. (1999). Teratology: General considerations and principles. J ALLERGY CLIN IMMUNOL FEBRUARY. VOL. 103, NUMBER 2, PART 2.

Sadeghi F.; Salaramoli; J.H.Gilanpour; M. Azarnia, T. Aliesfehni.(2015). Modified Double Staining Protocols With Alizarin red-S and Alcian blue in Laboratory Animals. Annals of Military& Health Science Research. 13(2): 76-81.

Erdogan, D. ; Kadiodla D. and Peker T.(1995). vsulisation of fetal skeletal system by Double Staining With Alizarin red-S and Alcian blue. J. Gazi Med. 6:55-8.

Horobin RW. How do dyes impart color to different components of the tissues In: Kumar GL, editor. *Educational guide special stains and H & E*. 2. Carpinteria.(2010) California:. pp. 159–166.

Karen M. Lyons and Diana R.(2014). Whole- Mount Skeletal Staining. Methods Mol.Vol.1130, pp.113-121.

Hedges, R. E. M.; Nielsen-Marsha, C.M; Mann, T.; Collins, M.J.(2000). A preliminary Investigation of The Application of Differential Scanning Calorimetry to The Study of Collagen Degradation in Archaeological Bone. *Thermochimica Acta*, Vol. 365, Issues (1-2). pp. 129-139.



## Estimation of Some Physiological Biomarkers Associated with Kidney Failure and Liver Damage in COVID Patients

Reem M. Obaid <sup>1</sup>  
 Aveen R. Mohsin <sup>2</sup>  
 Sama s. Salih <sup>3</sup>  
 Farah Tareq Yaseen <sup>4</sup>



© 2024 The Author(s). This open access article is distributed under a Creative Commons Attribution (CC-BY) 4.0 license.



### Abstract:

A coronavirus referred to by the term SARS-CoV-2 caused the most recent contagion, which was dubbed COVID-19. It has been demonstrated that the Covid-19 viral illness affects a number of systems and organs, including the kidneys and liver. Fever, cough, and dyspnea are the most typical signs of SARS-CoV-2 infection. Methodology look into anomalies in the liver functional testing the serum values of Liver Function Test (LFT) which includes alanine transaminase (ALT), aspartate aminotransferase (AST) and alkaline phosphatase (ALP) in COVID-19 individuals as well as the usefulness of two markers for renal failure (urea and creatinine), besides, the level of Na and K. In addition to the estimation of serum lactate dehydrogenase (LDH), and ferritin. Findings demonstrated that there was a non-significant difference in creatinine, Na, as well as in K levels between the patient and control groups, but a very significant difference in urea values between the two groups. There are notable variations in the patient and control groups' blood levels of liver enzyme tests, such as ALT, AST, and ALP. It appears that there is a very significant difference in the Mean  $\pm$  SE of D-dimer, ferritin, and LDH between the control group and patients. The p-value reflects the degree of statistical significance among both of the groups. Conclusion: The best indicator of mortality was ferritin, which was followed by LDH and D-dimer. These parameters should be carefully examined to help physicians assess primitive risks. In addition, close observation is likely to lower mortality. Based on the observations, the patient group's AST, ALT and ALP values in the serum were all higher than those of controls which indicate the significance of these parameters. These indicators may aid in the recognition of damage that may impact various organs within the body, thus aiding in clinical decision-making.

**Keywords:** Creatinine; D-dimer; Ferritin; Inflammation; Urea.



<http://dx.doi.org/10.47832/MinarCongress12-12>

- <sup>1</sup> Department of Biology, College of Science for women, University of Baghdad, Iraq [reem.m@csw.uobaghdad.edu.iq](mailto:reem.m@csw.uobaghdad.edu.iq)
- <sup>2</sup> Department of Biology, College of Science for women, University of Baghdad, Iraq [aveen.r@csw.uobaghdad.edu.iq](mailto:aveen.r@csw.uobaghdad.edu.iq)
- <sup>3</sup> Department of Biology, College of Science for women, University of Baghdad, Iraq [sama.s@csw.uobaghdad.edu.iq](mailto:sama.s@csw.uobaghdad.edu.iq)
- <sup>4</sup> University of Al-Mustansiriyah, Baghdad, Iraq [farah.tariq834@uomustansiriyah.edu.iq](mailto:farah.tariq834@uomustansiriyah.edu.iq)

## Introduction

A coronavirus referred to by the term SARS-CoV-2 caused the most recent contagion, which was dubbed COVID-19. COVID-19 has been officially identified by the WHO to be a global health crisis in March 2020 (Mohammed *et al.*,2022 ; Yunus *et al.*,2021). Positive-stranded RNA is the envelope of coronaviruses (Mohammed *et al.*, 2020). Fever, cough, and dyspnea are the most typical signs of SARS-CoV-2 infection (WHO, 2021). Additionally, there have been accounts of a range of systemic symptoms, including gastrointestinal symptoms (Cichoz-Lach and Michalak, 2021). As the number of COVID-19 instances rises, numerous investigations have shown that, after lung damage, the liver is the organ most frequently affected. Angiotensin-converting enzyme 2 (ACE2), which is highly seen in liver cells, cholangiocytes, and endothelial cells of the liver, is how SARS-CoV-2 enters the target cell (Lei *et al.*,2020) . This could help to partially explain why patients who have positive SARS-CoV-2 testing have abnormal liver function tests (Cai *et al.*,2020).

It's also important to consider how immune-mediated inflammation and underlying chronic liver disease may contribute to abnormal liver function tests (Zhang *et al.*, 2020) . An intermittent rise in ALT, and AST has frequently been linked to hepatic insult. Acute liver damage has, however, been identified less frequently (Li and Fan, 2020). COVID-19 infected patients are frequently hospitalized due to a cough, dyspnea, elevated fever, exhaustion, and anosmia. Respiratory distress is the primary cause of death, accounting for 2-3% of cases (Chai *et al.*,2020). Clinical manifestations of pathology can also arise in additional organs, including the cardiovascular system, the pancreas kidneys, as well as liver, even though pulmonary injury is the primary cause of clinical appearances.

This is probably because the primary viral entry ACE two receptor, sometimes referred to simply as the angiotensin-converting enzyme two receptor, is shown in a number of tissues (Zhou *et al.*,2020). Hepatic injury has frequently been described. Infected liver cells and cells from the bile duct may harbor SARS-CoV-2, leading to aberrant functioning of the liver observed in these individuals, because of the receptor's shipping all over the body (Chen *et al.*, 2020). Severe COVID-19 cases are associated with improper liver function test results; the rate has been reported to be between 14 and 53%, most frequently in a hepatocellular pattern (Shi *et al.*,2020 ; Yang *et al.*,2020) . The objectives assess the significance of two indicators of kidney failure in COVID-19 patients: creatinine and urea. Secondly, to look into factors that affect irregularities in tests for liver function among COVID-19 patients and whether or not the seriousness of COVID-19 is linked to such anomalies.

## **Materials and procedures:**

### **Subjects and research layout:**

The current research was conducted on 140 individuals, the ages of men and women was between Eighteen and over seventy 110 of them belong to patients and 30 indicate the unaffected category, which is made up of healthy individuals who are not COVID-affected. The individuals were collected from Al- Sheikh Zaid hospital from the month of February, till April 2023.

### **Blood Sample Collection:**

The subsequent biological investigations were investigated for their enzymes of the liver in blood (ALP, AST, ALT) and kidney function test (Urea, creatinine, Na, K) in addition to the estimation of LDH, and ferritin. 5 ml of blood was obtained from each patient by puncture of veins via disposable five milliliter injections, subsequently we centrifuged samples at three thousand round per minute for ten minutes for collecting the serum. The electro-chemiluminescence immunoassay was used to measure the blood amounts of LDH. Roche Cobas Integra 400 plus (Manheim, Germany: the Roche Diagnostics GmbH).

Simultaneously, ferritin concentration was measured via a miniVIDAS instrument using the Enzyme Linked Fluorescent Assay (ELFA). Each patients blood specimens were fed into the device, and an automated calculation of the LDH as well as ferritin concentrations was performed. The other tests as liver enzymes and kidney function test were also detected.

### **Statistical Analysis**

The Statistical Analysis System- SAS (2018) was employed to find the impact of various groupings (patients and control) in research variables. The t-test was employed for contrasting between means. Meaningful comparison between percentages (0.05 and 0.01 probability) was made using the Chi-square test. Correlation coefficient was also calculated among the study's parameters.

### **Results**

The levels of urea, creatinine, Na and K in patients as well as in controls are demonstrated in table 1. The results exposed a highly significant difference in urea value amongst patients in addition to controls, whereas a non significant difference in values of creatinine, Na and K between patients and control group.

**Table 1-** Comparison between control and patients groups in Kidney function test

Group	Mean $\pm$ SE			
	Urea (mg/dL)	Creatinine (mg/dL)	Na (mmol/L)	K (mmol/L)
Control	44.39 $\pm$ 3.58	1.085 $\pm$ 0.07	139.59 $\pm$ 3.09	4.54 $\pm$ 0.30
Patients	84.54 $\pm$ 5.03	1.129 $\pm$ 0.05	139.72 $\pm$ 0.62	4.55 $\pm$ 0.06
T-test	15.169 **	0.191 NS	1.860 NS	0.261 NS
P-value	0.0001	0.643	0.889	0.963
<b>** (P<math>\leq</math>0.01) Highly Significant NS: Non-Significant.</b>				

There were a highly significant differences in the serum values of hepatic enzymes test, which includes ALT, AST and ALP amongst patients and control group (table 2).

**Table 2-** Comparison between control and patients groups in Liver enzymes

Group	Mean $\pm$ SE		
	ALT (U/L)	AST (U/L)	ALP (U/L)
Control	6.62 $\pm$ 0.65	17.50 $\pm$ 1.26	45.93 $\pm$ 4.96
Patients	40.73 $\pm$ 4.95	55.83 $\pm$ 7.08	142.70 $\pm$ 29.35
T-test	14.121 **	20.213 **	83.752 **
P-value	0.0001	0.0004	0.0094
<b>** (P<math>\leq</math>0.01) Highly Significant</b>			

The p-value designates the statistical significance levels among the two groups, it appears a highly significant difference in the Mean  $\pm$  SE of LDH, Ferritin and D-dimer between control group and patients (table 3).

**Table 3-** Comparison between control and patients groups in inflammatory markers

Group	Mean $\pm$ SE		
	LDH (U/L)	Ferritin (mg/L)	D.dimer (mg/mL)
Control	189.40 $\pm$ 11.41	97.84 $\pm$ 11.41	0.490 $\pm$ 0.22
Patients	362.03 $\pm$ 39.64	382.15 $\pm$ 35.14	5.07 $\pm$ 0.42
T-test	113.33 **	101.19 **	1.223 **
P-value	0.0035	0.0001	0.0001
<b>** (P<math>\leq</math>0.01) Highly Significant</b>			

Table 4 shows the correlation coefficient (r) between study parameters in patients group, there is a highly significant positive correlation coefficient between Urea & Cr, Urea & D-

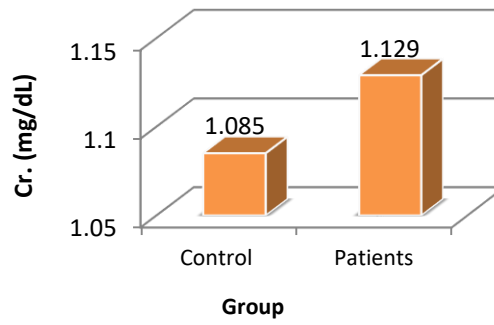


dimer, ALT & AST, ALT & ALP, ALT & Ferritin, AST & ALP, AST & Ferritin and between ALP & Ferritin. A significant positive correlation coefficient between Urea & Ferritin, Cr. & K, and between Cr. & D-dimer. A non-significant positive correlation coefficient between Urea & ALT, Urea & AST, Na & K, LDH & D-dimer, Ferritin & D-dimer and between Urea & ALP, we also observed that there was a highly significant correlation coefficient amongst Na & ALP, Na & Ferritin and between Na & ALT.

A significant negative correlation coefficient between ALT & D-dimer. Also a non-significant negative correlation coefficient between Urea & Na, Urea & K, Urea & LDH, Cr. & Na, Cr. & ALT, Na & LDH, Na & D-dimer, Cr. & AST, Cr. & ALP, Cr. & LDH, Cr. & Ferritin, AST & D-dimer, ALP & LDH, ALP & D-dimer and between LDH & Ferritin.

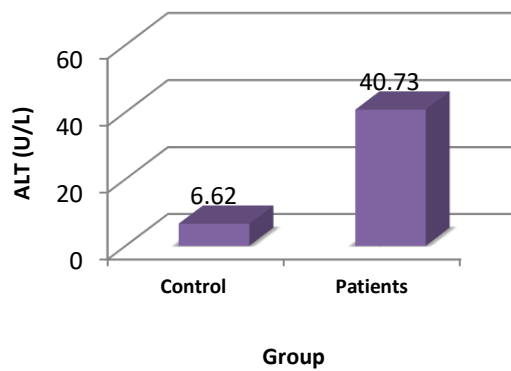
**Table 4-** Correlation coefficient between study parameters in patients group

Parameters	Correlation coefficient-r	P-value	Parameters	Correlation coefficient-r	P-value
Urea & Cr.	0.40 **	0.0098	Na & ALP	-0.50 **	0.0009
Urea & Na	-0.26 NS	0.0944	Na & LDH	-0.04 NS	0.799
Urea & K	-0.004 NS	0.978	Na & Ferritin	-0.40 **	0.0098
Urea & ALT	0.23 NS	0.155	Na & D-dimer	-0.04 NS	0.802
Urea & AST	0.15 NS	0.349	ALT & AST	0.92 **	0.0001
Urea & ALP	0.16 NS	0.332	ALT & ALP	0.77 **	0.0001
Urea & LDH	-0.04 NS	0.805	ALT & LDH	0.12 NS	0.438
Urea & Ferritin	0.30 *	0.050	ALT & Ferritin	0.74 **	0.0001
Urea & D-dimer	0.44 **	0.0045	ALT & D-dimer	-0.35 *	0.025
Cr. & Na	-0.12 NS	0.458	AST & ALP	0.64 **	0.0001
Cr. & K	0.34 *	0.028	AST & LDH	0.25 NS	0.110
Cr. & ALT	-0.22 NS	0.176	AST & Ferritin	0.74 **	0.0001
Cr. & AST	-0.14 NS	0.393	AST & D-dimer	-0.24 NS	0.132
Cr. & ALP	-0.21 NS	0.185	ALP & LDH	-0.15 NS	0.344
Cr. & LDH	-0.21 NS	0.187	ALP & Ferritin	0.44 **	0.004
Cr. & Ferritin	-0.09 NS	0.559	ALP & D-dimer	-0.15 NS	0.344
Cr. & D-dimer	0.35 *	0.024	LDH & Ferritin	-0.24 NS	0.004
Na & K	0.02 NS	0.916	LDH & D-dimer	0.21 NS	0.121
Na & ALT	-0.48 **	0.0015	Ferritin & D-dimer	0.25 NS	0.112
Na & AST	-0.53 **	0.0004		---	
* (P≤0.05) Significant ** (P≤0.01) Highly Significant NS: Non-Significant.					



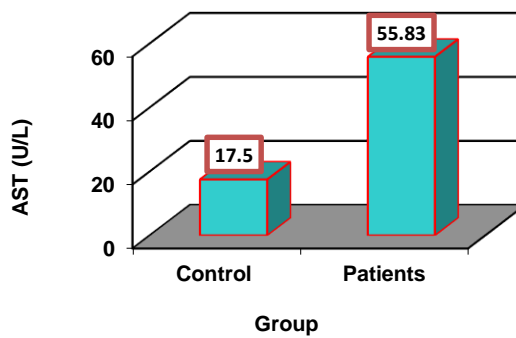
**Figure 1-** Comparison between control and patients groups in Creatinine

Figure 1 showing that the highest level of creatinine was in patients, while the lowest level was in control group



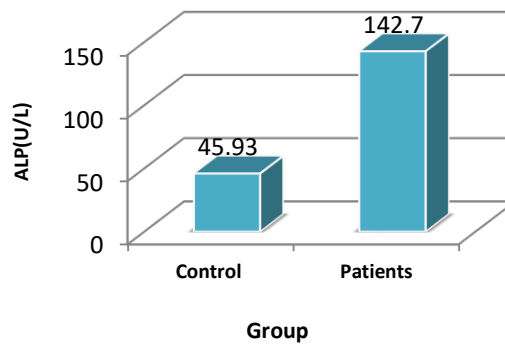
**Figure 2.** Comparison between control and patients groups in ALT (U/L)

In Figure 2, the maximum value of ALT was in COVID patients, while the lowest level was in controls



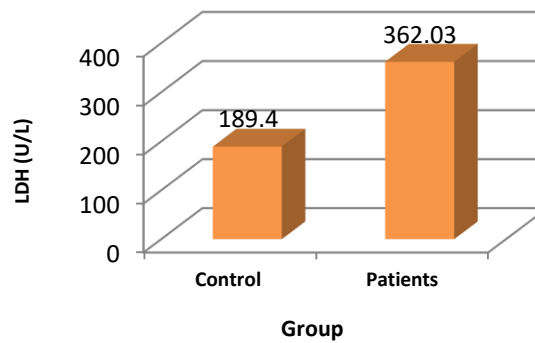
**Figure 3-** Comparison between control and patients groups in AST (U/L)

Figure 3 showed that, the highest level of AST was in COVID patients



**Figure 4-** Comparison between control and patients groups in ALP (U/L)

Furthermore, ALP was markedly raised in COVID-19 patients as in Figure 4



**Figure 5-** Comparison between control and patients groups in LDH (U/L)

The highest level of LDH was in COVID patients, while the lowest level was in controls (Figure 5)

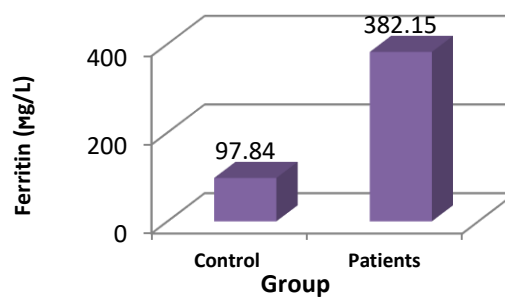


**Figure 6-** Comparison between control and patients groups in Ferritin

The highest level of ferritin was in patients, while the lowest level was in controls (fig. 6)

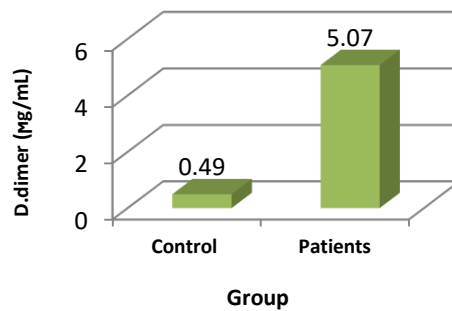


**Figure 7-** Comparison between control and patients groups in D.dimer

We observed in Figure 7, The highest level of D. dimer was in patients, while the lowest level was in controls.

### Discussion:

It has been demonstrated that the Covid-19 viral illness impacts a broad spectrum of systems and organs, together with the liver (Salman *et al.*, 2023). Patients infected with COVID-19 may have liver damage due to several reasons. Hepatocyte inclusions of viruses were not found in biopsy of liver from a COVID-19 patient, despite substantial microvesicular steatosis and modest lobular as well as portal action that were compatible with either direct infection with a virus or drug-induced hepatic injury (Xu *et al.*, 2020).

According to reports, those with severe liver illness may require more intense care and have a higher death rate (Fan *et al.*, 2020; Zhang *et al.*, 2020). According to new studies, an autoimmune thyroiditis may develop after contracting COVID-19 (Mori and Yoshida, 2010). Both Grave's disease (GD) as well as Hashimoto's thyroiditis (HT) are examples of autoimmune thyroid disorders (AITD) (Obaid *et al.*, 2020). Increases in Ferritin, LDH, D-dimer, along with other markers of inflammation have also been seen in biomarkers in Iraqi COVID-19 patients (Abdul Hussein and Fadhil, 2023).

According to our findings, COVID patients had the greatest level of AST, and the most frequent anomalies were raised levels of ALT and AST, both of whom pointed to hepatic destruction (Del Zompo *et al.*, 2020). Both AST and ALT have been connected to increased functioning of the liver. It was discovered that the inflammatory indicators D- dimer, ferritin, along with the enzyme (LDH) levels were significant predictors of the course of the illness. The body's stress is reflected in an elevated level of this inflammatory biomarker, which suggests systemic inflammation.



The amount increases to an even greater degree in situations if there's greater stress, especially in cases of really serious patients. Because of the seriousness of the condition, this inflammatory indicator so indirectly reveals the body's degree of stress (Zarei *et al.*, 2022). According to our research, serum ferritin levels were greater among individuals with COVID-19 than in controls; Each of these variations had a difference that was statistically significant ( $p < 0.001$ ). One of the inflammatory indicators required to diagnose hyperinflammatory syndrome (HI-S) in COVID-19 infected patients is ferritin (Manson *et al.*, 2020). Ferritin concentrations and the condition of the COVID-19 patient are closely correlated, according to a research conducted by Szarpak *et al.* and his coworker on twelve investigations.

Significantly elevated ferritin levels have been linked with raised death, exposure to critical care units, and more severe patient conditions (Szarpak *et al.*, 2020). Moreover, related research results demonstrated that the COVID-19 connection hyperinflammatory criteria (ferritin levels). As a modulator of immunological disorder, ferritin is extremely significant. It has been suggested that in cases of severe hyperferritinemia, ferritin directly exerts immunological suppressive and proinflammatory effects, which may contribute to the storm of cytokine observed in COVID-19 infected individuals. Because serum coagulation cascade proteins and oxides of iron interact with one another, hyperferritinemia results in regular cell death (RCD). Amongst COVID-19 patients, abnormalities in coagulation are extremely common, especially in those with the severe form of the illness (Perricone *et al.*, 2020). Iron overload may result from the virus's attack on the destruction of hemoglobin, which releases iron from porphyrins and discharges it into the bloodstream. Furthermore, iron is necessary for ATP hydrolysis, which is a need for the SARS-CoV helicases' normal function during viral replication (Ma *et al.*, 2021). Iron is probably necessary for SARS-CoV-2 viral RNA replication and function (Channappanavar *et al.*, 2017).

It is noteworthy that monocytes are believed to be infected by SARS-CoV-2. Therefore, it is anticipated that increased iron buildup in monocytes will promote viral replication. Systemic iron overload is associated with increased levels of oxidative stress in cells, the production of cytokines and malfunction of the mitochondria, a marked reduction in utilization of  $O_2$  in cells, peroxidation of lipids, and a shift in metabolism via lactic dehydrogenase (LDH) from aerobic (pyruvate) to anaerobic (lactate). Our results demonstrated a substantial increase in D-dimer and LDH levels in serious and critically ill individuals in contrast to controls ( $p < 0.001$ ).

The impairment of natural anticoagulants, the breakdown of fibrin irregular thrombin production, and activation of coagulation have all been associated with elevated D-dimer values in COVID-19 patients (Zheng *et al.*, 2020). Moreover, antibodies for phospholipids, coagulation disorders, and a rise in coagulation episodes in the arteries and veins, including brain damage, have been documented in a number of critically sick patients (Zhang *et al.*, 2020). Paliogiannis *et al.* investigated over 1,800 COVID-19 people, which is consistent with our findings. They discovered that plasma concentrations of D-dimer in people infected with COVID-19 were considerably greater than in controls (Lippi *et al.*, 2020). Since LDH found in pulmonary tissue, which is the areas primarily impacted by COVID-19, pulmonary tissue deterioration may be the cause of high LDH levels. Our results align with other studies that demonstrated elevated LDH levels were typical among COVID-19 patients (Paliogiannis *et al.*, 2020).

Our findings from the kidney function test showed that those with COVID had more creatinine than normal. Numerous research have examined the impact of kidney function or creatinine level about COVID-19 death and medical effects, and they have found a substantial correlation among elevated concentrations of creatinine and COVID-19 seriousness and death (Niculae *et al.*, 2022).

### **Conclusions:**

Increasingly prevalent systemic infection, there is a notable adverse impact of COVID-19 on the immune system. Enhanced pro-inflammatory biomarkers are a common consequence of COVID-19 infection. The best indicator of death was ferritin, which was followed by LDH and D-dimer. In addition, close observation can likely lower mortality. These parameters should be thoroughly examined at the beginning of the study to help physicians assess primitive risks. Based on the observation that the patient group's blood amounts of AST, ALT, and ALP were all greater than those of the control group, we draw the conclusion that certain biochemical parameters are significant. These indicators may aid in the recognition of destruction that may impact various tissues within the body, thus aiding in clinical decision-making.

**Acknowledgment:** The authors honestly respected the clinical staff's collaboration at Al-Sheikh Zaied hospital in Baghdad city, special thanks to manager of the hospital, Dr. Ahmed Tahir Al-Sultan.

**Conflict of Interest:** The authors have no conflict of interest.

**References:**

- Abdul Hussein T.A. and Fadhil H.Y.(2023). Impact of inflammatory markers, dread diseases and cycle threshold (Ct) Values in COVID-19 progression.Revis Bionatura. 8 (1)33. Available from: <http://dx.doi.org/10.21931/RB/2023.08.01.33> .
- Cai Q., Huang D., Yu H., Zhu Z., Xia Z., Su Y., Li Z., Zhou G., Gou J., Qu J., Sun Y., Liu Y., He Q., Chen J., Liu L., Xu L.(2020).COVID-19: Abnormal liver function tests. J.Hepatol.73(3):566-574. Available from: <https://doi: 10.1016/j.jhep.2020.04.006>.
- Chai X., Hu L., Zhang Y., Han W., Lu Z., Ke Z.L., Ke A., Zhou J., Shi G., Fang N., Fan J., Cai J., Fan J., Lan F.(2020). Specific ACE2 expression in cholangiocytes may cause liver damage after 2019-nCoV infection. bioRxiv. 02.03.931766. Available from: <http://dx.doi.org/10.1101/2020.02.03.931766>.
- Channappanavar R., Fett C., Mack M., Ten Eyck P.P., Meyerholz D.K., Perlman S.(2017).`Sex-Based Differences in Susceptibility to Severe Acute Respiratory Syndrome Coronavirus Infection. J Immunol. 15;198(10):4046-4053. Available from: <doi: 10.4049/jimmunol.1601896>. Epub 2017 Apr 3 .
- Chen N., Zhou M., Dong X., Qu J., Gong F., Han Y., Qiu Y., Wang J., Liu Y., Wei Y., Xia J., Yu T., Zhang X., Zhang L.(2020).Epidemiological and clinical characteristics of 99 cases of 2019 novel coronavirus pneumonia in Wuhan, China: a descriptive study.Lancet. 395: 507-513.  
Available from: [http://dx.doi.org/10.1016/S0140-6736\(20\)30211-7](http://dx.doi.org/10.1016/S0140-6736(20)30211-7) | Medline.
- Cichoż-Lach H. and Michalak A. (2021).Liver injury in the era of COVID-19. World J Gastroenterol. 27: 377-390. Available from: <https://doi: 10.3748/wjg.v27.i5.377>.
- Del Zompo F., De Siena M., Ianiro G., Gasbarrini A., Pompili M., Ponziani F.R.(2020). Prevalence of liver injury and correlation with clinical outcomes in patients with COVID-19: systematic review with meta-analysis. Eur Rev Med Pharmacol Sci.24(24): 13072-13088. Available from: [doi: 10.26355/eurrev\\_202012\\_24215](doi: 10.26355/eurrev_202012_24215).
- Fan Z., Chen L., Li J., Cheng X., Yang J., Tian C., Fan Z., Chen L., Li J., Cheng X., Yang J., Tian C., Zhang Y., Huang S., Liu Z., Cheng J.(2020). Clinical features of COVID-19-related liver damage. Clin Gastroenterol Hepatol.18(7):1561-1566. Available from: <http://dx.doi.org/10.1016/j.cgh.2020.04.002>.
- Lei H.Y., Ding Y.H., Nie K., Dong Y.M., Xu J.H., Yang M.L., Liu M.Q., Wei L., Nasser M.I., Xu L.Y., Zhu P., Zhao M.Y.(2021). Potential effects of SARS-CoV-2 on the gastrointestinal tract and liver. Biomed Pharmacother. 133: 111064. Available from: <https://doi: 10.1016/j.biopha.2020.111064>.
- Li J. and Fan J.G. (2020).Characteristics and mechanism of liver injury in 2019 coronavirus disease. J Clin Transl Hepatol. 28;8(1):13-17. Available from: <https://doi: 10.14218/JCTH.2020.00019>.
- Lippi G., Simundic A.M., Plebani M.(2020). Potential preanalytical and analytical vulnerabilities in the laboratory diagnosis of coronavirus disease 2019 (COVID-19). Clin Chem Lab Med. 25; 58(7):1070-1076. Available from: <doi: 10.1515/cclm-2020-0285>.

- Manson J.J., Crooks C., Naja M., Ledlie A., Goulden B., Liddle T.(2020). COVID-19-associated hyperinflammation and escalation of patient care: a retrospective longitudinal cohort study. *Lancet Rheumatol.* 2(10):e594-e602. Available from: [doi.org/10.1016/S2665-9913\(20\)30275-7](https://doi.org/10.1016/S2665-9913(20)30275-7). Epub 2020 Aug 21.
- Ma T.L., Zhou Y., Wang C., Wang L., Chen J.X., Yang H.H., Zhang C.Y., Zhou Y., Guan C.X.(2021). Targeting Ferroptosis for Lung Diseases: Exploring Novel Strategies in Ferroptosis-Associated Mechanisms. *Oxid Med Cell Longev.*6:2021:1098970. Available from: [doi.org/10.1155/2021/1098970](https://doi.org/10.1155/2021/1098970). eCollection 2021.
- Mohammed S.K., Taha M.M., Taha E.M., Mohammad M.N.A. (2022).Cluster Analysis of Biochemical Markers as Predictor of COVID-19 Severity. *Baghdad Sci J.* 19(6): 1423-1429. Available from: <https://doi.org/10.21123/bsj.2022.7454>.
- Mohammed M., Shafik N.S., Maher A., Hemdan S.B., Abd Elhamed R.M. (2020). Liver injuries in COVID-19 infected patients. *Sohag Medical Journal.* 24: 15-19. Available from: [https://smj.journals.ekb.eg/article\\_94834.html](https://smj.journals.ekb.eg/article_94834.html).
- Mori K. and Yoshida K.(2010). Viral infection in induction of Hashimotos thyroiditis: a key player or just a bystander? *Curr Opin Endocrinol Diabetes Obes.*17(5): 418- 424. Available from: [doi: 10.1097/MED.0b013e32833cf518](https://doi.org/10.1097/MED.0b013e32833cf518).
- Niculae A., Peride I., Nechita A.M., Petcu L.C., Tiglis M., Checherita I.A.(2022). Epidemiological Characteristics and Mortality Risk Factors Comparison in Dialysis and Non Dialysis CKD Patients with COVID-19-A Single Center Experience. *J. Pers. Med.* 12, 966. Available from: [doi: 10.3390/jpm12060966](https://doi.org/10.3390/jpm12060966).
- Obaid R.M., Yaseen F.T., Salim A.K. (2020): Correlation between vitamin D3(cholecalciferol) and thyroid diseases in Iraqi patients, *Ann Trop Med & Public Health:* 23(S16):SP231603. Available from: DOI: <http://doi.org/10.36295/ASRO.2020.231603>.
- Paliogiannis P., Mangoni A.A., Dettori P., Nasrallah G.K., Pintus G., Zinellu A.(2020). D-Dimer Concentrations and COVID-19 Severity: A Systematic Review and Meta-Analysis. *Frontiers in public health.* 8:432. Available from: <https://doi.org/10.3389/fpubh.2020.00432>.
- Perricone C., Bartoloni E., Bursi R., Cafaro G., Guidelli G.M., Shoenfeld Y., Gerli R. (2020).COVID-19 as part of the hyperferritinemic syndromes: the role of iron depletion therapy. *Immunol Res.* 68(4): 213–224. Available from: [doi: 10.1007/s12026-020-09145-5](https://doi.org/10.1007/s12026-020-09145-5).
- Salman Z.Z., Mohammed S.B., Muhi S.A. (2023).Studying the effect of COVID-19 on Liver Enzymes and Lipid Profile in Iraqi Recovering Patients. *Baghdad Sci.J.* 20(4(SI):1489 Available from:<https://doi.org/10.21123/bsj.2023.8347>.
- SAS. 2018. Statistical Analysis System, User's Guide. Statistical. Version 9.6<sup>th</sup> ed. SAS. Inst. Inc.Cary.N.C. USA.
- Shi H., Han X., Jiang N., Cao Y., Alwalid O., Gu J., Fan Y., Zheng C. (2020). Radiological findings from 81 patients with COVID-19 pneumonia in Wuhan, China: a descriptive study.*Lancet Infect Dis.* 20(4):425-434. [https://doi: 10.1016/S1473-3099\(20\)30086-4](https://doi.org/10.1016/S1473-3099(20)30086-4).



- Szarpak L., Zaczynski A., Kosior D., Bialka S., Ladny J.R., Gilis- Malinowska N., Smereka J., Kanczuga-Koda L., Gasecka A., Filipiak K.J., Jaguszewski M.J.(2020). Evidence of diagnostic value of Ferritin in patients with COVID-19. *Cardiol J.* 27(6):886-887 Available from: [doi: 10.5603/CJ.a2020.0171](https://doi.org/10.5603/CJ.a2020.0171). Epub 2020 Dec 21.
- WHO. (2021). Coronavirus (COVID-19) Dashboard .WHO Coronavirus Disease (COVID-19). Available from: <https://covid19.who.int/>.
- Xu Z., Shi L., Wang Y., Zhang J., Huang L., Zhang C. (2020). Pathological findings of COVID -19 associated with acute respiratory distress syndrome. *Lancet Respir Med.* Available from: [http://dx.doi.org/10.1016/S2213-2600\(13\)70187-5](http://dx.doi.org/10.1016/S2213-2600(13)70187-5) | Medline.
- Yang X., Yu Y., Xu J., Shu H., Xia J., Liu H., Xia J., Liu H., Wu Y., Zhang L., Yu Z., Fang M., Yu T., Wang Y., Pan S., Zou X., Yuan S., Shang Y. (2020).Clinical course and outcomes of critically ill patients with SARS-CoV-2 pneumonia in Wuhan, China: a single-centered, retrospective, observational study. *Lancet Respir Med.* Available from: [http://dx.doi.org/10.1016/S2213-2600\(13\)70187-5](http://dx.doi.org/10.1016/S2213-2600(13)70187-5) | Medline
- Yunus A.A., Yunus A.A., Ibrahim M.S., Ismail S. (2021). Future of Mathematical Modelling: A Review of COVID-19 Infected Cases Using SIR Model. *Baghdad Sci J.* 18(1): 824-9. Available from: [https://doi.org/10.21123/bsj.2021.18.1\(Suppl.\).0824](https://doi.org/10.21123/bsj.2021.18.1(Suppl.).0824) .
- Zarei M., Bose D., Nouri-Vaskeh M., Tajiknia V., Zand R., Ghasemi M. (2022). Long-term side effects and Ingering symptoms post COVID-19 recovery. *Rev Med Virol.* 32(3): 2289 Available from: <http://doi.org/10.1002/rmv.2289>.
- Zhang C., Shi L., Wang F.S. (2020). Liver injury in COVID-19: management and challenges. *Lancet Gastroenterol Hepatol.* 5(5):428-430. Available from: [http://doi.org/10.1016/S2468-1253\(20\)30057-1](http://doi.org/10.1016/S2468-1253(20)30057-1).
- Zhang Y., Xiao M., Zhang S. (2020). Coagulopathy and antiphospholipid antibodies in patients with Covid-19. *N Engl J Med.* 382(17):e38 Available from: [doi: 10.1056/NEJMc2007575](https://doi.org/10.1056/NEJMc2007575).
- Zhang Y., Zheng L., Liu L., Zhao Z., Xiao J., Zhao Q. (2020). Liver impairment in COVID-19 patients: a retrospective analysis of 115 cases from a single center in Wuhan city, China. *Liver Int,* 40(9):2095-2103. Available from: [doi: 10.1111/liv.14455](https://doi.org/10.1111/liv.14455). Epub 2020 Apr 28.
- Zheng S., Fan J., Yu F., Feng B., Lou B., Zou Q., Xie G., Lin S., Wang R., Yang X., Chen W., Wang Q., Zhang D., Liu Y., Gong ,Ma Z., Lu S., Xiao Y., Gu Y., Zhang J., Yao H., Xu K., Lu X., Wei G., Zhou J., Fang Q., Cai H., Qiu Y., Sheng J., Chen Y., Liang T. (2020). Viral load dynamics and disease severity in patients infected with SARSCoV- 2 in Zhejiang province, China, January-March 2020: retrospective cohort study. *BMJ.* 21:369:m1443 Available from: [doi: 10.1136/bmj.m1443](https://doi.org/10.1136/bmj.m1443) .
- Zhou P.,Yang X.L.,Wang X.G., Hu B., Zhang L., Zhang W., Zhou P., Yang X.L., Wang X.G., Hu B., Zhang L., Zhang W., Si H.R., Zhu Y., Li B., Huang C.L., Chen H.D., Chen J., Luo Y., Guo H., Jiang R.D., Liu M.Q., Chen Y., Shen X.R., Wang X., Zheng X.S., Zhao K., Chen Q.J., Deng F., Liu L.L., Shi Z.L.(2020). A pneumonia outbreak associated with a new coronavirus of probable bat origin. *Nature.* 579(7798):270-273. Available from: [https://doi: 10.1038/s41586-020-2012-7](https://doi.org/10.1038/s41586-020-2012-7).

# Investigation of the Optical Properties and Spectroscopy Diagnostic of Magnesium Oxide Plasma by Nd: YAG Laser Method

Wassan D. Hussain <sup>1</sup>

Arkan K. Buraihi <sup>2</sup>



© 2024 The Author(s). This open access article is distributed under a Creative Commons Attribution (CC-BY) 4.0 license.

## Abstract:

*The fundamental wavelength of a pulsed Nd:YAG laser (1064 nm) is used to generate a plasma from a solid MgO sample in air at atmospheric pressure. The optical characterization of thin films like transmittance and band gap energy and determined by UV-VIS spectrum, the transmissions in the visible region was 80%. and the band gap of the direct transition is 4 eV. The electron temperatures were calculated using the ratio of line intensities approach at various laser peak powers. The Saha-Boltzmann equation was used to derive electron densities. The impact of the peak power of the laser on the emission lines was examined, and only a small number of appropriate MgO lines were identified. The laser peak powers were changed from 22 to 11 MW, and as a result, electron concentrations of around  $10^{17} \text{ cm}^{-3}$  and temperatures between 0.36 and 0.44 eV were documented.*

**Keywords:** MgO, Band Gap; Optical; Thin Film Plasma; Electron Density; Electron Temperature.

---

 <http://dx.doi.org/10.47832/MinarCongress12-13>

<sup>1</sup>  Department Of Energy Engineering, College Of Engineering, University Of Baghdad , Iraq  
[wassan.hussain@coeng.uobaghdad.edu.iq](mailto:wassan.hussain@coeng.uobaghdad.edu.iq)

<sup>2</sup>  Department Of Energy Engineering, College Of Engineering, University Of Baghdad , Iraq  
[arkan.kareem@coeng.uobaghdad.edu.iq](mailto:arkan.kareem@coeng.uobaghdad.edu.iq)

**Introduction:**

Numerous practical uses have resulted from this study, including X-ray laser sources, pulsed laser produced plasma of solids, inertial confinement fusion, and laboratory astrophysics. The process of creating plasma involves exciting the analyte with a pulsed laser source and then vaporising it. You can figure out what the material is made of by looking at the optical emission that happens when excited species relax in the plasma.

Thermophysical features of the target and laser beam parameters (wavelength, energy, pulse width, and shape) determine the plasma and its properties (electrons' density and temperature, as well as their spatial and temporal behavior)[1,2]. Instead than focusing on the specific species, descriptions of plasma initially aim to describe the characteristics of the atomic, molecular, electron, and ion configuration. Plasma characteristics, including particle velocities and relative energy populations, can be defined in terms of temperature if thermodynamic equilibrium holds [3].

Additionally, there are a number of spectroscopic methods that can be used to assess the electron temperature, a crucial plasma characteristic, including the integrated line intensity ratio, continuum spectral form, line intensity to underlying continuum ratio [4]. Thomson scattering, microwave and laser interferometry, Langmuir probe, plasma spectroscopy, and some of the diagnostic methods used to find the electron density [5]. As far as equipment goes, spectroscopy is the simplest method. Using a solid Mg target in air at atmospheric pressure, we analyse the Nd:YAG nanosecond laser produced plasma in this work. Additionally, the report details the impact of the laser's peak power on the spectral line intensities. Research on plasma properties like electron density ( $n_e$ ) and electron temperature ( $T_e$ ) and how they relate to laser peak power is also detailed here. The density of electrons was calculated using the Saha-Boltzmann formula. The Mg I (333.06 nm) line was used to calculate the electron temperature using the relative intensity ratio method.

**Experimental setup:**

To diagnose laser-induced Mg plasma using optical emission spectroscopy (OES), the experimental setup is schematically shown in Figure (1). We used a Nd:YAG pulsed laser with a fundamental wavelength of 1064 nm, a pulse duration of 9 ns, a repetition rate of 1 Hz, and varying laser peak strengths to ablate Mg plasma. A lens with a focal length of 10 cm was employed to focus the laser beam. Each laser pulse was focused on a different area of the sample because the Mg target was manually rotated. To capture the 320–750 nm range of plasma

emission from the Mg plasma plume, an ocean optics (HR 4000 CG-UV-NIR) spectrometer was employed.

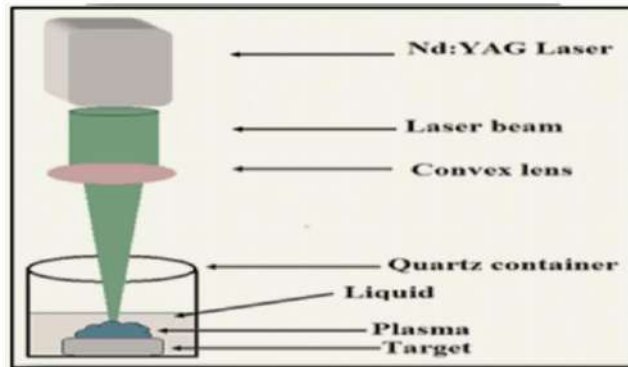


Figure 1- The experimental setup.

### Results and discussions:

Physical attributes, like absorption, transmittance, and band gap energy, can be inferred from optical characterization of thin films using the UV-VIS spectra. Spectra of MgO film transmittance measured in relation to wavelength range (200-800 nm. See Figure 2 for a plot of transmission vs wavelength for MgO thin films. In the visible spectrum, the films' transmission was 0.8%. Optoelectronic devices benefit from the film's reasonably high transmittance over the UV-VIS regions.

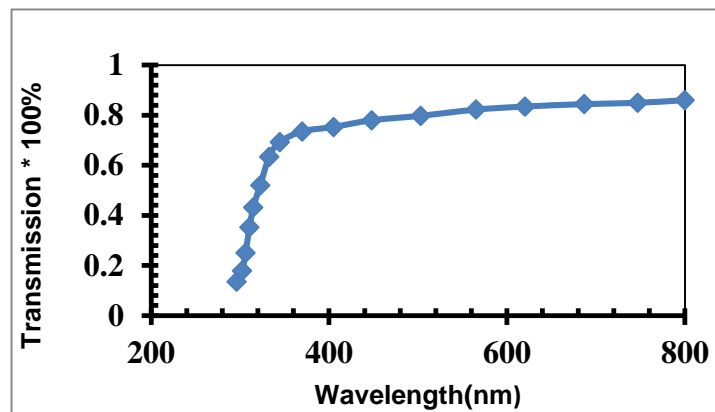


Figure 2- The Transmission as a function of wave length of MgO films

Figure (3) shows that while the MgO film has strong absorption in the short wavelength area, its absorption decreases as the wavelength increases.



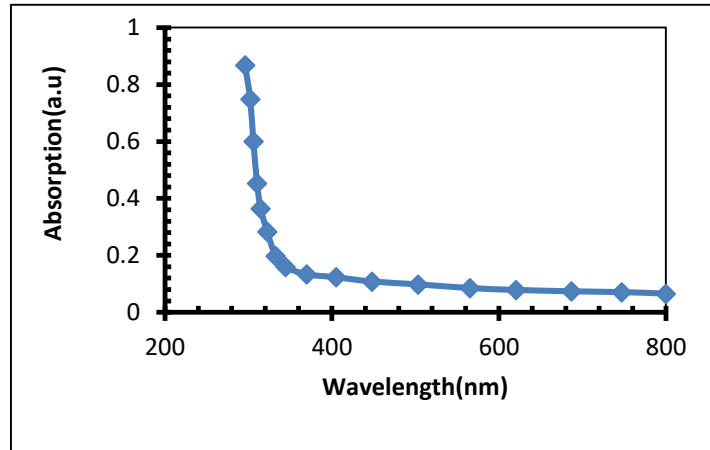


Figure 3- The Absorption as a function of wave length of MgO films

The absorbance readings were used to determine the absorption coefficient ( $\alpha$ ) of the MgO film, which was then computed using the given equation.

$$\alpha = 2.303A/t \dots \dots \dots (1)$$

Where t is thickness of the film (120 nm)

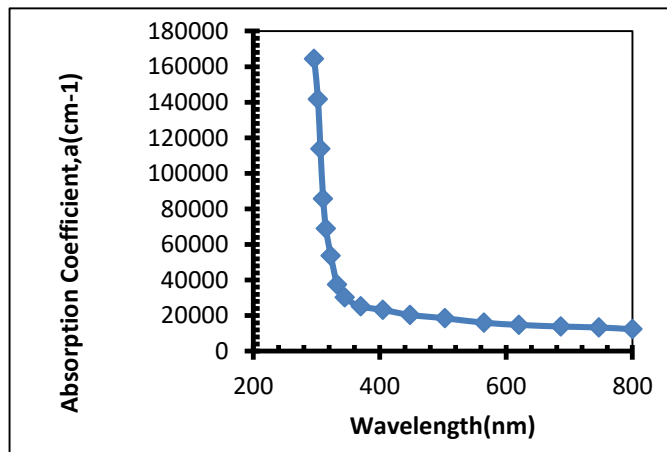


Figure 4- The Absorption coefficient as a function of wave length of MgO films

The extinction coefficient ( $k_0$ ) is plotted against wavelength in Figure (5). An attenuation coefficient k between 200 and 800 nm can be calculated from a transmittance spectrum using the following formula::

$$k = a \lambda / 4\pi \dots \dots \dots (2)$$

Figure 5 shows the relationship between the extinction coefficient (k) and wavelength spectra; the visible range (300 nm) is where the extinction coefficient begins to fall.

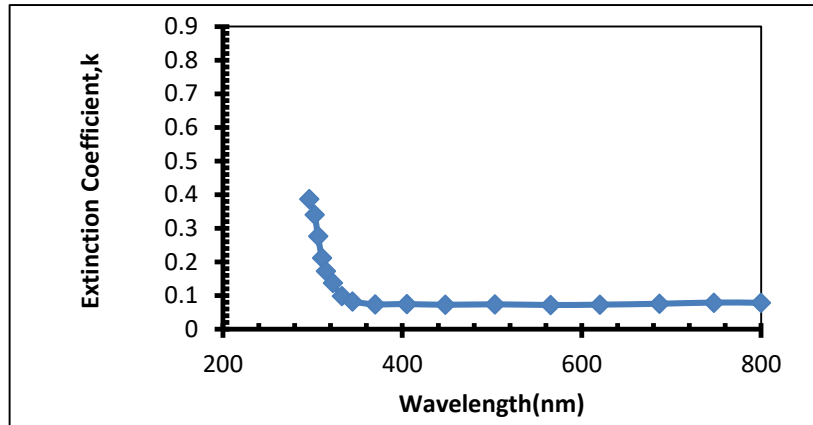


Fig 5- The Extinction coefficient as a function of wavelength of MgO films

The refractive index and reflectance both behave in very similar ways. The relationship between wavelength and the refractive index is seen in Figure 6. By utilising the transmission spectrum and the formula, one can ascertain the refractive index (n).

$$n = [(4R/(R-1) - (K^2) ]^{1/2} - R+1)/(R-1)] \dots \dots \dots (3)$$

The extinction coefficient is denoted by k and the reflectance is represented by R

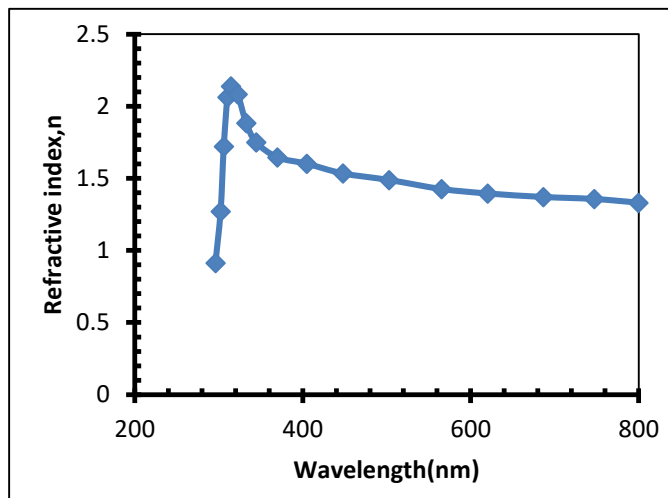


Figure 6- The Refractive index as a function of wave length of MgO films

It is possible to determine the films' optical band gaps by analysing their transmittance spectra. The layer thickness (t) is used in equation (1), [6], to determine the absorption coefficient (α). According to the given equation [7], there is a relationship between the incident photon energy (hv) and the absorption coefficient (α).

$$(\alpha hv) = A (hv - E_g)^r \dots \dots \dots (4)$$

A is a constant that inversely corresponds to amorphousness, α is the absorption coefficient, and hv is the incident photon energy. The values of r can range from 1/2 to 3,

depending on the material and the kind of optical transition (direct or indirect). As shown in Figure 7, we may determine the band gap values of the MgO thin film for the direct transition by extrapolating the straight line section of the  $(\alpha h\nu)^2$  Versus  $h\nu$ , with  $r=1/2$ .

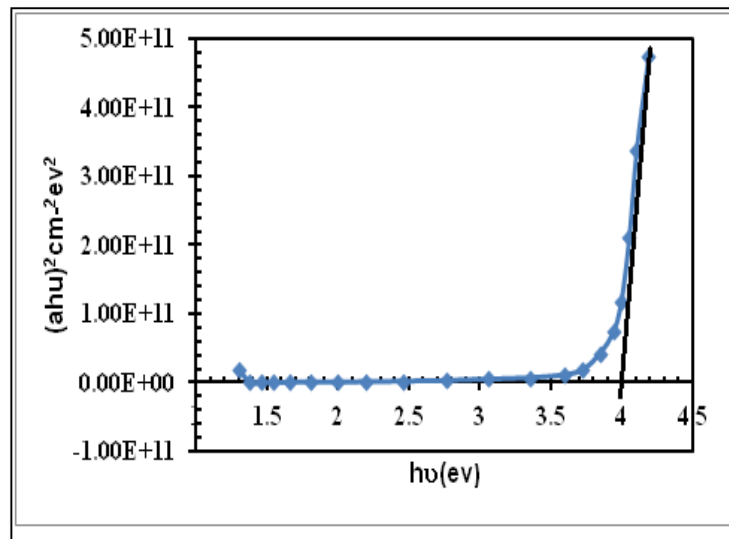


Figure 7- The  $(\alpha h\nu)^2$  as a function energy gap of MgO films

As shown in figure (8), the laser-induced Mg plasma displays an optical emission spectra in the 320-750 nm region. In ambient air, the most significant magnesium spectral lines are magnesium I at 380.101 nm, magnesium II at 579.918 nm, and magnesium II at 645.35 nm. Additionally, we have captured low-intensity spectral lines for Mg I, Mg II, and CsI at wavelengths of 326.233 nm, 333.06 nm, 365.577 nm, and 533.236 nm, respectively. The spectral database of the National Institute of Standards and Technology (NIST) is used to identify the transitions [8].

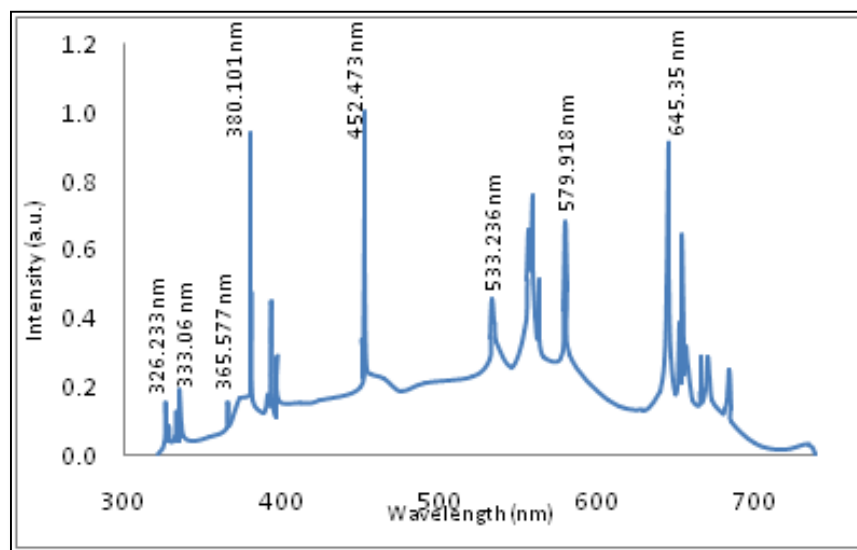


Figure 8- The emission spectrum of nanosecond laser induced Mg plasma at 55 MW laser peak power.

At varying laser peak strengths, the line intensities at 326.233 nm, 333.06 nm, and 607.326 nm were measured. Figure 9 shows that the intensities of the spectral lines are affected by the peak power of the laser. As the peak power of the laser increases from 22 MW to 88 MW, the emission intensity of the spectral lines also increases. Plasma permits more extensive target ablation since it absorbs and is relatively transparent to laser light. Plasma height and plasma emission are both increased as the target ablation is increased [9]. At higher laser peak powers, the plasma shielding effect becomes apparent, where the plasma reduces line intensities and blocks the laser beam, protecting the target [7].

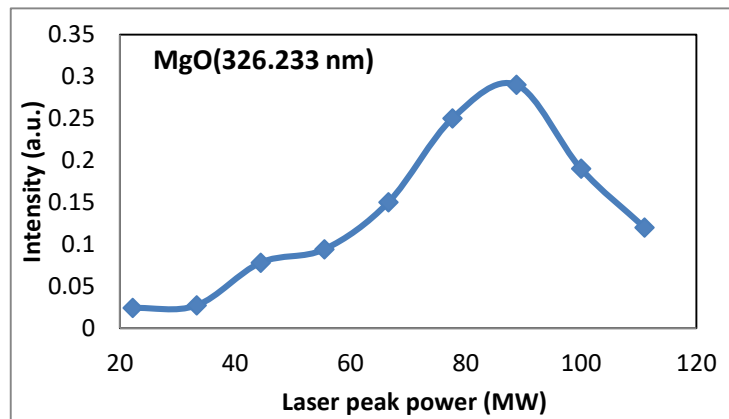


Figure 9- Variation of emission intensity with different laser peak power.

If the plasma is in LTE, the McWhirter criterion states that the electron density can't be lower than this:

$$n_e \geq 1.6 \times 10^{12} T_e^{1/2} \Delta E^3 \quad (5)$$

The energy difference between the states is denoted by  $\Delta E$  (eV), the electron temperature is  $T_e$ (K), and  $n_e$  is the density of electrons. From the Saha-Boltzmann equation, we derive the  $n_e$  values.:

$$n_e = \frac{2(2\pi m_e k_B T_e)^{3/2}}{h^3} \frac{I_{mn}^I A_{ij}^I g_i^I}{I_{ij}^I A_{mn}^I g_m^I} e^{-\frac{E_{ion} + E_i^I - E_m^I}{k_B T_e}} \quad (6)$$

$I$ , the mass of an electron,  $h$ , the ionisation potential of a neutral substance in its ground state, Boltzmann's constant, Planck's constant, and the equation itself all contain these variables. Electron density of laser-induced magnesium plasma with varying laser peak powers is illustrated in Figure (10). As the laser's peak power increases, the electron density grows. This happens because free electrons in the focal volume are accelerated when a collision-induced process is begun by irradiating a solid Mg sample with a Nd:YAG laser. These electrons then obtain energy through collisions with neutral atoms. The electron density increases in relation to the peak power of the laser because, once the electrons have amassed



enough energy, they can ionise atoms through collision. At high laser peak powers, the electron density drops considerably because of plasma shielding, which we've already covered.

By comparing two lines from the same ionisation stage species, we may get the electron temperature

$$(Te) \text{ as: } T_e = \frac{E_1 - E_2}{K_B \ln\left(\frac{\lambda_2^2 I_2 g_1 A_1}{\lambda_1^2 I_1 g_2 A_2}\right)} \quad (7)$$

There are three variables: the integrated line intensity ( $I$ ), the likelihood of transitions ( $A$ ), as well as the top-level statistical weight ( $g$ ). In order to find the electron temperature, we used the ratio of the Magnesium lines' brightness at 333.06 nm and 607.326 nm in conjunction with equation (7). Figure (11) shows the correlation between the maximum power output of a laser and the temperature of its electrons. The relationship between  $T_e$  and the peak power of the laser. Since the laser's peak power causes the target to evaporate, atomise, and ionise when concentrated on it, it stands to reason that the electron temperature is highly dependent on it [10].

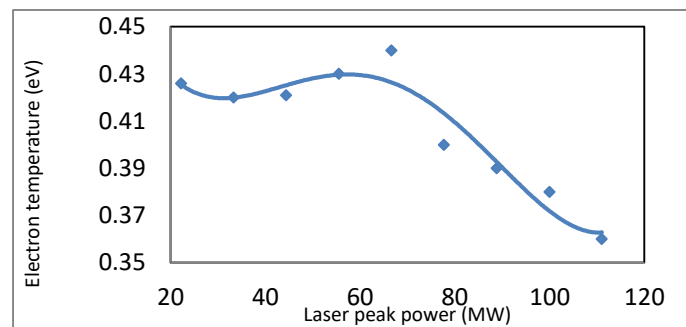


**Figure 10-** The electron density of laser induced Mg plasma at different laser peak power.

## Conclusions

This report presents the results of an optical emission spectroscopy (OES) study on laser-induced magnesium plasma. The discussion centres on the measured emission lines from atomic and ionic species and how their intensities are related to the laser peak power. From the intensity of the Mg I lines, we were able to derive the electron temperature of the magnesium plasma, which was found to be between 0.36 and 0.44 eV, and electron densities on the order of  $10^{17} \text{ cm}^{-3}$ .

## References:

- M. Autin, A. Briand and P. Mauchien, *Spectrochim. Acta Part B* 48, 851 (1993).
- J. B. Simeonsson and A.W. Miziolek, *Appl. Phys. B* 59,1 (1994).
- D. A. Cremers and L. J. Radziemski, *Handbook of laser induced breakdown spectroscopy* (John Wiley & Sons, Ltd, Chichester, 2006).
- M. A. Gigisos, S. Mar, C. Perez and I. de la Rosa, *Phys. Rev. E* 49, 1575 (1994).
- H. R. Griem, *plasma spectroscopy* (McGraw-Hill, New York, 1964).
- E. Florez, F. Mondragon, T.N. Truong, and P. Fuentealba., Transition metal atom adsorption on an F<sub>s</sub> defect site of MgO and the interaction with a hydrogen atom, *Phys. Rev.*, B73, pp.115423 – 115423-7, 2006.
- V. Kvachadze, G. Dekanozishvili, V.Vylet, M. G Galustashvili, Z. Akhvlediani, N Keratishvili, and D. Zardiashvili, Thermally stimulated luminescence of MgO ceramic and single crystal samples irradiate in reactor, *Radiat. Eff. & Defects in Solids*, 162, pp. 17-24, 2007.
- W.L. Wiese and G.A. Martin, *Wavelengths and Transition Probabilities for Atoms and Atomic Ions\_ Part II*, National Bureau of Standards, Washington, DC, (1980).
- Aadim, K.A.,Optical emission spectroscopic analysis of plasma parameters in tin–copper alloy co-sputtering system *Optical and Quantum Electronics*, 48(12), 545, 2016.
- Hehab, M.M., Aadim, K.A.Spectroscopic diagnosis of the CdO:CoO plasma produced by Nd:YAG laser *Iraqi Journal of Science*, 2021, 62(9), pp. 2948–2955.

## Design of Reconfigurable Antenna for UWB Operation and Dual-Band Rejection

Raad H. Thaher <sup>1</sup>

Lina M. Nori <sup>2</sup>

Adil S. Abduljabbar <sup>3</sup>



© 2024 The Author(s). This open access article is distributed under a Creative Commons Attribution (CC-BY) 4.0 license.



### Abstract:

The aim of this research paper is to design a microstrip antenna capable of changing the pass band region and different applications in the ultra wide band (UWB) and has a rejection characteristics using diodes so that at conduction give a certain band and in the OFF state give another application which give an equivalent to two different antennas. The antenna is proposed to make the switching operation depending on the design equation presented in the paper (initial parameters) and obtaining the optimum parameters that give reflection coefficient less than ( $S_{11} < -10\text{dB}$ ). It is found that proposed antenna is characterized by the following:

1. antenna reject the bands for WLAN (3.21-3.8) and WiMAX (5.16-5.9) GHz when all the pin diodes are OFF (i.e. D1, D2, D3)
2. The antenna reject the WiMAX (3.4-4.1) GHz when two diodes are in the ON state (D1, D2), and one diode is in the OFF state (D3)

Finally the antenna reject the WLAN (5.26-6.5) GHz when one of the diode is in the ON state (D3) while (D1 and D2) is in the OFF state. Also when all the diodes are in the ON state, the antenna operate as normal UWB antenna.

The variation of the voltage standing wave ratio (VSWR)(1:2) with frequency and the gain with frequency are obtained. Also the group delay of the proposed antenna is found in the acceptable range ( $\pm 3$  nsec). The proposed antenna is Simulated using the CST-19 program. It is intended to manufacture such antenna to get the practical results using the Vertical network analyser (VNA) and Compare the measured and Simulation results. The results of the proposed antenna is compared with other paper published in the literature.

**Keywords:** UWB; PIN Diode; Reconfigurable; WiMAX; WLAN; FR-4 Substrate; Reject Band; Microstrip.



<http://dx.doi.org/10.47832/MinarCongress12-14>



<sup>1</sup> Department of Biomedical Engineering, Al-Turath University, Baghdad, Iraq



<sup>2</sup> Department of Network Engineering, Al-Iraqia University, Baghdad, Iraq



<sup>3</sup> Department of Electrical Engineering, Al-Mustansiriyah University, Baghdad, Iraq

## Introduction

The rapid development of ultrawideband (UWB) communication systems necessitates efficient communication devices that can operate in their unique environments, as UWB systems are distinguished from others by their ultra-wide bandwidth for impedance, constant gain, omnidirectional radiation pattern, high radiation efficiency, constant group delay, low profile, and ease of manufacturing. Slot antennas, one of the recently proposed antenna designs, are a strong contender because of their very high radiation efficiency, low dispersion, and simple switch integration [1-5].

Both the research and industrial communities have been focusing more and more attention increasingly to reconfigurable antennas' capacity to rapidly change their operational frequency, polarization, and radiation pattern.. A lot of focus has been placed on the frequency agility trait because of the growing need to support virtually all telecommunication standards without sacrificing portability, efficiency, or simplicity. Several types of switches varactor diodes, and PIN diodes, are used to achieve this level of flexibility [6-11].

As an example, Due to their desirable characteristics, planar printed UWB antennas with band-stop performance have been researched., which include a straightforward design, a small footprint, a relatively low weight, a broad operating frequency range, and a low learning curve for integration. The elimination of interference with certain UWB-frequency wireless systems can be facilitated by making their rejected bands adjustable as needed. UWB systems, which operate at frequencies between (3.1-10.6) GHz, the issue of interference arises because the UWB spectrum is shared with other technologies, WLAN (5.15-5.825 GHz) and WiMAX (3.3-3.6 GHz) are some examples [12-16].

Many UWB antennas have considered adopting frequency-band-rejected function designs to get around the interference issue. Wideband to single and multiple band-notch monopole antennas are presented using a parasitic construction. The notch function is implemented with parasitic patches as well. A patch with slots was developed to get the band-notch qualities demand after a band-stop filter is employed. Other methods utilized for band-notch applications include fractal structure, defective ground structure (DGS) and pin diodes between slots in radiation patches or on the feed line are examples of how this is done, along with additional methods for switching between single and dual band-notch features[17-20].



An ultra-wideband (UWB) microstrip-fed antenna is used in this paper, and its notched-band performance can be adjusted. A reconfigurable electromagnetic bandgap (EBG) is integrated on both ends of a patch and center-fed line to achieve frequency agility.

Several publications indicate that modified planar antennas with band-notched features can be employed to construct the frequency band-notched function. propose a compact reconfigurable antenna that can operate in single- and dual-band stop modes, as well as multi-resonant. By varying the ON/OFF states of the PIN diodes, the antenna of the proposed design can be utilized to produce a single or dual-notch band to isolate and prevent interference in the UWB frequency range. The VSWR values and radiation pattern are calibrated for the relevant frequency range. The results of tests and modelling demonstrate the effectiveness of the recommended antenna arrangement for UWB applications [21–25].

### Proposed Antenna

On both sides of a FR-4 substrate, the suggested antenna construction with the desired parameters is printed with a thickness of 1.6 mm,  $\epsilon_r$  of 4.3, and a loss tangent of 0.002. The antenna consists of an electromagnetic band gap on the middle patch of a modified rectangular radiating patch with a defective ground structure. that has the shape of a star ( $2 \times 2$ ) mm<sup>2</sup>, and an antenna that is  $40 \times 30 \times 1.6$  mm<sup>3</sup>. The patch had two slits cut on either side, and a 0.1 mm-thick, inverted U-shaped ring was on the feed line. As seen in Figures (1) and (2), respectively, To allow for frequency reconfiguration of the antenna, The antenna patch and feedline are fitted with three PIN diodes. With the suggested antenna, eight of these states are feasible.

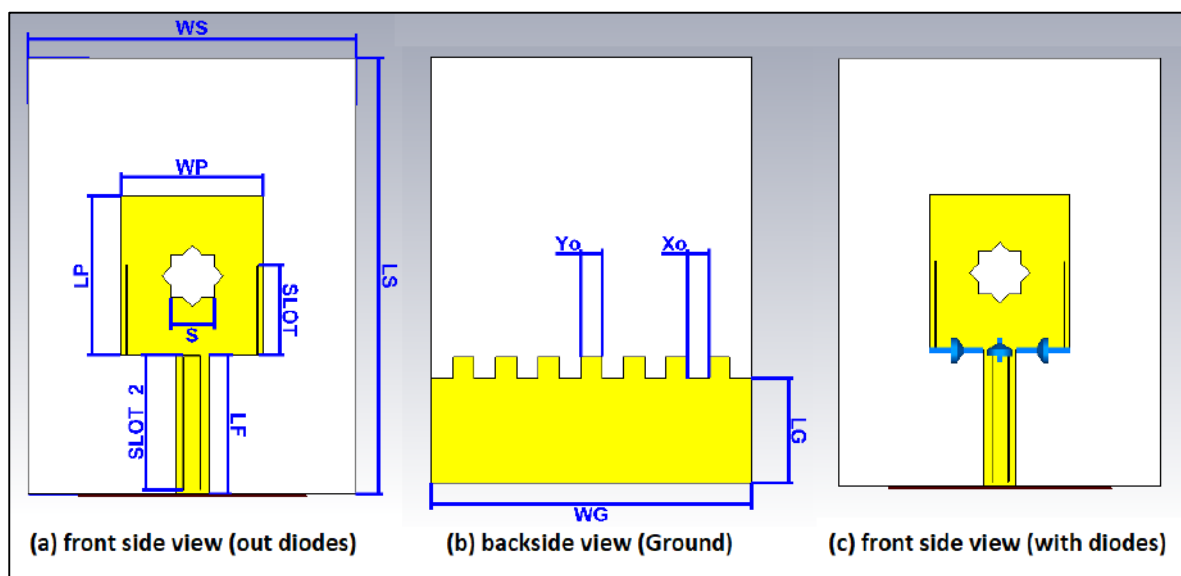


**Figure 1-** Antenna that can be reconfigured: (a) front side view(out diodes) and (b) backside view (Ground) and (c) front side view (with diodes)

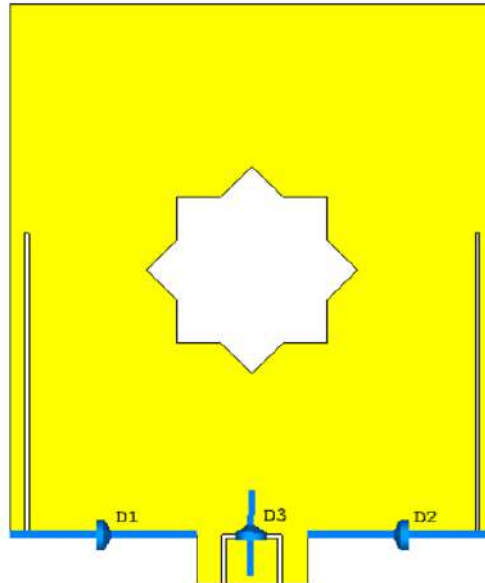


**Figure 2-** Reconfigurable pin diode antenna

The ground has been altered with forms and star DGS to obtain the (3.1–10.6) GHz Bandwidth, as seen in Figure (1b). A square patch was altered to take on the shape of a star in the centre in order to increase the impedance bandwidth. As an extra precaution, To provide an increased ground plane bandwidth for UWB applications, a partial ground plane is introduced, with a top side curved like a modified von Koch curve [26]. After the changes were generated by the simulation approach, it was discovered that the size of the adjustments was essential to getting the intended outcome. By connecting two slot strips to the side patch, the 5.15–5.8 GHz band rejection may be achieved. By adding an inverted U-shaped slot to the feedline, the band rejection of (3.2–3.8) GHz was accomplished, resulting in UWB performance with band rejection in the WLAN and WiMAX bands, respectively.

### **Switching operation:**

#### **1. Lumped Network Elements [27-29]:**

Circuit configurations such as RLC Serial, RLC Parallel, and Other are referred to as "Lumped Network Elements", which can be used to replicate basic electronic components.

Commonly used in switching applications are pin diodes. These pin diodes can be used as open or short circuits when put at different points, which will alter the effective resonant length and, consequently, the operating frequency of the antenna. For pin diode switches, Equivalent circuits are divided into two sets: one for operation and one for idleness. Prove that the circuit only makes use of a low-value resistor (represented by "R") and an inductor (represented by "L") linked in series, just like in the RL circuit. The (RLC) circuit, in which the letters "L" stand for an inductor, "R" for a high-value resistor, and "C" for a large capacitor, is what it looks like when it is in the off state. According to the CST program's modeling, its parameters are  $C = 0.015\text{pF}$ ,  $L = 0.15\text{nh}$ , and  $R = 4.7 \Omega$ . The same circuit model's on and off states are shown in Figure (3).

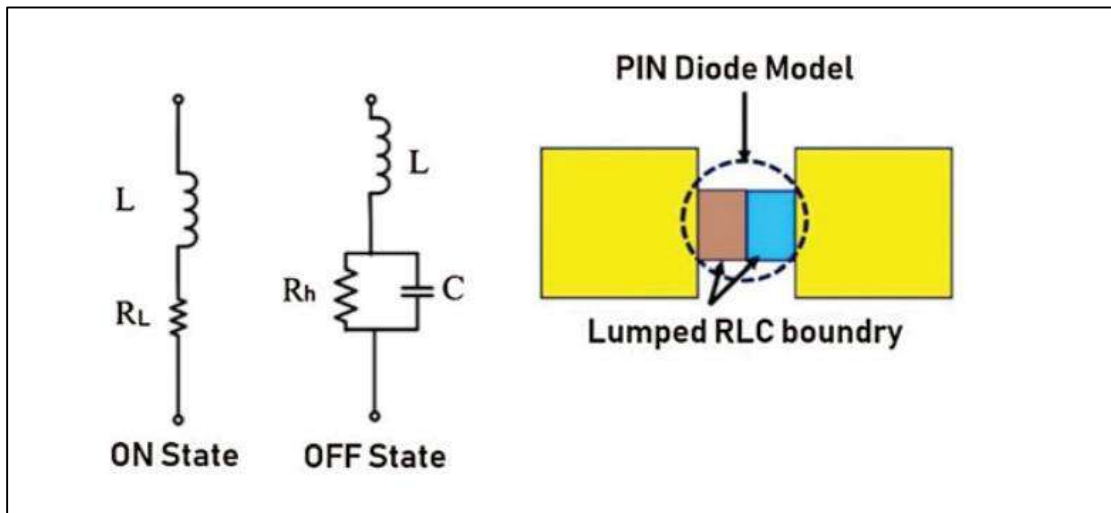


Figure 3- On and off states of an equivalent circuit model

### The suggested design of the antenna

The antenna is constructed to use the following design equation to determine the beginning values of the parameters: [5]

$$\epsilon_{reff} = \frac{\epsilon_r + 1}{2} + \frac{\epsilon_r - 1}{2} \left[ 1 + 12 \frac{h}{w} \right]^{-\frac{1}{2}} \quad (1)$$

$$L_{eff} = \frac{c}{2f_0 \sqrt{\epsilon_{reff}}} \quad (2)$$

$\Delta L$ , the length extension, is provided by

$$\frac{\Delta L}{h} = 0.412 \frac{(\epsilon_{reff} + 0.3) \left( \frac{w}{h} + 0.264 \right)}{(\epsilon_{reff} - 0.285) \left( \frac{w}{h} + 0.8 \right)} \quad (3)$$

The actual length ( $L$ ) of the patch is obtained by:

$$L = L_{eff} - 2\Delta L \quad (4)$$

$$f_r = \frac{1}{2L\sqrt{\epsilon_r\epsilon_0\mu_0}} = \frac{c}{2L\sqrt{\epsilon_r}} \quad (5)$$

The width of the patch element (W) is given by:

$$W = \frac{1}{2f_r\sqrt{\mu_0\epsilon_0}}\sqrt{\frac{2}{\epsilon_r+1}} \quad (6)$$

$$L_g = 6h + L \quad (7)$$

$$W_g = 6h + W \quad (8)$$

$$Z_c = \frac{120\pi}{\sqrt{\epsilon_{reff}}\left[\frac{W_0}{h}+1.393+0.667\ln\left(\frac{W_0}{h}+1.444\right)\right]} \quad \frac{W_0}{h} > 1 \quad (9)$$

$$L_{notch} = \frac{C}{2f_{notch}\sqrt{\epsilon_{reff}}} \quad (10)$$

$$L_{notch} = \frac{C}{4f_{notch}\sqrt{\epsilon_{reff}}} \quad (11)$$

$$\lambda = \frac{C}{2f_{notch}\sqrt{\epsilon_{reff}}} \quad (12)$$

Where:

$h$  : is the thickness of the substrate.

$L$  : is the length of the patch.

$L_{eff}$  : is the effective length of the patch.

$f_{notch}$  : Is the notch center frequency.

$L_{notch}$  : is the notch length.

$W$  : is the width of the patch.

$C$  : is the speed of light =  $3 \times 10^8$  m/sec.

$f_0$  : is the operating frequency.

$\epsilon_r$  : is the relative dielectric constant.

$\epsilon_{reff}$  : is the effective relative dielectric constant.

$L_g$  : is the length of a ground plane.

$W_g$  : is the width of a ground plane.

$W_0$  : is the microstrip line width.

$Z_c$  : is the microstrip line characteristic impedance.



It is possible to determine the Suitable values for each parameter in order to produce the desired results. The table displays the starting and optimal parameter values. (1).

**Table 1-** Values of the initial and Suitable parameters

Parameters	Initial value(mm)	Suitable value(mm)
$W_s$	34	30
$L_s$	42	40
$W_p$	14	13
$L_p$	16	14.5
$W_f$	3.1	2.96
$W_g$	34	30
$L_g$	42	9.75
a	1	0.4
b	0.4	0.1
c	2	1
d	1	0.8
e	22	19.5
$Y_0$	1.5	1
$Y_1$	2.5	2
$h_s$	1.6	1.6
$h_t$	0.035	0.035

## The Results

Spark that initiates the waveguide's action is supplied by a regular-sized port. Among the performance parameters are radiating structure, surface current, group latency, return loss, VSWR, and gain.

### (a) Resonant mode status Bandwidth and Loss of Return:

Using the suggested structure and adding three-pin diodes across the radiation patch and feedline slots, as seen in figure 2, create a UWB antenna with single and dual band notches. Between radiating patches, open and short circuit behaviour can be produced by flipping each pin diode between its ON and OFF states. It is possible to change the frequency of the suggested antenna. By varying the locations of the switches, the optimal frequency notched bands can be produced; the suggested architecture has eight potential operating modes.

1. When all pin diodes are off, the antenna rejects the following bands for WLAN and WiMAX, respectively: 3.21–3.81 GHz and 5.16–5.9 GHz
2. Only the WiMAX (3.4–4.1) was rejected (i.e., single band reject), while pin diodes D1 and D2 are functioning in the on state and pin diode D3 is operating in the off state.
3. When pin D3 is in the on state while pins D1 and D2 are in the off state. The WLAN (5.26–6.5 GHz) will be rejected by the antenna. When every pin diode is turned on, the suggested antenna functions as a UWB.

For this reason, the accidental symmetry does not account for the other status of D1, and D2 (i.e., D1 on, D2 off, and vice versa). Consequently, the four statuses shown in Table (2) represent the actual outcomes. Note that only D1, D2, and D3 (both ON or both OFF) are functional states. For each of the four effective statuses, the fluctuation of the reflection coefficient ( $S_{11}$ ) with frequency is depicted in Figure 4.

**Table 2-** Conditions of operation for pin diodes at various resonance frequencies

status	D1	D2	D3	Band Possible in GHz
1	OFF	OFF	OFF	(3.21-3.81) and (5.16-5.9) band rejected
2	ON	OFF	OFF	not in running
3	OFF	ON	OFF	not in running
4	ON	ON	OFF	(3.4-4.1) WiMAX band reject
5	OFF	OFF	ON	(5.2-6 GHz) WLAN band reject
6	ON	OFF	ON	not in running
7	OFF	ON	ON	not in running
8	ON	ON	ON	(3.1-10.6) Ultra Wide band pass

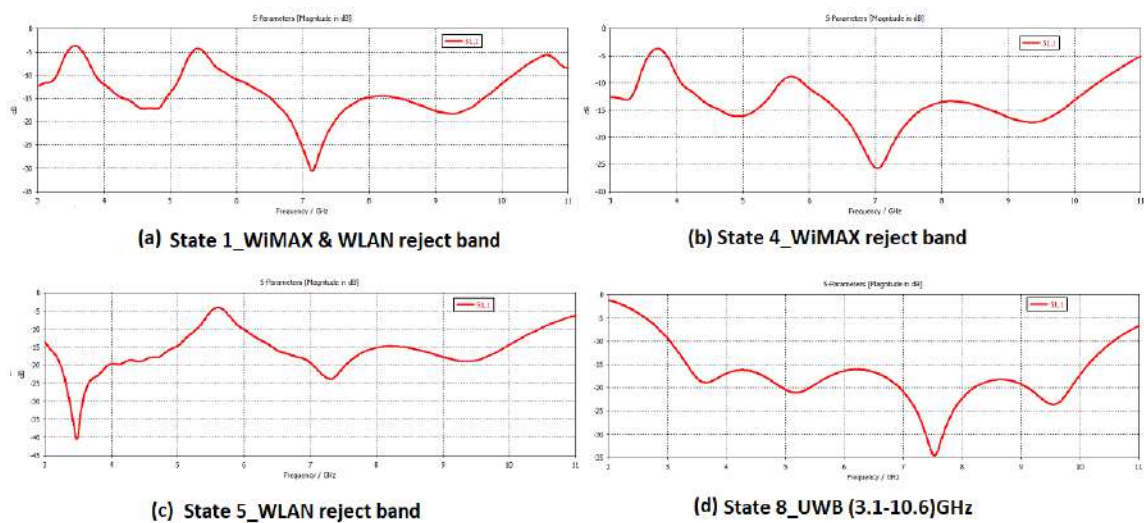


**Figure 4-** The  $S_{11}$  frequency variation for the various status

(b) Figure 5 illustrates how the Voltage Standing Wave Ratio (VSWR) varies with frequency throughout four states. It should be observed that the VSWR value is 1-2.

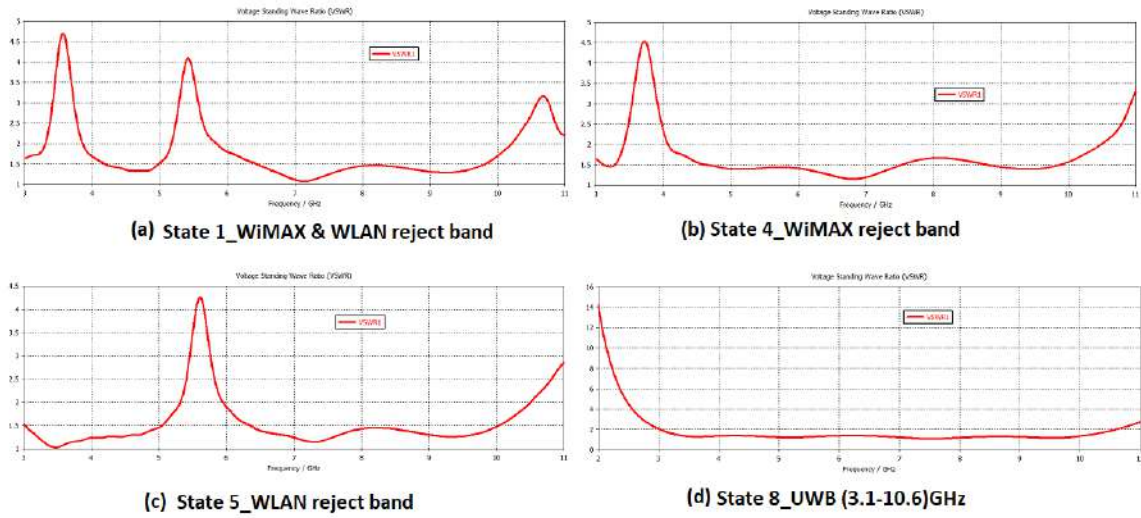


Figure 5- Voltage Standing Wave Ratio (VSWR).

However, Figure (6) indicates the varying values of the gain with frequency for various modes of operation; Table (3) displays the maximum gain value for each state

Table 3- highest gain value in several status.

Status	highest gain value
1	(-3.8, -2.2 and 3.8)
4	(-0.5,3.8)
5	(-1.6,3.4)
8	(2.5)

Since the antenna operates in the UWB (status 8), it is evident that the gain is positive in these bands, however in the notch bands (status 1,4,5) it is negative.

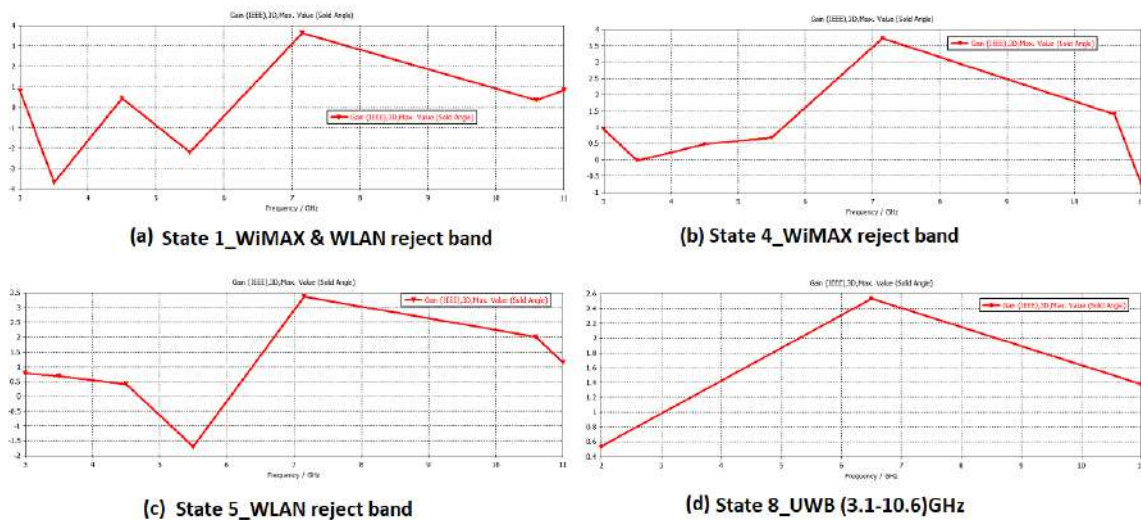
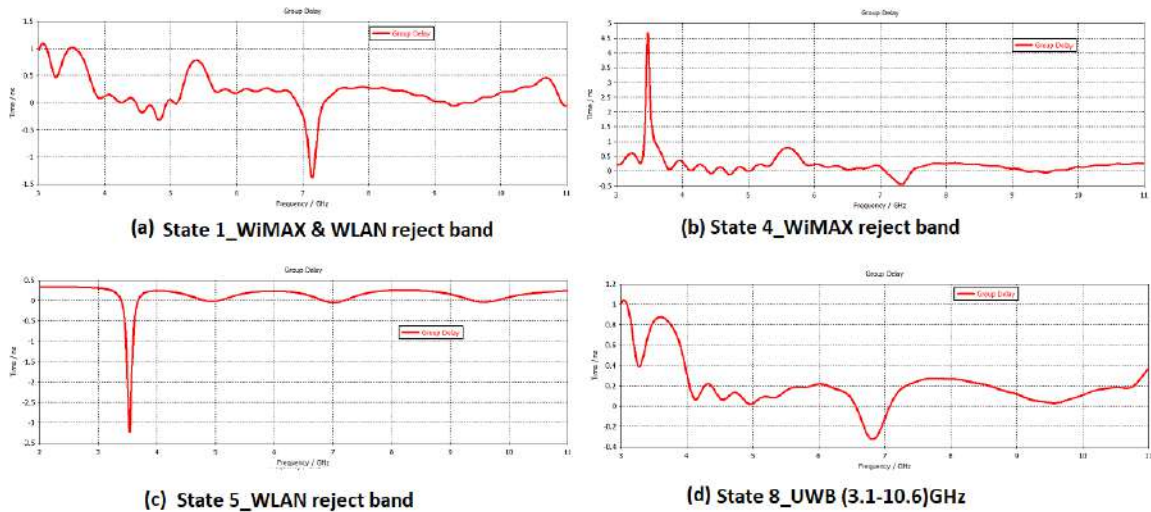


Figure 6- Gain is in agreement with simulations

## (c) Group delay

Since Group delay is a signal distortion metric, it is expected that it will be outside the allowed range ( $\pm 3$  nsec). In status 8, the UWB group latency is (-0.3 - 0.9) nsec. The four status group delays are displayed in Figure (7). Because of this, the antenna's operation can be classified as either notch band or regular UWB, depending on the D1, D2, and D3 states.



**Figure 7-** The suggested antenna's group delay

The surface current distribution for various operating statuses is displayed in Figure (8). Figures 8a, 8b, and 8c, in that order, show the surface current distribution of status 1 with dual-band reject (WiMAX, WLAN) and single passband (5.8-10.2) GHz. As seen in Figures 8d and 8e, the surface current of status 4 and 5 is single band rejects (WiMAX and WLAN), respectively. Only the UWB operation is displayed in Figure (8f) That is, without a notch. Figure (8c) illustrates the uniform distribution of surface current, which is mostly concentrated in the feed at a passband frequency of 7.15 GHz (outside the notched band). Nonetheless, it should be observed that for all states, Figures (8a), (8b), (8d), (8e), and (8f) show surface current distributions that are concentrated close to the slot margins at the center frequencies of the notched band, which are (3.5) and (5.5) GHz, respectively.



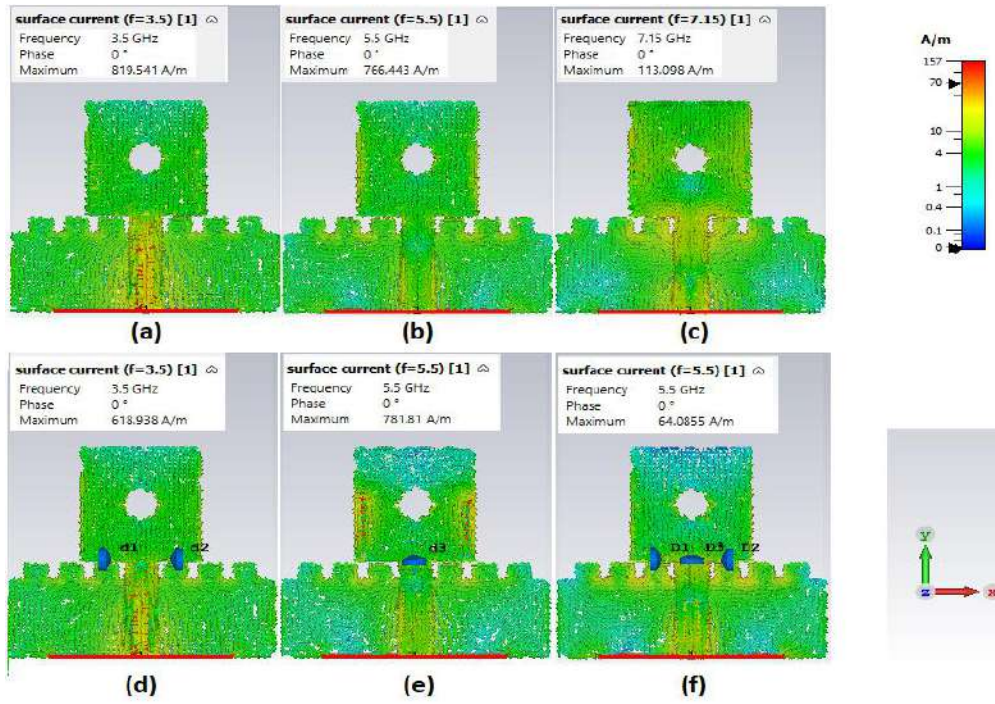


Figure 8- The spreading of surface currents

f) The Pattern of Far-Field Directivity Radiation

The proposed antenna's simulated Figure 9 shows the far-field radiation patterns for four distinct operating states in the H-field and E-field, respectively. The H-field and the E-field are two examples of far-field radiation patterns that demonstrate omnidirectional bidirectional patterns while maintaining an approximate dipole form

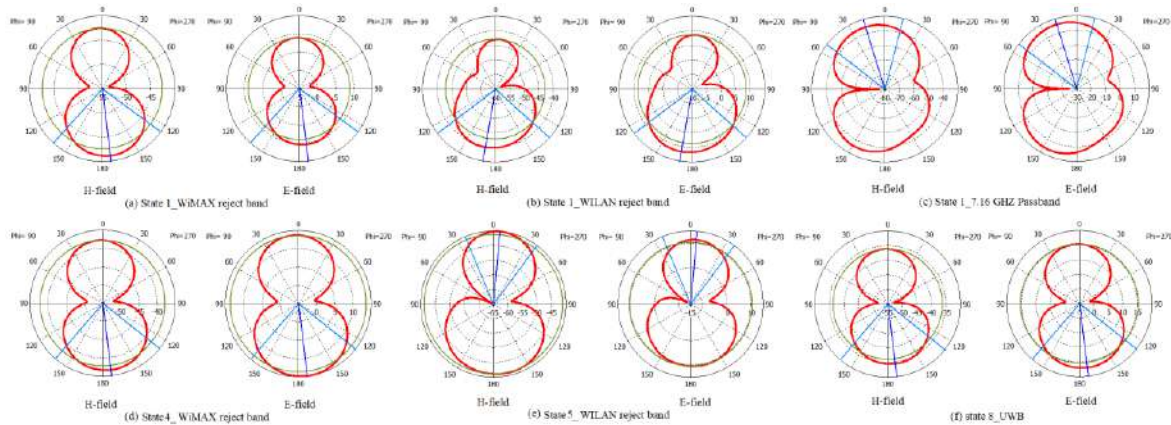


Figure 9- H-field and E-field Far-Field Radiation Patterns

**Table 4-** UWB antennas with customizable band-notches are compared in terms of their performance.

Reference	shape	size mm	Band reject	State mode
[1]	circular	(70X44)	WiMAX & WLAN	Single mode
[2]	circular	(36x32)	WiMAX & WLAN	multimode
[4]	circular	(42x32)	WiMAX & WLAN	Single mode
[28]	rectangular	(20x20)	WiMAX	Single mode
Proposed	rectangular	(30X40)	WiMAX & WLAN	Multi mode

**Conclusion:**

A notch band antenna was proposed and simulated to perform the single and dual band notch, the antenna size  $(30 \times 40 \times 1.6) \text{ mm}^2$  with epoxy substrate with  $\epsilon_r = 4.3$ , loss tangent  $\tan \delta = 0.002$ . It was noted that the antenna provides four effective states depending on the position of the pin diodes. Hence acceptable results were obtained in which WiMAX, WLAN can be rejected and offer the passband for the other frequencies. However, the proposed antenna offers normal operation in terms of gain and group delay. For the future work it is intended to fabricate such antenna and obtain the practical results using the Vector Network Analyzer (VNA) and compare the simulation and practical results. The group delay can be modified using other connections of pin diodes. Also it is suggest to arrange the diodes to get other rejection bands using MIMO applications.

**Conflicts of Interest:** Conflicts of interest are not disclosed by the authors.

**Author Contributions:** The authors have made the following research contributions: “Conceptualization, R.H. Thaher, and A.S. Abduljabbar ; methodology, R.H. Thaher; software, A.S. Abduljabbar; validation, R.H. Thaher, and L.M. Nori; formal analysis, L.M. Nori; investigation, L.M. Nori and A.S. Abduljabbar; data curation, R.H. Thaher, and L.M. Nori original draft preparation, L.M. Nori, review and editing, R.H. Thaher, L.M. Nori, and A.S. Abduljabbar; visualization, A.S. Abduljabbar; supervision R.H. Thaher

**Acknowledgments:** Authors thanks Al-Iraqia, Al-Turath, and Al-Mustansiriyah universities, sponsor and financial support acknowledgments.

**References:**

- Z. Chao, Z. Zitong, X. Pei, Y. Jie, L. Zhu, and L. Gaosheng, "A Miniaturized Microstrip Antenna With Tunable Double Band-Notched Characteristics For UWB Applications," *Sci Rep*, Vol. 12, No. 19703, pp. 1-13, 2022.
- M.S. Alam and A. Abbosh, "Reconfigurable band-rejection antenna for ultra-wideband applications," *IET Microwaves, Antennas and Propagation*, Vol. 12, No. 2, pp. 195-202, 2018.
- Francis Xavier Engineering College and Institute of Electrical and Electronics Engineers, Proceedings of the International Conference on Smart Systems and Inventive Technology (ICSSIT 2018): Francis Xavier Engineering College, Tirunelveli, India, date: December 13-14, 2018.
- S. Lakrit, S. Das, A. El Alami, D. Barad, and S. Mohapatra, "A compact UWB monopole patch antenna with reconfigurable Band-notched characteristics for Wi-MAX and WLAN applications," *AEU - International Journal of Electronics and Communications*, Vol. 105, pp. 106–115, 2019
- F. Zhu et al., "Multiple band-notched UWB Antenna With Band-Rejected Elements Integrated In The Feed Line", *IEEE Trans Antennas Propag*, Vol. 61, No. 8, pp. 3952–3960, 2013.
- H. Oraizi and N. V. Shahmirzadi, "Frequency- and time-domain analysis of a novel UWB reconfigurable microstrip slot antenna with switchable notched bands", *IET Microwaves, Antennas and Propagation*, Vol. 11, No. 8, pp. 1127-1132, 2017.
- N. F. Miswadi and M. T. Ali, "Design of compact reconfigurable UWB antenna with WiMAX and WLAN band rejection," *Indonesian Journal of Electrical Engineering and Computer Science*, vol. 17, no. 3, pp. 1427–1433, 2019.
- O. El Maleky and F. Ben Abdelouahab, "A UWB antenna with reconfigurable rejection band using split ring resonator for radio cognitive technology," in *Procedia Manufacturing*, Elsevier B.V., 2019, pp. 694–701
- B. Chen, A. G. Wang, and G. H. Zhao, "Design of a novel ultrawideband antenna with dual band-notched characteristics," *Microw Opt Technol Lett*, vol. 54, no. 10, pp. 2401–2405, Oct. 2012
- B. Chen, W. Leng, A. G. Wang, and G. H. Zhao, "Compact ultra-wideband antenna with reconfigurable notched bands," *Electron Lett*, vol. 48, no. 19, pp. 1175–1176, Sep. 2012
- Institute of Electrical and Electronics Engineers, IEEE Microwave Theory and Techniques Society, IEEE Instrumentation and Measurement Society, and Institute of Electrical and Electronics Engineers. Region 8, 2016 16th Mediterranean Microwave Symposium (MMS)
- IEEE Computer Society and Institute of Electrical and Electronics Engineers, Innovations'16: proceedings, 2016 12th International Conference on Innovations in Information Technology (IIT)
- D. Zhao, L. Lan, Y. Han, F. Liang, Q. Zhang, and B. Z. Wang, "Optically controlled reconfigurable band-notched UWB antenna for cognitive radio applications," *IEEE Photonics Technology Letters*, vol. 26, no. 21, pp. 2173–2176, Nov. 2014
- Loughborough University, Annual IEEE Computer Conference, Loughborough Antennas and Propagation Conference 8 2012.11.12-13 Loughborough, and LAPC 8 2012.11.12-13 Loughborough, Loughborough Antennas and Propagation Conference (LAPC), 2012 12-13 Nov. 2012
- J. Dong, X. Zhuang, and G. Hu, "Planar UWB monopole antenna with tri-band rejection characteristics at 3.5/5.5/8 GHz," *Information (Switzerland)*, vol. 10, no. 1, Dec. 2018

- W. A. E. Ali and R. M. A. Moniem, "Frequency Reconfigurable Triple Band-Notched Ultra-Wideband Antenna with Compact Size," 2017
- J. Perruisseau-Carrier, P. Pardo-Carrera, and P. Miskovsky, "Modeling, design and characterization of a very wideband slot antenna with reconfigurable band rejection," *IEEE Trans Antennas Propag*, vol. 58, no. 7, pp. 2218–2226, Jul. 2010
- IEEE Electrical Insulation Society Staff, 2013 13th Mediterranean Microwave Symposium (MMS). IEEE, 2013
- C. Singh and G. Kumawat, "A Compact Rectangular Ultra-Wideband Microstrip Patch Antenna with Double Band Notch Feature at Wi-Max and WLAN," *Wirel Pers Commun*, vol. 114, no. 3, pp. 2063–2077, Oct. 2020.
- Annual IEEE Computer Conference, Fla. Annual IEEE Wireless and Microwave Technology Conference 14 2013.04.07-09 Orlando, Fla. Annual Wireless and Microwave Technology Conference 14 2013.04.07-09 Orlando, Fla. IEEE Wireless & Microwave Technology Conference 14 2013.04.07-09 Orlando, and Fla. WAMICON 14 2013.04.07-09 Orlando, IEEE 14th Annual Wireless and Microwave Technology Conference (WAMICON), 2013 7-9 April 2013, Orlando, FL
- P. Mayuri, N. D. Rani, N. B. Subrahmanyam, and B. T. P. Madhav, "Design and Analysis of a Compact Reconfigurable Dual Band Notched UWB Antenna," 2020
- Institute of Electrical and Electronics Engineers Malaysia Section, Annual IEEE Computer Conference, IEEE Symposium on Computer Applications and Industrial Electronics 2015.04.12-14 Langkawi, and ISCAIE 2015.04.12-14 Langkawi, 2015 IEEE Symposium on Computer Applications & Industrial Electronics (ISCAIE) 12-14 April 2015, Langkawi, Kedah, Malaysia
- H. A. Atallah, A. B. Abdel-Rahman, K. Yoshitomi, and R. K. Pokharel, "Reconfigurable Band-Notched Slot Antenna Using Short Circuited Quarter Wavelength Microstrip Resonators," 2016
- S. Tripathi, A. Mohan, and S. Yadav, "A compact fractal UWB antenna with reconfigurable band notch functions," *Microw Opt Technol Lett*, vol. 58, no. 3, pp. 509–514, Mar. 2016
- Y. Shang, S. Xiao, M. C. Tang, Y. Y. Bai, and B. Wang, "Radar cross-section reduction for a microstrip patch antenna using PIN diodes," *IET Microwaves, Antennas and Propagation*, vol. 6, no. 6, pp. 670–679, Apr. 2012
- A. Karmakar, P. Chakraborty, R. Ghatak, and D. R. Poddar, "A Compact Fractal UWB Antenna with open-ended Quarter Wavelength Slot for Band Notch Characteristics."
- S. H. Zheng, X. Liu, and M. M. Tentzeris, "Optically controlled reconfigurable band-notched UWB antenna for cognitive radio systems," *Electron Lett*, vol. 50, no. 21, pp. 1502–1504, Oct. 2014
- N. Tasouji, J. Nourinia, C. Ghobadi, and F. Tofigh, "A novel printed UWB slot antenna with reconfigurable band-notch characteristics," *IEEE Antennas Wirel Propag Lett*, vol. 12, pp. 922–925, 2013
- [29] A. Musavand, Y. Zehforoosh, H. Ojaroudi, and N. Ojaroudi, "A Compact UWB Slot Antenna with Reconfigurable Band-Notched Function for Multimode Applications," 2016.



## Particle Pollution in University of Baghdad Campus

Nahla Shadeed Ajeel <sup>1</sup>

Hussein J. Khadim <sup>2</sup>



© 2024 The Author(s). This open access article is distributed under a Creative Commons Attribution (CC-BY) 4.0 license.

### Abstract:

*The aim of this research to determine particle pollution in the University of Baghdad campus. This study was chosen as a result of the University of Baghdad's location being close to sources of particulate pollution, such as the Doura refinery and traffic intersections that are crowded most of the time, as well as the frequent use of cars by university students and employees. Air samples were collected via portable particle mass counter device (Temptop) used to determine concentrations of total suspended particles TSP and particulate matters (PM (PM<sub>2.5</sub> and PM<sub>10</sub>)). Readings conducted in the first half of 2024 during day.*

*Particulates matters including PM with different diameters such as particulate matter 2.5 PM<sub>2.5</sub> µg/m<sup>3</sup> and particulate matter 10 PM<sub>10</sub> µg/m<sup>3</sup>, and larger suspended particles matters in air TSP µg/m<sup>3</sup> during the study periods which extend from January to June 2024.*


*The largest concentration value of PM<sub>2.5</sub> was founded in January was 48.3 µg/m<sup>3</sup> while the lowest one recorded in June was 14 µg/m<sup>3</sup>. As well as concentrations of PM<sub>10</sub> ranged from 74.9 µg /m<sup>3</sup> in January to 15 µg /m<sup>3</sup> in February, TSP recorded value found between 7197 and 1740 µg /m<sup>3</sup> in January and February respectively.*


*The averages of particulate matters and total suspended particles matters in some months were exceeded WHO suggested standards for ambient and in others months within WHO standards. This may be resulted due to the existence of relevant industries and crowded traffic around the campus that led to high concentrations. Therefore, effective strategies such as traffic management, industrial movement away from university can be effective in reducing airborne PM and TSP concentrations.*

**Keywords:** Particle Pollution; Aerosols; Campus; Particulate Matters; Crowded Traffic; University of Baghdad.



<http://dx.doi.org/10.47832/MinarCongress12-15>

<sup>1</sup>  Department of Environmental Engineering, Collage of Engineering, University of Baghdad, Iraq  
[nahla.shadeed@coeng.uobaghdad.edu.iq](mailto:nahla.shadeed@coeng.uobaghdad.edu.iq)

<sup>2</sup>  Department of Environmental Engineering, Collage of Engineering, University of Baghdad, Iraq  
[hussein.jabar@coeng.uobaghdad.edu.iq](mailto:hussein.jabar@coeng.uobaghdad.edu.iq)

## Introduction

Contamination of air is a serious environmental hazard to public health. Particles matter is small that they sometimes can stay suspended in the air, particulate matter harmful atmospheric pollutant. The scientific term for particles present in the air is aerosols, which include liquid, solid particles, and the mix of gases that keep particles in suspended. To stay suspended in the air, the particles must be less than 100 micrometers; larger particles fast precipitate to the ground, and in general can not to be transported over long distances. WHO estimated that 4.3 million deaths per year worldwide are attributable to exposure to PM (1). Particulate matter is a complex of a wide different of chemical species, like heavy metals, which are not metabolized through human body and accumulate in the some soft tissues. Airborne particles have been produce through natural sources (2). Natural sources are salt of sea, volcanic eruptions and mineral dust, while anthropogenic sources are non-exhaust and exhaust vehicle emissions, agricultural activities, biomass burning and fossil fuel combustion, mining activities. As well as particles matter can result from gases or physical or chemical processes (3). The remaining per cent of particles in the air are produced by anthropogenic (Manmade), and emissions in some places can be very large (4).

The aim of this paper is to determine the concentrations levels of particulate matters PM in ambient air of Baghdad University campus.

## Materials and Methods

### Sampling Site:

The sampling site was at the campus of University of Baghdad (Center of the university), samples were collected through January – June, 2024. Three samples were collected from different points on random days and during the morning, except for rainy days. The main sources of manmade emissions in this area are traffic with industrial activities (3). While natural PM sources, the study area is affected from dust storms that Baghdad is exposed to from time to time.

There are many methods of study the levels of particles in air, depending on the aim of the study and how performed (4). A measurement indicates particles number, chemical structure and mass. The studies that linked to public health focus on chemical structure of PM while studies on particles impact on the weather and climate focus on size and numbers of particle (5).

Air samples were collected from studied area by use portable particle mass counter device (Temtop) Figures (1) which put on 1.5 – 2 meter high above the ground surface to ensure accuracy in readings and avoid pollution.



Figure 1- Portable particle mass counter device

### Effects of Meteorological Factors on PM Concentrations

Temperature, relative humidity, atmospheric pressure, speed of wind, and direction of wind have been termed the important parameters in the movement of contaminants of air and have a huge effect on the particulate matter movement (6). When the wind speed is high, the high rapid and complete the dispersion of pollutants in the air (7,8). Meteorological factors which led to reduce of contaminants rates and chemical reactions and removal processes like wet and dry deposition that are important factors affecting the particle concentration in the air (11,12).

### Results and discussions

#### Air quality variables:

Average particulate matter concentrations PM<sub>2.5</sub>, PM<sub>10</sub>, and TSP measured during study period in sampling site are show in table (1)

Table 1- Mean concentrations of particulate matter PM<sub>2.5</sub>, PM<sub>10</sub>, and TSP in sampling site

Variable	PM 2.5 μg/m <sup>3</sup>	PM 10 μg/m <sup>3</sup>	TSP μg/m <sup>3</sup>
Months			
January	48.3	74.9	7197
February	8.6	15	1740
March	36	50	2705
April	26	41	3691
May	32	44	4324
June	14	22	2094

## Levels of Particulate Matter 2.5 PM2.5

Measured concentrations of PM<sub>2.5</sub> in the first six months of 2024 in the campus, results found that highest concentrations are more common in January, March and May compared with concentrations in the rest months as shown in figure (2). The highest level recorded in January was 48.3  $\mu\text{g}/\text{m}^3$ , while the lowest value found in February was 8.6  $\mu\text{g}/\text{m}^3$ . The WHO standard for PM<sub>2.5</sub> is 25  $\mu\text{g}/\text{m}^3$  for daily mean values. That means concentrations of PM<sub>2.5</sub> in January, March, April, and may exceed limits of WHO.

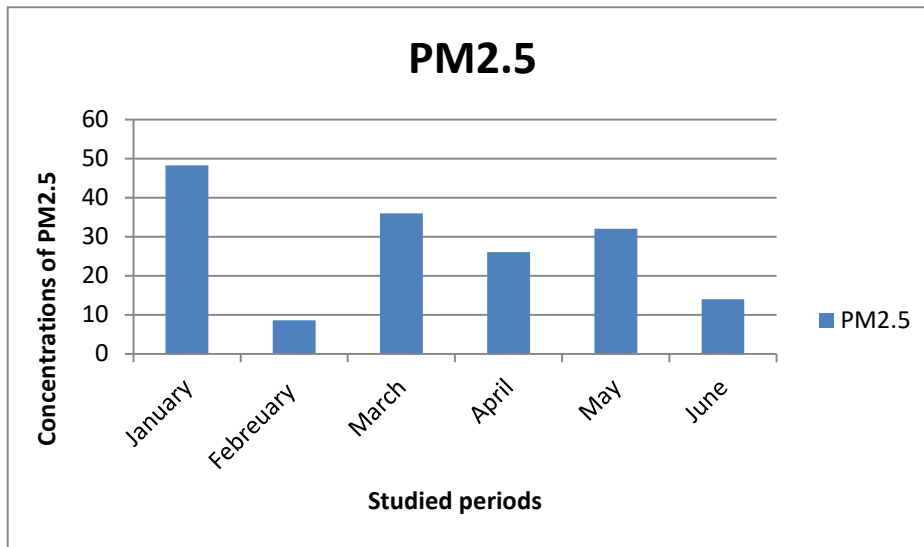


Figure 2- Mean concentrations of PM<sub>2.5</sub>  $\mu\text{g}/\text{m}^3$  during study periods (January to June 2024)

### 1. Levels of Particulate Matter 10 PM10:

Measured concentrations of PM<sub>10</sub> ranged from 15  $\mu\text{g}/\text{m}^3$  to 74.9  $\mu\text{g}/\text{m}^3$  in February and January respectively as shown in figure (3). The highest level recorded in January was, while the lowest value found in February. From results was observed that in January PM<sub>10</sub> found 74.9  $\mu\text{g}/\text{m}^3$  and this value exceeded WHO limits was 50 $\mu\text{g}/\text{m}^3$  for daily mean values. While in other months the concentrations within standards of WHO. Due to effects of weather factors



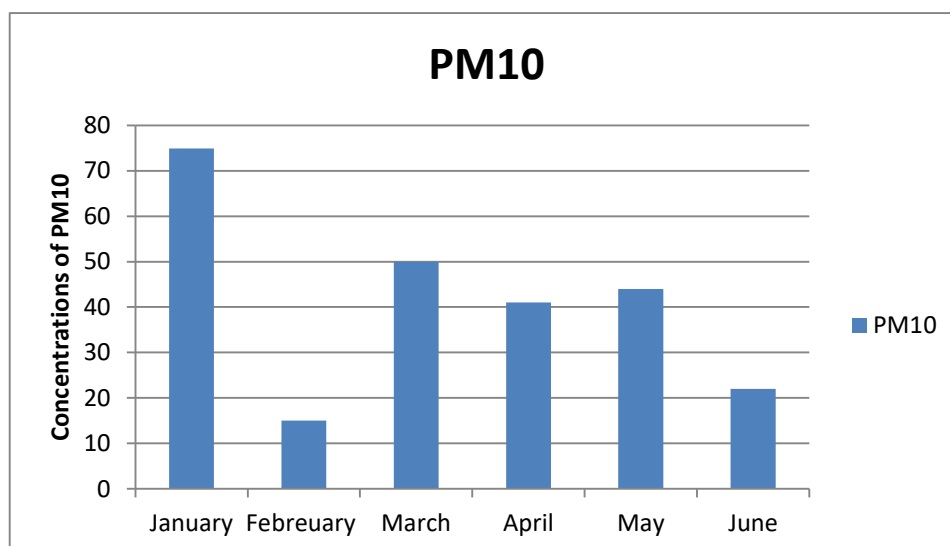


Figure 3- Mean concentrations of PM10  $\mu\text{g}/\text{m}^3$  during study periods

## 2. Levels of Total Suspended Particles TSP

Concentration of TSP ranged from 1740 in February to 7197  $\mu\text{g}/\text{m}^3$  in January. The results show levels of TSP in all studied months more than World Health Organization WHO limits  $150 \mu\text{g}/\text{m}^3$ , this may be due to meteorological factors that effects on accumulation and concentration of TSP as shown in figure (4). These concentrations of TSP are considered in the unhealthy to very unhealthy.

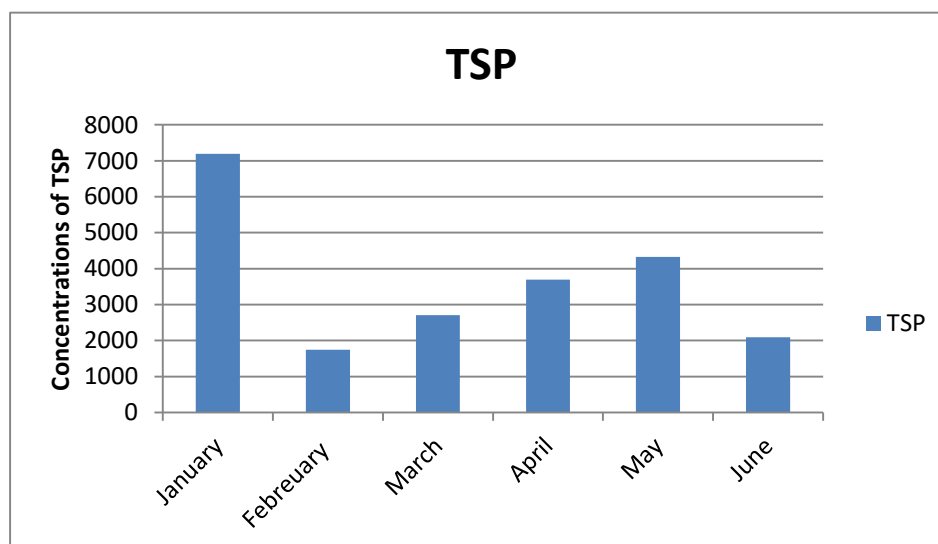


Figure 4- Mean concentrations of TSP  $\mu\text{g}/\text{m}^3$  during study periods

## Conclusion

According to the results the highest levels of TSP, PM 10, PM 2.5 are recorded in January, and in general most value more than WHO and EPA standards, while in others months most concentrations values within standards. The increase in concentrations in January is due to the overcrowding of the university campus and surrounding areas with

traffic, as this month represents the peak time for working hours at the university, as well as the time for taking samples during the first hours of the day, which is considered the time when traffic is at its most intense, and this increases the emission of pollutants.

As for the decrease in pollutant concentrations during the rest of the months, it may be due to the Iraqi government's decision to change working hours at universities and ministries, which reduced traffic momentum at the intersections near the University of Baghdad and at the university itself.

Particulate matter PM is a global problem, the high effective method to decrease particulate matter PM concentrations levels in the air is to decrease sources, therefore must be reducing and eliminating sources of pollution, as well as move factories and car garages away from residential areas to decrease dangerous on public health. The issue requires more studies to cover more areas and then estimate the extent of the impact of the concentrations of these pollutants on the environment and humans alike.

## References

- WHO (2014). 7 million premature deaths annually linked to air pollution. <http://www.who.int/media-centre/news/releases/2014/air-pollution/en/>.
- Environmental Protection Agency. Air and Environment 2023, Swedish.
- Alberto Izzotti, Paola Spatera, Zumama Khalid and Alessandra Pulliero. (2022). Importance of Punctual Monitoring to Evaluate the Health Effects of Airborne Particulate Matter. *Int. J. Environ. Res. Public Health* 2022, 19, 10587.
- Moryani, H.T.; Kong, S.; Du, J.; Bao, J. Health risk assessment of heavy metals accumulated on PM<sub>2.5</sub> fractioned road dust from two cities of Pakistan. *Int. J. Environ. Res. Public Health* 2020, 17, 7124.
- Kastury, F.; Smith, E.; Juhasz, A.L. A critical review of approaches and limitations of inhalation bioavailability and bioaccessibility of metal(loid)s from ambient particulate matter or dust. *Sci. Total Environ.* 2017, 574, 1054–1074.
- Shihab, A.S. Meteorological effects on particulate matter PM<sub>10</sub>, PM<sub>2.5</sub> concentrations with diurnal and seasonal variations in cities neighboring desert lands. *Nat Hazards* (2024). <https://doi.org/10.1007/s11069-024-06658-2>
- Filonchyk, M., Yan, H., Yang, S. et al. A study of PM<sub>2.5</sub> and PM<sub>10</sub> concentrations in the atmosphere of large cities in Gansu Province, China, in summer period. *J Earth Syst Sci* 125, 1175–1187 (2016). <https://doi.org/10.1007/s12040-016-0722-x>
- Javed, M., Bashir, M. and Zaineb, S. (2021). Analysis of daily and seasonal variation of fine particulate matter (PM<sub>2.5</sub>) for five cities of China. *Environ Dev Sustain* 23, 12095–12123 (2021).
- Alberto Izzotti, Paola Spatera, Zumama Khalid and Alessandra Pulliero. (2022). Importance of Punctual Monitoring to Evaluate the Health Effects of Airborne Particulate Matter. *Int. J. Environ. Res. Public Health* 2022, 19, 10587.
- Denis Vinnikov, Anel Abenova, Aizhan Raushanova and Venerando Rapisarda. (2023). Occupational exposure to fine particulate matter in the reinforced concrete production and its association with respiratory symptoms and lung function. *BMC Public Health.* (2023) 23:1813.
- Yumara Martín-Cruz 1, and Álvaro Gómez-Losada. (2023). Risk Assessment and Source Apportionment of Metals on Atmospheric Particulate Matter in a Suburban Background Area of Gran Canaria (Spain). *Int. J. Environ. Res. Public Health* 2023, 20, 5763.
- Francis Olawale Abulude. (2016). Particulate Matter: An Approach To Air Pollution. Preprints.

## Date Palm Pollen (*Phoenix dactylifera* L.) Supplementations: impact on the Fertility and Anti-Cancer Properties

Eslah S. rajab <sup>1</sup>

Mahmood A. Al-Azzawi <sup>2</sup>



© 2024 The Author(s). This open access article is distributed under a Creative Commons Attribution (CC-BY) 4.0 license.





### Abstract:

*Infertility and cancer are a major public health challenge globally. Date palm pollen (DPP), the male reproductive cells of the palm tree's flowers, has a long-standing use as a nutritional supplement, especially as an aphrodisiac and fertility ameliorative. Recently, some studies have looked into its effect against some types of cancer. This study sought to assay the impact of DPP extract (DPPE) supplementation on the fertility of adult healthy male Swiss albino mice in vivo and to evaluate its cytotoxic effect against human rhabdomyosarcoma (RD) cancer cell line in vitro. Forty male mice were randomly divided into two groups (n=20) including control and the treatment group. DPPE was dissolved in distilled water and orally given to the treatment group at a dose of 250 mg/kg once daily for 35 days while the control group received distilled water. At the end of the administration, serum levels of follicle-stimulating hormone (FSH), luteinizing hormone (LH), testosterone, estradiol, final body and male reproductive organs weights, and sperm parameters were evaluated. In addition, the percentage of cancer cell growth inhibition (GI) of eight concentrations in µg/ml (0.19, 0.39, 0.78, 1.56, 3.12, 6.25, 12.5, 25) were assessed in vitro using RD cell line. DPPE dose significantly increased the weight of reproductive organs (prostate gland, seminal vesicle, and epididymis), sperm indices (concentration, motility, morphology), estradiol levels ( $P < 0.001$ ), LH ( $P < 0.01$ ), and testosterone ( $P < 0.001$ ) compared to the control group. Concerning the anti-tumor properties of the extract, the results showed that they were a concentration-independent effect. DPPE recorded the best GI values on the RD cell line in the 0.19 and 1.56 µg/ml range. This study concluded that DPP has a clear effect on improving the male fertility profile and development of the male reproductive system in adult male Swiss albino mice, in addition to its concentration-independent anti-cancer effect.*

**Keywords:** Fertility; Anti-cancer; Infertility.

 <http://dx.doi.org/10.47832/MinarCongress-16>

<sup>1</sup>  Department of Microbiology, College of Science, Al-Karkh University of Science, Baghdad, Iraq  
[eslah\\_bio@kus.edu.iq](mailto:eslah_bio@kus.edu.iq)

<sup>2</sup>  Department of Forensic Science, College of Science, Al-Karkh University of Science, Baghdad, Iraq  
[dr.mahmood14@kus.edu.iq](mailto:dr.mahmood14@kus.edu.iq)



## Introduction

Infertility was defined as the inability to conceive and give birth after 12 months of unprotected intercourse. Infertility affects 10%-15% of couples [1, 2], making it one of the most common conditions among people between the ages of 20 and 45 years, it is a complicated disorder of medical and psychosocial significance [3, 4]. In one-third of infertile couples, the problem is with the male and nearly 50% of male infertility cases are treatable [5- 8].

The main causes of male infertility are some underlying problems that cause some signs and symptoms to appear. These conditions include genetic disorders, immunological issues, reproductive system diseases, endocrine disorders, lifestyle, dietary and environmental issues [9- 11]. Many of the factors causing infertility are acquired and develop over time. Therefore, it is possible to prevent or treat infertility in some cases, as many treatments (Pharmaceutical and Herbal Medicine) have been proposed. Recently, many isolated natural products or raw plant extracts have been broadly used in the treatment of male infertility, as they have been proven effective in treating oligospermia, sexual dysfunction, and other psychological and physiological disorders [12-15]. Date palm pollen (DPP) has been utilized in indigenous medicine in the Mideast and some Asiatic nations for many years to boost healthiness and better fertility in both males and females [14, 16-18]. The pharmacological action of DPP (*in vitro* and *in vivo*) on fertility has been assessed [19, 20].

DPP is a functional natural and nutritional supplement due to its great content of carbohydrates, proteins, vitamins, enzymes, cofactors, minerals, trace elements, organic acids, lipids, sterols, and nucleic acids, in addition to biologically active volatile unsaturated fatty acids and phenolic components, such as flavonoids, phenolic acids, which play a pivotal role as a powerful antioxidant and anti-cancer agent [21-27]. For the last decades, accumulating evidence has revealed that DPP supplementation can positively affect sperm parameters and is conducive to improving fertility in male rats [28-31]. Furthermore, due to phenolic compounds, flavonoids and anthocyanins, DPP can stimulate the activity and expression of antioxidant genes [32-34]. Even so, the antioxidant effect of DPP on human sperm parameters and its mode of action have not been well understood and documented, raising the hypothesis that DPP supplementation could lower ROS levels, mostly through peroxiredoxin genes. Thus, decoding this association potentially dispense insight into one of the molecular mechanisms of DPP in improving sperm parameters in infertile men. Conventionally, DPP is believed to be an erogenous and fertility strengthener and has lately been specified as a conventional medicine for male infertility treatment [35]. The erotic impact of DPP is likely ascribed to the existence

of estradiol-like hormones. The pharmaceutical actions of DPP are not restricted to males, also it has been shown to have a gonadal stimulating effect and enhance fertility in women [36]. DPP has been used in the treatment of impotence and has been found to cause significant increases in levels of follicle-stimulating hormone (FSH) and testosterone (T) in patients with azoospermia and oligoasthenozoospermia respectively [37]. Many studies indicated that DPP has shown an action on male fertility parameters. One survey observed that DPP induced a significant increase in the ratio of epididymis to body weight or testis, which was concurrent with an increase in estradiol (E2) and testosterone concentrations in male Wistar rats [38]. Another clinical trial indicated that DPPE (120 and 240 mg/kg) significantly improve fertility parameters in adult male rats [28].

In addition, a study conducted on adult male rats to evaluate the effect of DPP on some sexual behavior parameters indicated that DPP resulted in increased testicular weight and testosterone concentrations [39]. DPP was shown to have a preventive effect contra potential mechanisms of cadmium-stimulated testicular dysfunction in adult male albino rats, as oral consumption of DPP (240 mg/kg BW, daily for one month) significantly increased estradiol levels in normal rats and significantly restored testosterone levels, the weight of sexual organs, and sperm motility which were reduced by cadmium.. Furthermore, DPP treatment showed an increase in antioxidant systems in rat testes as assessed by the restoration of the levels of superoxide dismutase (SOD), catalase (CAT), and glutathione (GSH) [40].

In the same context, other study investigating the therapeutic prospect of DPP contra the toxic actions of cadmium on the testicles of adult male Wistar rats showed that treatment with DPP restored spermatogenesis and mitigated the damaging effects of cadmium on testicles, spermatogenesis, and oxidative stress [41].

Another study reported that date palm seed and DPPEs significantly improved aromatase, glutathione, superoxide dismutase, catalase, malondialdehyde, total antioxidant capacity, Estrogen, LH, FSH, testosterone, and sperm quality of male albino rats induced by cadmium [42]. In addition, a study that investigated the action of DPPE on male rats with streptozotocin-induced diabetes detected that DPP perfected levels of testosterone, FSH, and LH and may defend the testicular structure [43]. A similar study indicated that suspension of bee pollen and DPP (100 mg/kg BW/diurnally for 4 weeks) showed anti-hyperglycemic effects by normalizing destructive histological changes of the testis and dysfunction of the hypothalamic-pituitary-testicular axis, beside an amelioration in the antioxidant system in male Wistar rats with streptozotocin-induced diabetes [44]. Another study suggested that 5 and 10% DPPEs might be

beneficial for male infertility caused by diabetes [45]. Cancer is a group of diseases that develop over a long period, causing millions of deaths worldwide [46]. The Global Burden of Disease Study estimates that approximately 10 million people died from cancer in 2019. Cancer remains a major public health issue worldwide due to its highly aggressive nature, poor prognosis and low survival rate [47].

Natural products have protruded as an indicator in the uncovering and evolution of new drugs, especially those for anti-cancer and anti-infective agents [48, 49]. It is worth noting that about 50% of anti-cancer drugs and treatments are derived either from natural sources or from natural products [50]. Different herbal-derived components such as polyphenols, flavonoids, terpenoids, alkaloids, and polysaccharides are used for diverse types of cancer and infectious diseases [51, 52]. Although different therapeutic approaches and interventions are accessible for these diseases, most of them are immedicable owing to drug resistance, in addition to the undesirable side effects that some natural products are not free from [53]. Therefore, the discovery of new plant-derived products is imperative to perfect the effect and outcomes of therapeutic factors in Plant-Based therapies. DPPE has been proven to have an anti-cancer effect. An *in vitro* study showed that DPP could suppress the growth of breast carcinoma cells and stimulate apoptosis in dose-dependently; this activity was attributed to DPP's high content of bioactive compounds, including polyphenols and flavonoids. [54]. Another similar study reported the anti-cancer activity of DPPE on hepatocellular carcinoma cells, where was shown to inhibit their growth and proliferation and induce apoptosis in dose-dependently [55].

Other studies have also confirmed the potential anti-cancer effect of DPP [56–59]. Nevertheless, further research is indispensable to perceive the anti-cancer mechanisms of DPPE and assess its safety and competence in human clinical studies. In general, these results propose that DPPE, as a naturalistic product may be promising for the prevention and curing of several types of cancer. Accordingly, the major targets of this investigation were the evaluation (*in vivo*) of the effect of DPP on fertility and development of the male reproductive system in adult Swiss albino male mice and to evaluate (*in vitro*) its toxic effect on the rhabdomyosarcoma (RD) cell lines.

## **Materials and methods:**

### **1. Plant materials and extraction preparation:**

DPP plant was collected from the outskirts of Baghdad city (Iraq) in late spring 2023. Plant scientists (Department of Botany, Agricultural Resources and Animal Husbandry Research Center, University of Baghdad-Iraq) identified the plant. 50 grams of DPP grains

were extracted overnight in 250 ml of solvent (70% absolute ethanol) using maceration at room temperature. The pollen extract was filtered and then evaporated by a rotary vacuum evaporator at 45°C until dry. The resultant crude extract was frozen at 4°C until used to prepare the required doses and concentrations. [60].

## **2. Preparation of extract concentrations**

Stock solution of plants extracts was prepared by dissolving (1g) of plants extracts powder in 10 ml sterile distilled water. The plant extracts were prepared at concentration 100 mg/ml.

## **3. Animals and experimental procedures**

Forty healthy adult Swiss albino male mice (*muss musculus*), aged 8-10 weeks, and weighing 23 to 28 grams were selected for this experimental study. They were procured from the Biotechnology Research Centre- Al-Nahrain University-Iraq. The animals were housed for 2 weeks before the experiment in a well-ventilated room with a constant temperature of  $22 \pm 3^\circ\text{C}$ , a 12 h light-dark cycle, and 55% relative humidity.

They were supplied with standard rat food pellets and tap water ad libitum. After the adaptation period, mice were randomly divided into two groups (n=20) including control and the treatment group. Ethanolic extract of DPP was dissolved in distilled water and orally given to the treatment group at dose of 250 mg/kg BW, while the control group received only a similar volume of distilled water. These treatments continued for 35 sequential days. For the DPPE to have an action, mice require 48-52 days for the exact spermatogenic cycle [61]. Higher than half of this period is requisite to ascertain the effects of DPP on fertility potential in male mice [29, 40].

All experimental procedures were carried out between 8–10 am and precautions were taken to avert stressful conditions. All animal procedures and experimental protocols were approved by the Ethical Committee at the High Institute for Infertility Diagnosis and Assisted Reproductive Technologies-Al-Nahrain University-Iraq, and were performed following the directory for the care and use of laboratory animals.

## **4. Collecting of blood and reproductive organ samples:**

After the experimental duration, all mice were weighed separately and sacrificed after being anesthetized with diethyl ether and then blood specimens were withdrawn from the aorta. The blood was permitted to clot in plain tubes at 25°C for 20 minutes. The serum was aspirated

after centrifugation (3000 rpm) for 30 minutes and stored at -20°C to measure male reproductive hormones. All testes, epididymis, and seminal vesicles were then eradicated and weighed.

### **5. Hormones measurement:**

Serum concentrations of Estradiol (E2), and testosterone, were determined by solid phase enzyme-linked immunosorbent assay (ELISA), using Estradiol mouse ELISA kit, Testosterone rat/mouse ELISA kit, (Cat. #: DEV9999, Cat. #: DEV9911, Demeditec Diagnostics GmbH., Lise-Meitner-Germany) respectively. Follicle - stimulating hormone (FSH) and luteinizing hormone (LH) were assayed by solid-phase Sandwich Enzyme-Linked Immunosorbent Assay (ELISA) using mouse FSH ELISA Kit and LH Mouse ELISA Kit (Cat. #: EEL097, Cat. # EEL121, Invitrogen, Vienna, Austria) respectively. All procedures were achieved conforming to the manufacturer's prescript.

### **6. Epididymal sperm parameters :**

The scrotums of the mice were opened, the testicles were removed, and the fat was stripped. Next, the epididymis was carefully dissociated and fractionated in Dulbecco's modified Eagle's medium (DMEM) containing 5% fetal bovine serum (FBS). Using sperm suspension, the sperm parameters analysis (count, motility, morphology) were analyzed. For sperm counting, sperm suspension is set in the Neubauer chamber, and the sperm are ticked off on the four corners of the central square using an optical microscope [62]. Using the Papanicolaou staining method and by application of eosin staining, sperm morphology, and sperm viability were examined, respectively [63].

### **7. Evaluation of cell growth inhibition percentage:**

The *in vitro* anti-tumor activity of ethanolic extracts of DPP was performed at the Biotechnology Research Center (Nahrain University-Iraq). Preliminary screening of the cytotoxic activity of DPP grain extract was performed on RD tumor cell lines. This was applied under the method by Freshney, 2001 [64]. The cells (RD) were supplemented as a monolayer-attached cell in Falcon culture flasks (25 ml) containing RPMI-1640 medium (Cat#:11875093, Thermo Fisher Scientific Inc., USA). After washing the cells with PBS, one ml of trypsin-versene solution (Cat#: 15040066, Thermo Fisher Scientific Inc., USA) was added while continuing to shake gently to ensure the cells separated from the surface of the flask. The flask contents were then carried to other flask and incubated for 15 min at 37°C. Viable cell counting was performed using trypan blue stain (0.4%), where dead cells absorb the dye, seem blue under the microscope while live cells shut out the dye, and seem white. The neutral red cytotoxicity



test was used to perform the cytotoxicity test of the plant extract. Distilled water was used to dissolve the plant extract. Eight concentrations (in  $\mu\text{g/ml}$ ) of the plant extract were prepared (0.19, 0.39, 0.78, 1.56, 3.12, 6.25, 12.5, 25). 0.2 ml of the cultured cells were transferred to a 96-well microplate, each well containing 105 cells, and then 0.2 ml of the prepared plant extract concentrations were added. Some wells containing cultured cells were left untreated with the plant extract as a negative control. Cells were incubated at  $37^\circ\text{C}$  for three days and after washing with PBS solution, neutral red solution (0.8 ml) was added to each well, and then re-incubated at  $37^\circ\text{C}$  for 2 hours. Afterwards, the medium was disposed of and the wells were rewashed with PBS solution. 0.1 ml of phosphate buffered-ethanol (0.1 M  $\text{NaH}_2\text{PO}_4$ -ethanol; 1:1) was added to each cell. ELISA reader (492 nm wavelength) was used to read the cells, absorbance was recorded. The growth inhibition percentage (GIP) of the examined materials was calculated using the following formula:

$$\text{Growth inhibition (\%)} = ((\text{Control Abs.} - \text{Test Abs.}) / \text{Control Abs.}) \times 100$$

### Statistical analysis

The values of the measured parameters were expressed as mean $\pm$ SEM. One-way ANOVA and LSD post hoc tests using the SPSS software package for Windows were used to evaluate the statistical differences between groups. The P-value cutoff for significance was set at  $< 0.05$ .

### Results

#### 1. Phytochemical screening:

According to the results, the phytochemical screening of DPPE revealed the presence of alkaloids, flavonoids, phenols, glycosides, Saponins, steroids, Tannin, and Terpenes. (**Table 1**)

**Table 1-** Chemical detections of secondary metabolites in the DPPE

Secondary Metabolites	Reagents	Indication	Result of detection
Alkaloids	Mayer's reagent	white ppt.	+
Flavonoids	Ethanol with KOH	yellow color	+
Glycosides	Benedict reagent	Red precipitate	+
Saponins	shaking Extract ferric chloride	foam white ppt.	+
steroids	chloroform, acetic anhydride, sulphuric acid	Blue color	+
Tannin	Lead acetate 1%	Greenish blue	+
Terpenes carotenoid pigment	chloroform, acetic anhydride, sulphuric acid	brown precipitate	+

## 2. Body and reproductive organs weights:

Table 2 represents all weights. Administration of DPPE increased significantly ( $p < 0.05$ ) the weight of the prostate gland, seminal vesicle, and epididymis by 14.27 %, 17.21%, and 15.8 %, respectively as compared with the control group.

**Table 2-** Effect of DPPE on the weight of body and reproductive organs

Groups	Final body (g) (mean+SD)	Testes (mg) (mean+SD)	Prostate gland (mg) (mean+SD)	Seminal vesicle (mg) (mean+SD)	Epididymis (mg) (mean+SD)
Control group	28.5 ± 5.33a	104.22 ± 0.03a	42.65 ± 0.01a	215.79 ± 0.01a	98.35 ± 0.012a
Treated group	29.4 ± 7.27a	106.34 ± 0.05a	48.74 ± 0.03b	252.94 ± 0.05b	113.92 ± 0.013b

One-way ANOVA and LSD post hoc test showed that the mean differences were statistically significant between values in the same column that carried diverse superscripts compared to the control group. (a vs b:  $p < 0.05$ ).

## 3. Epididymal sperm parameters

Epididymal sperm parameters are shown in **Table 3** and Figures (1-3). DPPE administration caused a significant increase in sperm quality; concentration ( $P < 0.01$ , an increase of 33.1%), and motility ( $P < 0.05$ , an increase of 12.0 %), a significant decrease in immotile sperm ( $P < 0.001$ , a reduction of 34.5 %) and abnormal sperm morphology ( $P < 0.01$ , a reduction of 32.6) compared with the control group.

**Table 3-** Effect of DPPE on semen parameters of male albino mice

Groups	Sperm concentration ( $\times 10^6$ sperm.ml <sup>-1</sup> ) (mean+SD)	Motile sperms (%) (mean+SD)	Immotile sperms (%) (mean+SD)	Abnormal sperm morphology (%) (Head and Tail) (mean+SD)
Control	186.60 ± 12.44a	73.31 ± 4.32a	21.42 ± 6.20 a	4.01 ± 3.30a
Treated group	248.37 ± 15.30c	82.11 ± 6.43d	14.03 ± 5.10b	2.70 ± 2.90c

One-way ANOVA and LSD post hoc test showed that the mean differences were statistically significant between values in the same column that carried diverse superscripts compared to the control group. (a vs b:  $p < 0.001$ , a vs c:  $p < 0.01$ , a vs d:  $p < 0.05$ ).

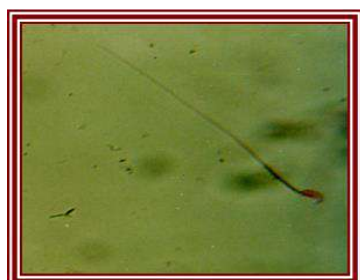


Figure 1- Normal sperm



Figure 2- Abnormal tail

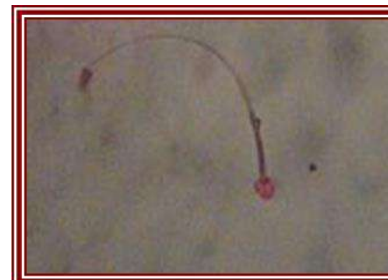


Figure 3- Abnormal head

#### 4. FSH, LH, testosterone and estradiol hormones:

A statistically significant increase in LH ( $p < 0.05$ , an increase of 22 %), testosterone ( $p < 0.001$ , an increase of 35.2 %), and estradiol ( $p < 0.001$ , an increase of 26.6 %) levels as compared to the control group (**Table 4**).

**Table 4-** Effect of DPPE on FSH, LH, testosterone, and estradiol levels of male albino mice

Groups	FSH (mIU/mL) (mean+SD)	LH (mIU/mL) (mean+SD)	Testosterone (ng/ml) (mean+SD)	Estradiol (nmol/L) (mean+SD)
Control	0.63 ± 1.06a	0.75 ± 0.35a	0.54 ± 1.08a	13.89 ± 3.33a
Treated group	0.74 ± 2.70a	0.92 ± 1.59C	0.73 ± 2.96b	17.59 ± 2.91d

One-way ANOVA and LSD post hoc test showed that the mean differences were statistically significant between values in the same column that carried diverse superscripts compared to the control group. (a vs b:  $p < 0.001$  a vs c:  $p < 0.05$  a vs d:  $p < 0.01$ ).

#### 5. Cytotoxic effects of DPP (ethanolic extract) on cell lines:

When the RD cancer cell line was treated with eight concentrations of ethanolic extract of DPP (0.19 to 25  $\mu\text{g/ml}$ ) the result (**Table 5**) showed a cytotoxic effect in a concentration-independent manner. The DPPE's first and fourth concentrations (0.19 and 1.56  $\mu\text{g/ml}$ ) recorded the highest percentage growth inhibition in Rhabdomyosarcoma cell lines (53 and 51) % respectively.

**Table 5-** Growth inhibition of the effect of DPPE on RD cancer cell line after 72 hr. of incubation

<b>Extract Concentration (<math>\mu\text{g/ml}</math>)</b>	<b>Growth inhibition % (Mean<math>\pm</math> SE)</b>
0.19	53.00 $\pm$ 1.20
0.39	37.30 $\pm$ 2.51
0.78	29.90 $\pm$ 1.10
1.56	51.00 $\pm$ 2.00
3.12	19.20 $\pm$ 3.10
6.25	3.20 $\pm$ 1.55
12.5	16.20 $\pm$ 3.15
25	31.9 $\pm$ 0.24

## Discussion

This study was conducted to determine the effectiveness of DPPE on the fertility of healthy adult male Swiss albino mice (in vivo) and to evaluate its antitumor effects on Rhabdomyosarcoma (RD) cell line (in vitro). The current results showed that DPP gave rise to a significant increase in serum estradiol, LH, and testosterone values, epididymal sperm count, motility, and a decreased percentage of sperm abnormalities in the experimental group.

These effects were associated with a significant increase in the weight of reproductive organs (prostate gland, seminal vesicle, and epididymis). Many studies, especially clinical trials have shown that date palm parts have a positive effect on male fertility indices. Elberry et al. [38], noted that DPP caused a significant increase in the ratio of epididymis to body weight or testis, which was concurrent with an increase in estradiol and testosterone concentrations in male Wistar rats. Moreover, Mehrabian et al. [28], found that after administering *A. ovinus* extract (500 mg/kg) and DPPE (120 and 240 mg/kg) to adult male rats, DPPE improved fertility factors, while *A. ovinus* adversely affected sperm parameters and gonad. Additionally, a study has been conducted on adult male rats to mark the effects of DPPE on some sexual behavioral standards. The outcomes evidenced DPPE augmented testicular weight and blood testosterone concentrations in tested male rats [39].

A study by Iftikhar et al. [31], found that DPPE enhanced testosterone concentrations with a synchronous increase in body weight in prepubertal rats. Khadem et al. [65], evaluated the protective effect of DPPE on thyroid dysfunction-induced testis dysfunction in male rats and found that DPPE supplementation increased sperm concentration and motility, estradiol (E2), LH, and testosterone in conjunction with an increase in the activities of 3-hydroxysteroid dehydrogenase and 17-hydroxysteroid dehydrogenase, in addition to an improvement in the state of antioxidants in the testicle. Mohamed et al. [44], evaluated the effect of DPP on male

sexual dysfunction of Streptozotocin-Induced Diabetic Wistar rats and indicated that DPP may have a prophylactic effect contra diabetic-induced pituitary testicle malfunction and testicle histological alterations concurrent with antihyperglycaemic effects. In the same context, El-Komy et al. [42], found that extracts of DPP and seed have a protective impact on infertility in male rats induced by cadmium. There was a remarkable amelioration in sperm properties, testosterone, estradiol, LH, FSH, SOD, CAT, TAC, GSH, Malondialdehyde (MDA), Xanthine oxidase (XO) activity, and testis histoarchitecture. Hassan et al. [40], found that oral administration of DPPE by testicular dysfunction-induced rats caused replenished sperm count, motility, weight of sexual organs, and level of testosterone, which were inhibited by CdCl<sub>2</sub> stimulation. DPP also retrieved the levels of SOD, GSH, and CAT. In the same context, DPPE treatment ameliorated reproductive destruction and adverse effects of cadmium on redox imbalance, spermatogenesis, and testicles in adult male Wistar rats [41].

The findings of El-Tahan et al. [45], indicated that DPPE (5 and 10%) might be advantageous for diabetes-induced male rat infertility. In the same context, Kazimenya et al. [43], reported that DPPE bettered levels of testosterone, LH, and FSH, and may preserve testicle structure in male rats with streptozotocin-induced diabetes. Also, the suspension of bee pollen and DPP (100 mg/kg BW/daily for one month) evidenced improvement in the antioxidant system, in addition to a hypoglycemic effect in male Wistar rats with streptozotocin-induced diabetes through normalization of destructive histological alterations in testis, and a defect in the testicular-pituitary axis [44].

The DPP's alcoholic extract on thyroid-induced male rat infertility showed the ability to restore reproductive organ weight, sperm count, and its motility, and levels of FSH, LH, and testosterone, which were reduced owing to induced hyper- and hypothyroidism [28]. In a similar study, DPPE showed a protective role against thyroid dysfunction-induced testis dysfunction [66]. The results showed that treatment with DPP prevents malformations caused by levothyroxine (LT<sub>4</sub>) or propylthiouracil (PTU). DPPE supplementation increased both motility and sperm count, levels of LH, and perfected testicular antioxidant status in normal rats. In addition, DPPE has been shown to cause a significant improvement in sex hormone disorders, testicular dysfunction, sperm quality, and testicular marker enzyme activities induced by hyper- or hypothyroidism [67].

The effect of eight different concentrations (0.19, 0.39, 0.78, 1.56, 3.12, 6.25, 12.5, 25) µg/mL with a period of 72 hours of ethanolic extract of DDP on the RD cell line was tested. The result showed that there was a dose-independent effect. The DPPE's first and fourth



concentrations (0.19 and 1.56  $\mu\text{g/ml}$ ) recorded the highest percentage growth inhibition in RD cell lines (53 and 51) % respectively, while other concentrations showed varying effects that did not depend on the dose concentration.

Several studies have shown that DPPE possesses anti-cancer activity. In particular, a study by Majumder et al. [45] confirmed that DPPE could suppress (in vitro) in a dose-dependent pattern the breast cancerous tumor and stimulate apoptosis. This study proposed that this effect might be ascribed to the high content of bioactive compounds, e.g., polyphenols and flavonoids in DPPE. Likewise, Kadry et al. [55], informed the anti-cancer activity of DPPE on hepatoma cells, which indicates that DPPE can suppress the growth and proliferation of these cells and induce apoptosis in a dose-dependent pattern. Different studies [56-59] indicated the potential of DPPE as an anti-cancer agent .

In a study by Barzin et al., 2011 [68], examined the anti-mutagenicity and anti-cancer effect of DPP grains, the results show the average hindrance percent of DPP grains was 46% in the anti-mutagenicity test. The average hindrance percent of DPP grains was 49% in the anti-cancer test. The study has revealed the anti-mutagenicity and anti-cancer effects of DPP grains. In addition, DPPE possesses anti-cancer effects against breast carcinoma (MDA), hepatoma (HepG-2), and colon carcinoma (Caco-2) cancer cell lines. It was observed that apoptosis in cells treated with DPPE occurred in a dose-dependent pattern, and cell cycle arrest was also detected. Additionally, DPPE down-regulated Bcl-2 and p21 in breast cancer cells and up-regulated p53 and Caspase-9 [69].

Mostly, the previous studies suggest that DPP may be promising as a natural product for the avoidance and curing of several types of cancers owing to its exclusive chemical structure and contents that may effectually withstand cancer besides lower toxicity and undesirable effects compared to conventional therapies. Even so, more research is still necessary to comprehend and clarify the mechanisms of action of DPPE's anti-cancer activity and assess its safety and activity in human clinical studies .

In general, the anti-cancer and antioxidant activities of some plant extracts are attributable to the biologically active compounds they contain [70]. A compound that shows anti-cancer activity usually has antioxidant properties. As we mentioned previously, DPP regarded as an effectual natural and functional dietary supplement due to its remarkable content of bioactive volatile unsaturated fatty acids, phenolic, and flavonoid compounds that play a crucial role as strong antioxidant and anti-cancer agents [71-73]. Prospective antioxidant and anti-cancer advantages have been suggested for phenolic phytochemicals. It is known that when normal

cells are injured in different ways, grow uncontrollably, or are mislocalized, they undergo programmed cell death [74]. An effective strategy for treating cancer is by targeting apoptosis, which involves changing the cell death machinery to devastate cancer cells [75]. The mechanisms of increased RONS resulting from oxidative stress are known to be positively associated with the pathology of many diseases such as cancer. Increased formation of RONS of endogenous or exogenous origin leads to oxidative stress due to pro-oxidant and antioxidant imbalance causing cellular damage in metabolism, subsequently, increasing cell inflammation, apoptosis, necrosis, DNA and protein cross-links, DNA base damage, mitochondrial malfunction, and lipid membrane peroxidation. Antioxidants can be known as a system that defends organism and biomolecules from the deleterious effects of free radicals, and minimizes or repairs the damage caused by RONS to the target molecule, this is termed antioxidant protection [76].

## Conclusions

DPP extract contains many advantageous components that play a pivotal role in fertility. DPP is a worthy source of macronutrients (carbohydrates, proteins, and unsaturated fatty acids), phytochemicals (phenolic components, such as flavonoids, phenolic acids), carotenes, triterpene glycosides, enzymes, cofactors, minerals, trace elements, organic acids that have a critical function in the body. On account of, the wide-ranging therapeutic potential of DPP, it may contribute to improving fertility. A positive effect on hormonal levels has been evident in male mice (estradiol, LH, and testosterone), weight of reproductive organs (prostate gland, seminal vesicle, and epididymis), and sperms (concentration, motility, viability, and morphology). The present study also showed that DPP extracts had a selective effect against RD cell lines in a dose-independent pattern. This impact can be ascribed to the synergistic effect of bioactive agents especially polyphenols and flavonoids present in DPP which have antioxidant and anti-cancer properties. Although many studies have examined the beneficial effect of DPP, most of these research studies were on mice, with human studies being limited. More research is still necessary to determine the active form of DPP and its appropriate daily dose to avert and handle infertility in humans, understand and elucidate the mechanisms of DPPE's anti-cancer action, and evaluate its safety and activity in human clinical studies.

## References

- Vander Borgh, M., & Wyns, C. (2018). Fertility and infertility: Definition and epidemiology. *Clinical biochemistry*, 62, 2–10. <https://doi.org/10.1016/j.clinbiochem.2018.03.012>
- Carson, S. A., & Kallen, A. N. (2021). Diagnosis and Management of Infertility: A Review. *JAMA*, 326(1), 65–76. <https://doi.org/10.1001/jama.2021.4788>
- Hyun Joo Lee, Jung Yeol Han, Han Zo Choi, Baeg Ju Na. Infertility Prevalence and Associated Factors among Women in Seoul, South Korea: A Cross-Sectional Study. *Clin. Exp. Obstet. Gynecol.* **2023**, 50(3), 54. <https://doi.org/10.31083/j.ceog5003054>
- Fatima, W., Akhtar, A. M., Hanif, A., Gilani, A., & Farooq, S. M. Y. (2024). Predicted risk factors associated with secondary infertility in women: univariate and multivariate logistic regression analyses. *Frontiers in medicine*, 10, 1327568. <https://doi.org/10.3389/fmed.2023.1327568>
- Öztekin, Ü., Caniklioğlu, M., Sarı, S., Selmi, V., Gürel, A., & Işıkay, L. (2019). Evaluation of Male Infertility Prevalence with Clinical Outcomes in Middle Anatolian Region. *Cureus*, 11(7), e5122. <https://doi.org/10.7759/cureus.5122>
- Agarwal, A., Mulgund, A., Hamada, A., & Chyatte, M. R. (2015). A unique view on male infertility around the globe. *Reproductive biology and endocrinology : RB&E*, 13, 37. <https://doi.org/10.1186/s12958-015-0032-1>
- Raman JD, Nobert CF, Goldstein M. Increased incidence of testicular cancer in men presenting with infertility and abnormal semen analysis. *J Urol* 2005; 174: 1819-1822.
- Kolettis Pn. Evaluation of the Subfertile Man. *Am Fam Physisan* 2003; 67: 2165-2172.
- Kamiński, P., Baszyński, J., Jerzak, I., Kavanagh, B. P., Nowacka-Chiari, E., Polanin, M., Szymański, M., Woźniak, A., & Kozera, W. (2020). External and Genetic Conditions Determining Male Infertility. *International journal of molecular sciences*, 21(15), 5274. <https://doi.org/10.3390/ijms21155274>
- Tahmasbpour, E., Balasubramanian, D., & Agarwal, A. (2014). A multi-faceted approach to understanding male infertility: gene mutations, molecular defects and assisted reproductive techniques (ART). *Journal of assisted reproduction and genetics*, 31(9), 1115–1137. <https://doi.org/10.1007/s10815-014-0280-6>
- Sengupta, P., Dutta, S., Karkada, I. R., & Chinni, S. V. (2021). Endocrinopathies and Male Infertility. *Life (Basel, Switzerland)*, 12(1), 10. <https://doi.org/10.3390/life12010010>
- Noh, S., Go, A., Kim, D. B., Park, M., Jeon, H. W., & Kim, B. (2020). Role of Antioxidant Natural Products in Management of Infertility: A Review of Their Medicinal Potential. *Antioxidants (Basel, Switzerland)*, 9(10), 957. <https://doi.org/10.3390/antiox9100957>
- Jaradat, N., Zaid, A.N. Herbal remedies used for the treatment of infertility in males and females by traditional healers in the rural areas of the West Bank/Palestine. *BMC Complement Altern Med* **19**, 194 (2019). <https://doi.org/10.1186/s12906-019-2617-2>
- Martins, R.V.L.; Silva, A.M.S.; Duarte, A.P.; Socorro, S.; Correia, S.; Maia, C.J. Natural Products as Protective Agents for Male Fertility. *BioChem* **2021**, 1, 122-147. <https://doi.org/10.3390/biochem1030011>

- Chorosh, S. H., Malik, N., Panesar, G., Kumari, P., Jangra, S., Kaur, R., Al-Ghamdi, M. S., Albishi, T. S., Chopra, H., Singh, R., & Murthy, H. C. A. (2023). Phytochemicals: Alternative for Infertility Treatment and Associated Conditions. *Oxidative medicine and cellular longevity*, 2023, 1327562. <https://doi.org/10.1155/2023/1327562>
- Falahati, A. M., Fallahi, S., Allamehzadeh, Z., Izadi Raieni, M., & Malekzadeh, K. (2023). Effects of Date Palm Pollen Supplementations on The Expression of PRDX1 and PRDX6 Genes in Infertile Men: A Controlled Clinical Trial. *International journal of fertility & sterility*, 17(3), 201–207. <https://doi.org/10.22074/ijfs.2022.549291.1264>
- Salhi S, Chentouf M, Harrak H, et al. Assessment of physicochemical parameters, bioactive compounds, biological activities, and nutritional value of the most two commercialized pollen types of date palm (*Phoenix dactylifera* L.) in Morocco. *Food Science and Technology International*. 2023;0(0). doi:[10.1177/10820132231168914](https://doi.org/10.1177/10820132231168914)
- Al-Karmadi, A., & Okoh, A. I. (2024). An Overview of Date (*Phoenix dactylifera*) Fruits as an Important Global Food Resource. *Foods* (Basel, Switzerland), 13(7), 1024. <https://doi.org/10.3390/foods13071024>
- Mahaldashtian, M., Naghdi, M., Ghorbanian, M. T., Makoolati, Z., Movahedin, M., & Mohamadi, S. M. (2016). In vitro effects of date palm (*Phoenix dactylifera* L.) pollen on colonization of neonate mouse spermatogonial stem cells. *Journal of ethnopharmacology*, 186, 362–368. <https://doi.org/10.1016/j.jep.2016.04.013>
- Laghouti, A., Belabbas, R., Castellini, C., Mattioli, S., Dal Bosco, A., Benberkane, A., & Iguer-Ouada, M. (2021). Impact of Algerian date palm pollen aqueous extract on epididymal and ejaculated rabbit sperm motility during in vitro incubation. *Italian Journal of Animal Science*, 20(1), 717–727. <https://doi.org/10.1080/1828051X.2021.1911696>
- El-Kholy, W. M., Soliman, T. N., & Darwish, A. M. G. (2019). Evaluation of date palm pollen (*Phoenix dactylifera* L.) encapsulation, impact on the nutritional and functional properties of fortified yoghurt. *PloS one*, 14(10), e0222789. <https://doi.org/10.1371/journal.pone.0222789>
- Shehzad, M.; Rasheed, H.; Naqvi, S.A.; Al-Khayri, J.M.; Lorenzo, J.M.; Alaghbari, M.A.; Manzoor, M.F.; Aadil, R.M. Therapeutic Potential of Date Palm against Human Infertility: A Review. *Metabolites* 2021, 11, 408. <https://doi.org/10.3390/metabo11060408>
- National Center for Biotechnology Information (2024). PubChem Compound Summary for . Retrieved June 28, 2024 from [https://pubchem.ncbi.nlm.nih.gov/compound/Alanine\\_-arginine\\_-aspartic-acid\\_-glutamic-acid\\_-glycine\\_-histidine\\_-isoleucine\\_-leucine\\_-lysine-ace](https://pubchem.ncbi.nlm.nih.gov/compound/Alanine_-arginine_-aspartic-acid_-glutamic-acid_-glycine_-histidine_-isoleucine_-leucine_-lysine-ace).
- El Ghouizi, A., Bakour, M., Laaroussi, H., Ousaaid, D., El Menyiy, N., Hano, C., & Lyoussi, B. (2023). Bee Pollen as Functional Food: Insights into Its Composition and Therapeutic Properties. *Antioxidants* (Basel, Switzerland), 12(3), 557. <https://doi.org/10.3390/antiox12030557>
- Hussain M.I., Farooq M., Syed Q.A. Nutritional and biological characteristics of the date palm fruit (*Phoenix dactylifera* L.)—A review. *Food Biosci.* 2020;34:100509. doi: 10.1016/j.fbio.2019.100509.
- Banu H., Renuka N., Faheem S.M., Ismail R., Singh V., Saadatmand Z., Khan S.S., Narayanan K., Raheem A., Premkumar K. Gold and silver nanoparticles biomimetically synthesized using date palm pollen extract-induce apoptosis and regulate p53 and Bcl-2 expression in human breast

- adenocarcinoma cells. *Biol. Trace Elem. Res.* 2018;186:122–134. doi: 10.1007/s12011-018-1287-0.
- Abu-Reidah I.M., Gil-Izquierdo Á., Medina S., Ferreres F. Phenolic composition profiling of different edible parts and by-products of date palm (*Phoenix dactylifera* L.) by using HPLC-DAD-ESI/MSn. *Food Res. Int.* 2017;100:494–500. doi: 10.1016/j.foodres.2016.10.018.
- Mehraban F, Jafari M, Akbartabar Toori M, Sadeghi H, Joodi B, Mostafazade M, et al. Effects of date palm pollen (*Phoenix dactylifera* L.) and *Astragalus ovinus* on sperm parameters and sex hormones in adult male rats. *Int J Reprod Biomed.* 2014;12(10):705–712.
- Bahmanpour S, Talaei T, Vojdani Z, Panjehshahin M, Poostpasand A, Zareei S, et al. Effect of phoenix dactylifera pollen on sperm parameters and reproductive system of adult male rats. *Iran J Med Sci.* 2015;31(4):208–212.
- Baharin A, Hashim NE, Sonsudin F, Hashim NH. Morphine and *Phoenix dactylifera* (dates) effects on the histological features of male rat reproductive organs. *J Res Med Sci.* 2020;25:20–20.
- Iftikhar S, Bashir A, Anwar MS, Mastoi SM, Shahzad M. Effect of date palm pollen (dpp) on serum testosterone levels in prepubertal albino rats. *Pak J Med Health Sci.* 2011;5(4):639–644.
- Al Alawi R, Alhamdani MSS, Hoheisel JD, Baqi Y. Antifibrotic and tumor microenvironment modulating effect of date palm fruit (*Phoenix dactylifera* L.) extracts in pancreatic cancer. *Biomed Pharmacother.* 2020;121:109522–109522.
- Saibabu V, Fatima Z, Khan LA, Hameed S. Therapeutic potential of dietary phenolic acids. *Adv Pharmacol Sci.* 2015;2015:823539–823539.
- Alahyane A, Harrak H, Ayour J, Elateri I, Ait-Oubahou A, Benichou M. Bioactive compounds and antioxidant activity of seventeen Moroccan date varieties and clones (*Phoenix dactylifera* L.). *S Afr J Bot.* 2019; 121: 402-409.
- Abdi, F.; Roozbeh, N.; Mortazavian, A.M. Effects of date palm pollen on fertility: Research proposal for a systematic review. *BMC Res. Notes* **2017**, 10, 1–4.
- Waly, M.I. Health benefits and nutritional aspects of date palm pollen. *Can. J. Clin. Nutr.* **2020**, 8, 1–3.
- Saeed, H.S.; Osman, B.; El-Hadiyah, T.M.H.; Mohamed, M.S.; Osman, W.J.; Abdoon, I.H.; Mothana, R.A. Date palm pollen grains as a potential manager for male sub-fertility: A clinical trial. *J. Pharm. Res. Int.* **2020**, 32, 83–95.
- Elberry, A.A.; Mufti, S.T.; Al-Maghrabi, J.A.; Abdel-Sattar, E.A.; Ashour, O.M.; Ghareib, S.A.; Mosli, H.A. Anti-inflammatory and antiproliferative activities of date palm pollen (*Phoenix dactylifera*) on experimentally-induced atypical prostatic hyperplasia in rats. *J. Inflamm.* 2011, 8, 40.
- Selmani, C.; Chabane, D.; Bouguedoura, N. Ethnobotanical survey of *Phoenix dactylifera* L. pollen used for the treatment of infertility problems in Algerian oases. *Afr. J. Tradit. Complement. Altern. Med.* 2017, 14, 175–186.
- Hassan, W.A.; El-kashlan, A.M.; Mohamed, N.A. Egyptian date palm pollen ameliorates testicular dysfunction induced by cadmium chloride in adult male rats. *J. Am. Sci.* 2012, 8, 659–669.



- El-Neweshy, M.; El-Maddawy, Z.; El-Sayed, Y. Therapeutic effects of date palm (*Phoenix dactylifera* L.) pollen extract on cadmium induced testicular toxicity. *Andrologia* **2013**, 45, 369–378.
- El-Komy, M.; Saad, H.O. Magda protective effect of date palm extracts on cadmium-induced infertility in male rats. *Egypt. J. Hosp. Med.* 2017, 69, 2181–2190.
- Kazeminia, S.M.; Kalaee, S.E.V.; Nasri, S. Effect of dietary intake alcoholic extract of palm pollen (*Phoenix dactylifera* L.) on pituitary-testicular axis in male diabetic rats. *J. Maz. Univ. Med. Sci.* 2014, 24, 167–175.
- Mohamed, N.A.; Ahmed, O.M.; Hozayen, W.G.; Ahmed, M.A. Ameliorative effects of bee pollen and date palm pollen on the glycemic state and male sexual dysfunctions in streptozotocin-Induced diabetic wistar rats. *Biomed. Pharmacother.* 2018, 97, 9–18.
- El-Tahan, N.R.; Mesilhy, S.; Abdelaziz, H.Y.A. Effect of date palm pollen on fertility of diabetic male rats. *J. Specif. Educ. Stud. Res.* **2019**, 3, 207–223.
- Bray, F., Laversanne, M., Sung, H., Ferlay, J., Siegel, R. L., Soerjomataram, I., & Jemal, A. (2024). Global cancer statistics 2022: GLOBOCAN estimates of incidence and mortality worldwide for 36 cancers in 185 countries. *CA: a cancer journal for clinicians*, 74(3), 229–263. <https://doi.org/10.3322/caac.21834>
- Global Burden of Disease 2019 Cancer Collaboration, Kocarnik, J. M., Compton, K., Dean, F. E., Fu, W., Gaw, B. L., Harvey, J. D., Henrikson, H. J., Lu, D., Pennini, A., Xu, R., Ababneh, E., Abbasi-Kangevari, M., Abbastabar, H., Abd-Elsalam, S. M., Abdoli, A., Abedi, A., Abidi, H., Abolhassani, H., Adedeji, I. A., ... Force, L. M. (2022). Cancer Incidence, Mortality, Years of Life Lost, Years Lived With Disability, and Disability-Adjusted Life Years for 29 Cancer Groups From 2010 to 2019: A Systematic Analysis for the Global Burden of Disease Study 2019. *JAMA oncology*, 8(3), 420–444. <https://doi.org/10.1001/jamaoncol.2021.6987>
- U Ferreira M. J. (2023). Natural Product-Derived Compounds for Targeting Multidrug Resistance in Cancer and Microorganisms. *International journal of molecular sciences*, 24(18), 14321. <https://doi.org/10.3390/ijms241814321>
- Martínez-Fructuoso, L., Arends, S. J. R., Freire, V. F., Evans, J. R., DeVries, S., Peyser, B. D., Akee, R. K., Thornburg, C. C., Kumar, R., Ensel, S., Morgan, G. M., McConachie, G. D., Veeder, N., Duncan, L. R., Grkovic, T., & O'Keefe, B. R. (2023). Screen for New Antimicrobial Natural Products from the NCI Program for Natural Product Discovery Prefractionated Extract Library. *ACS infectious diseases*, 9(6), 1245–1256. <https://doi.org/10.1021/acsinfecdis.3c00067>
- Shaik, B. B., Katari, N. K., & Jonnalagadda, S. B. (2022). Role of Natural Products in Developing Novel Anti-cancer Agents: A Perspective. *Chemistry & biodiversity*, 19(11), e202200535. <https://doi.org/10.1002/cbdv.202200535>
- Riaz, M., Khalid, R., Afzal, M., Anjum, F., Fatima, H., Zia, S., Rasool, G., Egbuna, C., Mtewa, A. G., Uche, C. Z., & Aslam, M. A. (2023). Phytobioactive compounds as therapeutic agents for human diseases: A review. *Food science & nutrition*, 11(6), 2500–2529. <https://doi.org/10.1002/fsn3.3308>
- Chaachouay, N.; Zidane, L. Plant-Derived Natural Products: A Source for Drug Discovery and Development. *Drugs Drug Candidates* 2024, 3, 184-207. <https://doi.org/10.3390/ddc3010011>

- Talib, W. H., Alsayed, A. R., Barakat, M., Abu-Taha, M. I., & Mahmud, A. I. (2021). Targeting Drug Chemo-Resistance in Cancer Using Natural Products. *Biomedicines*, 9(10), 1353. <https://doi.org/10.3390/biomedicines9101353>
- Majumder, M.; Nandi, P.; Omar, A.; Ugwuagbo, K.C.; Lala, P.K. EP4 as a Therapeutic Target for Aggressive Human Breast Cancer. *Int. J. Mol. Sci.* 2018, 19, 1019.
- Kadry, M.; Megeed, R.M.A.; Ghanem, H.; Abdoon, A.; Abdel-Hamid, A.-H. Does glycogen synthase kinase-3 \_ signaling pathway has a significant role in date palm pollen cancer therapy? *Egypt. Pharm. J.* 2019, 18, 208.
- El-Far, A.H.; Oyinloye, B.E.; Sepehrimanesh, M.; Allah, M.A.G.; Abu-Reidah, I.; Shaheen, H.M.; Razeghian-Jahromi, I.; Alsenosy, A.E.-W.A.; Noreldin, A.E.; Al Jaouni, S.K.; et al. Date Palm (*Phoenix dactylifera*): Novel Findings and Future Directions for Food and Drug Discovery. *Curr. Drug Discov. Technol.* 2019, 16, 2–10.
- Abdallah, W.E.; AbdelMohsen, M.M.; Awad, H.M. Phytochemical Composition, Antioxidant and Antitumor Activities of some Date Palm Pollen Extracts. *Egypt. J. Chem.* 2022.
- Teo, D.; Abdullah, B.; Zainatul, N.; Binti Zainol, N.; Hasraf, N.; Nayan, B.M.; Muhammad, N.B. A Systematic Literature Review: The Effect of Date Palms (*Phoenix Dactylifera*) toward Breast Cancer MCF-7 Cell Line. *Ann. Rom. Soc. Cell Biol.* 2021, 25, 5387–5393.
- El-Far, A.H.; Ragab, R.F.; Mousa, S.A. Date Palm Bioactive Compounds: Nutraceuticals, Functional Nutrients, and Pharmaceuticals. In *The Date Palm Genome*; Springer International Publishing: Cham, Switzerland, 2021; pp. 27–50.
- Daoud, A., Malika, D. and Gharsallah, N. (2015) Assessment of Polyphenol Composition, Antioxidant and Antimicrobial Properties of Various Extracts of Date Palm Pollen (DPP) from Two Tunisian Cultivars. *Arabian Journal of Chemistry*, 12, 3075-3086.
- Schroder JD. Reproduction and Breeding Techniques for Laboratory Animals. *Can J Comp Med* 1971; 35: 345.
- Lotfi N, Khazaei M, Shariatzadeh SM, Mehranjani MS, Ghanbari A. The effect of cannabis sativa hydroalcoholic extract on sperm parameters and testis histology in rats. *Int J Morphol.* 2013;31(1):82-86.
- Avendano C, Mata A, Sanchez Sarmiento CA, Doncel GF. Use of laptop computers connected to internet through Wi-Fi decreases human sperm motility and increases sperm DNA fragmentation. *Fertil Steril.* 2012;97(1):39-45.e2.
- Freshney, R.I., 2001. Application of cell culture to toxicology. *Cell Biol. Toxicol.* 17, 213–230.
- Khadem, N.; Sharaphy, A.; Latifnejad, R.; Hammod, N.; Ibrahimzadeh, S. Comparing the efficacy of dates and oxytocin in the management of postpartum hemorrhage. *Shiraz E-Med. J.* 2007, 8, 64–71.
- El-Kashlan, A.M.; Nooh, M.M.; Hassan, W.A.; Rizk, S.M. Therapeutic potential of date palm pollen for testicular dysfunction induced by thyroid disorders in male rats. *PLoS ONE* 2015, 10, e0139493.
- Barrett, K.E.; Boitano, S.; Barman, S.M.; Brooks, H.L. *Ganong's Review of Medical Physiology*, Lang, 23rd ed.; McGraw Hill: New York, NY, USA, 2010; p. 530.

- Barzin, G., Entezari, M., Hashemi, M., Hajiali, S., Ghafoori, M., & Gholami, M. (2011). Survey of Antimutagenicity and Anti-cancer effect of Phoenix dactylifera pollen grains. *Advances in Environmental Biology.*, 5(12), 3716–3718.
- Habib, H. M., El-Fakharany, E. M., El-Gendi, H., El-Ziney, M. G., El-Yazbi, A. F., & Ibrahim, W. H. (2023). Palm Fruit (Phoenix dactylifera L.) Pollen Extract Inhibits Cancer Cell and Enzyme Activities and DNA and Protein Damage. *Nutrients*, 15(11), 2614. <https://doi.org/10.3390/nu15112614>
- Godinho, P. I., Soengas, R. G., & Silva, V. L. (2021). Therapeutic Potential of Glycosyl Flavonoids as Anti-Coronaviral Agents. *Pharmaceuticals.*, 14(6), 546.
- Al-Samarai, A., Al-Salihi, F., & Al-Samarai, R. (2018). Phytochemical constituents and nutrient evaluation of date palm (Phoenix dactylifera, L.) pollen grains. *Tikrit journal of pure science.*, 21(1), 56–62.
- El-Azim, M. H. M. A., Yassin, F. A., Khalil, S. A., & El-mesalamy, A. M. D. (2015). Hydrocarbons, fatty acids and biological activity of date palm pollen (phoenix dactylifera L.) growing in Egypt. *IOSR J Pharm Biol Sci Ver I*, 10(3), 2319–7676. <https://doi.org/10.9790/3008-10314651>.
- Sadeq, O., Mechchate, H., Es-Safi, I., Bouhrim, M., Ouassou, H., Kharchoufa, L., et al. (2021). Phytochemical Screening, Antioxidant and Antibacterial Activities of Pollen Extracts from *Micromeria fruticosa*, *Achillea fragrantissima*, and *Phoenix dactylifera*. *Plants.*, 10(4), 676.
- Huang, H. -C., Wang, S. -S., Tsai, T. -C., Ko, W. -P., & Chang, T. -M. (2020). Phoenix dactylifera L. Seed extract exhibits antioxidant effects and attenuates melanogenesis in B16F10 murine melanoma cells by downregulating PKA signaling. *Antioxidants*, 9(12), 1270. <https://doi.org/10.3390/antiox9121270>
- Pfeffer, C. M., & Singh, A. T. (2018). Apoptosis: A target for anti-cancer therapy. *International journal of molecular sciences.*, 19(2), 448.
- Kıran, Tugba Raika, Otlu, Onder and Karabulut, Aysun Bay. "Oxidative stress and antioxidants in health and disease" *Journal of Laboratory Medicine*, vol. 47, no. 1, 2023, pp. 1-11. <https://doi.org/10.1515/labmed-2022-0108>.

## Study of the Runge-Kutta Scheme for Random Differential Equations

Ali Sami Abdullah <sup>1</sup>

Esraa Habeeb Khaleel <sup>2</sup>




© 2024 The Author(s). This open access article is distributed under a Creative Commons Attribution (CC-BY) 4.0 license.


### Abstract:


*Numerical methods are methodologies that use purely algebraic and arithmetic techniques to approximately solve complex equations or systems of equations, which analytically are very difficult or even impossible to solve. The slow convergence of Euler's method and the restrictedness of its region of absolute stability leads us to consider methods of higher order to attain the convergence of the solution. At each step, Euler's method moves along the tangent of a certain curve that is "close" to the unknown or sought curve. Because of the method's insufficiency, studying the Runge-Kutta methods that extend this geometric idea by using several intermediate derivatives or tangents instead of just one, to approximate the unknown function, makes up for what the Euler's method lacks.*

**Keywords:** Runge-Kutta; Numerical; equations

---

 <http://dx.doi.org/10.47832/MinarCongress12-17>

<sup>1</sup>  Tikrit University, Iraq [as230031pcm@st.tu.edu.iq](mailto:as230031pcm@st.tu.edu.iq)

<sup>2</sup>  Tikrit University, Iraq [esraa.h.khaleel@tu.edu.iq](mailto:esraa.h.khaleel@tu.edu.iq)

## Introduction

When a physical problem is translated into a set of mathematical equations, in order to study it, certain levels of uncertainty and complexity occur due to errors in the differential equations and therefore it is necessary to use numerical methods to solve them. Due to the randomness of some elements in the study of random differential equations, it is necessary to present sequences of second-order random variables. These variables are those whose range is formed by a finite number of elements, defined as

$$\delta^2 = E(X^2) - [E(X)]^2 \quad (1)$$

Convergence, continuity and mean square analyticity provide alternatives to numerical constructions of random initial value solutions for differential problems. Consider an initial value problem of the form:

$$\begin{aligned} X(t) &= G(X(t), t), \quad t \in I = [t_0, T] \\ X(t_0) &= X_0 \end{aligned} \quad (2)$$

There are many types of numerical methods for solving initial value problems for ordinary differential equations such as Eulers method and Runge-Kutta fourth order method (RK4). Runge-Kutta method is the powerful numerical technique to solve the initial value problems (IVP). This method widely used one since it gives reliable starting values and is particularly suitable when the computation of higher derivatives is complicated. Also, this method gives more accuracy of the numerical results and used in most computer programs for a differential equation. Many authors try to spread these methods to get more accurate solution of Initial Value Problems (IVP) [1]. In [2,3, and 4] authors presented different orders of Runge-Kutta method for solving ordinary differential equation, also, they presented a comparative study on numerical solutions of Initial Value Problems (IVP) for (ODE).

An explicit Runge-Kutta method is one of these methods, it can be written as following:

$$\begin{aligned} S_1 &= hG(t_n, X_n) \\ S_2 &= hG(t_n + c_2h, X_n + a_{2,1}S_1) \quad \vdots \\ S_r &= hG\left(t_n + c_rh, X_n + \sum_{j=1}^{r-1} a_{r,j}S_j\right) \\ X_{n+1} &= X_n + h \sum_{l=1}^r b_l S_{il} \end{aligned} \quad (3)$$



where,

$$X_{n+1} = X_n + \frac{1}{6}(S_1 + 2S_2 + 2S_3 + S_4), \quad n = 0,1,2, \dots \quad (4)$$

The computational cost is basically given by the number of evaluations for the function  $G$  in each step. Explicit  $r$  – step Runge-Kutta methods require  $r$  evaluations of  $G$ . Euler method can be written as a 1 – stage Runge Kutta method and will therefore at each step an evaluation of the function  $G$  are require.

This research is going to focus on the standard Runge-Kutta method of order 4, which is possibly the best known and most used Runge-Kutta method as it maintains a good balance between computational cost and precision.

### Numerical Method

In this section we will represent a method Runge-Kutta fourth order (RK4) for solving initial value problem (IVP) for ordinary differential equations (ODEs).

Theorem:

Consider  $G(X(t), t)$  defined as  $K \times I$  in  $L_2$ , where,  $K$  is a set bounded in  $L_2$  and  $G(X(t), t)$  satisfies the following conditions:

➤  $G(X, t)$  satisfies the Lipschitz condition in mean square.

$$\|G(X, t) - G(Y, t)\| \leq S(t) \|X - Y\| \quad (5)$$

where,

$$\int_{T_0}^T S(t)dt < \infty$$

➤  $G(X, t)$  it is uniformly continuous and randomly bounded.

Then, the fourth-order Runge-Kutta random scheme (4) is convergent to mean square.

Proof:

Under the hypotheses in this theorem, with the following error,

$$e_n = X_n - X(t_n) \quad (6)$$

that converges to zero in mean square, where  $X(t)$  is the theoretical solution of the following equation,

$$X(t) = G(X(t), t), \quad t \in I = [t_0, T], \quad X(t_0) = X_0$$

and,  $X_n, n \geq 0$  is the numerical approximation given by the fourth-order Runge Kutta random scheme. Whereas,

$$X(t_{n+1}) = X(t_n) + hG(X(t_\alpha), t_\alpha), \quad t_\alpha \in (t_n, t_{n+1}) \quad (7)$$

From equation (4),

$$e_{n+1} = X_{n+1} - X(t_{n+1}) + X_n - X_n - X(t_n) + X(t_n)$$

Reordering, taking norms and using equations (3), (4), and (5),

$$\begin{aligned} \|e_{n+1}\| &\leq \|X_n - X(t_n)\| + \|X(t_n) - X(t_{n+1}) + X_{n+1} - X_n\| \\ &= \|e_n\| + \left\| -hG(X(t_\alpha), t_\alpha) + \frac{h}{6}G(X_n, t_n) + \frac{h}{3}G\left(X_n + \frac{S_1}{2}, t_n + \frac{h}{2}\right) + \frac{h}{3}G\left(X_n + \frac{S_2}{2}, t_n + \frac{h}{2}\right) \right. \\ &\quad \left. + \frac{h}{6}G(X_n + S_3, t_n + h) \right\| \end{aligned} \quad (8)$$

By using,

$$M = \sup_{t_0 \leq t \leq T} \|\dot{X}(t)\| \quad (9)$$

and using the hypotheses in theorem (1),

$$\begin{aligned} &\|G(X_n, t_n) - G(X(t_\alpha), t_\alpha)\| \\ &\leq \|G(X_n, t_n) - G(X(t_n), t_n)\| + \|G(X(t_n), t_n) - G(X(t_\alpha), t_n)\| \\ &\quad + \|G(X(t_\alpha), t_n) - G(X(t_\alpha), t_\alpha)\| \\ &\leq S(t_n)\|e_n\| + S(t_n)Mh \\ &\quad + \delta(K, h) \end{aligned} \quad (10)$$

and,

$$\begin{aligned} &\left\| G\left(X_n + \frac{S_1}{2}, t_n + \frac{h}{2}\right) - G(X(t_\alpha), t_\alpha) \right\| \\ &\leq S\left(t_n + \frac{h}{2}\right)\|e_n\| + \frac{3}{2}MhS\left(t_n + \frac{h}{2}\right) \\ &\quad + \delta(K, h) \end{aligned} \quad (11)$$

$$\begin{aligned} & \|G(X_n + S_3, t_n + h) - G(X(t_\alpha), t_\alpha)\| \\ & \leq S\left(t_n + \frac{h}{2}\right) \|e_n\| + 2MhS\left(t_n + \frac{h}{2}\right) \\ & + \delta(K, h) \end{aligned} \tag{12}$$

$$\begin{aligned} & \|G(X_n + S_3, t_n + h) - G(X(t_\alpha), t_\alpha)\| \\ & \leq S\left(t_n + \frac{h}{2}\right) \|e_n\| + 2MhS\left(t_n + \frac{h}{2}\right) + \delta(K, h) \end{aligned} \tag{13}$$

Substituting equations (10), (11), (12) and, (13) into equation (8) to obtain,

$$\begin{aligned} \|e_{n+1}\| & \leq \left[1 + \frac{h}{6}S(t_n) + \frac{2h}{3}S\left(t_n + \frac{h}{2}\right) + \frac{h}{6}S(t_n + h)\right] \|e_n\| + M\frac{h^2}{6}S(t_n) \\ & + Mh^2S\left(t_n + \frac{h}{2}\right) + M\frac{h^2}{3}S(t_n + h) \\ & + h\delta(K, h) \end{aligned} \tag{14}$$

and taking,

$$a_n = 1 + \frac{h}{6}S(t_n) + \frac{2h}{3}S\left(t_n + \frac{h}{2}\right) + \frac{h}{6}S(t_n + h) \tag{15}$$

with,

$$b_n = M\frac{h^2}{6}S(t_n) + Mh^2S\left(t_n + \frac{h}{2}\right) + M\frac{h^2}{3}S(t_n + h) + h\delta(K, h) \tag{16}$$

Equation (14) can be rewritten as:

$$\|e_{n+1}\| \leq a_n \|e_n\| + b_n, \quad n = 0, 1, 2, \dots \tag{17}$$

and by successive substitution in equation (17) will get the following,

$$\|e_{n+1}\| \leq \left(\prod_{i=1}^n a_i\right) \|e_0\| + \sum_{l=0}^n \left(\prod_{j=l+1}^n a_j\right) b_l, \quad n=0, 1, 2, \dots \tag{18}$$

To prove that  $e_n \rightarrow 0$  when  $n \rightarrow \infty$ , with  $nh = T$  and  $h \rightarrow 0$ , suppose that the Lipschitz bounding function,  $S(t)$ , introduced in the first condition of theorem 1, is uniformly bounded on the interval  $[T_0, T]$  so,

$$S = \max_{T_0 \leq t \leq T} S(t)$$

Under this hypothesis it is satisfied,

$$\begin{aligned} \prod_{l=0}^n a_l &\leq \prod_{l=0}^n \exp\left(\frac{h}{6}\left[S(t_l) + 4S(t_l) + \frac{h}{2} + S(t_l) + h\right]\right) \\ &\leq \prod_{l=0}^n \exp\left(\frac{h}{6}[S + 4S + S]\right) = \prod_{l=0}^n \exp(Sh) \\ &= e^{S(n+1)h} \end{aligned} \tag{19}$$

Where in the first dimension we have applied the following inequality:  $1 + x \leq e^x$ ,  $x \geq -1$ . Applying that  $S(t) \leq S, \forall t \in [T_0, T]$ , from equation (16), the following limitation is also satisfied,

$$\begin{aligned} b_n &\leq M \frac{h^2}{6} S + Mh^2 S + M \frac{h^2}{3} S + h\delta(K, h) = Mh^2 S [1.5] + h\delta(K, h) \\ &= \frac{3}{2} Mh^2 \\ &\quad + h\delta(K, h) \end{aligned} \tag{20}$$

Now substituting the dimensions (19) and (20) in (18), with  $e_0 = 0$ , and equation (19) applied to a product that has  $n - l$  factors,

$$\begin{aligned} \|e_{n+1}\| &\leq \sum_{l=0}^n \left( \prod_{j=l+1}^n a_j \right) b_l \leq \sum_{l=0}^n e^{S(n-l)h} \left( \frac{3}{2} Mh^2 S + h\delta(K, h) \right) \\ &= \left( \frac{3}{2} Mh^2 S + h\delta(K, h) \right) e^{Snh} \sum_{l=0}^n e^{-lSh} \\ &= \left( \frac{3}{2} Mh^2 S + h\delta(K, h) \right) e^{ST} \frac{1 - e^{-S(n+1)h}}{1 - e^{-Sh}} \end{aligned} \tag{21}$$

where in the last step we have used that  $nh = T$ , and that,

$$\sum_{l=0}^n r_l = \frac{1 - s^{n+1}}{1 - s}, \quad s = e^{-Sh}$$

By using  $nh = T$ , and (21) can be written as follows,

$$\begin{aligned} \|e_{n+1}\| &\leq \left(\frac{3}{2}MhS + h\delta(K, h)\right) e^{ST} \frac{h(1 - e^{-Snh}e^{-Sh})}{1 - e^{-Kh}} \\ &= \left(\frac{3}{2}MhS \right. \\ &\quad \left. + h\delta(K, h)\right) e^{ST} \frac{h(1 - e^{-ST}e^{-Sh})}{1 - e^{-Sh}} \end{aligned} \tag{22}$$

By using L'Hôpital's rule, will have,

$$\lim_{h \rightarrow 0} \frac{h(1 - e^{-ST}e^{-Sh})}{1 - e^{-Sh}} = \frac{0}{0} = \lim_{h \rightarrow 0} \frac{(1 - e^{-ST}e^{-Sh} + hSe^{-ST}e^{-Sh})}{Se^{-Sh}} = \frac{1 - e^{-Sh}}{S} \tag{23}$$

With,

$$\lim_{h \rightarrow 0} \left(\frac{3}{2}MhS + h\delta(K, h)\right) = 0 \tag{24}$$

given that  $\delta(K, h) \rightarrow 0$  when  $h \rightarrow 0$ .

Therefore, taking limits when  $h \rightarrow 0$ ,  $n \rightarrow \infty$  with,  $nh = T$ , in (22), and using (23) and (24), it follows that  $\|e_{n+1}\| \rightarrow 0$  when  $n \rightarrow \infty$ , which proves the convergence of the Runge-Kutta method.

### Conclusion

The slow convergence of Euler's method and the restrictedness of its region of absolute stability leads us to consider methods of higher order to attain the convergence of the solution. At each step, Euler's method moves along the tangent of a certain curve that is “close” to the unknown or sought curve. Because of the method’s insufficiency, studying the Runge-Kutta methods that extend this geometric idea by using several intermediate derivatives or tangents instead of just one, to approximate the unknown function, makes up for what the Euler’s method lacks. From the method it has been concluded that the fourth order Runge-Kutta method is the best choice as it provides small margins of error with respect to the actual solution of the problem, with the advantage that it is easily programmable in software to perform the necessary iterations.



## References

- Hossain, M. J., Alam, M. S., & Hossain, M. B. (2017). A study on numerical solutions of second order initial value problems (IVP) for ordinary differential equations with fourth order and Butcher's fifth order Runge-Kutta methods. *American Journal of Computational and Applied Mathematics*, 7(5), 129-137.
- Rabiei, F., & Ismail, F. (2011, October). Fifth order improved Runge-Kutta method for solving ordinary differential equations. In *Proceedings of the 11th WSEAS international conference on Applied computer science* (pp. 129-133).
- Al-Juhaishi, E. H. K. (2022). Symbolic Solutions by Using the Functional Separation of Variables. *Iraqi Journal of Humanitarian, Social and Scientific Research*, (- عدد خاص لوقائع المؤتمر السادس-جامعة قم- (و.جامعة القاسم ورابطة التدريسيين وتربية كربلاء).
- Butcher, J. C. (1995). On fifth order Runge-Kutta methods. *BIT Numerical Mathematics*, 35(2), 202-209.
- Islam, M. A. (2015). A comparative study on numerical solutions of initial value problems (IVP) for ordinary differential equations (ODE) with Euler and Runge Kutta Methods. *American Journal of computational mathematics*, 5(03), 393-404.
- AL-JUHAISHI, E. H. K. (2022). Solving some linear equations by using enhanced theorem. In *MINAR CONGRESS 6* (p. 566).

## Applying A Medium Developed from Some Chelating Elements to Grow Some Microalgae

Maha Falah Al-Taie <sup>1</sup>

Mira Ausama Al-Katib <sup>2</sup>

Rana R. Abed <sup>3</sup>



© 2024 The Author(s). This open access article is distributed under a Creative Commons Attribution (CC-BY) 4.0 license.


### Abstract:


*The process of algae culturing is an important field in the biological applications of algae which is considered the crucial material for the production of bioactive compounds. It is also a basic organism in modern biological applications particularly of sustainable development; for instance, biofuels, bio fertilization, antibiotics, and pollution treatment. Hence, the present study aims to find economic and easy culturing conditions for algae. The nutrient medium is regarded as one of the most important influences on algae growth. The new medium supplemented with simple components (chelating elements) showed success in growing of Cosmarium and Diatom algae compared to the standard medium used Chu10, and the differences were clear in those which were separately grown for (15) days. The medium supplemented with chelating elements at a concentration of 2 ml/ 1 L recorded superior growth in Cosmarium algae based on the optical density at the wavelength of 436 nm, with the highest growth density (0.549). Whereas the standard Chu10 medium was (0.521), as well as the growth levels of Diatom algae were closed. The standard medium (Chu10) with the medium supplemented with chelating elements at a concentration of 2 ml/ 1L, were recorded (0.486) and (0.430) respectively. Thus, the results refer to the necessity of using other concentrations of these chelating elements in order to study their effect on algae development, and to depend on them as an economic alternative compared to the other growth methods.*


**Keywords:** Economic Growth Medium; Chelating Elements; Cosmarium, Diatoms.



<http://dx.doi.org/10.47832/MinarCongress12-18>

<sup>1</sup>  Department of Biology ,College of Education for Pure Sciences, University of Mosul, Iraq

<sup>2</sup>  Department of Biology ,College of Education for Pure Sciences, University of Mosul, Iraq

<sup>3</sup>  Department of Chemistry , College of Education for Pure Sciences, University of Mosul, Iraq

## Introduction

Algae, specifically macro algae and microalgae, are photosynthetic organisms. Macro algae are visible to the naked eye, while microalgae are too small to be seen without a microscope. Both types of algae may be found in aquatic environments, including fresh and marine water[1]. Microalgae are unicellular organisms categorized as diatoms (Bacillariophyceae), green algae (Chlorophyceae), and cyanobacteria (Cyanophyta). [2]. Algae can be regarded as a raw material for biofuel and other industrial byproducts. Additionally, algae have potential uses in pharmaceuticals, cosmetics, nutraceuticals, and the biofuel industry. [3]. In this study, we used two algae (*Cosmarium* and Diatoms) for testing efficiency of this new mixture of chelating elements coupled with glycerin. *Cosmarium*, Division: Chlorophyta, Class: Zygnematophyceae, Order: Desmidiiales Family: Desmidiaceae[4].

The Desmidiaceae It consists of two large green plastids in each half of the cell. The plastid has radial protrusions and in its middle there is a pyrenoid starch formation center. The nucleus is located in the waist area between the two halves of the cell, and one or more gaps. It reproduces in two ways: vegetatively (cell division) or sexually (conjugation) [5].

Diatoms possess a distinctive cell wall made of silica, which is referred to as a frustule. [6]. Diatoms are a highly successful group of single-celled creatures that use photosynthesis and belong to the domain of eukaryotes. Diatoms are a highly diversified category consisting of over 200 genera and encompassing around 10-12 thousand documented species. [7].

Plant nutrients are crucial environmental variables that are necessary for the growth and development of crops. Micronutrients such as iron (Fe), manganese (Mn), zinc (Zn), and copper (Cu) undergo oxidation or precipitation in soil, resulting in their inefficient usage. Chelated fertilizers have been created to enhance the efficiency of micronutrient utilization. This publication offers a comprehensive introduction to chelated fertilizers and the factors to consider when using them in commercial crop production. It is intended for county Extension instructors, producers, and students with an interest in this field. [8].

In most cases, the commonly used iron source for cultivating algae is Ethylenediaminetetraacetic acid ferric sodium salt (Fe-EDTA), which is considered the industry standard. The pH and light intensity conditions during algal formation are not conducive to preserving the integrity of the Fe-EDTA complex. Therefore, the availability of iron becomes the primary factor that limits growth. Several growth investigations and biomass assessments were carried out using various iron chelating agents in controlled settings. The control iron

source employed was Fe-EDTA in order to assess any potential benefits of the test chelates. The results indicated that chelating agents with greater stability constants than Fe-EDTA exhibited slower initial growth in short-term tests. Similarly, iron chelating agents with a stability constant similar to or lower than Fe-EDTA showed comparable results. Significant enhancements in the development of algae over lengthy periods (>7 days) were reported when using more stable chelates, specifically *Chlorella vulgaris* and *Spirulina platensis*. Enhancing the pH and light stability of chelating agents used as iron sources can effectively postpone the occurrence of iron deficiency situations. Optimized iron chelation in commercial batch operations might potentially offer advantages such as increased growth between cleanouts, enhanced lipid and biomass output, and potential savings of raw inputs. [9].

## Methods of Experiment

### 1. Algal liquid growth medium (Chu 10 medium) preparation:

A modified Chu 10 liquid medium for algal development was made using the specified proportions of the content, with Material Weight (g/L) as the unit of measurement. The composition of the solution is as follows: 0.4 M  $\text{Ca}(\text{NO}_3)_2$ , 0.1 M  $\text{K}_2\text{HPO}_4$ , 0.2 M  $\text{Na}_2\text{CO}_3$ , 0.25 M  $\text{MgSO}_4 \cdot 7\text{H}_2\text{O}$ , 0.25 M  $\text{Na}_2\text{SiO}_3$ , and 0.005 M Ferric Ammonium Citrate [10]. The constituents are dissolved in one liter of distilled water. Subsequently, the pH of the solution is adjusted to a range of 7.6-7.8 using a pH-Meter. The pH value is then equalized by adding dilute solutions of NaOH (0.1 N) and HCL (1 N). The prepared medium is evenly spread onto the flasks using aluminum paper. The aluminum is sterilized using an autoclave at a temperature of 121°C and a pressure of one atmosphere for a duration of 20 minutes. [1].

### 2. Resource and algal isolates detection:

A laboratory sample of Cosmarium and Diatoms algae was acquired from the Scientific Education Research Unit for Pure Sciences/Algae Research. Subsequently, the sample was scrutinized using a light microscope to verify the presence of the thallus, and photographic documentation of the sample was obtained. The algae were cultivated in 250 ml glass flasks using a sterile medium called Chu 10, along with a supporting media consisting of 5 ml of supporting materials per 100 ml of medium. Subsequently, following a week of development, the inoculum was extracted and transferred to uncomplicated photo reactors with a volume of 1 liter. The incubation process was conducted at a temperature of  $25 \pm 2^\circ\text{C}$  and a lighting intensity of 2500 lux. The air supplied during incubation was filtered using a 0.45 mm filter and a blower gas, as depicted in Figure. (1).

A fertilizer has been prepared that is added to the algae growth media to enhance its growth. It is composed of several elements such as Zinc, manganese, copper, chelated bi ethylene diamine tetra acetic acid. EDTA , in addition to potassium nitrate and glycerin.

After preparing the chelated elements, they are dried and weighed In calculated quantities and dissolve them with distilled water to obtain agricultural fertilizer containing the following proportions:

13%EDTA -Zn , 15%EDTA -Mn , 13%EDTA -Cu , 10% glycerin , and 3% potassium nitrate . Ponds containing algae are fertilized in a proportion 5 ml / 20 L Over the course of couple week we notice its significant growth.

The chelated elements were prepared by thermal sublimation for 3 hours for sodium ligand ethylenediaminetetraacetic acid with calculated amounts of the elements... dried and weighed to be used to prepare fertilizer.



**Figure 1-** A simple photoreactor

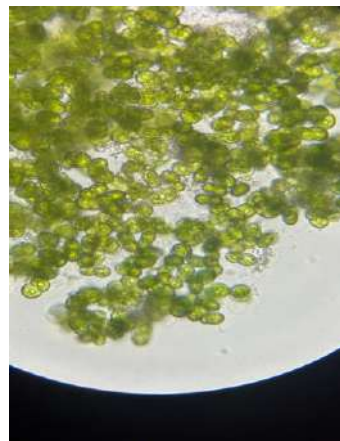
### 3. Algal detection

Algae growth in a photobioreactor was measured for *Cosmarium* and Diatoms algae using a spectrophotometer at various absorption lengths (436nm) based on different sources. [9], The identification of the algal samples was carried out by the utilization of references for algae classification. [10,11].



**Results and Discussion:**

Cosmarium alga is a solitary desmid that is seen freely floating in freshwater ponds, alongside other types of algae[5]. Therefore, our investigation extracted samples from the wells of the household reservoir. Cosmarium is composed of a diminutive and planar cell. This study employed various varieties of algal thallus, including Cosmarium, a unicellular Chlorophyta, and Diatoms, which are simple unbranched filaments (Figure 2).



**Cosmarium**



**Diatoms**

**Figure 2-** Microscopic image for algal samples

**1. Growth estimation:**

Algae culture growth

The discrepancy in culture media between the first and second week resulted in a minor increase in cell density. This change may be attributed to the achievement of a consistent growth rate at 14 to 30 days of culture in a photo bioreactor, with an absorption length of 436 nm. Fig.3.



**(Chu10 medium)**



**Chu10+supporting elements(SE)**

**Figure 3-** Growth of algae after 30 days left (Chu10) right (Chu10+supporting elements(SE))

### Determination of algae growth by optical density (O.D.)

The obtained data after culture periods Figure 4,5 , refers to growth value of each alga. The growth density differed according to media content too beside the differ between algal species. Water alone and with SE used too to compare with Chu10 standard media.

The results of Tables (1) and (2) show that there is variation in the growth of the algae under study in the new culture media used, as well as the results of its growth with the standard liquid Chu10 medium.

**Table 1-** Shows the absorbance values of *Cosmarium* alga growth in different agricultural media

Medium type 100 ml (medium)+ µl (SE)	Growth as Optical Density(O.D.) at 436 nm		
	7 days	15 days	30 days
<b>Chu 10</b>	0.401	0.521	0.419
<b>Water</b>	0.134	0.273	0.159
<b>Chu10 + 100 µl SE</b>	0.284	0.493	0.422
<b>Chu10 + 200 µl SE</b>	0.256	0.549	0.411
<b>Water + 100 µl SE</b>	0.174	0.247	0.144
<b>Water + 200 µl SE</b>	0.106	0.270	0.205

The results of the table showed that there was variation in the growth of *Cosmarium* moss in different cultural media, and that these media were an excellent alternative to the standard medium Chu 10, as the moss showed excellent growth in general in the second week in general, and the highest growth was in the standard medium with the addition of chelating elements at a concentration of 200 Microliter in the second week, with the highest growth density (0.549), exceeding the standard medium (0.521), followed by the standard medium with the addition of chelating elements at a concentration of 100 microliters, with a density of (0.493). Also, the rest of the media had good growth of the algae. Fig.4



**Chu10**

**Chu10+100 µl SE**

**Chu10+200 µl SE**

**Figure 4-** *Cosmarium* alga growth in different agricultural media

**Table 2-** Shows the absorbance values of Diatom growth in different cultural media

Medium type	Growth as Optical Density(O.D.) at 436 nm		
	7 days	15 days	30 days
100 ml (medium)+ µl (SE)			
<b>Chu 10</b>	0.444	0.486	0.364
<b>Water</b>	0.132	0.221	0.143
<b>Chu10 + 100 µl SE</b>	0.28	0.35	0.336
<b>Chu10 + 200 µl SE</b>	0.386	0.430	0.375
<b>Water + 100 µl SE</b>	0.165	0.366	0.191
<b>Water + 200 µl SE</b>	0.118	0.486	0.364



Chu10

Chu10+100 µl SE

Chu10+200 µl SE

**Figure 5-** Diatom growth in different cultural media

The results of Table (2) showed that the best growth of the diatom was in the two weeks, where it outperformed the standard medium and distilled water supplemented with chelating agents at a concentration of 200 microliters, with an optical density of 0.486), followed by the growth of the diatom in the standard medium supplemented with chelating agents at a concentration of 200 microliters, where it recorded (0.430) and approximately Water and standard medium supplemented with chelating agents at a concentration of 100 microliters had an optical density of 0.366 and 0.35, respectively, while distilled water alone had the least growth (0.221).

Given the importance of microalgae, which has recently become a promising source in the production of biofuels, antibiotics, and various by-products, it is necessary to develop this source and study the cost of its production. Many sources have been found to describe the

requirements of agriculture and development, but there are a limited number that discuss the cost of agriculture and obtaining an abundant product from it using few alternatives cost.

This study agrees with [12], as the highest growth rate of *Cosmarium* was reached in the second week in the standard medium with a growth density of (0.637). The results of [9] showed good initial growth in the medium supplemented with iron chelated in Fe-EDTA. Extended investigations (7 days) revealed substantial and enduring enhancements in algal growth when examining *Chlorella vulgaris* and *Spirulina Platensis*. Utilizing chelating agents to optimize the growth source can yield many benefits, including enhanced growth and elevated amounts of lipids and biomass. An optimal solution is to utilize chelating compounds, which have garnered increased interest due to their highly interactive nature with metal ions, resulting in a modification of their solubility in algae. Three often employed chelating compounds are ethylenediaminetetraacetic acid (EDTA), citric acid, and nitrilotriacetic acid (NTA). [13]. [14] used EDTA to generate low ash in algal biomass. Ethylenediaminetetraacetic acid (EDTA) is a synthetic chelating chemical that is frequently utilized as a necessary nutrient for microalgal metabolism. Fe-EDTA is commonly employed to keep iron in solution for the purpose of cultivating microalgae. This utilization of Fe-EDTA has opened up the possibility of enhancing microalgae cultivation, hence boosting production efficiency in photo bioreactors [15].

EDTA has been used as a metal chelator in hydroponics or microalgae growth media for coastal algae such as *Heterosigma akashiwo*, *Prymnesium parvum* and *Skeletonema marinodohrnii* improve the growth of these algae [16,17] It has been proven that the green marine algae *Tetraselmis suecica* and the diatom *nare* are able to grow in a medium containing glycerol, glucose and acetate [18].

There are several attempts to find different media in order to increase the biomass of algae, including growing algae in NPK bio fertilizer media alone and not as an improver of the existing standard media. [19] compared the use of NPK media (20:20:20+TE) to grow one species. Of the algae, which is *Chlorella*, the use of this medium was better in growing algae than Chu 10 medium. A comparison between the types of media used in growing algae and cyanobacteria was also used before [20]

In a study [21], it was found that the best growth of the cyanobacteria *Chroococcus* was in (BG-11) medium compared to Chu 10 medium, with the formula and (BG-11) medium. All of these media are artificial and have a cost in preparation, in addition to the presence of prohibited materials are rarely traded. There is no study that used multiple types of NPK fertilizers with varying proportions of elements. Confirmatory experiments have indicated that the lack of

stability of Fe-EDTA over extended tests is the primary factor that restricts the availability of iron, leading to subpar performance. [9].

## Conclusion

The field of algae cultivation and development is one of the most important axes for obtaining the algae biomass, which is the main raw material for all algae bio application research and recently it is considered the most important sustainable renewable sources. Therefore, algae development research has great importance in achieving sustainability and modern applied research. Hence the importance of obtaining an economic medium for producing biomass in a short period. The use of chelated iron with the most important nutrients used in this research (SE) as a support medium for the standard nutritional medium (Chu10) as well as a support medium when experimenting with the use of sterile water is a new experiment added to the algae development experiments referred to in algae development and cultivation research in order to reach useful results in this field the support medium (SE) at a concentration of 2 ml/L with the standard medium for development (Chu10) showed superiority in the growth of *Cosmarium* algae during a period of 15 days compared to the standard medium alone, and the concentration of 1 ml/L for the support medium was superior to the normal one during a period of 30 days of cultivation for the same algae. As for the Diatoms algae, the best growth was recorded for them during a period of 30 days with the support medium at a concentration of 2 ml/L added to sterile water and during the two growth periods of 15 and 30 days. The results show that adding the support medium had an effect in improving the growth of the two algae under study, whether by adding it to the water or to the standard algae medium, as the growth of *Cosmarium* increased in the standard medium with support medium, while the growth of Diatoms increased in the water to which the support medium was added, due to the effect of the type of algae that determined the most suitable medium for growth. However, in both types, adding the support medium had a positive effect on growth, so it is recommended to use it and try other nutritional media with it and test other concentrations added from it and study the optimal concentration for growth of these algae and other new algal genera.



## References

- Alobeady Mohammed A.H. and AL-Katib Mira Ausama (2022). Separation and identification of a number of unsaturated fatty acids from different types of algae. MINAR International Journal of Applied Sciences and Technology. v.4(3).145-159.
- Avragyan, Armen.(2018). The use of microalgae for biofuel production and need in improvements of global environmental policy. Proceeding of 11<sup>th</sup> world Bioenergy congress and expo ( July 2-4 , 2018 , Berlin , Germany )
- Abu Yousef .(2020) Microalgae Cultivation for Biofuels production . Chapter 12 , Microalgal Biorefineries for Industrial products : 187-195 .
- Bellinger, E.G. and Sigeo, D.C. (2010). Freshwater Algae Identification and use as Bioindicators. John Wiley and Sons, Ltd pp.271.
- Vashishta, B. R.,sinha, A. K. and Singh, V P. (2012). Botany for Degree stuents Algae. Chand Higher Academic. Printed on Gnvirion mental friendly ECF paper. S. Chanl Qublishing S. Chand and Company LTD
- Round,F.E. Crawford R.M.and D G Mann,D.G.(1990). The Diatoms: Biology & Morphology of the Genera, Cambridge University Press
- Seckbach J. and Kociolek, J.P. eds(2011). The Diatom World, Vol.19. Cellular Origin, Life in Extreme Habitats and Astrobiology. Dordrecht: Springer Netherlands.
- Guodong Liu, Edward Hanlon, and Yuncong Li Understanding and Applying Chelated Fertilizers Effectively Based on Soil Ph <https://search.app/En5JNXi3snRaW84QA>
- M. A. Kean\*#, E. Brons Delgado\*, B.P. Mensink\*, M.H.J. Bugter (2015). Iron chelating agents and their effects on the growth of Pseudokirchneriella subcapitata, Chlorella vulgaris, Phaeodactylum tricorutum and Spirulina platensis in comparison to Fe- EDTA .J. Algal Biomass Utln. 2015, 6 (1): 56-73 Iron chelating agents and their effects on the growth of algae ISSN: 2229 – 6905
- Prescott, G.W. (1982).Algae of the Western Great Lakes Areas. Willam, C.; Brown, C.O .Pub. Dubuque. I. Iowa,16th printing.
- Wehr, J. D. and sheath, R. G. (2003). Fresh water Algae of North America. Ecology and classification. Academic press. Elsevier science (USA).
- Al-Shabki, Badr Hussein Khurshid (2021). Production of biodiesel from some Iraqi macro- and micro-algae and estimation of their content of oils and fatty acids. Master's thesis, College of Education, University of Mosul
- Daramola,T.G.(2019).Application of Biodegradable and Recyclable chelating Agent for ash Removal from Algae.Civil &Environmental Engineering.
- Edmunds, C.W., et al., Using a chelating agent to generate low ash bioenergy feedstock. Biomass and bioenergy, 2017. 96: p. 12-18
- Sauvage,J. ;Wikfors,G.H.;Sabbe,K. ;Nevejan,N.;Goderis,S.;Claeys,p.;Li,X. and Joyce,A.(2021).Biodegradable ,metal –chelating compounds as alternatives to EDTA for cultivation of marine microalgae.Journal of Applied phycology .33:3519-3537.

- Hasegawa H, Nozawa A, Papry RI, Maki T, Miki O, Rahman MA (2018) Effect of biodegradable chelating ligands on Fe uptake in and growth of marine microalgae. *J Appl Phycol* 30:2215–2225
- Hasegawa H, Rahman MM, Kadohashi K, Takasugi Y, Tate Y, Maki T, Rahman MA (2012) Significance of the concentration of chelating ligands on Fe<sup>3+</sup>-solubility, bioavailability, and uptake in rice plant. *Plant Physiol Biochem* 58:205–211
- Smith JP, Hughes A, McEvoy L, Day J (2020) Tailoring of the biochemical profiles of microalgae by employing mixotrophic cultivation. *Bioresour Technol Rep* 9:100321
- AL-Mashhadani, Mahmood K.H. and Khudhair, Entisar Mohsin (2017). Experimental Study for commercial fertilizer NPK(20:20:20+TE N:P:K) in microalgae cultivation at different aeration periods. *Iraqi Journal of Chemical and Petroleum Engineering*. Vol.18(1):99-110
- Al-Husseini, Ahmed Idan; Hussein, Thamer Heba; Hammoud, Amal Hamza (2014). Propagation of algal cultures using several methods in different culture media. *Journal of Basic Education*, Volume 10 – Issue 84: 121.
- Fayyad, Raghad J. and Dwaish, Ahmed S. (2016). Examination of the growth of blue green alga, *Chroococcus turigidus* in different traditional media formulations. *Journal of the College of Basic Education*. Volume 22 – Issue 95: 51-60

# Evaluation of The Protective Effect of Propolis Extracts Against Atherosclerotic Lesions in Male Rats Exposed to Oxidative Stress Induced by Hydrogen Peroxide

Sadoon Mohammed Abdullah <sup>1</sup>

Sahib Jummah Abdul Rahman <sup>2</sup>

Adil Ali Haider <sup>3</sup>



© 2024 The Author(s). This open access article is distributed under a Creative Commons Attribution (CC-BY) 4.0 license.



## Abstract:

*Propolis, also known as bee glue, is a resinous substance collected by bees from plants. It contains phenolic compounds and flavonoids, with antibacterial, antifungal and antioxidant properties, traditionally used to support immunity and treat infections. The present study aimed to the assessment the role of propolis extracts (aqueous and alcoholic) and vitamin E in the prevention of atherosclerotic diseases in male rats exposed to oxidative stress. Blood samples were taken from rats exposed to oxidative stress induced by hydrogen peroxide after the end of the experiment period (21 days) for laboratory analysis to observe the effect of these extracts and vitamin E on some physiological and biochemical variables such Lipid profile include cholesterol (Chol), triglycerides (TG), low density lipoproteins (LDL-C), very low density lipoproteins (vLDL-C), high-density lipoproteins (HDL-C) and atherogenic indicators (AIP). The results of the current study showed a significant increase in ( $p \leq 0.05$ ) in the concentration of Chol, TG, LDL-C, vLDL-C, atherogenic indicators, Urea, and Creatinine level and it showed decrease in the level of HDL-C, While the treatment with propolis extracts and vitamin E led to a significant decrease in the concentration of Chol, TG, LDL-C, vLDL-C, atherogenic indicators, Urea, and Creatinine level and it showed decrease in the level of HDL-C in the propolis treatment groups, which confirms the positive role of Propolis in the prevention of atherosclerosis, and that this role is affected by the type of solvent used in the preparation of the extract has shown the extract prepared with ethanol a more positive role in the variables studied when compared to the extract prepared with water.*

**Keywords:** Propolis; Atherogenic Indicators; lipid profile; Antioxidant.



<http://dx.doi.org/10.47832/MinarCongress12-19>

<sup>1</sup> Biology Department, College of Education for pure Sciences, University of Kirkuk, Iraq  
[sadoonm1993@gmail.com](mailto:sadoonm1993@gmail.com)

<sup>2</sup> Biology Department, College of Education for pure Sciences, University of Kirkuk, Iraq  
[drsahib68@uokirkuk.edu.iq](mailto:drsahib68@uokirkuk.edu.iq)

<sup>3</sup> Biology Department, College of Education for pure Sciences, University of Kirkuk, Iraq  
[777ali@uokirkuk.edu.iq](mailto:777ali@uokirkuk.edu.iq)

## Introduction

Propolis is one of the most important products of the honey bee and is characterized by its various medicinal effects. It is defined as a resinous substance consisting of a mixture of different plant parts and molecules secreted by honey bees *Apis mellifera*, while chemically it is described as a complex matrix containing biologically active parts. It includes within its composition more than 824 compounds [1] that are responsible for its various biological activities and potential therapeutic properties [2] such as its antioxidant activity [3], its anti-atherosclerotic activity and its ability to prevent other cardiovascular diseases through several mechanisms, the most important of which is improving the lipid profile in plasma [4]. Regulation of metabolism, Reducing blood glucose level, reducing insulin resistance, Positive effect on the intestinal microflora [5], Regulation of gene expression, Prevention of cytokines activity and accumulation as well as its role in reducing endothelial dysfunction [6].

All of the above mechanisms contribute to reducing the lesions of atherosclerosis, which is defined as a chronic disease that occurs as a result of the accumulation of fat in the layers of the walls of the large and medium arteries, except for the outer layer, producing a decrease in the diameter of the lumen of the artery [7]. It is one of the leading causes of 80% of deaths in developed countries [8] and occurs as a result of the oxidation of LDL-C and their aggregation under the inner lining in its oxidized form OX-LDL [9]. They are devoured by phagocytes, turning them into foam cells loaded with fat [10]. Vascular sclerotic lesions occur as a result of the accumulation of free radicals and the occurrence of oxidant that causes the accumulation of foam cells [11].

Based on the above, the study aimed to :

1. To evaluate the efficacy of both extracts in mitigating damage caused by hydrogen peroxide.
2. To compare the protective effect of aqueous and alcoholic propolis extracts in reducing the development of atherosclerotic lesions in rats subjected to oxidative stress.

## Materials and Methods

### 1. Animals used in the study:

A total of 25 rat males of the Sprague Dawley strain (*Rattus norvegicus*) weighing between 160 and 200 grams were used; the University of Tikrit's Faculty of Veterinary

Medicine provided them, and the Ethics Committee approved the use of them with letter No. 3/7/1555 dated 18/7/2023.

The animals placed in plastic cages measuring (46x28x13) cm and under the appropriate conditions of the appropriate temperature (25) °C and a light period divided into 12 hours of light and 12 hours of darkness, in addition to the availability of good ventilation for a period of 21 days

## **2. Experiment design:**

Five groups comprising the animals were assigned to them: Until the study's conclusion, the first group, known as the control, was given nothing except food and water ; The second group was administered 0.5% H<sub>2</sub>O<sub>2</sub> in drinking water for 21 days, as suggested by [3] for inducing oxidative stress; the third group received the same H<sub>2</sub>O<sub>2</sub> dose but additionally received treatment with an aqueous extract of propolis (A.E.P.) at a concentration of 4% for 21 days. The fourth group was given 0.5% H<sub>2</sub>O<sub>2</sub> in drinking water and 1% alcoholic extract of propolis (E.E.P.) for 21 days, while the fifth group received 0.5% H<sub>2</sub>O<sub>2</sub> in drinking water and 50 mg/kg of vitamin E for 21 days.

## **3. Collection of samples propolis and Preparing the extracts :**

The samples were taken straight from the *Apis mellifera* honey beehives and stored in plastic containers in the freezer or refrigerator to solidify and make them suitable for grinding with an electric grinder. Following that, the alcoholic extract was prepared using the procedure described in [12], and this was done by dissolving 30 grams of propolis powder in 100 mL of absolute ethyl alcohol for 7 days at room temperature with periodic shaking. The solution was then filtered using filter paper, and afterward, the solvent was removed using a rotary evaporator at a temperature of 40°C for 35 minutes .

The aqueous extract was prepared using the [13] method by dissolving 20 grams of propolis in 200 mL of water and thoroughly mixing it using a magnetic stirrer while heating. The solution was then filtered first using medical gauze and subsequently through filter paper multiple times. After that, drying was performed using an electric oven at 40°C to obtain the powder.

## **4. Determination of active dose:**

The most effective dose for the alcoholic and aqueous extracts of propolis was determined using a method [14]. The proper dose of hydrogen peroxide to induce oxidative stress in the



male rats was determined using prior research, such as the study of [15], and the proper dose of vitamin E was determined using prior research, such as the study of [16].

### 5. Collection of blood samples:

The animals were fasted for 12 hours, then anesthetized using chloroform, and blood samples were directly drawn from the heart. The samples were placed in test tubes and transferred to the incubator for 30 minutes at a temperature of 37°C. Afterward, the serum was separated from the other blood components using a centrifuge at a speed of 3000 revolutions per minute for 15 minutes. The serum was then withdrawn using a micropipette and stored in a deep freezer at -20°C until the required tests were performed.

### 6. Estimation of the variables studied:

Ready-made analysis tools from the Swiss company Aggabbe were used based on the enzymatic method and according to the method of action attached with each kit to estimate the concentration of total cholesterol according to the method of [17], triglycerides according to the method of [18], high-density lipoproteins of cholesterol according to the method of [19], LDL - C was calculated according to the equation of [20] v LDL-C was calculated according to the equation of [21] and AIP I, AIP II and AIP III were calculated according to the equations of [22] and shown below :

$$AIP I = \frac{TC}{HDL - C Con.}$$

$$AIP II = \frac{vLDL - C Con. + LDL - C Con.}{HDL - C Con.}$$

$$AIP III = \frac{LDL - C Con.}{HDL - C Con.}$$

### 7. Statistical Analysis:

Statistical results were analyzed by using the SPSS statistical program and extracted morale through the Anova-One Way test and then the significant differences were identified according to the Duncans Multiple Ranges test ( $p \leq 0.05$ ) [23].

### Results and discussion :

The results of the study shown in Table 1 and Table 2 indicated a significant increase at the level of ( $P \leq 0.05$ ) in the levels of lipid profile elements and atherogenicity indicators, except

for high-density lipoprotein cholesterol, which showed a significant decrease in the group treated with hydrogen peroxide when compared to the control group, while the groups treated with vitamin E and propolis extracts showed a significant decrease in lipid profile elements and atherogenicity indicators, except for high-density lipoprotein cholesterol, which showed a significant increase when compared to the hydrogen peroxide group.

**Table 1-** The level of lipid profile in studied groups

Groups Parameters	Group 1	Group 2 (H <sub>2</sub> O <sub>2</sub> )	Group 3 (H <sub>2</sub> O <sub>2</sub> +A.E .P)	Group 4 (H <sub>2</sub> O <sub>2</sub> +E.E. P)	Group 5 (H <sub>2</sub> O <sub>2</sub> +Vit. E)
<b>Cholesterol (mg/dl)</b>	202.39 ±1.87 bc	238.56±0.4 2 a	207.25±3.7 7 b	198.98 ± 3.69 c	204.75 ±1.26 b
<b>Triglycerides (mg/dl)</b>	86.16±2.86 D	274.61±6.7 1 a	112.30±4.7 3b	104.90 ±4.05 c	113.13±3.5 9 b
<b>vLDL-C (mg/dl)</b>	17.23±0.58 c	54.92±1.23 a	22.46±0.95 b	20.98±0.81 b	22.63±0.72 b
<b>HDL-C (mg/dl)</b>	98.33 ± 1.84 a	91.22±0.91 b	99.84±2.32 a	100.29±2.55 a	97.55±1.48 a
<b>LDL-C (mg/dl)</b>	86.64 ±0.57 b	92.41 ±1.67 a	84.95 ±1.31 b	77.70 ± 4.4 c	84.57 ± 1.88 b

**Note:** A significant difference is shown by different letters horizontally at the ( $p \leq 0.05$ )

**Table 2-** The level of atherogenic markers in studied groups

Groups Parameters	Group 1	Group 2 (H <sub>2</sub> O <sub>2</sub> )	Group 3 (H <sub>2</sub> O <sub>2</sub> +A. E.P)	Group 4 (H <sub>2</sub> O <sub>2</sub> +E. E.P)	Group 5 (H <sub>2</sub> O <sub>2</sub> +Vit .E)
<b>AIP I</b>	2.06 ± 0.02 a	1.62 ± 0.03 b	2.08 ± 0.02 a	1.99 ± 0.07 c	2.10 ± 0.03 a
<b>AIP II</b>	1.06 ± 0.02 a	1.62 ± 0.03 b	1.08 ± 0.02 a	0.99 ± 0.07 c	1.10 ± 0.03 a
<b>AIP III</b>	0.88 ± 0.02 b	1.01 ± 0.02 a	0.85 ± 0.02 b	0.78 ± 0.06 c	0.87 ± 0.03 a

**Note:** A significant difference is shown by different letters horizontally at the ( $p \leq 0.05$ )

The tables 1 and 2 show the effectiveness of Propolis extracts and vitamin E in improving lipid profile and the atherogenic indicators (AIP) in the males of rats exposed to H<sub>2</sub>O<sub>2</sub>. The results have shown a significant height ( $p \leq 0.05$ ) in the values of both cholesterol, triglycerides and LDL-C. The VLDL-C and AIP in the positive control group, when compared to the negative control group. These results were consistent with the result of study [24].

The significantly increasing of cholesterol concentrations level as been attributed to the exposure of pancreatic beta cells to the oxidative stress resulting from interactive oxygen types, which leads to a decrease in glucose-stimulated insulin secretion [25]. Insulin weakens the body's ability to remove cholesterol. [26] indicated that insulin inhibits the production of  $\alpha$ -Hydroxylated that enhances the absorption of intestinal cholesterol and inhibits the absorption of hepatic cholesterol, or may be attributed to the oxidation of the APO B-100 protein .[27] Found in LDL-C and v LDL-C, which prevents the transmission of cholesterol and triglycerides from the blood to the liver, [28] mediates the decomposition of fat within the blood vessels of the fatty proteins rich in triglycerides such as Chylomicons and v LDL-C for by degradation to fatty acids and glycerin, whose weak activity leads to high triglycerides in the blood [29].

Table (1) also shows the low concentrations of HDL-C may be attributed to the increase in the concentrations of cholesterol, triglycerides and LDL-C because the function of HDL-C is to transport cholesterol from the various tissues of the body to the liver, if the concentrations of cholesterol and triglycerides in tissues and blood vessels increase, this constitutes a disability that reduces the efficiency of HDL-C in the transport of cholesterol [20], and that the oxidation of LDL-C and the destruction of internal cholesterol in the body due to reactive types of oxygen leads to a reduction in HDL-C concentrations [30], which is the main carrier of cholesterol from the cells and tissue in the body to the liver and thus reduce its level in the blood vessels and this is characteristic of atherosclerosis and dyslipidemia disorder and reflects an unhealthy lifestyle, poor metabolism and an increased risk of cardiovascular disease [31].

Giving male rats with  $H_2O_2$  with drinking water at a concentration of 0.5% is sufficient to create a state of oxidative stress and increase the concentrations of free radicals, which increases the oxidative processes of LDL-C and v LDL-C, as well as the removal of nitric oxide NO secreted from cells lining blood vessels [32], which it works to reduce atherosclerosis [33].

$H_2O_2$  is also characterized by its ability to generate the free radicals represented by the Hydroxyl OH radical, which is characterized by its high ability to destroy cells and tissues, causing the excessive increase in the iron voltage inside the cells and freed from the protein that carries iron known as Ferritin [34]. Interactive species also lead to damage to the channels The ionic pumps in the plasma membrane, which enhances the process of atherosclerosis [35] that the results confirms the validity of the interpretations and hypotheses above.

The high concentrations of triglycerides , LDL-C and v LDL-C or HDL-C decrease can raise the signs of the atherogenic indicators, which reflects growth and development in the risk

of sclerosis caused by changes in body fat metabolism [36], This is consistent with what he reached [22] in his equations to calculate the AIP that the Atherogenic sclerosis pests are inversely proportional to the high -density sebaceous protein of cholesterol and expelled with the rest of the lipid elements, as [35] emphasized the high indicators are an inevitable result of increasing the concentrations of blood fat and low HDL-C, due to the fact that the flow of blood in the arteries and its capacity is a response to the worker called methacholine, whose level is less in cases of increased levels of harmful fats in the blood, as it was recently noticed that the hydrogen peroxide with a concentration of 0.5 % The ability to raise blood pressure in the ventricle and reduce the level of adenosine triple phosphate in cells, which interferes with the expansion function of the cells lining the arteries [37]. After the formation of OX-LDL by free radicals and its deposition on the walls of blood vessels, it is directly attacked by phagocytes and subjected to a cytophage process producing foam cells that adhere to the blood vessel and recruit a large number of pro-inflammatory agents laying the foundation for atherosclerosis lesions [38].

Giving rats concentrations of aquatic and alcoholic extracts of propolis gave positive results regarding the lipid profile, and this is consistent with the [39] in their study of a significant decrease ( $p \leq 0.05$ ) at the level of both total cholesterol, triglycerides and low-density lipoproteins, and the very low-density lipoprotein and a significant HDL level in the male rats treated with the aquatic extract of proposals, as well as the results of our study agreed with the [40] that the use of different concentrations of alcoholic extract (150-250) mg/kg It led to a desirable change in the Lipid profile This has been indicated by several other studies conducted on diabetic rats that the use of ethanolic and aqueous propolis extracts has improved the lipid profile, increasing the level of good lipids and reducing the level of harmful fats [41] due to the ability of propolis to promote the expression of ATP-binding cassette transporters in liver proteins associated with HDL formation [42], on the other hand, propolis can increase the regulation of the ABCA1 pathway by stimulating PPAR-gamma and expression of the hepatitis X receptor which can lead to lower cholesterol in macrophage cells [43] and as well as its role in lowering TG by improving insulin sensitivity and increasing insulin-mediated lipoprotein lipase activity [44].

It also works to reduce oxidative stress by breaking free radical chains that attack cell membranes due to its phenolic compounds such as chlorogenic acid, Cumaric Acid and Ferulic Acid [45], and this reduces the harmful effect of oxidative stress and excessive production of free radicals On the lipid profile which was referred to when interpreting the results of the

second group exposed to hydrogen peroxide 0.5 % with drinking water, all the mechanisms that the propolis use to show his various biological activities that earn him the ability to prevent atherosclerosis [46].

Reduce the development of atherosclerosis lesions by activating the reverse transport of cholesterol or by inhibiting the expression of lectin-like low-density lipoproteinuripoprotein receptor (LOX-1) found in endothelial cells of blood vessels, which prevents the deposition of OX-LDL on the walls of blood vessels in the form of plaques, which forms the onset of atherosclerosis lesions [47].

[33]It also prevents narrowing of the arteries due to the deposition of lipids by regulating blood lipids and inhibiting oxidative stress and inflammation [48] as the antioxidant and anti-inflammatory activities of propolis are responsible for protecting the lining of blood vessels containing NO-synthase-producing cells that have a role in reducing atherosclerosis [33].

The results shown in Table 1 and 2 also showed the positive role of vitamin E in influencing the lipid profile and AIP in male albino rats exposed to H<sub>2</sub>O<sub>2</sub> it was consistent with the study of [16] which showed that the dose of male rats with 50 mg/kg of vitamin E led to a significant decrease ( $p \leq 0.05$ ) in cholesterol and triglyceride concentrations, LDL-C and vLDL-C and a significant increase in HDL-C concentration due to its ability to activate the enzyme LPL and the enzyme hepatic lipase (HL), which stimulate cells to withdraw cholesterol and triglycerides from the blood [49].

[51] The activation of the enzyme LPL, which is mainly present in adipose tissue and muscles, increases fat metabolism, especially triglycerides, if it decomposes triglycerides carried in chylomicrons and vLDL-c into fatty acids and glycerol , as well as its participation in the reverse transport of cholesterol, which helps to transport cholesterol from the blood to the liver for secretion [50],while Hepatic lipase removes lipoprotein residues from the circulatory system, this is critical to the generation of residues that can be efficiently absorbed by the liver [51] and manufactured by liver cells and located on the surface of sinus capillaries in the liver and involved in the reshaping of LDL residues and high-density lipoproteins (HDL) and the production of small low-density lipoproteins (sd-LDLs) Small [52].

The role of vitamin E in improving the lipid profile positively according to many mechanisms, including what is mentioned above, in addition to its role as an antioxidant and its effect similar to the effect of propolis extracts on fat elements leads to reducing the incidence of atherosclerosis lesions, and The results agree with have reached and are consistent with the



results of [53], which showed the role of vitamin E in preventing atherosclerotic lesions through its antioxidant properties.

### **Conclusions:**

The study found that propolis extracts and vitamin E significantly decreased cholesterol, triglyceride, LDL-C, and atherogenic indicators, while increasing HDL-C levels. Propolis's positive role in atherosclerosis prevention was influenced by the solvent used, with ethanol extracts showing a more positive effect than water-prepared extracts.

### **Study limitations**

No limitations were known at the time of the study.

- 1. Acknowledgements:** I would like to express my sincere gratitude to Dr. Abbas Fadel for his invaluable guidance, support, and expertise throughout the duration of this project. His insightful feedback and encouragement were instrumental in shaping the direction of this work.
- 2. Funding source:** This research was funded by the authors.
- 3. Competing Interests:** I declare that there are no competing interests related to this research.
- 4. Human and animal -related studies (Ethical Approval):** The approval of the Chairman of the Ethics Committee at Kirkuk University was obtained on the study plan, including conducting experiments on laboratory animals represented by white male rats.

## References

- L. Šturm and N. P. Ulrih, 'Advances in the Propolis Chemical Composition between 2013 and 2018: A Review', *eFood*, vol. 1, no. 1, pp. 24–37, Feb. 2020, doi: 10.2991/efood.k.191029.001.
- E. Ören et al., 'Antioxidant, antidiabetic effects and polyphenolic contents of propolis from Siirt, Turkey', *Food Sci. Nutr.*, vol. 12, no. 4, pp. 2772–2782, Apr. 2024, doi: 10.1002/fsn3.3958.
- S. M. Abdullah, S. J. Abdulrahman, and A. A. Hayder, 'Assessment of the Effect of Propolis Extract on Enzymatic Antioxidants and Lipidperoxidation', *JHTD*, vol. 4, no. 02, pp. 13-25, Mar. 2024.
- H. Silva, R. Francisco, A. Saraiva, S. Francisco, C. Carrascosa, and A. Raposo, 'The Cardiovascular Therapeutic Potential of Propolis—A Comprehensive Review', *Biology*, vol. 10, no. 1, p. 27, Jan. 2021, doi: 10.3390/biology10010027.
- R. Guan et al., 'Ethanol extract of propolis regulates type 2 diabetes in mice via metabolism and gut microbiota', *J. Ethnopharmacol.*, vol. 310, p. 116385, Jun. 2023, doi: 10.1016/j.jep.2023.116385.
- A. Braakhuis, 'Evidence on the Health Benefits of Supplemental Propolis', *Nutrients*, vol. 11, no. 11, p. 2705, Nov. 2019, doi: 10.3390/nu11112705.
- S. P. Grover and N. Mackman, 'Tissue factor in atherosclerosis and atherothrombosis', *Atherosclerosis*, vol. 307, pp. 80–86, Aug. 2020, doi: 10.1016/j.atherosclerosis.2020.06.003.
- E. Bezsonov, I. Sobenin, and A. Orekhov, 'Immunopathology of Atherosclerosis and Related Diseases: Focus on Molecular Biology', *Int. J. Mol. Sci.*, vol. 22, no. 8, p. 4080, Apr. 2021, doi: 10.3390/ijms22084080.
- S. Gencer, B. R. Evans, E. P. C. Van Der Vorst, Y. Döring, and C. Weber, 'Inflammatory Chemokines in Atherosclerosis', *Cells*, vol. 10, no. 2, p. 226, Jan. 2021, doi: 10.3390/cells10020226.
- C. L. Miller and H. Zhang, 'Clarifying the Distinct Roles of Smooth Muscle Cell–Derived Versus Macrophage Foam Cells and the Implications in Atherosclerosis', *Arterioscler. Thromb. Vasc. Biol.*, vol. 41, no. 6, pp. 2035–2037, Jun. 2021, doi: 10.1161/ATVBAHA.121.316287.
- A. V. Poznyak, A. V. Grechko, V. A. Orekhova, Y. S. Chegodaev, W.-K. Wu, and A. N. Orekhov, 'Oxidative Stress and Antioxidants in Atherosclerosis Development and Treatment', *Biology*, vol. 9, no. 3, p. 60, Mar. 2020, doi: 10.3390/biology9030060.
- T. Krupp et al., 'Natural rubber-propolis membrane improves wound healing in second-degree burning model', *Int. J. Biol. Macromol.*, vol. 131, pp. 980–988, 2019.
- M. Zheng-Mu, 'Antimutagenic activity by the medicinal plants in traditional chinese medicines', *Pharmacy Journal, Jpn. J. Pharmacogn.*, vol. 44, no. 3, pp. p225-229, 1990.

- S. Chakrabarti et al., 'Advanced studies on the hypoglycemic effect of *Caesalpinia bonducella* F. in type 1 and 2 diabetes in Long Evans rats', *J. Ethnopharmacol.*, vol. 84, no. 1, pp. 41–46, 2003.
- J. Saheb, 'Effect of Alcoholic Leaf Extract of *Hellotropium Earopiam* on the Levels of Testosterone, Prolactin, TSH, T3 and T4 Hormones in Blood of Male Albino Rats Exposed to Oxidative Stress by H<sub>2</sub>O<sub>2</sub>', 2015, Accessed: Apr. 24, 2024. [Online]. Available: <https://core.ac.uk/download/pdf/234655479.pdf> pp.I-III
- A. F. Khudhur and M. A. Ahmed, 'Effect of water extract of rosemary Plant and olive oil and vitamin E on some physiological and biochemistry changes in male rats with induced hyperlipidemia', M.SC., Tikrit, Tikrit -Iraq, 2018.
- C. C. Allain, L. S. Poon, C. S. G. Chan, W. Richmond, and P. C. Fu, 'Enzymatic Determination of Total Serum Cholesterol', *Clin. Chem.*, vol. 20, no. 4, pp. 470–475, Apr. 1974, doi: 10.1093/clinchem/20.4.470.
- N. J. Jacobs and P. J. Van Denmark, 'Triglycerides *liquicolor mono*', *Arch. Biochem. Biophys.*, vol. 88, no. 1, pp. 250–255, 1960.
- T. Gordon, W. P. Castelli, M. C. Hjortland, W. B. Kannel, and T. R. Dawber, 'High density lipoprotein as a protective factor against coronary heart disease', *Am. J. Med.*, vol. 62, no. 5, pp. 707–714, May 1977, doi: 10.1016/0002-9343(77)90874-9.
- T. E. Anderoli, J. Carpenter, and T. B. Bennett, 'Cecil essentials of medicine : Disorder of lipid metabolism ,5th ed', Herbert P.N. W.B. Standers company, London , Tronto, vol. 16, no. 2001, pp. 526–532, 2001.
- M. H. Dominiczak, 'Tietz Textbook of Clinical Chemistry. By C.A. Burtis and E.R. Ashwood, editors', *Clin. Chem. Lab. Med.*, vol. 37, no. 11–12, pp. 840–843, Jan. 1999, doi: 10.1515/cclm.2000.37.11-12.1136.
- T. Temelkova-Kurktschiev and M. Hanefeld, 'The Lipid Triad in Type 2 Diabetes - Prevalence and Relevance of Hypertriglyceridaemia/Low High-Density Lipoprotein Syndrome in Type 2 Diabetes', *Exp. Clin. Endocrinol. Diabetes*, vol. 112, no. 02, pp. 75–79, Mar. 2004, doi: 10.1055/s-2004-815753.
- J. Duncan, 'Attention, intelligence, and the frontal lobes.', 1995, Accessed: Apr. 24, 2024. [Online]. Available: <https://psycnet.apa.org/record/1994-98810-045>
- J. S. Ali, 'The effect of walnut leaf infusion on blood lipids level was improved in rats treated with hydrogen peroxide and cholesterol', M.SC., Bagdad, Iraq, 2001.

- J. Fu et al., 'Low-Level Arsenic Impairs Glucose-Stimulated Insulin Secretion in Pancreatic Beta Cells: Involvement of Cellular Adaptive Response to Oxidative Stress', *Environ. Health Perspect.*, vol. 118, no. 6, pp. 864–870, Jun. 2010, doi: 10.1289/ehp.0901608.
- X. Xiao, Y. Luo, and D. Peng, 'Updated Understanding of the Crosstalk Between Glucose/Insulin and Cholesterol Metabolism', *Front. Cardiovasc. Med.*, vol. 9, p. 879355, Apr. 2022, doi: 10.3389/fcvm.2022.879355.
- S. Chakraborty, Y. Cai, and M. A. Tarr, 'In vitro oxidative footprinting provides insight into apolipoprotein B-100 structure in low-density lipoprotein', *PROTEOMICS*, vol. 14, no. 21–22, pp. 2614–2622, Nov. 2014, doi: 10.1002/pmic.201300174.
- A. Cisse et al., 'Dynamics of Apolipoprotein B-100 in Interaction with Detergent Probed by Incoherent Neutron Scattering', *J. Phys. Chem. Lett.*, vol. 12, no. 51, pp. 12402–12410, Dec. 2021, doi: 10.1021/acs.jpcclett.1c03141.
- S. A. Wu, S. Kersten, and L. Qi, 'Lipoprotein Lipase and Its Regulators: An Unfolding Story', *Trends Endocrinol. Metab.*, vol. 32, no. 1, pp. 48–61, Jan. 2021, doi: 10.1016/j.tem.2020.11.005.
- A. C. Guyton and J. E. Hall, *Textbook of medical physiology*, 11th ed. Philadelphia: Elsevier Saunders, 2006. pp.140-144
- S. A. Adefegha, O. S. Omojokun, and G. Oboh, 'Modulatory effect of protocatechuic acid on cadmium induced nephrotoxicity and hepatotoxicity in rats in vivo', *SpringerPlus*, vol. 4, no. 1, p. 619, Dec. 2015, doi: 10.1186/s40064-015-1408-6.
- N. Takeuchi, M. Ito, and Y. Yamamura, 'Cholesterol metabolism of rats to high cholesterol diet', *Am. J. Physiol. Cell*, vol. 285, no. 5, pp. 1322–1329, 2004.
- K. Inoue et al., 'Aerobic exercise training-induced irisin secretion is associated with the reduction of arterial stiffness via nitric oxide production in adults with obesity', *Appl. Physiol. Nutr. Metab.*, vol. 45, no. 7, pp. 715–722, Jul. 2020, doi: 10.1139/apnm-2019-0602.
- S. Y. Abd Al-Rahman, 'Effect of hunger and experimental diabetes on glutathione and liposomal levels in rat tissues', .PhD .Thesis in Veterinary Physiology, College of Veterinary Medicine, University of Mosul, Iraq, 1995.
- I. Williams, S. Wheatcroft, A. Shah, and M. Kearney, 'Obesity, atherosclerosis and the vascular endothelium: mechanisms of reduced nitric oxide bioavailability in obese humans', *Int. J. Obes.*, vol. 26, no. 6, pp. 754–764, Jun. 2002, doi: 10.1038/sj.ijo.0801995.

- Khudiar K. K, 'The role of aqueous extracts of olive (*Olea europaca*) leaves and garlic (*Allium sativum*) in ameliovating the effects of experrimentally infused atherosclerosis', PhD. Thesis, College of Veterinary Medicen., Bagdad, 2000.
- A. Hara, H. Matsumura, and Y. Abiko, 'Lidocaine attenuates both mechanical and metabolic changes induced by hydrogen peroxide in the rat heart', *Am. J. Physiol.-Heart Circ. Physiol.*, vol. 265, no. 5, pp. H1478–H1485, Nov. 1993, doi: 10.1152/ajpheart.1993.265.5.H1478.
- J. Zhang et al., 'Contradictory regulation of macrophages on atherosclerosis based on polarization, death and autophagy', *Life Sci.*, vol. 276, p. 118957, Jul. 2021, doi: 10.1016/j.lfs.2020.118957.
- N. M. AL Assaafi, 'Study of the physiological activity in female laboratory rats fed on dandelion, propolis and lemon juice, and induced infection with calcium oxalate deposits', M.SC., Tikrit, Iraq, 2023.
- D. K. Salem, 'Mohammed and H. M. Saleh . Effect of Propolis and Liquorice Extract on Some Biochemical and Tissue Characteristics of Male Rats Exposed to Acrylamide. M.Sc. Thesis.Tikrit University,Iraq.2023.', M.SC.Thesis, Tikrit, Iraq, 2023.
- H. Sameni, A. Bandegi, A. Ramhormozi, M. Taherian, M. Safari, and M. Tabriziamjad, 'Effects of hydroalcoholic extract of Iranian Propolis on blood serum biochemical factors in streptozotocin-induced diabetic rats', *koomesh*, vol. 15, no. 3, pp. 388–395, 2014.
- N. Samadi, H. Mozaffari-Khosravi, M. Rahmanian, and M. Askarishahi, 'Effects of bee propolis supplementation on glycemic control, lipid profile and insulin resistance indices in patients with type 2 diabetes: a randomized, double-blind clinical trial', *J. Integr. Med.*, vol. 15, no. 2, pp. 124–134, Mar. 2017, doi: 10.1016/S2095-4964(17)60315-7.
- A. Iio et al., 'Ethanollic extracts of Brazilian red propolis increase ABCA1 expression and promote cholesterol efflux from THP-1 macrophages', *Phytomedicine*, vol. 19, no. 5, pp. 383–388, Mar. 2012, doi: 10.1016/j.phymed.2011.10.007.
- Y. Li, M. Chen, H. Xuan, and F. Hu, 'Effects of Encapsulated Propolis on Blood Glycemic Control, Lipid Metabolism, and Insulin Resistance in Type 2 Diabetes Mellitus Rats', *Evid. Based Complement. Alternat. Med.*, vol. 2012, pp. 1–8, 2012, doi: 10.1155/2012/981896.
- N. Ecem Bayram, 'A STUDY ON FREE-RADICAL SCAVENGING ACTIVITY, INDIVIDUAL PHENOLIC COMPOUNDS AND ELEMENT CONCENTRATION OF PROPOLIS', *Uludağ Arıcılık Derg.*, vol. 20, no. 2, pp. 145–156, Nov. 2020, doi: 10.31467/uluarıcılık.778751.
- M. S. Mohd Suib, W. A. Wan Omar, E. A. Omar, and R. Mohamed, 'Ethanollic extract of propolis from the Malaysian stingless bee *Geniotrigona thoracica* inhibits formation of THP-1 derived



- macrophage foam cells', *J. Apic. Res.*, vol. 60, no. 3, pp. 478–490, May 2021, doi: 10.1080/00218839.2020.1720125.
- Y. Fang et al., 'Ethanol extract of propolis protects endothelial cells from oxidized low density lipoprotein-induced injury by inhibiting lectin-like oxidized low density lipoprotein receptor-1-mediated oxidative stress', *Exp. Biol. Med.*, vol. 239, no. 12, pp. 1678–1687, Dec. 2014, doi: 10.1177/1535370214541911.
- C. Ji et al., 'Propolis ameliorates restenosis in hypercholesterolemia rabbits with carotid balloon injury by inhibiting lipid accumulation, oxidative stress, and TLR4/NF- $\kappa$ B pathway', *J. Food Biochem.*, vol. 45, no. 4, Apr. 2021, doi: 10.1111/jfbc.13577.
- R. J. Glynn, P. M. Ridker, S. Z. Goldhaber, R. Y. L. Zee, and J. E. Buring, 'Effects of Random Allocation to Vitamin E Supplementation on the Occurrence of Venous Thromboembolism: Report From the Women's Health Study', *Circulation*, vol. 116, no. 13, pp. 1497–1503, Sep. 2007, doi: 10.1161/CIRCULATIONAHA.107.716407.
- S. Santamarina-Fojo, 'LPL and hepatic lipase: new insights into enzyme function', *Atherosclerosis*, vol. 109, no. 1–2, pp. 86–92, 1994.
- S. Chang and J. Borensztajn, 'Hepatic lipase function and the accumulation of  $\beta$ -very-low-density lipoproteins in the plasma of cholesterol-fed rabbits', *Biochem. J.*, vol. 293, no. 3, pp. 745–750, Aug. 1993, doi: 10.1042/bj2930745.
- J. Kobayashi, K. Miyashita, K. Nakajima, and H. Mabuchi, 'Hepatic Lipase: a Comprehensive View of its Role on Plasma Lipid and Lipoprotein Metabolism', *J. Atheroscler. Thromb.*, vol. 22, no. 10, pp. 1001–1011, 2015, doi: 10.5551/jat.31617.
- P. Bozaykut, R. Ekren, O. U. Sezerman, V. N. Gladyshev, and N. K. Ozer, 'High-throughput profiling reveals perturbation of endoplasmic reticulum stress-related genes in atherosclerosis induced by high-cholesterol diet and the protective role of vitamin E', *BioFactors*, vol. 46, no. 4, pp. 653–664, Jul. 2020, doi: 10.1002/biof.1635.

# A Review a Bout Educational of Students' Academic Performance Using Data Mining Algorithms

Douaa Ibrahim Alwan Al Saadi <sup>1</sup>

Hind Abdul Razzaq Mohammed Ali <sup>2</sup>



© 2024 The Author(s). This open access article is distributed under a Creative Commons Attribution (CC-BY) 4.0 license.

## Abstract:

Secondary and academic education is regarded as one of the most significant periods of a student's life, and students must work very hard to succeed and earn good grades. However, there has been a recent rise in the percentage of students failing in many nations, including Portugal, India, and others, achieving long-term economic success requires education. The educational attainment of students has increased during the past few decades. Organizational and company databases have grown exponentially as a result of information technology advancements, sparking interest in business intelligence (BI) and data mining (DM). The wealth of information included in all of this data, including trends and patterns, can be leveraged to enhance decision-making and maximize outcomes. However, human specialists are finite and often miss crucial information. Therefore, an automated tool to evaluate the raw data and extract valuable, high-level information for the decision-maker is the alternative, so I started Higher education institutions use artificial intelligence-based data mining tools and techniques to help students perform better academically. These tools include data mining algorithms like support vector machines, logistic regression, decision trees, neural networks, and others that can be used with data collected through the Weka program, RapidMiner, and other programs.

In this research paper, we will look at previous research on the topic, assessing the advantages and disadvantages of each, and reviewing data collection techniques, methods used for obtaining the best outcomes, and ways to enhance student data.

**Keywords:** Students Performance; Data Mining Algorithms; Educational Data Mining Performance;

 <http://dx.doi.org/10.47832/MinarCongress12-20>

<sup>1</sup>  Software Computer Engineering Department, Higher Health institute, Najaf, Iraq  
[inas.a.abood@nahrainuniv.edu.iq](mailto:inas.a.abood@nahrainuniv.edu.iq)

<sup>2</sup>  Civil Engineering Department, University of technology, Baghdad, Iraq [40125@uotechnology.edu.iq](mailto:40125@uotechnology.edu.iq)

## Introduction

To support institutional goals of providing high-quality educational environmental systems, there has been a recent surge in interest in determining the key elements that influence university students' academic performance as well as the cause of the decline in the number of students experiencing early learning difficulties and improving their educational outcomes (Abu Saa et al., 2019). Since student performance is one of the most crucial indicators of a university's quality, evaluation is essential to preserving both student performance and the efficiency of the educational process. A strategic program can be well-planned for students during their time at the institution by analyzing their performance. (Shahiri & Husain, 2015).

The literature offers various definitions for forecasting students' academic performance. Various scholars analyze students' performance using different student aspects or attributes. The majority of writers employed students' extracurricular activities, GPA, final test results, internal and external assessments, and final exam scores as prediction factors (Kumar et al., 2017).

There are no fixed standards for evaluating students' academic performance. Some universities use curricula and internal assessment; some use academic records as a criterion for evaluation; and other universities use students' previous grades, classroom performance, student demographics, and social status (Abu Saa et al., 2019).

According to (Francis & Babu, 2019), they used features from common fundamental machine learning algorithms, such as SVM, KNN, DT, etc., to choose features for each student through the initial test to improve accuracy.

These characteristics are used to divide the students into three categories. After obtaining the characteristics, the K-Means clustering algorithm produces clusters representing high, average, and low-performing students. A majority of the students in these groupings vote to assign designations to the freshmen who are represented in them. On this test set, the accuracy is then computed, and the suggested hybrid algorithm's application to the student data set revealed a substantial correlation between the academic success of the students and their conduct. When applied to academic, behavioral, and other variables of the student dataset, the suggested hybrid model combining clustering and classification has an accuracy of 0.7547 and was shown to be better than other existing techniques.

As such, to fully comprehend the meaning of data extraction, visualization, and analysis, we need to go over earlier literary works that discuss the numerous projects that the authors worked on.

In this study, our primary objective is:

1. Diagnosing methods used in data mining prediction of academic performance.
2. recognize and comprehend the various characteristics of students that are mostly utilized to forecast their performance.
3. Predicting the best data mining techniques for academic performance.
4. Proposing a new methodology for predicting students' academic performance.

The main objective of the literature search is to find the methods and utilize historical facts to generate new insights and diagnose the methods used in prediction as well as to find some suggestions and gaps in the research conducted by researchers to help us identify the different characteristics of students which are mostly used to predict their performance and predict the techniques used in data mining, we have to read the literature for more than five years so that our study can be considered relevant and we can suggest a new methodology to predict the academic performance of students.

#### **Methodology for doing a literature review search:**

We conducted searches across multiple databases, including Science Direct, Elsevier, AE CS Library, ICEEE, and specialized computer-related journals. We conducted a search using the following keywords: academic performance prediction, data mining techniques, educational data mining performance, students' performance, and data mining algorithms.

The literature from 2015 to 2023 was the period that was examined. The downloads included complete research papers in PDF format.

#### **The key variables that were utilized to forecast students' performance:**

Researchers in 2018. used the WEKA program to compare classification strategies between decision tree and random forest To create a model for academic prediction for incoming students they distributed questionnaires to Kalabat University's computer science department students to gather data, In this research, they selected demographic information (gender, family relationship, father's and mother's educational position) Because male and female students have distinct learning styles, the personal data for this study consists of the time

they spend with their friends, their weekly study time, and their free time after school (Kaunang & Rotikan, 2018). machine learning algorithms. When tested using different features related to online learning platforms, each model displayed a different accuracy.

To assess student performance, they employed five machine learning techniques: random forest, logistic regression, decision trees, support vector machines, and Perceptron classifiers. Student demographic, academic, and behavioral data are some of the features that have been observed to have the most impact on the data.

With an accuracy of 70.8%, the support vector machine is the best algorithm. The results obtained indicate that while student absence days have an impact on academic achievement, student class grades have no bearing on academic performance. Further features, like the motivating and encouraging tactics employed by teachers and facilitators, as well as psychological aspects that influence student performance, should be gathered for the study. (Masangu et al., 2021).

Researchers used the Weka program to collect data from various colleges in the Indian state of Assam. They collected about 300 data records with 24 attributes. The data consisted of socio-economic, demographic, and academic information., deleting some attributes for which there was insufficient information. To forecast the student's success, the data that comprised their technical and extracurricular skills was retrieved using a variety of classification methods.

There were four classification techniques used: Random Forest, J48, PART, and Bayes Network Classifiers. WEKA was the data mining tool utilized. To forecast students' performance, the data can be augmented to include some extracurricular activities and technical skills of the students. These can then be retrieved using various classification methods. Based on accuracy and classification mistakes, Random Forest fared better than other classifiers, according to the data.

The optimal rules were also displayed, and the Apriori method was utilized to find association rule mining between all characteristics. (Hussain et al., 2018). To determine whether academic performance could be impacted, the authors in 2020, tracked how staff members and students used the university's learning management system. To ascertain whether the quantity of participation was gauged by the amount, they employed 712 records of data on university students in an African nation to measure the patterns of students and staff in using the LMS's services. For gathering, categorizing, and visualizing the data for the WEKA system tools, machine learning techniques were employed. Tools used by the professor and students,



such as the test, assignment, chat, forum, URL, folder, and files, are included in the data. (Okike & Mogorosi, 2020). Research in the subject of education is growing because there is a vast amount of data that can be used to identify patterns connected to students' learning behavior. To ascertain the degree of students' achievement in the first semester, the authors of this study put up a framework for forecasting the academic performance of first-year students in the Department of Computer Science. The data they gathered covered the student demographics prior academic records and details on the family history and was gathered during the years 2006/2007 and 2013/2014, Classification approaches based on decision tree, Naïve Bayes, and rule were applied to the student data to generate the best model to predict the academic achievement of the students.

Subsequently, the data was cleaned and split into two sets using the open-source WEKA software: a training set for model construction and a test set for model validation. The model prediction that Rule Based (RB) extracted for the experiment has the greatest accuracy value among the algorithms that were chosen. The tiny amount of data resulting from incomplete and missing values in the obtained data is one of the study's weaknesses. (Ahmad et al., 2015).

It is now feasible to extract educational data to raise the caliber of educational processes, thanks to developments in the data mining sector. Data was taken out of this study to examine undergraduate students' performance. Predicting students' academic achievement after a four-year study program and examining usual progress and combining it with prediction results for low- and high-achieving students were the two main areas of attention for the data during the project, to enhance the data and forecast pupils' academic success, six algorithms were applied.

Every year, students often receive the same kind of grades—low, average, or high—for every course. So, they are separated into high-performing and low-performing students since this trend keeps happening over time. The study's researchers might broaden the study's focus beyond student grades and improve the findings by using different kinds of data. (Asif et al., 2017).

Institutions of higher learning prioritize giving pupils a top-notch education to improve their academic performance. In this study, student academic data was gathered through the use of questionnaires. To eliminate anomalies, decrease the complexity of the data, and gain an advantage, factor analysis, and data pre-processing were applied to the acquired data set. Most pertinent. The machine learning methods are compared using the Python 3 tool, following pre-processing, 80% of the 85 students who were collected were used as training data, and 20%

were kept as testing data, which was used to train and test the model. All of the selected attributes were considered input variables, along with the cumulative GPA up to the fifth semester. The output variable was the cumulative GPA of the sixth semester of final-year students at the chosen institution. Multiple linear regression, support vector regression\_rbf, support vector regression\_poly, and support vector regression linear were used to model the data for the training data set. Predictions were then produced for the test data, and the outcomes were examined and contrasted. With an accuracy of 83.44%, the linear model is shown to be the greatest fit, to improve accuracy, a bigger dataset can be employed, together with additional machine learning methods and algorithms. (Dabhade et al., 2021).

The majority of the studies focused on how well university and institute students performed academically. The performance of public-school pupils and lowering the secondary school failure rate will be the focus of this study. There were two sets of data gathered. Variables from the first set of data were acquired before the start of the academic year, whereas the second set was obtained two months after the semester began. For each dataset, classification models based on a gradient boosting machine (GBM) were developed to forecast academic outcomes of student performance at the end of the school year.

The neighborhood, the student's place of residence, and school statistics were the most significant factors in student failure; on the other hand, the student's grade and attendance records were the most significant variables in predicting his performance. The study's objective is to boost the effectiveness of educational support provided to students, which will raise their chances of success after the academic year and lower their overall failure rate. It is feasible to investigate additional factors influencing high school pupils and enhance their academic achievement. (Fernandes et al., 2019).

Also, the Portuguese school gathered actual data utilizing the questionnaire approach and school reports to forecast kids' behavior and academic success. A study was carried out to compare the efficacy of four EDM techniques for early identification of students who are likely to fail in beginning programming courses: decision tree, support vector machines, neural network, and naive Bayes theory.

The information was sufficiently evaluated to identify students' academic failure early on and then give teachers or educators pertinent information to assist them in making judgments. The data came from two distinct and independent sources, one from campus and the other from distance education. (Athani et al., 2017). A variety of factors, including the student's factor, the

family factor, or the teacher's factor, have been used by some studies to help teachers identify students who are likely to fail the course early on and help them improve their academic performance. Numerous elements or a collective impact There exist multiple elements that impact student performance, and these vary across nations, institutions, cultures, and student groups. Because of his crucial function in this area, the instructor needs to engage with the students more, offer helpful advice, and inspire them, three decision tree approaches (C4.5), a multi-layer perceptron, and a naïve Bayes model were employed in this investigation. These methods were all used using student data that was gathered from two semesters' worth of university courses. With an overall prediction accuracy of 86%, the naive Bayes classifier outperformed the other two classifiers, according to the data. (Mueen et al., 2016).

Some educational data mining: To raise the standard of instruction in educational institutions, unique mining approaches are employed to uncover hidden information from student data. In this study, data mining techniques were used to measure the impact of two feature categories, such as behavioral behavior and student absenteeism from class. For a more precise forecast, group filtering technology was also used (Rahman & Islam, 2017).

To identify students who are likely to fail academically at a time when action can be taken to lower the failure rate, this study examines the efficacy of techniques used to predict students' academic failure. It also examines the effects of data pre-processing and algorithmic fine-tuning tasks on the effectiveness of the techniques. Early failure detection of pupils and the efficacy of some of these methods have been enhanced through the use of data pre-processing and algorithmic optimization(Costa et al., 2017).

In these research projects, many WEKA classifiers were used, their accuracy was compared, various error metrics were employed to identify the best classifier, and data mining approaches were examined to forecast the degree of student achievement (Jalota & Agrawal, 2019), there aren't any universal tools that can be applied in all kinds of learning environments. Standardization, more efficient mining tools, the creation of a broad framework, and research into the variables influencing the process of teaching and learning are all necessary to raise the standard of education (Khanna et al., 2016).

Educational data mining has emerged as a powerful method for identifying hidden patterns in educational data and forecasting students' academic performance on final exams. The most efficient machine learning techniques have been found, and early identification of students at high risk of failing has been made possible by relying on midterm exam results as a

data source. They have computed and compared the learning algorithms' performances. Automatic and early detection of students who are more or less motivated to study is important, as this study aids in the development of a framework for learning analysis and decision-making in higher education. (Yağcı, 2022).

Since this will be the start of the development of intelligent learning methods, the study focuses on making the best selections regarding the most appropriate academic supervision for the seamless learning process and academic success of students. In a setting of education, like a university, where ineffective teaching is said to make it harder for students to complete their coursework or, worse, increase their risk of quitting altogether. In this study (Triayudi et al., 2024), student data from an information technology class at a private institution in Jakarta was examined and tested.

This study employs decision trees, neural networks, and naive Bayes modeling techniques, utilizing academic data from 300 students enrolled in the Information Systems and Information Science study program for the 2017–2019 and 2018–2020 academic years. Moreover, the cumulative hierarchical clustering algorithm is used to discuss the psychological traits of students. Psychometric analysis and segmentation should be used by stakeholders to develop students with the best personalities and performance.

### **Techniques that have been applied to forecast academic achievement:**

The academic achievement of students can be predicted using a variety of methods. These methods are intended to be used for data extraction, analysis, visualization, and regression analysis. The research papers listed all employ different methods, but we will concentrate on a few of them. For example (Decision Tree (DT), Naive Bayes (NB), K- Nearest Neighbor (KNN), Support Vector Machine (SVM), Neural Network (NN), and Random Forest Trees (RF)), Table 1 lists several research papers along with the names of the authors and the key characteristics that are useful for prediction accuracy when using various data mining algorithms.

**Table 1-** The distinction between earlier works in terms of the features and algorithms employed

Authors	Features that impact the accuracy of student's predictions	DT	NB	KNN	SVM	NN	RF
(Mueen et al., 2016)	the student's personal factor, the family factor	---	86.0%	---	---	---	---
(Rahman & Islam, 2017)	behavioral behavior and student absenteeism from class	76.2 %	73.8 %	75.3 %	---	78.6%	77.3 %
(Yağcı, 2022)	midterm exam results as a data source	---	77.5 %	77.5 %	77.5 %	77.5 %	77.5 %
(Francis & Babu, 2019)	substantial correlation between the academic success of the students and their conduct	0.660377	0.528302	---	0.641509	0.641509	---
(Kaunang & Rotikan, 2018)	select demographic information (gender, family relationship, father's and mother's educational position)	66.85%	---	---	---	---	61.14%
(Masangu et al., 2021)	They used academic, and behavioral data	46.8 %	---	---	70.8%	---	69.7%
(Hussain et al., 2018)	the data which comprised their technical and extracurricular skills was retrieved using a variety of classification methods	---	65.33%	---	---	---	99%
(Asif et al., 2017)	First, grades alone were used to forecast the pupils' performance. Second, by identifying the courses Third, Students were classified as high-performing or low-performing	60.58%	83.65%	74.04%	62.50%	62.50%	---
(Jalota & Agrawal, 2019)	Five classifiers are used under weka and the comparisons are made based on the accuracy among these classifiers and different error measures are used to determine the best classifier.	73.6 0%	64.40%	---	75.40%	---	67.40%

Table (1) shows the distinction between earlier works in terms of the features and algorithms employed, and we noticed that due to the use of novel mining techniques to extract hidden information from student data, Hasibur Rahman and Rabiul Islam's research yielded accuracy rates of 78.6% for the Neural Network (NN) algorithm and 77.3% for the Random Forest Trees (RF) algorithm, which is thought to be the highest accuracy among prior works. Data mining techniques have also been used to measure the influence of two types of variables, such as behavioral behavior and student absenteeism from class, to improve instruction in



educational institutions. Additionally, a crowd-filtering technique was applied to produce more accurate projections.

## **Discussion**

Decision Tree (DT), Naive Bayes (NB), K-Nearest Neighbor (KNN), Support Vector Machine (SVM), Neural Network (NN), and Random Forest Trees (RF) are a few of the techniques that were employed. The decision tree algorithm yields an accuracy of 76.2%, with 46.8% being the lowest.

To enhance instruction in educational institutions, Haseeb Rahman and Rabiul Islam's (Rahman & Islam, 2017) research employed data mining techniques to quantify the impact of two types of variables, such as behavioral behavior and student absenteeism from class, to achieve the best accuracy. Furthermore, crowd-filtering technology has been used to provide more accurate projections.

The Random Forest Trees algorithm had 99% accuracy at its greatest and 61.14% accuracy at its lowest points. Sadiq Hussain (Hussain et al., 2018) and his colleagues achieved the highest accuracy in predicting student achievement by retrieving data on their technical and extracurricular talents using a range of classification techniques.

The greatest accuracy in the Naive Bayes (NB) method is 86.0%, while the lowest accuracy is 64.40%. Mueen A, Zafar B (Mueen et al., 2016), and Manzoor U achieved the highest accuracy in this algorithm. Numerous aspects were taken into consideration, such as the student's personal factor, family factor, or teacher factor. In certain studies, these characteristics have been utilized to assist teachers in identifying students who are at risk of failing a course early on and in assisting them in improving their academic performance.

The K-Nearest Neighbor (KNN) algorithm yielded an accuracy of 74.04% at its lowest and 77.5% at its greatest. The researchers Yağcı M (Yağcı, 2022). Were able to attain great accuracy. They used the midterm exam results as their primary source of information. They computed and contrasted the learning algorithms' performances. Automatic and early identification of students who are somewhat motivated to learn, since this research contributes to the creation of a framework for decision-making and learning analysis in higher education.

The maximum accuracy achieved with the Support Vector Machine (SVM) method was 77.5%, while the lowest accuracy recorded was 62.50%. The person with the highest accuracy was Yağcı M (Yağcı, 2022).

Finally, there was the Neural Network (NN) algorithm, which had a 78.6% accuracy as well as a 62.50% accuracy. Rahman M. and Islam M. researchers, obtained high accuracy. (Rahman & Islam, 2017).

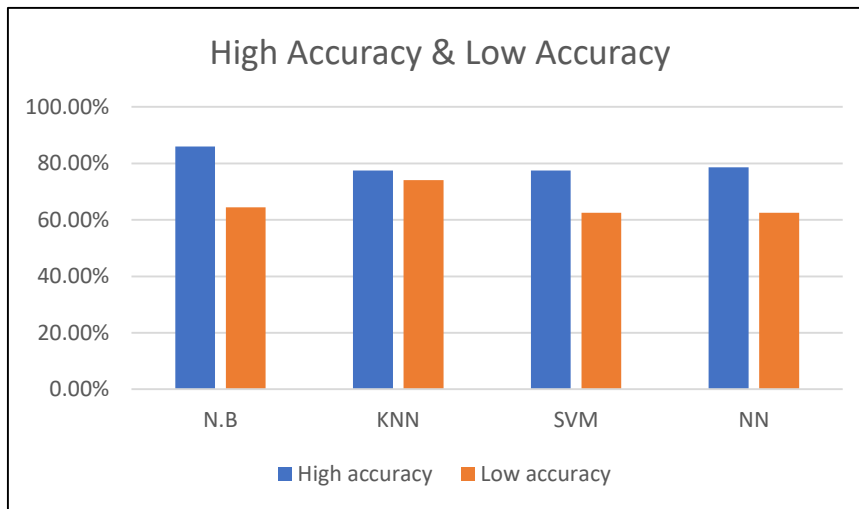


**Figure 1-** High & Low accuracy of algorithms

In the chart above we explain the high accuracy and the low accuracy of the algorithms used in the previous works according to their result, as we show that (N.B) algorithms have the highest accuracy than others (86.0%) after that (NN) (78.6%), (SVM) and (KNN) have the same accuracy (77.5%).

### Conclusion and Future Work

To succeed academically and get good grades, students must work hard. Given the recent decline in student performance, student data is currently being collected. Specialized data mining and analysis techniques are being applied to produce highly accurate results that improve the data while also predicting what methods should be used to improve student performance in universities and schools.

Research studies have utilized a variety of data, such as student demographics, previous academic records, family history information, grades, and course information that can be useful in predicting whether a course will be completed or not, such as test and assignment data, chat and forum data, URLs, folders and files, where a variety of algorithms have been applied, including Naive Bayes Decision Tree, K-Nearest Neighbor, Support Vector Machine, Neural Network, and Random Forest Trees, to achieve high prediction accuracy.

Finally, through our research study, we find that the best techniques used in terms of high performance are SVM and KNN, followed by NB, DT, and NN.

For future work, we will propose a method to predict the academic performance of students in one of the universities of Arab countries, especially in Iraq, to know the obstacles that enable us to improve academic performance in universities and institutes, as well as collect more new features that have not been addressed in studies such as the encouraging and motivational strategies adopted by facilitators and teachers and consider more materials available to students in e-learning platforms, and focus more on the psychological aspects of students and social and environmental factors because they are among the factors that most negatively affect student performance.

**Acknowledgements:** I would like to express my deep gratitude and appreciation to my research colleagues who contributed a lot to completing this research in the best possible way.

## References

Abu Saa, A., Al-Emran, M., & Shaalan, K. (2019). Factors affecting students' performance in higher education: a systematic review of predictive data mining techniques. *Technology, Knowledge and Learning*, 24(4), 567–598.

- Ahmad, F., Ismail, N. H., & Aziz, A. A. (2015). The prediction of students' academic performance using classification data mining techniques. *Applied Mathematical Sciences*, 9(129), 6415–6426.
- Asif, R., Merceron, A., Ali, S. A., & Haider, N. G. (2017). Analyzing undergraduate students' performance using educational data mining. *Computers & Education*, 113, 177–194.
- Athani, S. S., Kodli, S. A., Banavasi, M. N., & Hiremath, P. G. S. (2017). Student academic performance and social behavior predictor using data mining techniques. 2017 International Conference on Computing, Communication and Automation (ICCCA), 170–174.
- Costa, E. B., Fonseca, B., Santana, M. A., de Araújo, F. F., & Rego, J. (2017). Evaluating the effectiveness of educational data mining techniques for early prediction of students' academic failure in introductory programming courses. *Computers in Human Behavior*, 73, 247–256.
- Dabhade, P., Agarwal, R., Alameen, K. P., Fathima, A. T., Sridharan, R., & Gopakumar, G. (2021). Educational data mining for predicting students' academic performance using machine learning algorithms. *Materials Today: Proceedings*, 47, 5260–5267.
- Fernandes, E., Holanda, M., Victorino, M., Borges, V., Carvalho, R., & Van Erven, G. (2019). Educational data mining: Predictive analysis of academic performance of public school students in the capital of Brazil. *Journal of Business Research*, 94, 335–343.
- Francis, B. K., & Babu, S. S. (2019). Predicting academic performance of students using a hybrid data mining approach. *Journal of Medical Systems*, 43(6), 162.
- Hussain, S., Dahan, N. A., Ba-Alwib, F. M., & Ribata, N. (2018). Educational data mining and analysis of students' academic performance using WEKA. *Indonesian Journal of Electrical Engineering and Computer Science*, 9(2), 447–459.
- Jalota, C., & Agrawal, R. (2019). Analysis of educational data mining using classification. 2019 International Conference on Machine Learning, Big Data, Cloud and Parallel Computing (COMITCon), 243–247.
- Kaunang, F. J., & Rotikan, R. (2018). Students' academic performance prediction using data mining. 2018 Third International Conference on Informatics and Computing (ICIC), 1–5.
- Khanna, L., Singh, S. N., & Alam, M. (2016). Educational data mining and its role in determining factors affecting students academic performance: A systematic review. 2016 1st India International Conference on Information Processing (IICIP), 1–7.
- Kumar, M., Singh, A. J., & Handa, D. (2017). Literature survey on student's performance prediction in education using data mining techniques. *International Journal of Education and Management Engineering*, 7(6), 40–49.

- Masangu, L., Jadhav, A., & Ajoodha, R. (2021). Predicting student academic performance using data mining techniques. *Advances in Science, Technology and Engineering Systems Journal*, 6(1), 153–163.
- Mueen, A., Zafar, B., & Manzoor, U. (2016). Modeling and predicting students' academic performance using data mining techniques. *International Journal of Modern Education and Computer Science*, 8(11), 36–42.
- Okike, E. U., & Mogorosi, M. (2020). Educational data mining for monitoring and improving academic performance at university levels. *International Journal of Advanced Computer Science and Applications*, 11(11).
- Rahman, M. H., & Islam, M. R. (2017). Predict student's academic performance and evaluate the impact of different attributes on the performance using data mining techniques. *2017 2nd International Conference on Electrical & Electronic Engineering (Iceee)*, 1–4.
- Shahiri, A. M., & Husain, W. (2015). A review on predicting student's performance using data mining techniques. *Procedia Computer Science*, 72, 414–422.
- Triayudi, A., Aldisa, R. T., & Sumiati, S. (2024). New Framework of Educational Data Mining to Predict Student Learning Performance.
- Yağcı, M. (2022). Educational data mining: prediction of students' academic performance using machine learning algorithms. *Smart Learning Environments*, 9(1), 11.

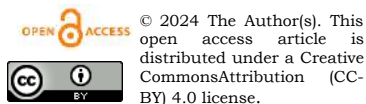


## In Vitro Activity of Spirulina Against Some Pathogenic Bacteria

Zahraa khalid Al- kheroo <sup>1</sup>

Sura M.Y. Al-Tae <sup>2</sup>

Mahmood Abd Aljabbar Al Tobje <sup>3</sup>



### Abstract:


*Increasing resistance to antibiotics is one of the most important global problems threatening public health. Therefore, alternative methods to reduce pathogens are being sought. The current study aims to study the effect of spirulina on some pathogenic species. Two concentrations of spirulina (250 and 500 mg/mL) were used and tested for their effects on Gram-positive bacteria (Staphylococcus aureus and Bacilli), Gram-negative bacteria (Escherichia coli, Klebsiella, and Pseudomonas aeruginosa) and fungi (Candida albicans and Candida tropicalis). The antibiotic susceptibility of the same species used in the study was also compared. The study showed the sensitivity of P. aeruginosa, Bacillus, and E. coli and S. aureus to the spirulina extract, while Klebsiella and the fungal species used in this study did not show clear sensitivity to this extract.*

*S. aureus was sensitive to all types of antibiotics used, while E. coli was resistant to most of them. The remaining*


**Keywords :** *Spirulina Platensis; Staphylococcus Aureus; Antifungal Activity; Sensitivity Test.*

---

 <http://dx.doi.org/10.47832/MinarCongress12-21>

<sup>1</sup>  Department of Biology, College of Sciences, University of Mosul, Mosul, Iraq  
[zahraa.alkhero@uomosul.edu.iq](mailto:zahraa.alkhero@uomosul.edu.iq)

<sup>2</sup>  Department of Biology, College of Sciences, University of Mosul, Mosul, Iraq  
[suramahmoud@uomosul.edu.iq](mailto:suramahmoud@uomosul.edu.iq)

<sup>3</sup>  Department of Biology, College of Sciences, University of Mosul, Mosul, Iraq  
[mahtsbio30@uomosul.edu.iq](mailto:mahtsbio30@uomosul.edu.iq)

## Introduction

Spirulina, a cyanobacterium of the class cyanophyte microalgae, is edible, multicellular, microscopic, photoautotrophic, filamentous, and alkalophilic (1). Its extract contains essential compounds that measured antioxidant properties (2-4), such as phycocyanin, phenolics, and polyunsaturated fatty acids. It has been used for many years as a human food because it contains high range of protein 50% to 70% of its dry weight(5), Carbohydrate of ample value is myoinositol phosphate, it is source of organic phosphorus and inositol, essential fatty acids such as copper, manganese, magnesium, iron, zinc, selenium, B-complex vitamin, vitamin E, vitamin B12 and provitamin A( $\beta$ -carotene)(6-9). The microalgae can be used as a portion of potential food, fuel, and feed source (10).

Clinical trials have demonstrated excellent human use of spirulina carotenoids (11). Furthermore, one gram of spirulina taken once a day proved to be remarkably helpful in treating chronic vitamin A deficiency in a research involving five thousand preschool-aged Indian children. Children with severe vitamin A insufficiency, or those with conjunctival Bitot's spots, experienced a decline from 80% to 10% after five months (12). Spirulina pays more attention not only to the aspects of food but also to the production of potentially harmful pharmaceutical products with corrective properties anti-anemia, anti-tumor, and anti-malnutrition capabilities (13).

Spirulina and its extracts are shown to have biological activities such as cancer prevention, decreased levels of blood cholesterol, increased immune system protection, reduced nephrotoxicity of pharmaceuticals, toxic metals, antibacterial, antiviral, antifungal, and anti-parasite activity (14,15).

Antibiotic resistance is a common result of indiscriminate use of antibiotics, which has led to a considerable increase in antibiotic use in recent years due to heavy infections. A wealth of structurally unique and physiologically active metabolites can be found in spirulina.

A potential bioactive compound of the pharmaceutical industry may be primary or secondary metabolites formed by these species. Toxic, inflammatory, antineoplastic, and antimicrobial effects are correlated with secondary metabolites from cyanobacteria. Polyphenols, terpenoids, alkaloids, glycolipids, fatty acids, and an unidentified group of bacteriocins are among the antimicrobial substances found in cyanobacterial exudates. (16). The current study aims to study the effect of spirulina on some pathogenic species

## Materials and method

Spirulina obtained from Dynamic excellent Network DXN Company which manufactures food supplements (health care). Prepared by dissolve 250mg of spirulina in 1ml of distilled water, and 500mg of spirulina in 1ml of distilled water. This study uses two fungus (*Candida albicans* and *Candida tropicalis*), two different Gram positive bacteria (*Staphylococcus aureus* and *Bacillus*) and three Gram negative bacteria (*Escherichia coli*, *Klebsiella*, and *Pseudomonas aeruginosa*) cultures

The microorganisms were sub cultured into petri dishes(nutrient agar) and incubated for 24 hours at 37c° for bacteria and 24 hours for 28c° for fungal(sabouraud dextrose agar ). Five milliliters of sterile saline were used to inoculate three to five bacterial colonies obtained from agar plates. The bacterial cultures in the saline test tubes were then compared to 0.5 MacFarland's standard. Each bacteria was cultured in Petri dishes containing Muller Hinton agar, and discs of filter paper impregnated with spirulina and sterilized for 15 minutes at 63°C in a water bath were placed then the dishes were incubated at 37°C for a full day.

Preparation of spirulina disc for antibacterial activity by using sterile Whitman filter paper. The discs were prepared by impregnating them with sterile spirulina for 15 minutes at 63°C in a water bath. After that, they were placed on the plate surface using sterile forceps and gently pressed to make sure the disc made contact with the agar surface. Observing and measuring the millimeter-scale zone of inhibition, the plates were incubated at 37°C for a whole day.

The same method are applied for cultivating the fungus except that the incubation done at 28°C for 24 hours instead of 37°C (17).

## Sensitivity test for antibiotics

Using the Kirby Bauer method, test tubes containing 5 milliliters of sterile saline were inoculated with three to five bacterial colonies obtained from agar plates. The bacterial cultures in the saline test tubes were then compared to 0.5 MacFarland's standard to standardize the bacteria. To create 100 milliliters of Muller Hinton agar, 3.8 grams of the agar were dissolved in 100 milliliters of distilled water. Autoclaving the agar at 121°C for 15 minutes sterilized it. Following sterilization, the aseptic pouring of Muller Hinton agar onto sterile petri dishes was performed. After giving the agar a few minutes to firm, each bacterial culture was aseptically swabbed onto the surface of the Muller-Hinton agar and allowed to dry with the aid of sterile swabs.

With the use of sterile forceps, the antibiotic disc (Bacitracin , Azithromycin ,Trimethoprim, Vancomycin, Gentamicin and Ciprofloxacin) was carefully placed on the plate's surface and pressed to ensure aseptic contact with the agar surface. The plates were incubated for twenty-four hours at 37°C. Millimeters were used to measure and observe the zone of inhibition (18)

## Results and Discussion

Table (1) shows that *S. aureus* bacteria were sensitive to all antibiotics used in this research with different degrees ranging between (16mm) for Bacitracin to (31 mm) for Gentamicin, whereas *Klebsiella* showed resistance to Vancomycin and Bacitracin but was high sensitivity to Ciprofloxacin and of variant sensitivity to the rest of the antibiotics used. *E. coli* bacteria showed high resistance to most of the antibiotics used except Gentamicin which showed efficiency against *E. coli*. *Bacillus* bacteria were resistant only to Trimethoprim and sensitive to other antibiotics in a range of (9mm) for Bacitracin and (31 mm) for Azithromycin. *P. aeruginosa* was resistant to Vancomycin and Trimethoprim but highly sensitive to Ciprofloxacin and Azithromycin and of medium sensitivity to Bacitracin and Gentamycin. Sensitivity test was performed for these antibiotics to check their effect compared to Spirulina extract in this research.

**Table 1-** Sensitivity of bacteria species used in the research towards different types of antibiotics.

Antibiotic	<i>S. aureus</i>	<i>Klebsiella</i>	<i>E. coli</i>	<i>Bacillus</i>	<i>P.aeruginosa</i>
<b>Trimethoprim</b>	27	15	R	R	R
<b>Azithromycin</b>	30	21	R	31	30
<b>Bacitracin</b>	16	R	R	9	10
<b>Vancomycin</b>	23	R	R	16	R
<b>Ciprofloxacin</b>	29	35	5	29	30
<b>Gentamicin</b>	31	21	23	26	13

Table (2) shows the effect of Spirulina extract with different concentrations for the same microbes used in table (1). *E. coli* bacteria showed medium sensitivity (11mm, 16mm) to the concentrations of (500 mg/ml, 250 mg/ml) compared to Trimethoprim, Azithromycin, Bacitracin, Vancomycin and Ciprofloxacin to which it showed evident resistance and with less effect to Gentamicin, and this makes clear the efficacy of the extract against *E. coli* compared to some types of antibiotics; Spirulina extract is used as antibiotic against infections caused by *E. coli* and it gives a safe and effective treatment in case the body responds to it. The bacteriological study which synthetically generating Spirulina in Mexico (19) and in USA (20) assures the complete absence of diseases' causes like Salmonella, Shigella and *S. aureus* and

nonexistence of any contamination with dysenteric amoeba whither in natural resources (Lake Chad) or in the experimental reservoirs which contain Spirulina (21) in addition to its use as nutrient agent; a research was conducted in Zaire between January and November in 1989 on 28 child suffering obvious (protein- energy disease) (22) and this analysis's evaluation of the data showed that spirulina generally has a good impact on patients' nutritional state. Bacillus bacteria showed resistance to Spirulina extract of (500 mg/ml) ; its sensitivity was the same to (250 mg/ml) Vancomycin and to (500mg/ml) of Bacitracin, and with higher effect than Trimethoprim (23).

The study (24) indicated the presence of toxic effects and side effects of antibiotics, therefore, the use of the safe and nontoxic Spirulina is preferred, taking into consideration it is a rich source of proteins; tests were conducted on children and adults who suffer from malnutrition in Hospital Bichat- France where they were given high doses of Spirulina (80-90 gram/ day), and despite the very large doses, no significant increase in uric acid in blood was noticed (25) and this indicates the absence of side effects of Spirulina extract even when high doses are given, compared to antibiotics. *S. aureus* bacteria showed sensitivity (16 mm) towards Spirulina similar to that of Bacitracin for the concentration of (250mg/ml), and a less effective than that of Trimethoprim, Azithromycin, Vancomycin, Ciprofloxacin and Gentamicin for the concentration of (500mg/ml) concentrations; it is preferred to use the extract of Spirulina instead of the non- regular uses of antibiotics against microbes of multiple resistance like Methicillin-resistant *Staphylococcus aureus* (MRSA) which causes food poisoning and blood infection (26, 27). According to a 2009 study by Parisi et al., phenolic compounds isolated from *Spirulina platensis* using methanol have strong antibiotic action against Gram-positive *S. aureus* (28).

*Klebsiella* bacteria showed medium sensitivity towards (500mg/ml) of Spirulina extract compared to the apparent resistance against types of antibiotics used in the research (Vancomycin and Bacitracin), and of equal effect (15 mm) to that of Trimethoprim for the concentration of (250mg/ml) and less effect than Gentamicin, Ciprofloxacin and Azithromycin. Spirulina is distinguished from other antibiotics by its high content of phenolic compounds which makes it an active extract with antioxidants even more than commercial algae (*Chlorella*) (29).

*P. aeruginosa* bacteria showed high effect sensitivity (17mm) to (250mg/ml) Spirulina extract compared to antibiotics against which it showed resistance; Trimethoprim and Vancomycin, medium effect by Bacitracin and Gentamicin, and of less effect towards Spirulina



than Ciprofloxacin and Azithromycin for the concentration of (500mg/ml), the thing that demonstrates the efficacy of Spirulina extract against bacteria *P. aeruginosa* compared to some types of antibiotics. Anvar and Nowruzi, conducted a study on Spirulina for its treating characteristic and its inclusion of biologic active compounds (30). Useful medical applications of Spirulina also contributed to the attraction of many scientists' attention as it was being used to treat many diseases like diabetes, excessive blood cholesterol, and arteriosclerosis (31-33). *Candida.sp* showed resistance to the extract of Spirulina of (500mg/ml) concentration, and medium sensitivity to concentration of (250 mg/ml) compared to the antifungal fluconazole used in the research of (Berkow and Lockhart, 2017)(34). Denfert and Hube (2007) conducted a study on *Candida albicans* demonstrating its effect by the ethanol extract of *Spirulina platensis* as these diploid fungi grow as yeast or thread cells, and that it is the factor causing opportunistic infection in the mouth and sex organs in humans and this confirms the biological activity of the ethanol extract of *Spirulina platensis* (35).

**Table 2-** The sensitivity of microbes used in the research against different concentrations of Spirulina extract

Spirulina	<i>S. aureus</i>	<i>Klebsiella</i>	<i>E. coli</i>	<i>Bacillus</i>	<i>P. aeruginosa</i>	<i>Candida albicans</i>	<i>Candida tropicalis</i>
250 mg/ml	16	15	16	16	17	12	15
500mg/ml	10	10	11	9	15	11	10

## Conclusion

The study proved that the concentration of (250) mg/ml of Spirulina had higher effect on *P. aeruginosa* than the other concentration, whereas *Bacillus*, *S. aureus*, *Klebsiella* and *E. coli* as well as the used species of fungi showed medium sensitivity to the same concentration of this extract.

Hence, we conclude that it is possible to use Spirulina extract of (250) mg/ml concentration to treat infections caused by *P. aeruginosa* instead of using antibiotics that have side effects on the body.

It can also be used to treat other infections caused by other pathogenic species of bacteria used in this study which showed medium sensitivity to the extract, due to its safety of use.

**Acknowledgment** We send thanks to bacterial strain bank in biology department for providing bacterial strain, we also send thankful to the Collage of Science and epartment of biology for providing this work.

## Reference

- Soni, R. A., Sudhakar, K., & Rana, R. S. (2017). Spirulina–From growth to nutritional product: A review. *Trends in food science & technology*, 69, 157-171.
- Bhat, V. B., & Madyastha, K. M. (2001). Scavenging of peroxy nitrite by phycocyanin and phycocyanobilin from *Spirulina platensis*: protection against oxidative damage to DNA. *Biochemical and biophysical research communications*, 285(2), 262-266..
- Estrada, J. P., Bescós, P. B., & Del Fresno, A. V. (2001). Antioxidant activity of different fractions of *Spirulina platensis* protean extract. *Il farmaco*, 56(5-7), 497-500.
- Nagaoka, S., Shimizu, K., Kaneko, H., Shibayama, F., Morikawa, K., Kanamaru, Y., ... & Kato, T. (2005). A novel protein C-phycocyanin plays a crucial role in the hypocholesterolemic action of *Spirulina platensis* concentrate in rats. *The Journal of nutrition*, 135(10), 2425-2430.
- Saranraj, P., & Sivasakthi, S. (2014). *Spirulina platensis*–food for future: a review. *Asian J. Pharm. Sci. Technol*, 4(1), 26-33.
- Liestianty, D., Rodianawati, I., Arfah, R. A., Assa, A., Patimah, Sundari, & Muliadi. (2019, May). Nutritional analysis of spirulina sp to promote as superfood candidate. In *IOP Conference Series: Materials Science and Engineering* (Vol. 509, p. 012031). IOP Publishing.
- Rao, C. K., & Annadana, S. (2017). Nutrient biofortification of staple food crops: Technologies, products and prospects. *Phytonutritional improvement of crops*, 113-183.
- Sharoba, A. M. (2014). Nutritional value of spirulina and its use in the preparation of some complementary baby food formulas. *Journal of food and dairy sciences*, 5(8), 517-538.
- Gaur, K., Wal, A., Sharma, P., Parveen, A., Singh, P., Mishra, P., and Mishra, N. P. (2024). Natural Resources for Human Health. *Lipids*, 5, 7.
- Nasima Akhtar, N. A., Ahmed, M. M., Nishat Sarker, N. S., Mahbub, K. R., & Sarker, A. M. (2012). Growth response of *Spirulina platensis* in papaya skin extract and antimicrobial activities of *Spirulina* extracts in different culture media.
- Karkos, P. D., Leong, S. C., Karkos, C. D., Sivaji, N., & Assimakopoulos, D. A. (2008). *Spirulina* in clinical practice: evidence-based human applications.
- Li, L., Zhao, X., Wang, J., Muzhing, T., Suter, P. M., Tang, G., & Yin, S. A. (2012). *Spirulina* can increase total-body vitamin A stores of Chinese school-age children as determined by a paired isotope dilution technique. *Journal of nutritional science*, 1, e19.

- Gaur, K., Wal, A., Sharma, P., Parveen, A., Singh, P., Mishra, P. and Mishra, N. P. (2024). Natural Resources for Human Health. *Lipids*, 5, 7..
- Farag, M. R., Alagawany, M., El-Hack, M. E. A., & Kuldeep Dhama, K. D. (2016). Nutritional and healthical aspects of *Spirulina* (*Arthrospira*) for poultry, animals and human.
- Khan, M. T. H., Ather, A., Thompson, K. D., & Gambari, R. (2005). Extracts and molecules from medicinal plants against herpes simplex viruses. *Antiviral research*, 67(2), 107-119.
- Nandagopal, P., Steven, A. N., Chan, L. W., Rahmat, Z., Jamaluddin, H., & Mohd Noh, N. I. (2021). Bioactive metabolites produced by cyanobacteria for growth adaptation and their pharmacological properties. *Biology*, 10(10), 1061.
- Bonnet, M., Lagier, J. C., Raoult, D., & Khelaifia, S. (2020). Bacterial culture through selective and non-selective conditions: the evolution of culture media in clinical microbiology. *New microbes and new infections*, 34, 100622.
- Hudzicki, J. (2009). Kirby-Bauer disk diffusion susceptibility test protocol. *American society for microbiology*, 15(1), 1-23.
- De Obeso Fernandez Del Valle, A., & Scheckhuber, C. Q. (2021). From past to present: Biotechnology in Mexico using algae and fungi. *Plants*, 10(11), 2530.
- Saraswathi, K., & Kavitha, C. N. (2023). *Spirulina*: Pharmacological Activities and Health Benefits. *Journal of Young Pharmacists*, 15(3), 441-447.
- RAMIANDRISOA, B. C. R., & Patrick, H. (2024). Essai de la culture de spiruline biologique *Arthrospira platensis* à la ferme Masoandro d'Ambovo dans la commune urbaine de Mahajanga Madagascar.
- Anvar, A. A., & Nowruzi, B. (2021). Bioactive properties of spirulina: A review. *Microb. Bioact*, 4, 134-142.
- Rehman, K., Kamran, S. H., & Akash, M. S. H. (2020). Toxicity of antibiotics. In *Antibiotics and Antimicrobial Resistance Genes in the Environment* (pp. 234-252). Elsevier.
- Algammal, A. M., Hetta, H. F., Elkelish, A., Alkhalifah, D. H. H., Hozzein, W. N., Batiha, G. E. S., and Mabrok, M. A. (2020). Methicillin-Resistant *Staphylococcus aureus* (MRSA): one health perspective approach to the bacterium epidemiology, virulence factors, antibiotic-resistance, and zoonotic impact. *Infection and drug resistance*, 3255-3265.
- Prete, V., Abate, A. C., Di Pietro, P., De Lucia, M., Vecchione, C., & Carrizzo, A. (2024). Beneficial Effects of *Spirulina* Supplementation in the Management of Cardiovascular Diseases. *Nutrients*, 16(5), 642.

- Chakraborty K, Lipton AP, Paulraj R and Chakraborty RD,(2010). Guaiane sesquiterpenes from seaweed *Ulva fasciata* Delile and their antibacterial properties. *Eur J Med Chem.* 45(6):2237-2244.
- Bouhlal R, Riadi H and Bourgougnon N.,(2010). Antiviral activity of the extracts of Rhodophyceae from Morocco. *Afr J Biotechnol.* 9(46):7968-7975.
- Parisi, A.S., S. Younes, C.O. Reinehr and L.M. Colla,( 2009). Assessment of the antibacterial activity of microalgae *Spirulina platensis*. *Revista de Ciências Farmacêuticas Básicæ Aplicada, Araraquara,* 30(3) 97-301.
- Wu, L.C., J.A.A. Ho, M.C. Shieh and W. Lu ,. (2005). Antioxidant and antiproliferative activities of *Spirulina* and *Chlorella* extracts. *Journal of Agriculture and Food Chemistry,* 53(10): 4207-4212.
- Anvar, A. A., & Nowruzi, B. (2021). Bioactive properties of spirulina: A review. *Microb. Bioact,* 4, 134-142
- Al-Obaidi, J. R., Alobaidi, K. H., Al-Taie, B. S., Wee, D. H. S., Hussain, H., Jambari, N. N., & Ariffin, N. S. (2021). Uncovering prospective role and applications of existing and new nutraceuticals from bacterial, fungal, algal and cyanobacterial, and plant sources. *Sustainability,* 13(7), 3671.
- Sonawane, T. N., Khairnar, V. S., & Chaudhari, R. R. (2023). A Review Article on ‘Spirulina’.
- Pankaj PP, and Varma MC.,(2013). Potential role of *Spirulina platensis* in retaining altered blood parameters in alloxan induced diabetic mice. *Int J Pharm Sci.* 5(4):450-456.
- Berkow, E. L., & Lockhart, S. R. (2017). Fluconazole resistance in *Candida* species: a current perspective. *Infection and drug resistance,* 237-245.
- d'Enfert, C., & Hube, B. (Eds.). (2007). *Candida: comparative and functional genomics* (Vol. 5). Norfolk: Caister Academic Press.

## Preparing Titanium Dioxide Nanofibers for Bacterial & Fungal Selectivity

Thamir Abdul Ameer Hassan <sup>1</sup>

Ali Q Tuama <sup>2</sup>

Ghaiath A. Fadhil <sup>3</sup>



© 2024 The Author(s). This open access article is distributed under a Creative Commons Attribution (CC-BY) 4.0 license.



### Abstract:

*Titanium oxide nanofibers were prepared using hydrothermal method for anti-bacterial and anti-fungal selectivity. These oxides were examined as agents for bacterial and fungal inhibition. This is mainly due to their nontoxicity, hydrophobicity and antifogging effect. The present study tests the viability of using TiO<sub>2</sub> nanofibers prepared using the simple and cost-effective hydrothermal process against a variety of bacterial (Staphylococcus, E. coli and Pseudomonas) and fungal (Candidiasis) organisms. The samples characteristic were examined mainly using, mainly: Field Emission-Scanning electron microscopy and x-ray diffraction. The selectivity of these oxides was tested against Staphylococcus, E. coli and Pseudomonas bacteria and Candidiasis fungus. No observable effect for TiO<sub>2</sub> on the bacterial growth was reported while a successful inhibition of Candidiasis fungus was achieved. The results shed a new light on the activity of Titanium oxide nanofibers as an anti-bacterial and -fungal selection for biological and environmental issues.*

**Keywords:** Titanium; Dioxide; Bacterial; Nanofibers.



<http://dx.doi.org/10.47832/MinarCongress12-22>



<sup>1</sup> Al karkh University of Science, Baghdad-Iraq



<sup>2</sup> College of Science, Al karkh University of Science, Baghdad-Iraq



<sup>3</sup> Department of Medical Physics, College of Science, Alkarkh University of Science, Baghdad-Iraq  
[ghaiath.fadhil@kus.edu.iq](mailto:ghaiath.fadhil@kus.edu.iq)



## Introduction

Titanium oxide nanostructures have attracted much attention recently due to their unique characteristics and wide-range applications [1]. Titanium oxides have two main polymorphs, anatase and rutile and represents a promising choice for a wide range of applications. Among these uses, Titanium oxides has two main polymorphs, anatase and rutile [2, 3]. Their mechanical, electronic and optical properties are extremely useful for efforts of finding cost-effective nanostructures that can be used in sensing [4], solar cells [5, 6], photo-catalysts [7], water treatment [8] and pharmaceutical activities [9]. TiO<sub>2</sub> nanoparticles has been studies extensively for bacterial and antimicrobial selectivity [10-13]. This is due to their nontoxicity, hydrophobicity and antifogging effect [12], which makes them an excellent candidate for eliminating disliked organic materials from water and air [12]. TiO<sub>2</sub> nanostructures were prepared previously using electrospinning process [14], sol-gel [15] and hydrothermal methods [16]. These nanostructures can be in the form of nanoparticles, nanotubes, nanofibers, nanowires depending on the processing conditions set during fabrication [16-18]. Hydrothermal emerges as a cost-effective and simple process compared to other techniques. In the hydrothermal process, the starting material, processing conditions and post processing treatment play a major role in determining the features of resulted nanoparticles and nanotubes [11, 19]. On the other hand, nanofibers emerged as candidate for optoelectronic and biological applications, due to their high photo-catalytic activity and the high surface-to-volume ratio [20-22]. Previous studies have reported the use of nanoparticles [10, 13] and nanotubes [23, 24] for inhibiting microbial and bacterial activity. These studies aimed to improve the inhibition capability of TiO<sub>2</sub> by fabricating it in the form of nanoparticles, which have a higher surface area compared to nanotubes. Furthermore to the surface area, it is essential to TiO<sub>2</sub> nanoparticles to be synthesized in the anatase form since it has a higher photocatalytic activity than the rutile form [25]. Other than nanoparticles and nanotubes, nanofibers produced by electrospinning process for eliminating microbes were reported to increase in the contact area with microbes [26, 27]. The present study tests the viability of using TiO<sub>2</sub> nanofibers prepared using the simple and cost-effective hydrothermal process against a variety of bacterial (*Staphylococcus*, *E. coli* and *Pseudomonas*) and fungal (*Candidiasis*) organisms. The morphological and structural analysis of these nanofibers can help in the evaluation of their selectivity on the different pathogens.

## Experimental

In this experiment, TiO<sub>2</sub> (Titanium Oxide Nanopowder, anatase, 99.5%,) powder was utilized with 10-30 nm nanoparticles size purchased from SkySpring Nanomaterials, Inc. The TiO<sub>2</sub> nanopowder and sodium hydroxide (NaOH) were used without any intermediate purification or treatment. Next, one gram of TiO<sub>2</sub> powder was added to a 20 ml of NaOH with the concentrations shown in table 1. The mixture was magnetically stirred for 30 minutes and eventually transferred into a Teflon-lined stainless steel autoclave with a 30 ml capacity. The NaOH solution up filled the autoclave up to 80% of its capacity and maintained the determined temperature for each experiment. The preparation parameters for each sample shown below (table 1). The processing temperature & NaOH concentration were varied as shown in the table while TiO<sub>2</sub> powder composition was fixed. This procedure was performed in order to analyze the effect of processing conditions.

**Table 1- Preparation parameters for the four samples used in this study**

Sample name	NaOH concentration (M)	Time (hours)	Temperature (°C)
<i>a3</i>	3	6	100
<i>a4</i>	4	6	100
<i>b3</i>	3	6	120
<i>b4</i>	4	6	120

At the end of the process, the autoclave was turned off and left to cool naturally to room temperature. The resulting precipitate was dried out by heating at 140 °C for an hour and then filtered and washed repeatedly with distilled water and hydrochloric acid in order to have the pH levelled at 7. The structural and morphological characterization of TiO<sub>2</sub> was performed using Powder X-ray diffraction (XRD) and Field Emission scanning electron microscopy. XRD was performed using Empyrean X-ray diffractometer with Cu-K $\alpha$  radiation ( $\lambda = 1.5418 \text{ \AA}$ ) while SEM was performed using Inspect F Fe-SEM. Overnight Culture of Staphylococcus, E. coli, Pseudomonas bacteria and Candidiasis fungus were added to 100 ml of nutrient broth according to Kirby Bauer disk diffusion Technique [28]. The disks were placed over the media and incubated at 37°C for 24 hours.

## Results and Discussion

Figures 1a and 1b show SEM images of the TiO<sub>2</sub> nanofibers, which were synthesized hydrothermally at 100 °C for 6 hours in controlled conditions with concentrations of 3M

(sample *a3*) and 4M (sample *a4*) of NaOH, respectively. The resulting nanofibers exhibited high linearity for both concentrations,. Some white residuals (annotated with arrows in fig. 1a) existed even with the extensive post-processing efforts, which indicates that an excessive washing of post-processing materials is required. Surprisingly, the nanofibers in sample *a4* were observed to exceed 3  $\mu\text{m}$ , which is not reported previously. These fibers showed some unevenness at their surfaces. Regarding samples *b3* and *b4*, SEM images (fig. 1c and 1d) showed a more obvious fibrous structure in both samples. The lengths of these nanofibers varied between 20-35  $\mu\text{m}$ . In all samples, the nanofibers have a straight structure with entanglement between different nanofibers. Features of layered structures in these nanofibers can be suggested from the SEM images. This is supported by the variation in contrast along the fibre structure. Such observation was reported previously in nanofibers produced using the hydrothermal process [20].

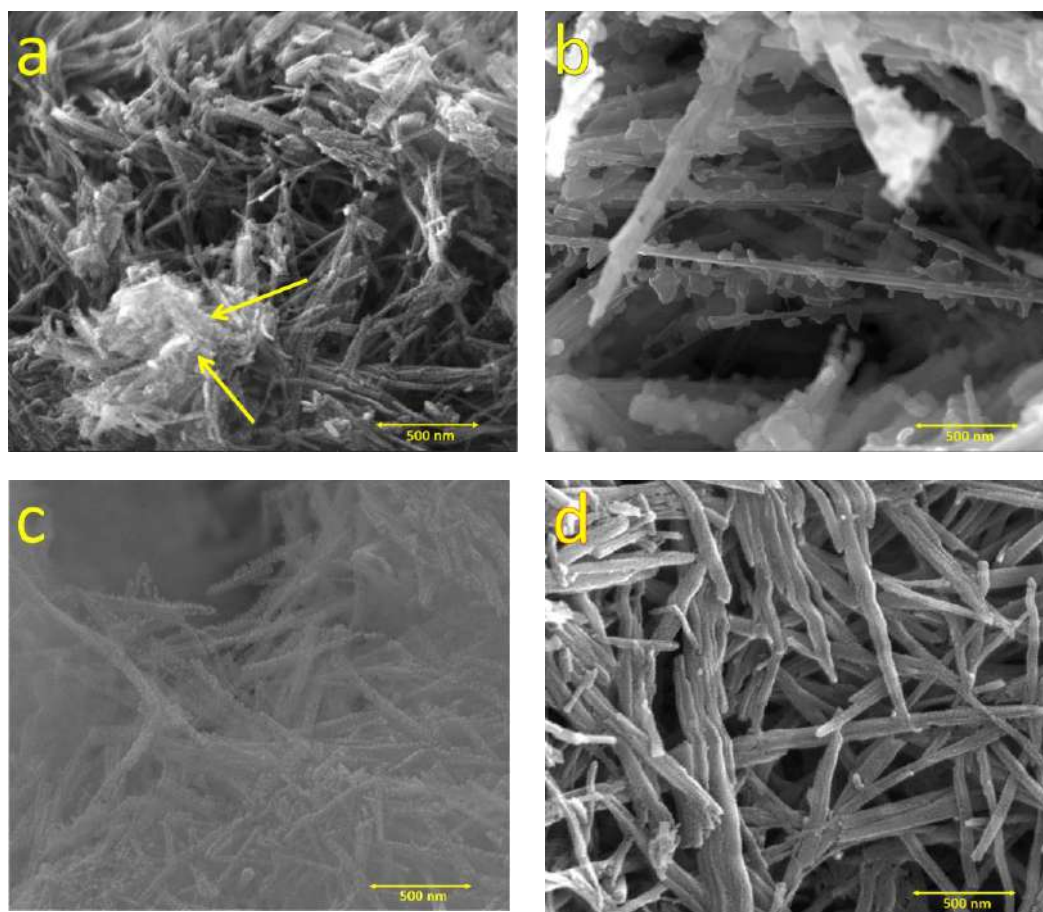


**Figure 1** - SEM images of  $\text{TiO}_2$  nanofibers synthesized through hydrothermal reaction (a) sample *a3*, (b) sample *a4* and (c) sample *b3* and (d) sample *b4*.

The X-ray diffraction (XRD) patterns shown in Fig. 3 reveal that the resulted  $\text{TiO}_2$  structures have anatase phase, as confirmed by the diffraction peak at plane (200) of the tetragonal phase in all samples. Sample *a4* showed a strong intensity at (101) plane of anatase

along with other non-indexed peaks that did not match any of the titania phases. This possible to be related to the irregular surfaces of this sample's fibers.

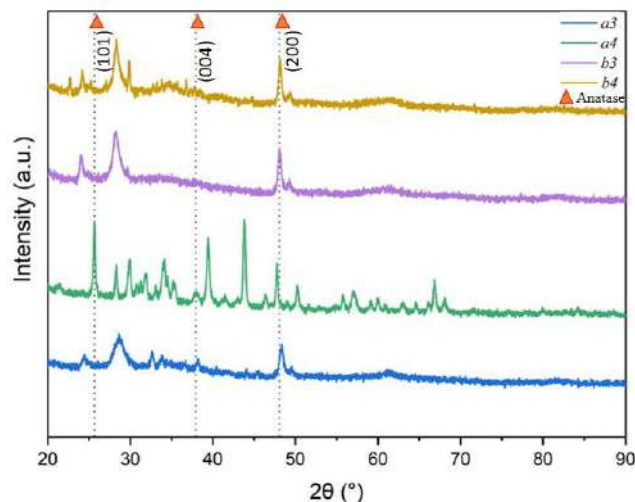


**Figure 2** - XRD patterns of TiO<sub>2</sub> nanofibers synthesized through hydrothermal reaction (a) sample a3, (b) sample a4, (c) sample b3 and (d) sample b4. The symbol ( $\Delta$ ) with red colour represents the Anatase phase peaks [29].

Hydrothermal process of anatase Nanopowder using different concentrations of NaOH and temperature. The characterisation of the resulted structures using SEM revealed fibrous structures with significant length to width ratio that are similar to previously reported structures. XRD data suggested that the hydrothermal process succeeded to produce the anatase phase in all samples. However, the processing of these structures at 100 °C led to the creation of white residual in samples a3 and a4 that is suggested by XRD to be the rutile titania phase or the titanate phase with the (Na<sup>+</sup>) cation. The processing of TiO<sub>2</sub> nanopowder at 120 °C (sample b3 and b4) has produced nanofibers with higher smoothness in their surfaces compared to samples a3 and a4. These insights reveal that higher temperature of hydrothermal process can reduce the possibility of forming unprocessed or non-preferable structures that might affect the efforts of bacterial inhibition.

In this study, the impact of titania nanofibers, produced using various hydrothermal processing conditions, on the growth of *E. coli*, *Staphylococcus*, and *Pseudomonas* bacteria, as well as *Candidiasis* fungus, was evaluated. Interestingly, almost no effect of TiO<sub>2</sub> nanoparticles was observed on *E. coli* (fig.3a), *Staphylococcus* (fig.3b) and *Pseudomonas* (fig.3c). The bacterial growth in liquid media with different processing conditions of TiO<sub>2</sub> nanofibers suffered no obvious delay. On the other hand, TiO<sub>2</sub> nanoparticles inhibition of *Candidiasis* fungus was noticeable compared to bacterial inhibition (fig.3d). These observations are related to the quality of nanofibers produced using the processing conditions listed above.

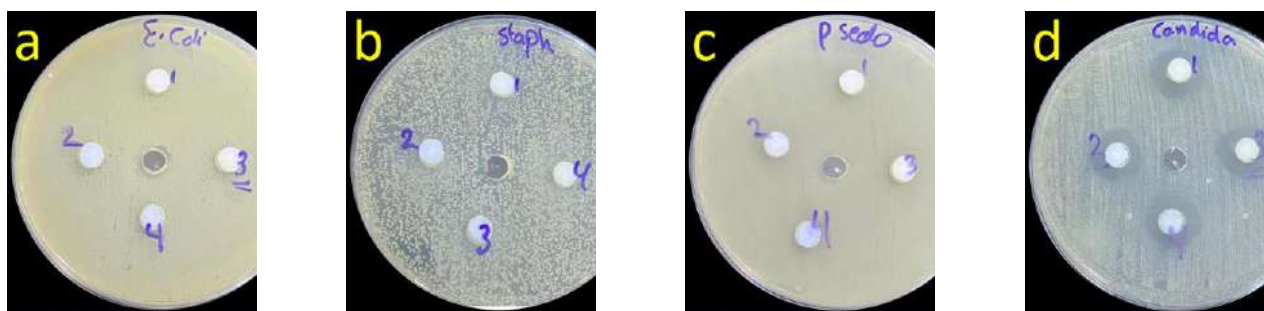


**Figure 3** - Overnight Culture of (a) Staphylococcus, (b) E. coli, (c) Pseudomonas and (d) candida fungus in the presence of TiO<sub>2</sub> nanofibers.

The effect of the residuals in the fibrous Titania nanostructure was noticed by measuring the growth of E. coli, Staphylococcus, and Pseudomonas bacteria in the presence of these nanostructures. The absence of a clear effect on the bacterial growth suggests that these residuals led to the deactivation of the polarity of the titania nanofibers phase. On the other hand, the successful inhibition of Candidiasis fungus showed promising results for the use of titania nanofibers for anti-fungal selectivity. The discrepancy between anti-bacterial and anti-fungal effect of these nanofibers can be attributed to the biological differences between these organisms and their reaction to characteristics of titania nanofibers. The optimization of hydrothermal processing conditions (processing temperature & NaOH concentration) for titania nanofibers and the interpretation of their mechanism of bacterial and fungal inhibition are vital milestones towards their use as successful anti-microbial agents. Future research on the processing parameters and materials composition of titania nanofibers is important for a more efficient bacterial and fungal inhibition.

## Conclusions

The selectivity of titanium oxide nanofibers produced using hydrothermal was tested against Staphylococcus, E. coli and Pseudomonas bacteria and Candidiasis fungus. No observable effect for TiO<sub>2</sub> on the bacterial growth was reported while a successful inhibition of Candidiasis fungus was achieved. This is directly related to the processing conditions of the hydrothermal process. Further optimization of the processing parameters of the hydrothermal process to produce titania nanofibers with no-residual structures can help efforts of using these fibrous structures in biological applications.



## References

- Chen, X. and S.S. Mao, Titanium dioxide nanomaterials: synthesis, properties, modifications, and applications. *Chemical reviews*, 2007. 107(7): p. 2891-2959.
- Kamat, P.V., Photophysical, photochemical and photocatalytic aspects of metal nanoparticles. 2002, ACS Publications. p. 7729-7744.
- Awati, P., et al., Photocatalytic decomposition of methylene blue using nanocrystalline anatase titania prepared by ultrasonic technique. *Catalysis Communications*, 2003. 4(8): p. 393-400.
- Galstyan, V., et al., TiO<sub>2</sub> nanotubes: recent advances in synthesis and gas sensing properties. *Sensors*, 2013. 13(11): p. 14813-14838.
- George, J.M., A. Antony, and B. Mathew, Metal oxide nanoparticles in electrochemical sensing and biosensing: a review. *Microchimica Acta*, 2018. 185: p. 1-26.
- Selema, T., et al., Advancements in black titanium dioxide nanomaterials for solar cells: a comprehensive review. *Emergent Materials*, 2024: p. 1-26.
- Ma, Y., et al., Titanium dioxide-based nanomaterials for photocatalytic fuel generations. *Chemical reviews*, 2014. 114(19): p. 9987-10043.
- Lazar, M.A., S. Varghese, and S.S. Nair, Photocatalytic water treatment by titanium dioxide: recent updates. *Catalysts*, 2012. 2(4): p. 572-601.
- Ziental, D., et al., Titanium dioxide nanoparticles: prospects and applications in medicine. *Nanomaterials*, 2020. 10(2): p. 387.
- Mahdy, S.A., et al., The antibacterial activity of TiO<sub>2</sub> nanoparticles. *J. Univ. Babylon*, 2017. 25: p. 955-961.
- Khashan, K.S., et al., Antibacterial activity of TiO<sub>2</sub> nanoparticles prepared by one-step laser ablation in liquid. *Applied Sciences*, 2021. 11(10): p. 4623.
- Haghi, M., et al., Antibacterial effect of TiO<sub>2</sub> nanoparticles on pathogenic strain of E. coli. *International Journal of Advanced Biotechnology and Research*, 2012. 3(3): p. 621-624.
- Lin, X., et al., Toxicity of TiO<sub>2</sub> nanoparticles to Escherichia coli: effects of particle size, crystal phase and water chemistry. *PLoS one*, 2014. 9(10): p. e110247.
- Kim, J.-H., et al., Synthesis of aligned TiO<sub>2</sub> nanofibers using electrospinning. *Applied Sciences*, 2018. 8(2): p. 309.
- Kim, W.-T., et al., Effects of electrospinning parameters on the microstructure of pvp/tio<sub>2</sub> nanofibers. *Nanomaterials*, 2021. 11(6): p. 1616.

- Yuan, Z.-Y. and B.-L. Su, Titanium oxide nanotubes, nanofibers and nanowires. *Colloids and Surfaces A: Physicochemical and Engineering Aspects*, 2004. 241(1-3): p. 173-183.
- Liu, N., et al., A review on TiO<sub>2</sub>-based nanotubes synthesized via hydrothermal method: Formation mechanism, structure modification, and photocatalytic applications. *Catalysis Today*, 2014. 225: p. 34-51.
- Zhang, Y., et al., Hydrothermal synthesis and photoluminescence of TiO<sub>2</sub> nanowires. *Chemical Physics Letters*, 2002. 365(3-4): p. 300-304.
- Zhang, F.-B. and H.-L. Li, Hydrothermal synthesis of TiO<sub>2</sub> nanofibres. *Materials Science and Engineering: C*, 2007. 27(1): p. 80-82.
- Yuan, Z.-Y., W. Zhou, and B.-L. Su, Hierarchical interlinked structure of titanium oxide nanofibers. *Chemical Communications*, 2002(11): p. 1202-1203.
- Yu, J., et al., Preparation and photocatalytic activity of mesoporous anatase TiO<sub>2</sub> nanofibers by a hydrothermal method. *Journal of Photochemistry and Photobiology A: Chemistry*, 2006. 182(2): p. 121-127.
- Altaf, A.A., et al., Titania nano-fibers: a review on synthesis and utilities. *Inorganica Chimica Acta*, 2020. 501: p. 119268.
- Tan, A., et al., Review of titania nanotubes: Fabrication and cellular response. *Ceramics International*, 2012. 38(6): p. 4421-4435.
- Ou, H.-H. and S.-L. Lo, Review of titania nanotubes synthesized via the hydrothermal treatment: Fabrication, modification, and application. *Separation and Purification Technology*, 2007. 58(1): p. 179-191.
- Fu, G., P.S. Vary, and C.-T. Lin, Anatase TiO<sub>2</sub> nanocomposites for antimicrobial coatings. *The journal of physical chemistry B*, 2005. 109(18): p. 8889-8898.
- Lee, B.-Y., et al., Titanium dioxide-coated nanofibers for advanced filters. *Journal of Nanoparticle Research*, 2010. 12: p. 2511-2519.
- Kobayashi, S., et al., Preparation of TiO<sub>2</sub> hollow-fibers using supramolecular assemblies. *Chemistry of materials*, 2000. 12(6): p. 1523-1525.
- Wanger, A., Disk diffusion test and gradient methodologies. *Antimicrobial susceptibility testing protocols*, 2007. 1: p. 53-73.
- Howard, C., T. Sabine, and F. Dickson, Structural and thermal parameters for rutile and anatase. *Acta Crystallographica Section B: Structural Science*, 1991. 47(4): p. 462-468.

## ST2 Concentration as Cardiac Biomarker in Cvd Patients with Hyperglycemia

Maryam Kadhim Al-Shemery <sup>1</sup>

Fatema Ali AL kafhage <sup>2</sup>



© 2024 The Author(s). This open access article is distributed under a Creative Commons Attribution (CC-BY) 4.0 license.

### Abstract:

**Background:** During vascular remodeling, fibrosis, including damage to the myocardium, ST2 is crucial. Since their development, high-sensitivity persistent Inhibition of Tumor formation-2 (sST2) tests have proven to provide useful tools in the diagnosis and surveillance for cardiovascular disorders. . **Objectives:** The research presented here aims to improve existing comprehension of sST2 in cardiovascular illness, particularly a focus upon the connection underlying hypoglycemia as well as The ST2.

**Materials and methods:** The region of Al-Najaf el-Ashraf's Hospital Al Sader General Teaching was used as the investigation's site. A collection mainly sixty individuals were analyzed, comprising of thirty-five individuals who had cardiovascular disease (CVD) with twenty-five healthy. The median age of the patients was 35 to 65. Age, creatinine, urea, fasting glucose level, the random blood sugar levels in patients having Cardiovascular have been assessed for the research patients. This investigation additionally confirmed the individual's ST2 levels.

**Result:** The results of the investigation show that, as compared to controls, those suffering from Cardiovascular had substantially greater levels of ST2, urea, which and creatinine levels, as well as arbitrary blood sugar and fasting glucose levels. In the research subjects, this genetic marker showed an upward trend with both creatinine and (fasting glucose and random blood sugars).

**Conclusions:** Individuals having Cardiovascular died at increased rates when their circulation ST2 content was increased. Kinase ST2 is positively regulated by hypoglycemia. Thus, in patients with CVD, there is a correlation between ST2 level increasing the incidence of diabetes. According to what we have discovered, there's is a highly substantial clinical correlation between ST2 with kidney problems.

**Keywords:** Hyperglycemia, CKD , CRS, ST2 and CVD.



<http://dx.doi.org/10.47832/MinarCongress12-23>

<sup>1</sup> Department of pathological analysis, College of Science, university of Kufa. Iraq  
[shemeriya1992@gmail.com](mailto:shemeriya1992@gmail.com)

<sup>2</sup> College of Veterinary medicine, university of Karbala.Iraq  
[fatimah.m@uokerbala.edu.iq](mailto:fatimah.m@uokerbala.edu.iq)

## Introduction

Just every other organ in the body, the cardiovascular system is made up of many different kinds of cells as well as among which the most prevalent of which are the cells known as endothelial cells, which are the components that form elements of arteries and veins (1). Endothelial cells are the cells that regulate the flow of oxygen and other nutrients into the cardiovascular system that aid in defending against immunity (2). The health of the heart is ultimately impacted by the dysfunction of cells called endothelial cells, which also affect nearby cells. Consequently, it is acknowledged that endothelial cells are believed to play a crucial part in the emergence of cardiovascular conditions (3).

Cardiorenal disease (CRS) is a word used to describe heart failure (HF) that results in impaired kidney function and reverses the other. As CRS increases morbidity as well as mortality among individuals with acute kidney injury (AKI), heart failure (HF), or chronic kidney disease (CKD), it is considered usually of these poorest diagnostic indications. (4). Additionally, biomarkers are crucial for cardiovascular remodeling, inflammation, and damage to myocardium.

Recently 2017, the American College of Cardiology and the American Heart Association (AHA) updated their recommendations on coronary artery disease, recognizing the value of high-sensitivity solubility Inhibition of The development of tumors-2 (sST2) tests for prediction as well as tracking of heart failure (3). It has been discovered that solubility ST2 is a significant determinant in failing heart treatment outcomes as well as an indication of morbidity and mortality for the context of serious cardiovascular conditions (5,6). Belonging to the subfamily of Rapid transmitters interacting interleukin 1, (TIR, Toll/interleukin1 receptor), contains intracellular and able to dissolve ST-2 proteins (29). It originates with 2 forms that are therapeutically important to consider: solubility or transdermal. The transdermal form (ST-2L, ST-2 ligand) is primarily found on the tissue called the end cardiomyocytes were and cells involved in inflammation.

According to research on mammals, interleukin 33 (IL-33) prevents cardiopulmonary hypertrophy and inflammation via interacting with ST-2L, which has been identified onto coronary arteries (7). This solubility structure, also known as solubility ST-2 or sST-2, is widely circulated in the blood and can be detected using a common biochemistry test that involves blood. Cells, that have been encouraged during development, as well as cytokines that promote inflammation, involving interleukin six (IL-6) and tumor necrosis element  $\alpha$  (TNF- $\alpha$ ), influence the production of sST-2. An overabundance of sST-2 inhibits IL-33 from interacting onto the

ST-2L proteins, which can lead to detrimental structural alterations in the heart. It has been shown that the presence of the IL33/ST-2 connection contributes to the advancement of atherosclerotic in addition to scarring and cardiac remodeling (8). prevailing knowledge regarding sST2 in heart failure will substantially updated by the present research, particularly a focus on the hyperlink connecting both the ST2 and hyperglycemia.

## Materials and methods

The investigation in question was conducted in Iraq between April and June of twenty-three. The municipality of Al-Najaf al-Ashrf's General Hospitals Al Sader General Teaching served as the research project's site.

### 1. Study Design

Each of the sixty specimens analyzed, of which thirty-five fell under the sick category while twenty-five were in the unaffected category. During every phase comprising the research, an everyday population of adults, males and females, age thirty to sixty-five (together with acceptance or exclusion conditions) was gathered.

### 2. Collection of Blood Sample

Using five milligrams of sterile collaborations, specimens of blood were taken into veins. Specimen placed inside container with labeling. The use of blood was permitted to coagulate lasting ten minutes at temperatures of room temperature, and subsequently centrifuged for an additional fifteen minute at 6000 revolutions per minute. The blood sample followed by separation as well as frozen at -80 °C unless the experiment's laboratory examination was completed.

### 3. Laboratory parameters

**A. Determination of Blood Urea concentration:** The amount of urea in the blood sample was determined using the colorimetric technique. Biolabo SA, France provided a specialized kit for measuring human urea amounts in serum.

**B. Determination serum creatinine concentration:** The amount of creatinine in the serum was ascertained by colorimetric response. The French company Biolabo SA provided the serum with its creatine content.



**C. Determination blood glucose:** This substance was developed to utilization in laboratories by professionals using a computerized procedure. It makes it possible to measure the quantity of glucose found in individual plasma and bloodstreams quantitatively also determine the amount in urinate. God oxidizes glucose to produce the compounds hydrogen peroxide and the acid gluconic acid, that when combined with POD, which stands interacts into PAP and chloro-4-phenol to make a crimson quinoneimine. At the wavelength of 500 nm the absorbance of the colored complex will be determined, and it corresponds to the amount of carbohydrates present in the specimen being examined.

**D. ST2:** Automated serum's ST2 quantities were measured employing an enzyme-linked immunosorbent assay ( , in accordance with Elabscience's prepared protocol).

#### 4. Statistical Analysis

The software package SPSS was used for statistically analyzing the data (SPSS, Version 26). The test for significance was employed, or descriptive analyses of means and standard error were performed comparing the participants and healthy subgroups. To determine the correlation between markers and criteria, correlation coefficients were calculated. The statistics were created with Microsoft Office 2016's EXCELL application. Every one among these factors was statistically tested at  $P < 0.05$  significance.

### Results and discussion

#### 1. Study subject:

An aggregate of Forty circumstances—20 individuals suffering from cardiovascular illnesses as well as Twenty healthy —were looked at in this investigation. The individuals receiving treatment ranged in age from forty to sixty-five years, and the participants were all male.

#### 2. Biochemical test of study subject:

##### A. Kidney function test:

The kidney function test results among the study groups are displayed in Figures (4-1) and (4-2). Serum concentrations of urea as well as creatinine among individuals with CVD are significantly higher ( $p < 0.05$ ) than in other research categories, which the data show.

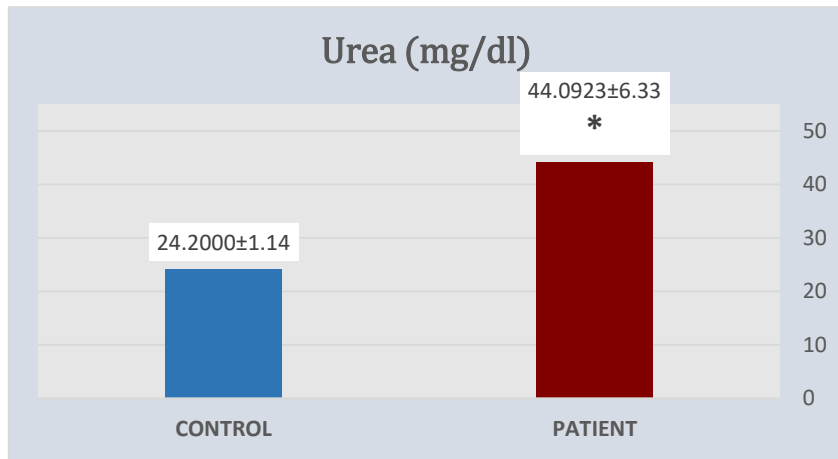


**Figure 1-** Comparison of the urea (mg/dl) between Groups of Patients with CVD and healthy group

\* P < 0.05 statistically significant with control group

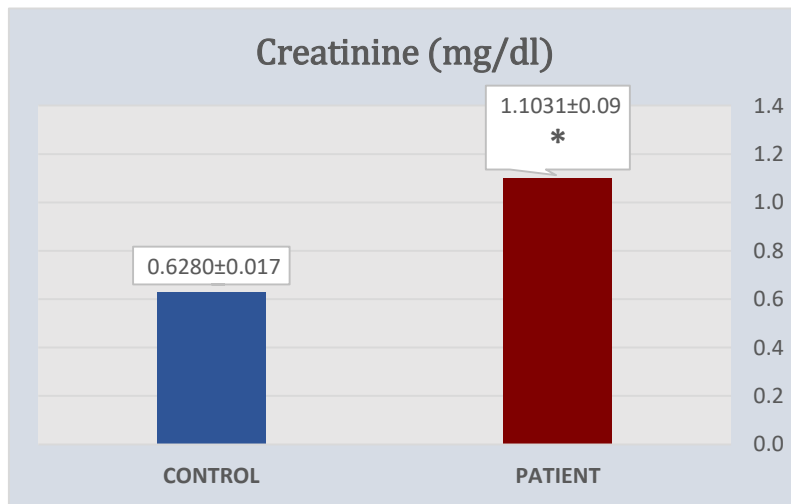


**Figure 2-** Comparison of the creatinine (mg/dl) between Groups of Patients with CVD and healthy group

\* P < 0.05 statistically significant with control group

**B. Blood sugar test:**

Figures (3,4) demonstrate that patients with CVD had significantly higher levels in their serum of both randomized blood sugar levels (RBS) and rapid blood sugar (FG) (p<0.05) than other group in the research.

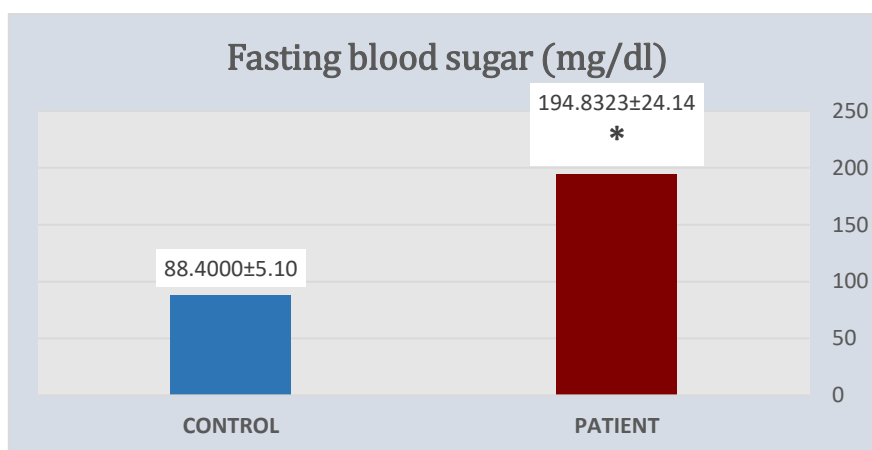


**Figure 3-** Comparison of the fasting blood sugar (mg/dl) between Groups of Patients with CVD and healthy group

\* P < 0.05 statistically significant with control group

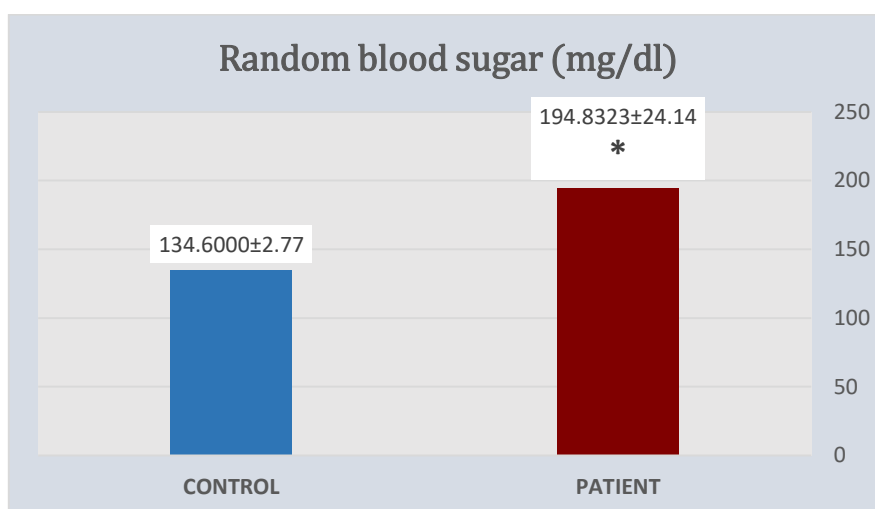


**Figure 4-** Comparison of the Random blood sugar (mg/dl) between Groups of Patients with CVD and healthy group

\* P < 0.05 statistically significant with control group

### 3. ST2 concentration:

The figure (5) shown the specific biomarker test levels between the studied groups According to this figure there was a significant increase (p < 0.05) of ST2 level in patients with CVD comparison with other study groups.

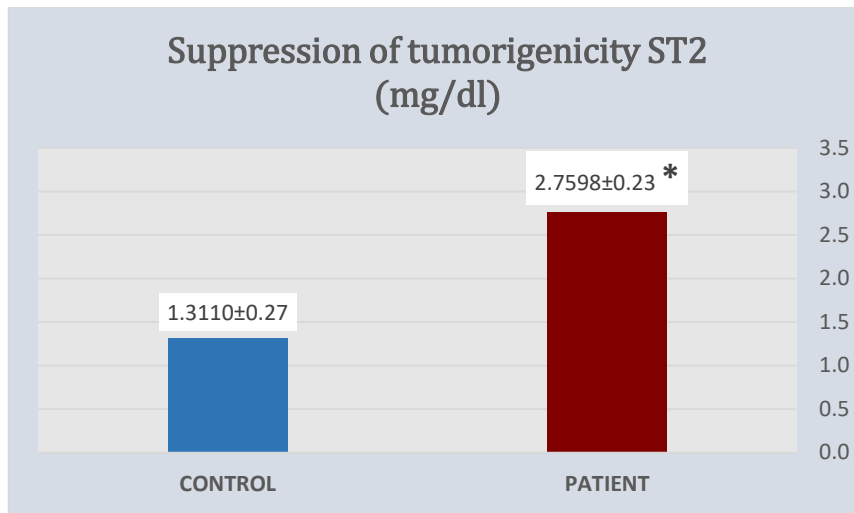


**Figure 5-** Comparison of the ST2 (pg) between groups of patients with CVD and healthy group

\* P< 0.05 statistically significant with control group

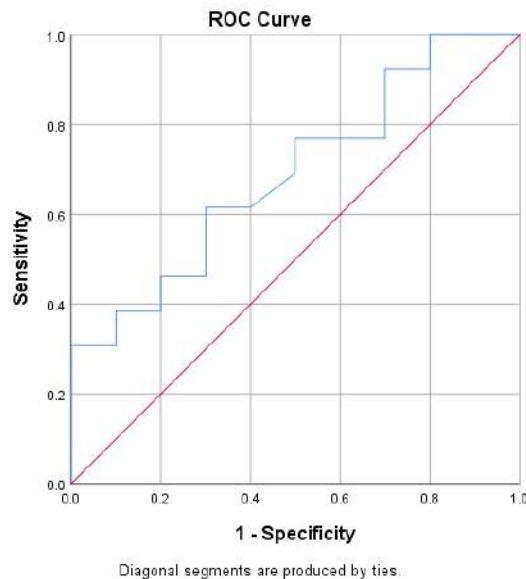


**Figure 6-** ROC curve for discrimination of the ST2 (pg) in all subjects

ROC AUC	Std. Error <sup>a</sup>	Cut off value
.688	0.11	1.9350

### Correlation

the table (4-2) displays the conclusions of the relationship and regression analyses amongst the individuals with CVD. It shows that there was a substantial positive correlation involving ST2 and the outcomes of the individuals s.cr, fg, and RBS. In contrast, the other

finding in the previous table showed that among those suffering from cardiovascular disease, a connection among ST2 as well as urea was not of statistical significance.

**Table 1- Correlation between the clinical characteristics and patients with CVD**

	Correlations	AGE	UREA	S.CR	FG	RBS
ST2	Pearson Correlation	.425*	0.385	.429*	587**	.416*
	Sig. (2-tailed)	0.043	0.069	0.040	0.003	0.048

\* Correlation is significant at the 0.05 level (2-tailed).

\*\*Correlation is significant at the 0.01 level (2-tailed).

## Discussion

Cardiac combined kidney conditions collectively are referred to as cardiorenal syndromes; acute or chronic failure of one of the organs results in malfunctioning of the opposite organ. It combines hemodynamically thru changes in neurohormonal indicators, a combination of heart-kidney connections throughout multiple channels, overall elevated arterial and the kidneys pressure—all of the above being indicative of possible symptoms. (9)

The results of the present investigation demonstrated that, as compared with the remaining participants, individuals who had CVD had significantly higher urea levels. These conclusions corresponded to accordance those of Hong et al. (2023), who discovered that a greater BUN percentage is a predictor of both mortality from all causes and cardiovascular disease (CVD). (10) Previous research shows found increased blood sugar levels are linked to unfavorable consequences in heart failure patients in particular when there is a sudden decrease in function (11).

Regularly employed as a diagnostic tool to evaluate kidney functioning, blood urea nitrogen, also known as BUN, is a waste result of protein metabolism that is generated by the body's liver then eliminated by the renal system (12, 13). In the research, kidney performance indicators like creatinine, filtration rate of the kidneys, and Urea have been connected to mortality from cardiovascular diseases (14, 15). Research investigations have shown that people with Cardiovascular had elevated the BUN levels, which, when combined with various additional kidney-related indicators, makes this indicator of kidney function an accurate indicator of Cardiovascular mortality (16,17, 18). BUN, on the opposite together, provides an



indication underlying kidney function with neurohumoral activation which may additionally suggest the pathogenesis of Cardiovascular.

Dehydration, or bleeding from the digestive tract, steroid injections and protein consumption are just some among the variables that affect BUN levels. Additionally, Urea is an essential indicator for metabolic disorders along with additional disorders that may demonstrate the connection among dietary position, the metabolism of proteins, and kidney activity (19).

The current study's findings support those of Bagheri et al. (2019), who found a strong correlation between creatinine concentrations and the incidence and degree of CAD (20). An indicator of the state of the kidneys, creatinine is the anhydride version of urea. Insulin targets muscle, which is additionally the primary generator of serum creatinine (21). Thus, it is expected that creatinine will serve as a marker for cardiovascular illness, diabetes, particularly insulin (CAD) (22, 23).

Particularly for males, there is an U-shaped relationship between CAD and creatinine in the blood, a measure of kidney condition (24, 25). Between twenty and forty percent of individuals admitted for heart failure may have elevated creatinine levels. (26, 27) Aggravating kidney function (WRF) is linked with the rise in the following cases: male gender; (28) advanced age; (29) heart failure past; (30,31) chronic kidney diseases; (32) diabetic; (33) anemia; (34) antihypertensive; (30,31) greater reduction in arterial pressure; (35,36); along with elevated prescriptions of medications (54,57). Prolonged stays in hospitals, higher incidences of hospitalized and for a long time death rates, and greater hospitalization again rates are all linked to larger amounts of creatinine and a greater rise in the creatinine level in the blood (37) A rise in creatinine in the blood did not, nevertheless, appear to be independently correlated with findings for particular investigations (38, 39).

The results of this research demonstrated that, compared with the remaining group members, individuals with Cardiovascular had a significantly higher ) concentration. The results of this research are consistent with those of Park et al. (2023), who show that when fasting blood glucose levels rose above more than 100 mg/dL, the likelihood of cardiac infarction, angiogenic cerebrovascular accident, overall ischaemic coronary heart disease improved gradually, whereas with likelihood of stroke caused by hemorrhaging increased significantly. Lower than 70 milligrams per deciliter of fasting blood glucose levels was linked to a greater likelihood for strokes overall in males (danger proportion 1.06, which is 95% confidence interval (CI) 1.01–1.11) and female (danger ratio 1.11, 1.05–1.17). (40) Through

the a non-en hyperglycemia of LDL ) cholesterol, for example, other the proteins involved, as well as coagulation variables hyperglycemia may negatively impact the endothelium or plaque caused by atherosclerosis of blood arteries (41).

Fisman et al. initially discovered a significant relationship among nondiabetic insulin levels and premature death among people with a constant persistent stage of cardiovascular illness. In their investigation, those who were not diabetic alongside were classified through groupings of fasting blood glucose levels (b110, 110 towards 126, as well as N126 mg per deciliter); preliminary findings about their research demonstrated that fatalities raised considerably within every one of the categories. Multiple research demonstrate that whenever the blood glucose level falls beneath the threshold for the diagnosis of insulin resistance, this represents an extraordinarily significant likelihood of passing away over people with the early stages of CAD as well as people who require coronary angioplasty (42).

According to the latest research, higher levels of fasting glucose in people without diabetes are linked to increased and more catastrophic instances of MI, a stroke, overall death by any cause (44). Furthermore, rising rapid glucose levels was linked to an elevated likelihood of cardiovascular disease in non-diabetic individuals, according to two separate meta-analyses (45). Several possible causes have been identified. Through the process of oxidative stress (46) the action of protein kinase C installation, that accelerated glycogen merchandise activates receptors (47) an elevated glucose state impairs regular functioning of endothelial cells, which speeds up the production of plaque associated with atherosclerosis and increases arterial rigidity (48)

The results from this research demonstrated that, in contrast to other participants in the study, people with non-diabetic Cardiovascular had a significantly higher (RBS) concentration. Despite inside the usual range of plasma glucose levels, reduced RBG concentrations have been linked to decreased chances all severe CVDs among adult Chinese without hypertension. (49). Compared to randomized blood glucose levels, that could be more prone to intraindividual combined interindividual variance, fasted combined randomised glucose levels in the blood constitute potentially dependable hyperglycemia measurements. Nonetheless, given that humans devote the majority of their lives not intermittent fasting, blood glucose levels might be a better indication of Cardiovascular hazards. (50)

Numerous possible causes have been treated as documented for the adverse impacts of carbohydrate discrimination, among them the immediate implications of hypoglycemia the repercussions of insulin resistance, or related changes in metabolism ranging elevated levels of

free fatty acids. Cells death with stiffness can arise from hyperglycemia's induction of nonenzymatic proteins glycosylation is engagement of cellular protein kinases C, stress caused by oxidation, and elevated tumor necrosis factor- (51). Elevated intracellular calcium heightened sympathetic function, that breakdown of blood vessel permeability are among the many heart damaging consequences of high free fatty acid levels (52). Cardiac hypertrophy as well as accumulation of collagen have been scientifically linked to high insulin levels (53). While there is evidence linking inadequate glycemic management to an elevated likelihood in heart failure (54)

In line with the present research's findings, individuals who had CVD had significantly higher (ST2) levels than those in the other investigation subgroups. The results obtained corresponded to line with what Zhang et al., 2021 (81) discovered. Although more recent study indicates increased reduction of the development of tumors 2 (the ST2) is linked to cardiovascular disease (CVD a meta-analysis of ST2 concentrations in various cardiovascular disease has not yet been carried out. Solvent ST2 (also known (sST2) concentrations in those who have ischemia cardiovascular disease , myocardium infarction (MI), and hypertension were the primary objective of current investigation. 55.

Numerous investigations revealed how the stretching of heart muscle cells neutralizes the binding protein of sST2, which is produced (56, 57). Additionally, it is linked to inflammatory alongside heart failure and MI. A suitable quantity for the SST2 can stop uncontrollably high levels of inflammatory because it is a masquerade transmitter of the IL-33 receptors (ST2L). Since it performs its strong rivalry function versus ST2L, superfluous sST2 may also impede the beneficial biological action of IL-33, ultimately leading to HF (58). Lately, there have been numerous reports linking sST2 to cardiovascular diseases, particularly HF (59).

According to the latest research, IL-33/ST-2 signaling is triggered to the aftermath of inflammatory with ventricular anxiety, resulting in the expulsion of the water-soluble form of ST2 into the bloodstream. Greater circulation concentrations of ST2 are associated with a higher probability about heart attack; this finding may be explained by the solubility version of ST2 acting as a dummy receptor in question, which sequesters as well as inhibits IL-33.(60)

This research additionally shows that there is not a significant association among the individual's aged with The ST2. This research supports an investigation conducted in 2016 by Villacorta et al. that showed no correlation between sST2 concentrations and age, BMI, prior HF evaluation, heart rate, or HF etiology (an ischemic vs. non-ischemic). Like established in the earlier investigation, sST2 proved a highly reliable indicator of death. However, sST2 was

a highly accurate indicator of death. Significantly greater amounts (1.08 vs. 0.18 grams per milliliter) were found among individuals whose passed away at the 1-year mark, indicating strong correlation amongst SST, which is 2 amounts that fatalities, particularly greater quantities indicating the greatest danger. (61)

**Conclusions:**

The research sheds light on the relationship between raised creatinine or urea levels and high blood sugar in CRS patients. Our findings demonstrate a highly substantial therapeutic relationship between kidney conditions with ST2. Individuals having Cardiovascular died at increased rates when their circulation ST2 content was increased. An additional instance of CRS is additionally linked to elevated ST2 concentrations. In this latest study, researchers showed that sST2 level represented linked to FG therefore RBS markers as well as constituted an independent risk contributor to elevated hypreglycemia in non-diabetic patients with cardiovascular disease.

**Acknowledgments:**

Our express our gratitude for the support that was provided by Iraqi citizens in conducting this research. The researchers also acknowledge the Faculty of Pathological Analysis at the Faculty of Medicine of Kufa, Iraq's College of Science. for being so helpful with this research.

## References

- Patric, B., Camille, A., Mauro, I., Angelika, H., Tobias, B., Christian, M., ... & Frank, R. (2019). Soluble ST2—a new biomarker in heart failure. *Cardiovasc Med*, 1.
- Pinto, A. R., Ilinykh, A., Ivey, M. J., Kuwabara, J. T., D'antoni, M. L., Debuque, R., ... & Tallquist, M. D. (2016). Revisiting cardiac cellular composition. *Circulation research*, 118(3), 400-409.
- Aird, W. C. (2007). Phenotypic heterogeneity of the endothelium: I. Structure, function, and mechanisms. *Circulation research*, 100(2), 158-173.
- Parker ED, Lin J, Mahoney T, et al. Economic costs of diabetes in the U.S. in 2022 *Diabetes Care* 1 November 2023 [Epub ahead of print].
- Schrier, R. W. (2007). Cardiorenal versus renocardiac syndrome: is there a difference?. *Nature clinical practice Nephrology*, 3(12), 637-637.
- Parikh, R. H., Seliger, S. L., Christenson, R., Gottdiener, J. S., Psaty, B. M., & deFilippi, C. R. (2016). Soluble ST 2 for Prediction of Heart Failure and Cardiovascular Death in an Elderly, Community-Dwelling Population. *Journal of the American heart association*, 5(8), e003188.
- Kakkar, R., & Lee, R. T. (2008). The IL-33/ST2 pathway: therapeutic target and novel biomarker. *Nature reviews Drug discovery*, 7(10), 827-840.
- Weinberg, E. O., Shimpo, M., De Keulenaer, G. W., MacGillivray, C., Tominaga, S. I., Solomon, S. D., ... & Lee, R. T. (2002). Expression and regulation of ST2, an interleukin-1 receptor family member, in cardiomyocytes and myocardial infarction. *Circulation*, 106(23), 2961-2966.
- Aird, W. C. (2007). Phenotypic heterogeneity of the endothelium: I. Structure, function, and mechanisms. *Circulation research*, 100(2), 158-173.
- Hong, C., Zhu, H., Zhou, X., Zhai, X., Li, S., Ma, W., ... & Cao, J. (2023). Association of blood urea nitrogen with cardiovascular diseases and all-cause mortality in USA adults: results from NHANES 1999–2006. *Nutrients*, 15(2), 461.
- Giamouzis, G., Kalogeropoulos, A. P., Georgiopoulou, V. V., Agha, S. A., Rashad, M. A., Laskar, S. R., ... & Butler, J. (2009). Incremental value of renal function in risk prediction with the Seattle Heart Failure Model. *American heart journal*, 157(2), 299-305.
- Peng, R., Liu, K., Li, W., Yuan, Y., Niu, R., Zhou, L., ... & Wu, T. (2021). Blood urea nitrogen, blood urea nitrogen to creatinine ratio and incident stroke: The Dongfeng-Tongji cohort. *Atherosclerosis*, 333, 1-8.
- You, S., Zheng, D., Zhong, C., Wang, X., Tang, W., Sheng, L., ... & Liu, C. F. (2018). Prognostic



- significance of blood urea nitrogen in acute ischemic stroke. *Circulation Journal*, 82(2), 572-578.
- Smilde, T. D., Damman, K., van der Harst, P., Navis, G., Daan Westenbrink, B., Voors, A. A., ... & Hillege, H. L. (2009). Differential associations between renal function and “modifiable” risk factors in patients with chronic heart failure. *Clinical Research in Cardiology*, 98, 121-129.
- Smith, G. L., Lichtman, J. H., Bracken, M. B., Shlipak, M. G., Phillips, C. O., DiCapua, P., & Krumholz, H. M. (2006). Renal impairment and outcomes in heart failure: systematic review and meta-analysis. *Journal of the American College of Cardiology*, 47(10), 1987-1996.
- Matsue, Y., Van Der Meer, P., Damman, K., Metra, M., O'Connor, C. M., Ponikowski, P., ... & Voors, A. A. (2017). Blood urea nitrogen-to-creatinine ratio in the general population and in patients with acute heart failure. *Heart*, 103(6), 407-413.
- Bhatia, K., Mohanty, S., Tripathi, B. K., Gupta, B., & Mittal, M. K. (2015). Predictors of early neurological deterioration in patients with acute ischaemic stroke with special reference to blood urea nitrogen (BUN)/creatinine ratio & urine specific gravity. *Indian Journal of Medical Research*, 141(3), 299-307.
- Lin, H. J., Chao, C. L., Chien, K. L., Ho, Y. L., Lee, C. M., Lin, Y. H., ... & Chen, M. F. (2009). Elevated blood urea nitrogen-to-creatinine ratio increased the risk of hospitalization and all-cause death in patients with chronic heart failure. *Clinical research in cardiology*, 98, 487-492.
- Arihan, O., Wernly, B., Lichtenauer, M., Franz, M., Kabisch, B., Muessig, J., ... & Jung, C. (2018). Blood Urea Nitrogen (BUN) is independently associated with mortality in critically ill patients admitted to ICU. *PloS one*, 13(1), e0191697.
- Bagheri, B., Radmard, N., Faghani-Makrani, A., & Rasouli, M. (2019). Serum creatinine and occurrence and severity of coronary artery disease. *Medical archives*, 73(3), 154.
- Hsieh MC, Hsiao JY, Tien KJ, et al. Chronic kidney disease as a risk factor for coronary artery disease in Chinese with type 2 diabetes. *Am J Nephrol*. 2008;28(2):317–323. doi: 10.1159/000111388.
- Harita N, Hayashi T, Sato KK, et al. Lower serum creatinine is a new risk factor of type 2 diabetes: the Kansai healthcare study. *Diabetes Care*. 2009;32(3):424–426. doi: 10.2337/dc08-1265
- Lorenzo C, Nath SD, Hanley AJ, et al. Risk of type 2 diabetes among individuals with high and low glomerular filtration rates. *Diabetologia*. 2009;52(7):1290–1297. doi: 10.1007/s00125-009-1361-4.
- Rasouli M, Trischuk TC, Lehner R. Calmodulin antagonist W-7 inhibits de novo synthesis of cholesterol and suppresses secretion of de novo synthesized and preformed lipids from cultured hepatocytes. *Biochim Biophys Acta*. 1682;2004(1-3):92–101.

- Lorenzo C, Nath SD, Hanley AJ, et al. Risk of type 2 diabetes among individuals with high and low glomerular filtration rates. *Diabetologia*. 2009;52(7):1290–1297.
- Butler, J., Chirovsky, D., Phatak, H., McNeill, A., & Cody, R. (2010). Renal function, health outcomes, and resource utilization in acute heart failure: a systematic review. *Circulation: Heart Failure*, 3(6), 726-745.
- Metra, M., Nodari, S., Parrinello, G., Bordonali, T., Bugatti, S., Danesi, R., ... & Cas, L. D. (2008). Worsening renal function in patients hospitalised for acute heart failure: clinical implications and prognostic significance. *European journal of heart failure*, 10(2), 188-195.
- Krumholz, H. M., Chen, Y. T., Vaccarino, V., Wang, Y., Radford, M. J., Bradford, W. D., & Horwitz, R. I. (2000). Correlates and impact on outcomes of worsening renal function in patients  $\geq 65$  years of age with heart failure. *The American journal of cardiology*, 85(9), 1110-1113.
- Testani, J. M., Coca, S. G., McCauley, B. D., Shannon, R. P., & Kimmel, S. E. (2011). Impact of changes in blood pressure during the treatment of acute decompensated heart failure on renal and clinical outcomes. *European journal of heart failure*, 13(8), 877-884.
- Forman, D. E., Butler, J., Wang, Y., Abraham, W. T., O'Connor, C. M., Gottlieb, S. S., ... & Krumholz, H. M. (2004). Incidence, predictors at admission, and impact of worsening renal function among patients hospitalized with heart failure. *Journal of the American College of Cardiology*, 43(1), 61-67.
- Butler, J., Forman, D. E., Abraham, W. T., Gottlieb, S. S., Loh, E., Massie, B. M., ... & Krumholz, H. M. (2004). Relationship between heart failure treatment and development of worsening renal function among hospitalized patients. *American heart journal*, 147(2), 331-338.
- Savira, F., Magaye, R., Liew, D., Reid, C., Kelly, D. J., Kompa, A. R., ... & Wang, B. H. (2020). Cardiorenal syndrome: Multi-organ dysfunction involving the heart, kidney and vasculature. *British Journal of Pharmacology*, 177(13), 2906-2922.
- Cowie, M. R., Komajda, M., Murray-Thomas, T., Underwood, J., & Ticho, B. (2006). Prevalence and impact of worsening renal function in patients hospitalized with decompensated heart failure: results of the prospective outcomes study in heart failure (POSH). *European Heart Journal*, 27(10), 1216-1222.
- Voors, A. A., Dittrich, H. C., Massie, B. M., DeLucca, P., Mansoor, G. A., Metra, M., ... & Givertz, M. M. (2011). Effects of the adenosine A1 receptor antagonist rolofylline on renal function in patients with acute heart failure and renal dysfunction: Results from PROTECT (placebo-controlled randomized study of the selective A1 adenosine receptor antagonist rolofylline for patients hospitalized with acute decompensated heart failure and volume overload to assess treatment effect on congestion and renal function). *Journal of the American College of Cardiology*, 57(19),

1899-1907.

- Ljungman, S., Kjekshus, J., Swedberg, K., & Consensus Trial Group. (1992). Renal function in severe congestive heart failure during treatment with enalapril (the Cooperative North Scandinavian Enalapril Survival Study [CONSENSUS] Trial). *The American journal of cardiology*, 70(4), 479-487.
- Voors, A. A., Davison, B. A., Felker, G. M., Ponikowski, P., Unemori, E., Cotter, G., ... & Pre-RELAX-AHF Study Group. (2011). Early drop in systolic blood pressure and worsening renal function in acute heart failure: renal results of Pre-RELAX-AHF. *European journal of heart failure*, 13(9), 961-967.
- Damman, K., Jaarsma, T., Voors, A. A., Navis, G., Hillege, H. L., & van Veldhuisen, D. J. (2009). Both in-and out-hospital worsening of renal function predict outcome in patients with heart failure: results from the Coordinating Study Evaluating Outcome of Advising and Counseling in Heart Failure (COACH). *European journal of heart failure*, 11(9), 847-854.
- Metra, M., Davison, B., Bettari, L., Sun, H., Edwards, C., Lazzarini, V., ... & Dei Cas, L. (2012). Is worsening renal function an ominous prognostic sign in patients with acute heart failure? The role of congestion and its interaction with renal function. *Circulation: Heart Failure*, 5(1), 54-62.
- Testani, J. M., Chen, J., McCauley, B. D., Kimmel, S. E., & Shannon, R. P. (2010). Potential effects of aggressive decongestion during the treatment of decompensated heart failure on renal function and survival: insights from the ESCAPE trial limited dataset. *Journal of Cardiac Failure*, 16(8), S104.
- Park, C., Guallar, E., Linton, J. A., Lee, D. C., Jang, Y., Son, D. K., ... & Samet, J. M. (2013). Fasting glucose level and the risk of incident atherosclerotic cardiovascular diseases. *Diabetes care*, 36(7), 1988-1993.
- Leon B.M., Maddox T.M. Diabetes and cardiovascular disease: Epidemiology, biological mechanisms, treatment recommendations and future research. *World J. Diabetes*. 2015;6:1246–1258.
- Zhao Q., Zhang T.Y., Cheng Y.J., Ma Y., Xu Y.K., Yang J.Q., Zhou Y.J. Impacts of triglyceride-glucose index on prognosis of patients with type 2 diabetes mellitus and non-ST-segment elevation acute coronary syndrome: Results from an observational cohort study in China. *Cardiovasc. Diabetol*. 2020;19:108. doi: 10.1186/s12933-020-01086-5
- Park C., Guallar E., Linton J.A., Lee D.C., Jang Y., Son D.K., Han E.J., Baek S.J., Yun Y.D., Jee S.H., et al. Fasting glucose level and the risk of incident atherosclerotic cardiovascular diseases. *Diabetes Care*. 2013;36:1988–1993.

- Lee, G., Kim, S. M., Choi, S., Kim, K., Jeong, S. M., Son, J. S., ... & Park, S. M. (2018). The effect of change in fasting glucose on the risk of myocardial infarction, stroke, and all-cause mortality: a nationwide cohort study. *Cardiovascular diabetology*, 17, 1-10.
- Levitan EB, Song Y, Ford ES, Liu S. Is nondiabetic hyperglycemia a risk factor for cardiovascular disease? A meta-analysis of prospective studies. *Arch Intern Med*. 2004;164(19):2147–55.
- Khatri JJ, Johnson C, Magid R, Lessner SM, Laude KM, Dikalov SI, Harrison DG, Sung H-J, Rong Y, Galis ZS. Vascular oxidant stress enhances progression and angiogenesis of experimental atheroma. *Circulation*. 2004;109(4):520–5.
- Gerich JE. Clinical significance, pathogenesis, and management of postprandial hyperglycemia. *Arch Intern Med*. 2003;163(11):1306–16.
- Van Popele NM, Elizabeth Hak A, Mattace-Raso FU, Bots ML, Van Der Kuip DA, Reneman RS, Hoeks AP, Hofman A, Grobbee DE, Witteman J. Impaired fasting glucose is associated with increased arterial stiffness in elderly people without diabetes mellitus: the Rotterdam Study. *J Am Geriatr Soc*. 2006;54(3):397–404.
- Bragg, F., Li, L., Bennett, D., Guo, Y., Lewington, S., Bian, Z., ... & China Kadoorie Biobank (CKB) Collaborative Group. (2016). Association of random plasma glucose levels with the risk for cardiovascular disease among Chinese adults without known diabetes. *JAMA cardiology*, 1(7), 813-823.
- Benn M, Tybjaerg-Hansen A, McCarthy MI, Jensen GB, Grande P, Nordestgaard BG. Nonfasting glucose, ischemic heart disease, and myocardial infarction: a Mendelian randomization study. *J Am Coll Cardiol*. 2012;59(25):2356-2365.
- Shanmugam, N., Reddy, M. A., Guha, M., & Natarajan, R. (2003). High glucose-induced expression of proinflammatory cytokine and chemokine genes in monocytic cells. *Diabetes*, 52(5), 1256-1264.
- Bell, D. S. (2003). Heart failure: the frequent, forgotten, and often fatal complication of diabetes. *Diabetes care*, 26(8), 2433-2441.
- Mizushige, K., Yao, L., Noma, T., Kiyomoto, H., Yu, Y., Hosomi, N., ... & Matsuo, H. (2000). Alteration in left ventricular diastolic filling and accumulation of myocardial collagen at insulin-resistant prediabetic stage of a type II diabetic rat model. *Circulation*, 101(8), 899-907.
- Iribarren, C., Karter, A. J., Go, A. S., Ferrara, A., Liu, J. Y., Sidney, S., & Selby, J. V. (2001). Glycemic control and heart failure among adult patients with diabetes. *Circulation*, 103(22), 2668-2673.
- Zhang, T., Xu, C., Zhao, R., & Cao, Z. (2021). Diagnostic value of sST2 in cardiovascular diseases: a systematic review and meta-analysis. *Frontiers in cardiovascular medicine*, 8, 697837.

- Weinberg EO, Shimpo M, De Keulenaer GW, MacGillivray C, Tominaga S, Solomon SD, et al. Expression and regulation of ST2, an interleukin-1 receptor family member, in cardiomyocytes and myocardial infarction. *Circulation*. (2002) 106:2961–6. doi: 10.1161/01.CIR.0000038705.69871.D9
- Parikh RH, Seliger SL, Christenson R, Gottdiener JS, Psaty BM, deFilippi CR. Soluble ST2 for prediction of heart failure and cardiovascular death in an elderly, community-dwelling population. *J Am Heart Assoc*. (2016) 5:e003188.
- Marino R, Magrini L, Orsini F, Russo V, Cardelli P, Salerno G, et al. Comparison between soluble ST2 and high-sensitivity troponin i in predicting short-term mortality for patients presenting to the emergency department with chest pain. *Ann Lab Med*. (2017) 37:137–46. doi: 10.3343/alm.2017.37.2.137
- Dudek M, Kałuzna-Oleksy M, Migaj J, Straburzyńska-Migaj E. Clinical value of soluble ST2 in cardiology. *Adv Clin Exp Med*. (2020) 29:1205–10
- Kakkar R, Lee RT. The IL-33/ST2 pathway: therapeutic target and novel biomarker. *Nat Rev Drug Discov*. 2008; 7:827–840.
- Villacorta, H., & Maisel, A. S. (2016). Soluble ST2 testing: a promising biomarker in the management of heart failure. *Arquivos brasileiros de cardiologia*, 106, 145-152.



# The Study of the Effect of Different Concentrations of Grape Seed Oil On Growth Rates and Some Biochemical Parameters of Common Carp Fish

دراسة تأثير تراكيز مختلفة من زيت بذور العنب على معدلات النمو وبعض المعايير الكيموحيوية

## لأسماك الكارب الشائع

Israa Adel Fadhil<sup>1</sup>

Layla Abboud Aufy<sup>2</sup>

Khulood Abdul Ali<sup>3</sup>

Shaymaa A.J. Al-jumaiee<sup>4</sup>



© 2024 The Author(s). This open access article is distributed under a Creative Commons Attribution (CC-BY) 4.0 license.



## الملخص

أجريت الدراسة لمعرفة تأثير زيت بذور العنب كمحفز مناعي ولدعم النمو عند إضافته. إلى علائق صغار أسماك الكارب الشائع. Cyprinus carpio. استعملت 90 سمكة تراوح معدل أوزانها 36.5 غم. وضعت الأسماك في أحواض نظام مائي دوار (ARS) وأقلمت لمدة 14 يوماً. غذيت بنسبة 3% من وزن الجسم على علائق مضاف لها تراكيز مختلفة من مستخلص زيت بذور العنب: معاملة السيطرة (0%)، المعاملة الأولى (0.2%)، المعاملة الثانية (0.5%)، المعاملة الثالثة (1%)، T3 قيست العوامل البيئية خلال التجربة وهي درجة حرارة الماء، الأوكسجين، الأس الهيدروجيني والملوحة أوضحت نتائج الدراسة الحالية أن أعلى قيمة لإنزيم الفوسفاتيز القاعدي كانت في المعاملة الثالثة بعد 40 يوم من التغذية (77.60) وحدة دولية/ لتر على التوالي في المعاملة الثالثة (1%)، كما بينت نتائج التحليل الإحصائي عدم وجود فروق معنوية ( $P > 0.05$ ) في تركيز إنزيم الفوسفاتيز القاعدي في المعاملات T1 و T2 مقارنةً بعينة السيطرة، بالإضافة إلى عدم وجود فروق معنوية في تركيز إنزيم ناقل الاثنين في دم الأسماك في جميع معاملات التجربة عدا المعاملة الثالثة سجلت اختلافاً معنوياً إذ بلغت (8.89) وحدة دولية/ لتر. كذلك لم تكن هناك فروق معنوية في تركيز ناقل الأسبارتيز في دم أسماك المعاملة الأولى والثانية بينما سجلت المعاملة الثالثة اختلافاً معنوياً مقارنةً بمعاملة السيطرة، إذ بلغت (56.28) وحدة دولية/ لتر بعد 40 يوم من التغذية.

الكلمات المفتاحية: زيت بذور العنب، تحفيز المناعة، معايير النمو، المعايير الكيموحيوية

## Abstract:

The study was conducted to know the effect of grape seed oil as an immune stimulant and to support growth when added to the diet of young common carp *Cyprinus carpio*. 90 fish were used with average weights rang was 36.5g. The fish were placed in recirculating water system (ARS) tanks and acclimatized for 14 days. They were fed at a rate of 3% of their body weight on diets to which different concentrations of grape seed oil extract were added: control treatment C (0%), first treatment T1 (0.2%), second treatment T2 (0.5%), third treatment T3 (1%). The environmental factors were measured during the experiment, which were water temperature, oxygen, pH and salinity. The results of the current study showed that the highest value of alkaline phosphatase enzyme was in the third treatment after 40 days of feeding (77.60) IU/L, respectively, in the third treatment (1%). The results of the statistical analysis also showed that there were no significant differences ( $P > 0.05$ ) in the concentration of alkaline phosphatase enzyme in treatments T1 and T2 compared to the control sample, in addition to the absence of significant differences in the concentration of the urinary transporter enzyme in the blood of fish in all experimental treatments except the third treatment, which recorded a significant difference, reaching (8.89) IU/L. There were also no significant differences in the concentration of the vector in the blood of fish in the first and second treatments, while the third treatment recorded a significant difference compared to the control treatment, as it reached ( 56.28) IU/L after 40days feeding.

**Keywords** Grape Seed Oil; Immune Stimulation; Growth Standards; Biochemical Standards.



<http://dx.doi.org/10.47832/MinarCongress12-24>

<sup>1</sup> Marine Science Center, University of Basra, Iraq

<sup>2</sup> Marine Science Center, University of Basra, Iraq

<sup>3</sup> Marine Science Center, University of Basra, Iraq

<sup>4</sup> Marine Science Center, University of Basra, Iraq

## المقدمة

تعتبر الأسماك أحد أكبر وأهم المجاميع الفقرية التي تقطن البيئة المائية، وتقع في قمة المستهلكات في السلسلة الغذائية في النظام البيئي المائي، وتمثل الأسماك 17% من البروتين الحيواني المتناول عالمياً (FAO, 2016) تغذية الأسماك تلعب دوراً حاسماً في الاستزراع السمكي لأنها تؤثر على تكلفة الإنتاج من خلال تأثيرها المباشر على النمو (Gatlin, 2002) تزايدت في الوقت الحاضر الدراسات لاستخدام النباتات الطبية كإضافات علفية في تربية الأسماك أكثر من الإضافات العلفية التقليدية التي غالباً ما تسبب مشاكل مترافقة مع التلوث البيئي (Shalaby, وآخرون 2006). يعد استخدام الأعشاب نهجاً قديماً لعلاج مجموعة من المشكلات الصحية وتقوية مناعة الجسم.

العنب أحد أكثر أنواع النباتات أهمية من الناحية الاقتصادية نظراً لاستخداماته المتنوعة في إنتاج عصير العنب والمنتجات الغذائية الأخرى. Ali et al. (2010) يُزرع في جميع القارات في المناطق المعتدلة حيث الأمطار الكافية والصيف الدافئ والجاف وكذلك الشتاء المعتدل نسبياً وهي أنماط مناخية طبيعية (Vivier and Pretorius, 2000) تتميز صفات منتجات العنب بتركيباتها الأيضية. تمثل مركبات الفلافونويد مجموعة واسعة الانتشار وشائعة من مادة البوليفينول الطبيعية التي ينتجها. (Ananga et al., 2013 and Vogt, 2010)

استخدم (Nader and Abdul Rahman 2017) مخلفات العنب الأسود في علائق أسماك الكارب الشائع ودراسة تأثيرها على عدد خلايا الدم الحمر، خلايا الدم البيض، العد التفريقي لكريات الدم البيض، نسبة الهيموكلوبين. كما استخدمت السعد (2017) المستخلص المائي لورق الغار (2%) في عليقة صغار أسماك الكارب الشائع الذي أدى إلى تحسين أداء النمو والحالة الصحية للأسماك مقارنةً بالمعاملات الأخرى (1% و3%) ومعاملة السيطرة.

## أهداف الدراسة

هدفت الدراسة لاستعمال بعض المحفزات المناعية مثل زيت بذور العنب، وإضافته إلى عليقة صغار أسماك الكارب الشائع بثلاث تراكيز مختلفة (0.2% و0.5% و1%) وتأثيرها على معدلات النمو وبعض المعايير الكيموحيوية لأسماك الكارب الشائع.

## المواد وطرائق البحث

نقلت الأسماك إلى المختبر باستخدام أكياس بلاستيك سعة 3 لتر، حاوية على ماء من نفس بيئة الأسماك لتقليل الإجهاد على الأسماك أثناء عملية النقل. كان معدل الوزن الكلي للأسماك 36.36 ± 0.38 غم ومعدل الطول الكلي 1.24 ± 13.65 سم.

وزعت الأسماك بشكل عشوائي ومتساوٍ على الأحواض البلاستيكية ذات حجم 30 x 40 x 60 سم لغرض أقلمتها لمدة 14 يوماً، إذ غذيت على عليقه سيطرة بنسبة 3% من وزن الجسم إلى نهاية التجربة من أجل إقامة الأسماك على الأحواض البلاستيكية والعلائق التجريبية. وزعت الأسماك على أحواض التربية بواقع 8 أسماك للحوض الواحد بعدها وزعت الأسماك بواقع مكررين لكل معاملة وحسب نسب إضافة زيت بذور العنب إلى العلائق السمكية (0.0%، 0.2%، 0.5%، 1%). وضع العلف في موضع محدد من الحوض وبواقع وجبتين لليوم الواحد إذ أعطيت الوجبة الأولى عند الساعة

التاسعة صباحاً والوجبة الثانية عند الساعة الثانية ظهراً أجريت عملية وزن الأسماك لجميع الأحواض كل أسبوعين بوساطة ميزان حساس.

### تحضير العلائق

جمعت المواد العلفية من الأسواق المحلية المستخدمة في تصنيع علائق التجربة وهي مركز مسحوق السمك، فول الصويا، ذرة صفراء، الحنطة المحلية، مجموعة الفيتامينات والأملاح والأحماض الأمينية اللايسين والميثونين. كما جلبت المادة المضافة (زيت بذور العنب) المراد اختبار كفاءتها من الأسواق المحلية إذ تم طحن المواد العلفية جيداً وغرلت باستعمال منخل مختبري ذي فتحات 0.4 ملم، بعدها وزنت كل مادة لوحدها وحسبت النسب المحسوبة، ثم خلطت المواد العلفية لتكوين العلائق جيداً لغرض التجانس، أضيف ما يقارب 300 مل ماء مغلي لكل 500 غم من الخليط بعدها تم مزج الخليط جيداً، ثم أضيفت الفيتامينات والأملاح والزيت، بعدها شكلت العلائق باستعمال ماكينة الفرز ذو فتحات متوسطة وجففت في درجة حرارة الغرفة لمدة 24 ساعة، ثم وضعت العلائق في أكياس بلاستيكية (البولي إيثيلين) وحفظت في الثلاجة لحين الاستعمال (Lovell, 1989).

### أنزيم الفوسفاتيز القاعدي (ALP) : Alkaline phosphatase

قدرت فعالية أنزيم ALP في مصلى دم الأسماك باستعمال جهاز المطياف الضوئي وعلى طول موجي 510 نانومتر، بوساطة عدة تقديرية جاهزة kit من إنتاج شركة Randox، وحسبت فعالية الأنزيم حسب المعادلة التالية:

$$\text{فعالية الأنزيم (وحدة دولية / لتر)} = (\text{قراءة النموذج} - \text{قراءة العينة الضابطة} / \text{القراءة القياسية}) \times 142$$

### أنزيم Aspartate amino transferase (AST)

قدرت فعالية أنزيم AST في مصلى دم الأسماك باستعمال جهاز المطياف الضوئي وعلى طول موجي 510 نانومتر، بوساطة عدة تقديرية جاهزة kit من إنتاج شركة Randox، وحسبت فعالية الأنزيم حسب المعادلة التالية:

$$\text{فعالية الأنزيم (وحدة دولية / لتر)} = (\text{قراءة النموذج} - \text{قراءة العينة المقارنة} / \text{القراءة القياسية}) - \text{قراءة العينة الضابطة} \times 100$$

### أنزيم Alanine amino transferase (ALT)

قدرت فعالية أنزيم ALT في مصلى دم الأسماك باستعمال جهاز المطياف الضوئي وعلى طول موجي 510 نانومتر، بوساطة عدة تقديرية جاهزة kit من إنتاج شركة Randox، وحسبت فعالية الأنزيم حسب المعادلة التالية:

$$\text{فعالية الأنزيم (وحدة دولية / لتر)} = (\text{قراءة النموذج} - \text{قراءة العينة المقارنة} / \text{القراءة القياسية}) - \text{قراءة العينة الضابطة} \times 100$$

## النتائج :

بين جدول ( 1 ) نتائج تحليل التركيب الكيميائي للعلائق السمكية المستخدمة في التجربة إذ كانت متقاربة في نسبة الرطوبة في العليقة المضاف لها زيت بذور العنب في المعاملات T1 و T2، إذ بلغت نسبتها 2.96 و 2.89 على التوالي مقارنة بعينة السيطرة 2.85 مع ازدياد طفيف غير معنوي ( $p>0.05$ ) في نسبة الرطوبة عند المعاملة T3 البالغ نسبتها 7 في حين كانت نسبة البروتين والدهن متقاربة في جميع المعاملات عدا المعاملة T2، إذ لوحظ ارتفاع طفيف غير معنوي ( $p>0.05$ ) في نسبة البروتين، في حين كانت قيم الرماد متقاربة في عينة السيطرة و T2 و T3 (5.87 , 5.88, 5.95) % وحصول ارتفاع طفيف غير معنوي في المعاملة T1 التي بلغت فيها نسبة الرماد (6.) كما لم يلاحظ اختلافات معنوية في قيم الكربوهيدرات لكل معاملات التجربة (T1 49.3 و T2 48.88 و T3 48.22) % مقارنة بمعاملة السيطرة (50.28) %.

جدول 1- التركيب الكيميائي % للعلائق المستخدمة في الدراسة الحالية

المحتويات	عينة السيطرة	عينة T1 (0.2%)	عينة T2 (0.5%)	عينة T3 (1%)
رطوبة	2.85 <sup>A</sup>	2.96 <sup>A</sup>	2.89 <sup>A</sup>	3.07 <sup>A</sup>
بروتين	30.35 <sup>A</sup>	30.1 <sup>A</sup>	31.71 <sup>A</sup>	30.64 <sup>A</sup>
دهن	9.61 <sup>A</sup>	9.49 <sup>A</sup>	9.62 <sup>A</sup>	9.31 <sup>A</sup>
رماد	5.95 <sup>A</sup>	6.0 <sup>A</sup>	5.88 <sup>A</sup>	5.87 <sup>A</sup>
كربوهيدرات	50.28 <sup>A</sup>	49.3 <sup>A</sup>	48.88 <sup>A</sup>	48.22 <sup>A</sup>

القيم التي تحمل حروفاً متشابهة في نفس الصف لا تختلف معنوياً ( $p>0.05$ ).

## أنزيم الفوسفاتيز القاعدي (ALP) Alkaline phosphatase:

بين جدول (2) نتائج تركيز أنزيم ALP في مصبل دم أسماك الكارب الشائع والمغذيات على علائق مضاف لها نسب مختلفة من زيت بذور العنب (0.2, 0.5, 1) % وعينت السيطرة في نهاية تجربة التغذية، إذ لوحظ حصول ارتفاعاً معنوياً ( $p<0.05$ ) (نتيجة سلبية) في تركيز الأنزيم في المعاملة T3 عند مستوى معنوية (0.05 77.60 وحدة دولية/ لتر) مقارنةً مع عليقة السيطرة غير المضاف لها زيت بذور العنب التي وصل فيها التركيز إلى 61.60 وحدة دولية/ لتر.

## أنزيم ناقل الأمين ألانين (ALT) Alanine amino transferase:

لوحظ من خلال نتائج التحليل الإحصائي لإنزيم ALT بعد 40 يوم من التغذية على علائق مختلفة من زيت بذور العنب عدم وجود فروقات معنوية ( $p>0.05$ ) في جميع المعاملات المدروسة الموضحة في الجدول (2) عدا الارتفاع المعنوي السلبي في المعاملة T3 المضاف لها زيت بذور العنب بنسبة 1% التي وصل فيها التركيز إلى 8.79 وحدة دولية/ لتر مقارنةً مع المعاملات الأخرى (عينة السيطرة والمعاملة T1 و T2) التي بلغ فيها التركيز (5.20، 6.52، 6.33) وحدة دولية/ لتر على التوالي لإنزيم ALT في دم أسماك الكارب الشائع المغذاة على علائق مختلفة.

## أنزيم ناقل الأمين أسبارتيز (AST):

كان تركيز أنزيم AST في نهاية تجربة التغذية بين المعاملات المضاف لها زيت بذور العنب ومعاملة السيطرة، إذ حصل ارتفاع سلبي في تركيز أنزيم ناقل الأسبارتيز في المعاملة T3 المضاف لها زيت بذور العنب بنسبة 1% بعد 40 يوماً من التغذية مقارنةً بمعاملة السيطرة والمعاملة T1 والمعاملة T2، في حين توجد فروقات معنوية (نتائج سلبية) بين عينة السيطرة الإيجابية والمعاملة T3 وهذا ما موضح في الجدول ...

جدول 2- تركيز أنزيم الفوسفاتيز القاعدي وأنزيمات ناقلات الأمين في دم أسماك الكارب الشائع المغذات 40 يوم على نسب مختلفة من زيت بذور العنب.

المعاملة الثالثة (%)	المعاملة الثانية (%0.5)	المعاملة الأولى (%0.2)	معاملة السيطرة	المعاملات
المعدل + الانحراف المعياري				
1.00±77.60 B	1.27±64.83 A	±1.41±64.76 A	2.41±61.60 A	الفوسفاتيز القاعدي ALP
0.09±8.89 B	0.05±6.33 A	0.40±6.52 A	0.22 ±5.20 A	انزيم ناقل الأمين الألتين ALT
2.41±56.28 B	1.86±42.44 A	1.30±44.24 A	2.49±40.32 A	انزيم ناقلالأمين الاسبارتيز AST

## المناقشة

## المعايير الكيموحيوية

إن الهدف الأساسي من دراسة هذه المعايير هو معرفة الإجهاد التأكسدي للأسماك والتخلص منه عن طريق إزالة الجذور الحرة من أنسجة الجسم، لا سيما جذر الأوكسجين الحر (Bashan et al., 2009) ROS تتمثل عملية إزالة السموم أثناء التمثيل الغذائي عن طريق الإجهاد التأكسدي (Stankiewicz et al., 2002) فإن تناول أي مادة ضارة وينسب مرتفعة تؤدي إلى تكون جذور ROS داخل الكبد والكلية؛ مما يسبب تلف هذه الأنسجة، والذي بدوره يؤدي إلى إحداث تلف وخلل وظيفي أثناء عمل هذه الأنسجة. (Ortiz et al., 2005).

تعد إنزيمات ALT و AST و ALP من أهم الإنزيمات الموجودة في الكائن الحي، لا سيما أنسجة الكبد، وأي تغيير يصيب الكائن الحي يؤدي إلى الخلل في عمل هذه الإنزيمات؛ مما يلحق الضرر في عمل وظيفة الكبد، عادة ما تكون هذه الإنزيمات داخل خلايا الكبد والقلب والعضلات والكلية والخياشيم والأعضاء الأخرى، ويتحرر من الخلايا في حالة تلفها، - (Mammary et al., 2002).

يعد إنزيم ناقل الأسبارتيز AST الأكثر تحديدا لمشاكل الكبد، والمستويات العالية منه ممكن أن تلاحظ عند الإصابة بالتهابات الكبد، أما أنزيم ناقل الألتين ALT فالمصدر الرئيسي له هو الكبد أيضاً، بالرغم من وجوده في أنسجة أخرى، وأن هذا الأنزيم له دوراً مهماً في أيض الأحماض الأمينية والكاربوهيدرات في أنسجة الكائنات الحية ومنها الأسماك، لذا فإن قياس نشاطه يساعد في تشخيص العديد من الأمراض الكبدية. (Rajamanickam and M.husband, 2008).



أما أنزيم الفوسفاتيز القاعدي ALP ، فيوجد في أنسجة مختلفة وخصوصاً أغشية الخلايا، إذ يحفز التحلل المائي لأسترات أحادية الفوسفات Monophosphate esters ، وهذا الإنزيم يكون واسع الانتشار في الجسم، يوجد في الكبد والأمعاء والكلى، ويساعد خلايا الأمعاء في نقل الفسفور اللاعضوي، وفي امتصاص الدهون، بالإضافة إلى أنه يساعد في عمليات تكلس العظام، ويرتفع تركيز هذا الأنزيم عند الإصابة بأمراض الكبد وخلل في عمل الكلى وأمراض العظام (Mohamed et al., 2019).

بينت نتائج التحليل الإحصائي SPSS ارتفاع معنوي في مستوى إنزيم ALT و AST و ALP للمعاملة T3 فقط مقارنة مع مجموعة السيطرة، وكانت المعاملة T2 هي الأفضل مستوى في قياس الإنزيمات المدروسة، التي كانت نتائجها مقارنة إلى عينة السيطرة، يعود ذلك إلى وجود المجاميع الفعالة في زيت بذور العنب بالتركيز المناسب في المعاملة الثانية ربما أدت إلى الحفاظ على مستوى تركيز هذه الإنزيمات بالمدى الملائم مقارنةً بالمعاملات الأخرى.

يعتبر زيت بذور العنب مضاد أكسدة طبيعي جيد ضد الأيونات الحرة التي تتحرر نتيجة عوامل الإجهاد التأكسدي، ومنها عملية الأيض التي تحدث داخل الخلايا، وعند زيادة مستوى الأيونات الحرة المتحررة أكبر من مستوى مضادات الأكسدة، فإنه يؤدي إلى تحطم خلايا الجسم وزيادة إفراز إنزيمات الكبد، ولكون وجود مركب البروسيين في العنب الذي له تأثير مباشر في عملية كسح جذور الأوكسجين الحرة؛ مما أدى إلى تقليل الإجهاد التأكسدي. (Li anything, 2004).

إن زيادة تركيزه يؤدي إلى حدوث تسمم الكبد أو تضرر خلاياه (Wang et al., 2015) ، وهذا ما تم ملاحظته في المعاملة T3 المضاف لها زيت بذور العنب بنسبة 1%، وقد يعود السبب في هذا الارتفاع إلى حاجة الأنسجة إلى الطاقة نتيجة الإجهاد وضعف الأنسجة، لأن بعض من هذه الإنزيمات وسيط رئيسي في دورة كريبس Krebs cycle (James et al., 1991)، وهذا يتفق مع ما توصل إليه العتاي (2012) عند استخدامه لمسحوق جذور نبات الزنجبيل وفصوص الثوم المطحون المضافة لصغار أسماك الكارب الشائع، وهذا ما أكدته (Zamani and Moafi 2018) في دراسته وتسجيل الانخفاض غير المعنوي بهذه الإنزيمات مقارنةً بعينة السيطرة في أسماك التراوت القزحي عند تغذيته على عليقة تحتوي على زيت بذور العنب بنسبة 50% استبدال عن زيت السمك، وقد أوعز السبب في هذا إلى وجود المكونات الفعالة المفيدة في العنب، عند ارتفاع تراكيز هذه الأنزيمات في مصد الدم تؤدي إلى مرض نخر الكبد؛ وبالتالي يؤثر على عضلة القلب والعضلات الأخرى (Srinivasan and Krishnamurthy, 1977).

### معايير النمو

يوضح الجدول (3) معايير النمو لأسماك الكارب المعدلات على علائق ذات نسب مختلفة من زيت بذور العنب، بينت النتائج عدم وجود فروقات معنوية ( $P>0.05$ ) في معدل الأوزان عند بداية التجربة لكافة المعاملات، وبينت أن أعلى معدل نمو وزيادة وزنية بعد 40 يوماً من التغذية حققها أسماك المعاملة الثانية والثالثة، إذ وصل معدل الوزن النهائي 44.13 و 40.37 غم ومعدل الزيادة الوزنية 7.76 و 4.14 غم على التوالي مقارنة بمعاملة السيطرة.

بينت نتائج التحليل الإحصائي أن معدل النمو النسبي للمعاملة الأولى لم يختلف معنوياً ( $P>0.05$ ) عن معاملة السيطرة (4.76 و 4.79%) على التوالي، بينما أظهرت المعاملة الثالثة اختلافاً معنوياً عن معاملة السيطرة والمعاملة الأولى

(11.45%)، أما المعاملة الثانية، فقد أظهرت تفوقاً معنوياً ( $p < 0.05$ ) في معدل النمو النسبي الذي بلغ 21.46% عن بقية المعاملات.

أوضحت النتائج أن أسماك المعاملة الأولى كان لها أفضل نسبة تحويل غذائي (19.52) مقارنة مع معاملة السيطرة. بينت نتائج التحليل الإحصائي عدم وجود فروقات معنوية ( $P > 0.05$ ) بين معاملة السيطرة والمعاملة الأولى في قيم كفاءة التحويل الغذائي (4.13 و 5.19) في حين أظهرت المعاملة الثانية والثالثة (21.34 و 11.97) اختلافاً معنوياً عن معاملة السيطرة والمعاملة الأولى أظهرت فروقاً معنوية فيما بينها.

جدول 3- معايير النمو لأسماك الكارب المغذات على علائق ذات نسب مختلفة من زيت بذور العنب

المعاملة الثالثة (%)	المعاملة الثانية (%0.5)	المعاملة الأولى (%0.2)	معاملة السيطرة	المعاملات
المعدل + الانحراف المعياري				معايير النمو
0.40 +36.22 A	0.39 +36.30 A	0.37 +36.15 A	0.38 +35.36 A	معدل الوزن الابتدائي (غم)
0.41 +40.37 B	1.13 +44.13 C	0.16 +37.88 A	0.14 +35.88 A	معدل الوزن النهائي (غم)
0.06 +4.14 B	0.80 +7.76 C	0.24 +1.72 A	0.24 +1.73 A	معدل الزيادة الوزنية (غم)
0.21 +11.45 B	2.06 +21.46 C	0.71 +4.79 A	0.71 +4.76 A	معدل النمو النسبي (%)
0.005 +0.21 B	0.032 +0.38 C	0.015 +0.093 A	0.016 + 0.19 A	معدل النمو النوعي (غم/يوم)
0.13 +8.35 B	0.37 +4.70 C	2.84 +19.52 A	1.87 +17.23 A	نسبة التحويل الغذائي
0.19 +11.97 B	1.76 +21.34 C	0.76 +5.19 A	0.65 +4.13 A	كفاءة التحويل الغذائي

\*القيم التي تحمل حروفاً متشابهة في نفس الصف لا تختلف معنوياً ( $p > 0.05$ ).

اتفقت النتائج الحالية مع تلك نتائج التي وجدها (Seden et al., 2009) والذي أشار إلى أن تغذية اصبعيات أسماك البلطي على غذاء مدعم بتركيز مختلفة من مستخلص *O. vulgare* أدى إلى تحسين أداء النمو (الوزن النهائي، الزيادة الوزنية، معدل النمو النوعي، معدل التحويل الغذائي ومعدل البقاء) وأعزى السبب إلى وجود الزيوت الأساسية التي تحتوي على مضادات ميكروبية ومضادات أكسدة ومواد أخرى نشطة بيولوجياً. في حين أشار (Ahmad et al., 2009) إن التركيز 0.5% من مستخلص *O. vulgare* أعطى أفضل وزن نهائي وزيادة وزنية ومعدل نمو نوعي لأسماك البلطي النيلي مقارنة مع التركيزين 1% و 2% وأعزى السبب لزيادة تناول العلف وهضم المغذيات فضلاً عن احتواء *O. vulgare* على العديد من العناصر الغذائية كالزيوت الأساسية والفيتامينات والمعادن، والتي تساعد على تعزيز النمو. بين (Abdel-Latif and Khalil (2014) إن إضافة زيت *O. vulgare* لغذاء أسماك البلطي النيلي أعطى أفضل زيادة وزنية ومعدل نمو نوعي أفضل كفاءة تحويل غذائي ومعامل تحويل غذائي، نتيجة تحسن هضم البروتين وتخليقها وزيادة الكولاجين للنسيج

العضلي. بين (Diler et al., 2017) إن زيت O.vulgare المضاف بتركيز مختلفة أدى إلى زيادة الوزن ومعدل النمو وتحسين كفاءة التحويل الغذائي، وأعزى السبب لاحتواء O.vulgare على نكهة عطرية مميزة؛ مما يؤدي إلى زيادة تناول العلف كما يحتوي على العديد من المركبات النشطة التي تحث إفراز الإنزيمات الهاضمة؛ ومن ثمَّ زيادة استهلاك الغذاء وامتصاص العناصر الغذائية. اتفقت النتائج الحالية مع ما توصل إليه (Rashidian et al., 2021) إذ بين أن المستخلص زيت بذور العنب 0.5% كان له تأثير قوي على النمو والزيادة الوزنية ومعدل النمو وانخفاض نسبة التحويل الغذائي مقارنة مع السيطرة، وأشار إلى أن الآليات المسؤولة عن ذلك غير مفهومة تماما لاحظ ((El Araby and El-Arabey, 2016) التأثير المعزز للنمو عند استخدامه لمستخلص O.vulgare في علائق أسماك البلطي النيلي، وإن التركيز 0.5% أعطى أعلى زيادة وزنية وأفضل معدل نمو نوعي لاحتوائه على زيوت عطرية وتوربينات ذات الفعالية المضادة للميكروبات ومضادات أكسدة وأنشطة بيولوجية أخرى. بين (El-Hawarry et al., 2018) إن زيت O.vulgare عمل على تحسن في أداء النمو مع زيادة التركيز المضاف عند استزراع أسماك البلطي النيلي بكثافات مختلفة، وأن تعزيز النمو يعود محتواه العالي من الثيمول والكارفاكروال التي تعمل على تحفيز إفراز ونشاط الإنزيمات الهاضمة.

بين (Rourkela et al., 2021) إن إضافة زيت O.vulgare في علف أسماك البلطي النيلي عامل رئيسي لنجاح أنظمة الاستزراع المكثف، إذ عمل على تحفيز النمو وزيادة قدرة مضادات الأكسدة، وأعزى السبب إلى دور زيت O.vulgare في تحمل الحموضة العالية في الجهاز الهضمي؛ مما يضمن فعاليته وتأثيره، إضافة إلى محتواه من الزيوت الطيارة التي تحفز الجينات المرتبطة بالشهية، كذلك قدرته كمضاد للجراثيم التي تساعد في القضاء على الكائنات الدقيقة الضارة، وتسمح للنافعة بالمساعدة في هضم العناصر الغذائية عن طريق إفراز الإنزيمات الهاضمة.

مع التحسن الملحوظ في أداء نمو الكارب الشائع في الدراسة الحالية، أظهرت العديد من الدراسات أن البوليفينول الغذائي قادر على التأثير على امتصاص العناصر الغذائية في الخلايا المعوية (Johnston et al., 2005) ويمكن أن يعزى التحسن الحالي إلى هذه النتيجة. علاوة على ذلك، من الممكن أن يكون للبوليفينول الغذائي تأثيرات مفيدة في عملية التمثيل الغذائي الوسيط، والتي يمكن أن تساهم في زيادة كفاءة العناصر الغذائية لنمو الحيوان (Fiesel et al.2014).

#### الإستنتاجات:

1. إن استعمال زيت بذور العنب كمضاف غذائي طبيعي إلى علائق صغار أسماك الكارب الشائع له تأثير إيجابي في زيادة النمو للأسماك، وأن أفضل تركيز لزيت بذور العنب كان في المعاملة T2
- 2- تحسن الصورة الدموية للأسماك ، وكانت المعاملة T2 هي الأفضل مستوى في قياس الإنزيمات المدروسة، التي كانت نتائجها مقارنة إلى عينة السيطرة.

## المراجع

- السعد, صفاء عدنان شعبان (2017). تأثير استخدام المستخلص المائي لورق الغار *Laurus nobilis* كسابق حيوي في النمو والحالة الصحية لأسماك الكارب الشائع *Cyprinus carpio* L. رسالة ماجستير, كلية الزراعة, جامعة البصرة: 94 صفحة.
- Abdel-Latif, H. M.; Abdel-Tawwab, M.; Khafaga, A. F. and Dawood, M. A. (2020). Dietary oregano essential oil improved the growth performance via enhancing the intestinal morphometry and hepato-renal functions of common carp (*Cyprinus carpio* L.) fingerlings. *Aquaculture*, 526: 735432.
- Ahmad, M. H.; El-Gamal, R. M.; Hazaa, M. M.; Hassan, S. M. and El Araby, D. A. (2009). The use of *Origanium vulgare* extract in practical diets as a growth and immunity promoter for Nile tilapia, *Oreochromis niloticus* (L.) fingerlings challenged with pathogenic *Pseudomonas aeruginosa* and *Pseudomonas flourescence*. *Egypt. J. Exp. Biol.(Zoology)*, 5: 457-463
- Alishahi, M.; Ranjbar, M.M.; Ghorbanpour, M.; Peyghan, R.; Mesbah, M. and Razi Jalali, M. (2010). Effects of dietary Aloe vera on some specific and nonspecific immunity in the common carp (*Cyprinus carpio*). *Int. J. Vet. Res.*, 3: 189-195.
- Bashan, N., J. Kovsan, I. Kachko, H. Ovadia, A. Rudich, 2009. Positive and negative regulation of insulin signaling by reactive oxygen and nitrogen species. *Physiol. Rev.*, 89(1): 27-71
- El Araby, D. A., and El-Arabey, A. A. (2016). New Approach to use *Origanium Vulgare* Extract as Immunostimulant to Increase Resistance to *Pseudomonas aeruginosa* and *Pseudomonas flourescence*. *J. Mar. Sci.: Res. Dev.* 6(1): 182-187.
- El-Hawarry, W. N.; Mohamed, R. A. and Ibrahim, S. A. (2018). Collaborating effects of rearing density and oregano oil supplementation on growth, behavioral and stress response of Nile tilapia (*Oreochromis niloticus*). *Egypt. J. Aquat. Res.*, 44(2):173-178.
- FAO (2016). The state of world fisheries and aquaculture. Rome, 200 pp .
- Fegan, M.; Paul F. P.; Hayward, A. C.; Davis, H. G. AND Fuerst, J. A. (1990) Phenotypic Conversion of *Pseudomonas aeruginosa* in Cystic Fibrosis. *Journal of Clinical Microbiology*, 28(6): 1143-1146.
- James, R.; Sivakumar, V.; Sampath, K. and Rajendran, P. (1991). Individual and combined effects of zinc; cadmium and copper on growth of *Oreochromis mossambicus*. *Indian J. Fish*, 38(3): 198-200.

- Li, L. and Zhong, J. (2004). Effect of grape procyanidins on the apoptosis and mitochondrial transmembrane potential of thymus cells. *Wei. Sheng Yan. Jiu.*, 33: 191.
- Mohamed, A.S., Gad, N.S. and El Desoky, M.A. (2019). Liver enzyme activity of *Tilapia zillii* and *Mugil capito* collected seasonally from Qarun Lake, Egypt. *Fish Aqua. J.* 10(1): 1-4.
- Nader, P. J. and Abdulrahman, N. M. (2017). Impact of black grape by products on blood picture in common carp (*Cyprinus carpio* L.). *Basrah J. Agric. Sci.*, 30(1): 32-37
- Rajamanickam, V. and Muthuswamy, N. (2008). Effect of heavy metals induced toxicity on metabolic biomarkers in common carp (*Cyprinus Carpio* L.). *Maejo Int. J. Sci. Technol.*, 2(1): 192–200
- Rashidian, G., Boldaji, J. T., Rainis, S., Prokić, M. D. and Faggio, C. (2021). Oregano (*Origanum vulgare*) extract enhances zebrafish (*Danio rerio*) growth performance, serum and mucus innate immune responses and resistance against *Aeromonas hydrophila* challenge. *Animals*, 11(2), 299.
- Seden, M. E. A.; Abbass, F. E. and Ahmad, M. H. (2009). Effect of *Origanum vulgare* as a feed additive on growth performance, feed utilization and whole body composition of Nile tilapia (*Oreochromis niloticus*) fingerlings challenged with pathogenic *Aeromonas hydrophila*. *Journal of Animal and Poultry Production*, 34(3): 1683-1695.
- Shalaby, A. M.; Khattab, Y. A. and Abdel Rahman, A. M. (2006). Effects of Garlic (*Allium sativum*) and chloramphenicol on growth performance, physiological parameters and survival of Nile tilapia
- Shourbela, R. M.; El-Hawarry, W. N.; Elfadadny, M. R. and Dawood, M. A. (2021). Oregano essential oil enhanced the growth performance, immunity, and antioxidative status of Nile tilapia (*Oreochromis niloticus*) reared under intensive systems. *Aquaculture*, 542, 736868.
- Srinivasan, K. and Krishnamurthy, R. (1977). Effects of  $\beta$  and  $\gamma$  isomers of hexachlorocyclohexane on some liver and kidney enzymes in albino rats. *Current Sci.*, 46(17): 598-600.
- Stankiewicz, A.; Skrzydlewska, E, and Makiela, M. (2002). Effects of amifostine on liver oxidative stress caused by cyclophosphamide administration to rats. *Drug Metabol. Drug Interact.*, 19(2): 67-82.
- Wang, Z.; Zhang, Z.; Wang Du.N.K.; and Li, L. (2015). Hepatoprotective effects of grape seed procyanidin B2 in rats with carbon tetrachloride-induced hepatic fibrosis. *Altern. Ther. Health Med.*, 2: 12-21.
- Zamani, A. and Moafi A. (2018). Effect of replacement of fish oil by grape seed oil on growth indices and protease enzymes activity in *Oncorhynchus mykiss*. *J. Fishe. Sci. Technol.*, 7(1): 71-79.



## Effect of Hydrocortisone On Some Physiological and Morphological Changes in Mice Fetus

Maha Khalaf Ali <sup>1</sup>

Amina Jasim Al-Hayani <sup>2</sup>

Hassan I Mohamed <sup>3</sup>




© 2024 The Author(s). This open access article is distributed under a Creative Commons Attribution (CC-BY) 4.0 license.

### Abstract:


*The purpose of the current study was to investigate the effects of hydrocortisone during the prenatal stage and its subsequent effects on various phenotypic abnormalities and morphologies in pregnant mice and their offspring. Rats were given hydrocortisone acetate treatment from the first day of pregnancy to day eighteen, at varying doses of 0.10–0.15–0.20 mg/day. An experiment using thirty-two pregnant mice was conducted. Three groups of eight pregnant mice each make up each experimental set-up. Eight untreated pregnant mice (control group) were included in the first group; eight pregnant mice treated with hydrocortisone dosage of 0.20 milligrams per kilogram, these animals treated with a body weight of 0.15 mg/kg, and these mice treated with 0.01 mg/Kg of hydrocortisone were included in the second group. The statistical analysis showed that the typical embryo's length, weight, and quantity in pregnant mice decreased significantly in contrast to the group under authority. Additionally, the organs of the pregnant mice— The placenta, brain, spleen, liver, heart, kidney, lung, and reproductive system all significantly decreased. The dosage of hydrocortisone mostly causes the following physiologic malformations: head cap atrophy, tissue invasions, many bleeding sites, particularly the bloody area at the mid-dorsum, and hooked tails. Based on the previously provided information, we deduced that the administration of hydrocortisone resulted in the malformation of several organs. With the exception of the (0.2 mg/Kg) group, all embryos exhibited decreased mother weight upon adsorption. Pregnant women tend to become sedentary with accumulated bulk in their stomach and broiler, particularly when they are on 0.20 mg/kg of medication, during the behavior terms with greater attention. suggesting that the central nervous system has been partially defeminized and masculinized.*

**Keywords:** *Embryos; Hydrocortisone; Behavior; Morphological Alteration.*

 <http://dx.doi.org/10.47832/MinarCongress12-25>

<sup>1</sup>  University of Mosul, college of science, biology department, Mosul. Iraq

<sup>2</sup>  Ninevah University, college of Nursing, Department of Basic Nursing Sciences, Mosul. Iraq

<sup>3</sup>  University of Telafer, Agricultural college, Mosul, Iraq

## Introduction

To enhance prenatal lung maturation and reduce the incidence of respiratory distress syndrome—a condition that lowers the mortality and morbidity of newborns— In obstetric clinical practice, corticosteroids are commonly administered to expectant mothers who are at risk of preterm delivery. (Kapugi and Cunningham 2019). However, some medications given to newborns and/or pregnant women may interfere with the offspring's hypothalamus sexual differentiation (Pereira et al., 2003).

One substance that is a member of the corticosteroid drug class is hydrocortisone. Within the human body, corticosteroids function to prevent specific immune responses that result in inflammation and edema. There are several ways to get hydrocortisone, such as oral pills, topical creams and ointments, and rectal creams and suppositories. Oral treatments are only accessible with a prescription; topical creams are available in over-the-counter and prescription strengths. (Et al., Mohammed, 2020).

When given as a medication, the hormone cortisol is known as hydrocortisone. (Becker, 2001). It is used to treat a variety of conditions, including dermatitis, asthma, COPD, rheumatoid arthritis, thyroiditis, and adrenaline syndrome.[1] For adrenocortical insufficiency, it is the recommended course of treatment (Hamilton 2015). Edema (swelling), elevated risk of infection, and mood swings are possible side effects. Common long-term side effects include candidiasis (yeast infections), osteoporosis, upset stomach, muscular weakness, and easy bruising. It is not known if using it while pregnant is safe. Miranda and Rojas-Suarez, 2022). A glucocorticoid, hydrocortisone suppresses the immune system and reduces inflammation. 1936 saw the patenting of hydrocortisone, which was authorized for use in medicine in 1941 (Fischer and Ganellin 2006). It is listed as one of the Essential Medicines by the World Health Organization (WHO 2019).It can be purchased as a generic drug. With over 3 million prescriptions, it ranked as the 149th most often prescribed drug in the US in 2020. Endogenous hydrocortisone has a negative impact on domestic animal products and public health. However, the possible mechanisms are still unknown. The brief estrous cycle in female rats and mice makes them perfect for examining alterations that take place during the reproductive cycle. Currently, the gold standard for assessing the extent of organ damage during long-term drug exposure is organ-specific histological examination. Consequently, certain tissue architecture in adult mice has a different histology. Determining the mechanism(s) of and lowering the degree of uncertainty in risk assessment for this medication will be made easier with a deeper comprehension of the target organs of hydrocortisone, with an emphasis on tissue architecture

at crucial places.

## Materials and Methods

This research looks at a few morphological aspects of embryos.

**Preparation of animals:** The mice were sent from the University of Mosul's College of Veterinary Medicine. They were selected with a weight range of 20–30 grams and an age range of 10–12 weeks for both sexes. Each box had a 3:1 (three females to one male) female to male ratio, which underwent modification. Per week, two to three times. Throughout the week, water food—specific food—supplied this box. By keeping an eye on the vaginal plug the following morning, the mating was confirmed [Siddiqi.N&Al nazwani.N.(2019)] as well as, The box container has the date written on it; the following day is the first day of pregnancy. , and the mating day is regarded as day zero ,[Siddiqi.N&Al nazwani.N.(2019)]. Doses of hydrocortisone are administered to male and pregnant mice. The animals were given a 100 mg injection of hydrocortisone, which was diluted in 100 milliliters of distilled water. An insulin needle was used to inject the animals, supplying each animal with a dose of (0.1, 0.15, or 0.2 mg/Kg), until the animal died, at which point 0.2 mg/animal was administered.

**Experiment design:** (32) Two divisions were created using pregnant female mice:

**A\_1st division:** First group (control): eight pregnant mice not given any medication.

– 2 nd by injecting hydrocortisone for 18 days at 0, 15, or 20 mg/kg of the drug.

**Animal dissection:** After the animals were anesthetized by either at day (18), the abdomen was cut upward, After the pregnant mice's targeted organs were removed, physiologic solution NaCl 0.95% was used to clean them. Following weighting and measuring, the organs and embryos were deposited in (formalin10%), which was modified the next day in accordance with the protocol of (Rahman et al., 2014).

**Statistical analysis:** The SPSS software is utilized for data analysis, and a completely randomized design is employed to examine the differences between the proportionate average adjectives for each weight category (brain, reproductive system, heart, liver, kidney, and spleen). The number of adsorbed embryos and their proportion are displayed in the analysis of pregnant mice using chi square.

**Brain:** The brain weights of all hydrocortisone-treated groups were considerably lower than those of the control group, but these groups did not differ and the concentration showed

significantly lower brain weights (as displayed in Table 1). According to Shina et al. (2018), this result increased free radical production, which had an impact on the brain. Ensuring that folic acid played a preventive role against the neurotoxicity effect of hydrocortisone.

**Reproductive system:** When compared to the control group, all groups receiving hydrocortisone had a substantial drop, and when compared between these groups, a significant decrease was also seen (see table 1).and this is connected to the direct impact of hydrocortisone, which affects the weight of embryos and, ultimately, the reproductive system after passing through the placenta (Aljuboury, 2021).

**Heart:** Table 1 indicates that all groups significantly decreased when compared to the control group. This is due to the effect of hydrocortisone on the bloodstream and alimentary materials, which reduces their admission into the heart and therefore lowers the heart's weight (Aljuboury, 2021).

**Liver:** In contrast to the group under influence, all groups showed a significant decrease; however, there was a significant decrease between these groups (as shown in table 1), which can be attributed to the liver's inability to receive food materials, which ultimately results in a lack of proliferation and a reduction in liver size (Aljuboury, 2021).

**Kidney:** As contrasted with the control group, all groups exhibited a significant drop. These groups also collected adipose tissue surrounding the systems and showed a significant decrease with high concentration of hydrocortisone (as in table 1).and this may be because they require a transition period to detoxify the drug as a result of a drop in average fluid and mineral intake (Aljuboury, 2021).

**Lung:** All groups showed a statistically significant increase in lung size and pulse compared to the control group. These differences were seen between the groups (see table 1).

**Spleen:** When compared to the control group, every group had a substantial drop; these groups also demonstrated significant decreases amongst them (as in table 1).this may be the result of a lack of cell growth and reproduction, which may be brought on by an inadequate blood supply to the organs (Aljuboury, 2021).

The organ weights in pregnant mice treated with hydrocortisone (0.1,0.15, 0.20) mg/kg of body weight are explained in Table 1.

**Table 01-** The organ weights in pregnant mice treated with hydrocortisone

Group/standerd	Spleen	Lung	kidney	Liver	heart	Reproductive system	Brain
Control	0.36 a	0.27 c	0.30a	2.09 a	0.33 a	14.86 a	0.52 a
0.1 mg/Kg	0.30 ab	0.29 b	0.26 b	1.75 b	0.20 b	10.46 b	0.44 b
0.15 mg/Kg	0.14 d	0.31a	0.22c	1. 67b	0.17 c	7.60 c	0.33 b
0.20 mg/Kg	0.11 cd	0.33 a	0.19c	1.49 c	0.13.4 c	5.48 d	0.30 b

**Table 2-** Determine placenta weight and the weight, length, and number of embryos

Sample	Embryos number	Embryos length	Embryos weight	Placenta weight
Control	9.30 a	22.71 a	1.45 a	0.19 a
0.1 mg/Kg	8.00 b	17.51 c	1.05 b	0.14 b
0.15 mg/Kg	7.50 c	13.1 d	0.70 b	0.10 c
0.2 mg/Kg	died	died	died	Died

**Placenta:** All groups treated with hydrocortisone acetate demonstrated a considerable decline in comparison to the control, but there were variations when compared to one another. (as in table 2), which is consistent with Omrany (2013). However, there was no significant change among the 0.1, 0.15, or 0.20 mg/Kg groups. this is due to hydrocortisone, which affects the supplemental food to the embryonic cycle, circulating in the blood at the embryo greater than moms and going through the placenta (Wenger et al., 1992). (Aljuboury, 2021).

**Embryos weight:** When the open abdomen of the groups 0, 20 mg/kg demonstrated the absorption of all embryos, all pregnant mice had perished, but all other groups demonstrated a significant drop when in contrast to the group under control (as shown in table 2).

**Embryos length:** When compared to the control, all groups exhibited a substantial drop; however, those treated with hydrocortisone had a significant decrease as the concentration rose (as shown in table 2). The decrease in the average length of embryos may be due to blood flow interruptions and reductions inside the placenta and uterus, which subsequently impact the placenta's function. This study is consistent with the decrease in the length and weight of the embryos, On the other hand, growth is slowed when intrauterine growth declines. (Kacirova et al,2015).



**Embryos number:** Every group exhibited a noteworthy decline when compared to the control. It also considerably dropped at high hydrocortisone concentrations. (as seen in Table 2).

**Average of absorbed embryos:** showed that the average number of absorbed embryos in pregnant mice treated with hydrocortisone increased significantly ( $p < 0.05$ ); the percentage of absorbed embryos reached 100% in 0.20 mg/Kg and 19.8% in 0.15 mg/Kg, while the percentage of absorbed embryos in pregnant mice treated with hydrocortisone reached 12% in 0.1 mg/Kg compared to control.

**The percentage of pregnant mice:** Comparing the 0.20 mg/kg group to the control, the percentage of absorbed embryos reached 100%, whereas the 0.15 mg/kg group's 25% of absorbed embryos reached 19% in the 0.10 mg/kg group.(as in figure 3). Due to a reversible relationship When comparing the average number of embryos to the number of absorbed embryos, the rise in absorbed embryos is thought to be the cause of the average number of embryos' decline (Dillasamolla et al,2016). Table 3 explains the quantity and percentage of absorbed embryos as well as the quantity and percentage of pregnant mice that showed absorbed embryos.

**Table 3-** The quantity and percentage of absorbed embryos

Sample	Number of absorbed embryos as a percentage	Total number of embryos absorbed	Ratio of mice in pregnancy with absorbed embryos	Mice in pregnancy with displayed absorbed embryos
Control	0	0	0	0
0.2 mg/Kg	100%	All of them	8	100%
0.15 mg/Kg	19.8%	9	25%	5
0.1 mg/Kg	12%	5	19%	3

## Results

While the men in this study were adults, the females were evaluated at embryonic days six (E 6.0) of pregnancy. Four male and female embryos made up the normal total number of live embryos. The current study's morphologic investigations revealed that a percentage of embryos at various gestational ages had exencephaly, a brain abnormality that results in perinatal death, and neural tube closure abnormalities (NTDs). When compared to the control group (A), embryos also displayed a number of abnormalities that were consistent with an aberrant neural tube closure (Fig. 1).

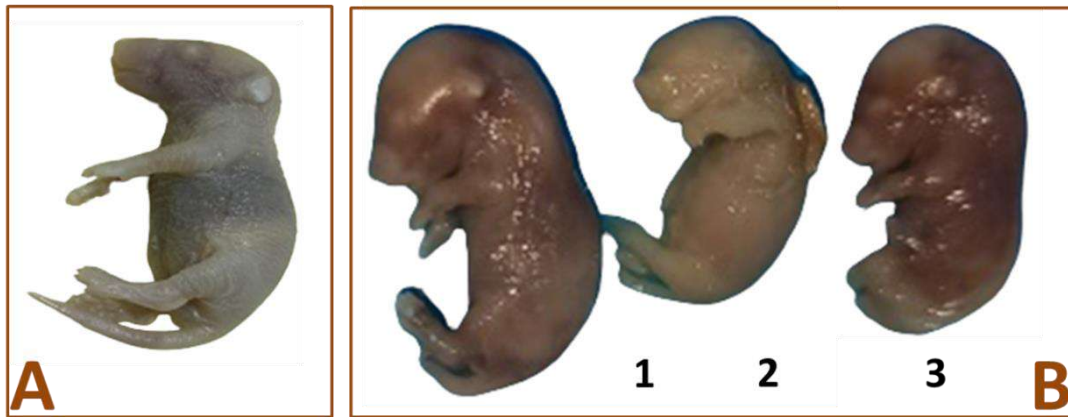


**Figure 1-** Lateral view in mouse embryos injected with hydrocortisone (0.1ml/kg) showing abnormal development and different defects. (A- control embryos injected with distilled water)

Additional abnormalities in the development of the face in exencephalic fetuses lacking hydrocortisone. When hydrocortisone-deficient babies were analyzed at treated embryos with 15/mg, more facial feature problems were discovered. First, limbs were fused and twisted in exencephalic individuals, and their mouths were closed with a protruding tongue—a feature never seen in fetuses of the wild type (Fig. 2A 1,2). Additionally, the results revealed aberrant embryos with partial heads (Fig. 2A4).



**Figure 2-** Lateral view in mouse embryos injected with hydrocortisone (0.15 ml/kg) showing abnormal development and different defects. (A- control embryos injected with distilled water)

## Discussion

In contemporary obstetric clinical practice, corticosteroids are used more frequently despite the associated risks of elevated corticosteroid levels during reproduction. In most animals, failure of the reproductive system has also been linked to increased plasma corticosterone levels during stressful situations (Retana-Marques et al., 1998). In the current investigation, a male adult's testes were reshaped and aberrant embryos were created as a result

of hydrocortisone treatment during pregnancy. As a result, the hydrocortisone medication showed symptoms of toxicity at the recommended dosage in the latter stages of pregnancy. These positive therapeutic outcomes, however, do not shield the medication from negative side effects in the future. According to Nyirenda et al. (2001), giving rats dexamethasone, a synthetic glucocorticoid, during the third week of pregnancy significantly decreased both the mother's mass gain and the offspring's birth mass. Similarly, Dahlof et al. (1978) reported that the injection of hydrocortisone to pregnant rats led to a drop in the mother's adrenal mass and a dose-dependent decrease in the fetal adrenals.

As a result, hydrocortisone therapy during pregnancy at the prescribed dosage displayed harmful effects. These positive outcomes for the treatment do not, however, absolve the medication. According to Nyirenda et al. (2001), giving rats synthetic glucocorticoids, such as dexamethasone, reduced the mass gain of the mother and the birth mass of the child by a significant amount during the third week of pregnancy. Nevertheless, neither the mother's mass growth nor the birth mass of the child changed when the treatment was restricted to the last two days of pregnancy. Both the women who received the medicine and the female pups that were delivered showed a significant drop in plasma corticosterone levels and adrenal wet mass, as expected given its inhibition of the hypothalamus-pituitary-adrenal axis.

Pain, fever, and the presence of blood in the semen are clinical signs of infections in the male reproductive system. Corticosteroids and stress function similarly, which lends credence to the theory that male progeny of stressed mothers experience demasculinization and feminization due to elevated corticosteroid production in the mother. As a result, the methodology used in this study could also be viewed as a model of prenatal and/or maternal stress that is administered to the pups. This study may possibly be an attempt to replicate how stress affects sexual differentiation by administering corticosteroids to pregnant female rats.

In additional embryos, embryonic adsorptions and exophthalmos (as seen in the picture). One group had slightly larger-than-normal embryos that lacked the skull cap and showed no signs of progress. another group showed bleeding in numerous locations, particularly the head with dorsal petechiae (as in the picture) showed multiple areas of body hemorrhaging (as seen in images), brain extrusion, skin wrinkles, tail twisting (in a few samples), and a loss of the carniun cap.

Regarding development delay, these findings are in line with those of (Saeed et al., 2020; Aljuboury, 2023) brain tumor, dorsal hemorrhage, and deformity of the extremities. Growth retardation, abdominal invagination, organ protrusion from the body, mid-dorsal bleeding, and

body and brain atrophy are all mentioned in the current study. (Mohamed & others, 2021).

The results of this inquiry are in line with the following: growth retardation, embryonic adsorption, loss of certain sites, abnormal ribs, skeletal deformity, and reduction in the size and length of the embryos. Hemorrhages in the brain, orbit, and extracranial areas are indications of epilepsy.

Brain protrusion and a skull-base puncture can arise from disruption of neural tube closure caused by brain loss (Alchalabi et al., 2017). (Mohamed & others, 2021). reduction in the size and length of the embryos, loss of certain regions, abnormal ribs, skeletal deformity, and growth retardation and embryonic adsorption are all consistent with the findings of this investigation. Hemorrhages in the brain, orbit, and extracranial areas are indicative of epilepsy. According to Alchalabi et al. (2017), brain protrusion and a puncture through the base of the skull may occur when brain loss impairs neural tube closure.

## **Conclusion**

The findings of the present study show that hydrocortisone, even at modest concentrations (0.10,0.15,0.20 mg/kg), can lead to defective embryos that have abnormalities in the testicular histopathology that may affect how well the male gonads operate. Standardized application of precautionary measures is required to lessen the risks associated with hydrocortisone, the medication source used for therapy.

**Acknowledgment:** I would be irresponsible if I did not mention my family, especially my father and sister. confidence in me has sustained my enthusiasm and attitude throughout my studies. I want to express my sincere gratitude to Dr. Najwa Elias for all of her help and encouragement as I got ready to conduct this research. I am also appreciative of my peers' moral support. Finally, I would like to thank the College of Pure Science's biology department and the university's research participants for their inspiration and impact.

## References

- Becker, K. L. (Ed.). (2001). Principles and practice of endocrinology and metabolism. LippincottWilliams&Wilkins.
- Fischer J, Ganellin CR (2006). Analogue-based Drug Discovery. John Wiley & Sons. p. 484. ISBN 9783527607495.
- Hamilton R (2015). Tarascon Pocket Pharmacopoeia 2015 Deluxe Lab-Coat Edition. Jones & Bartlett Learning. p. 202. ISBN 9781284057560.
- Kapugi, M., & Cunningham, K. (2019). Corticosteroids. *Orthopaedic Nursing*, 38(5), 336-339.
- Mohamed, Z. U., Prasannan, P., Moni, M., Edathadathil, F., Prasanna, P., Menon, A., ... & Menon, V. (2020). Vitamin C Therapy for Routine Care in Septic Shock (ViCTOR) trial: effect of intravenous vitamin C, thiamine, and hydrocortisone administration on inpatient mortality among patients with septic shock. *Indian Journal of Critical Care Medicine*,24(8).
- Pereira, O.C.M., Coneglian-Marise, M.S.P., Gerardin, D.C.C., 2003b. Effects of neonatal clomiphene citrate on fertility and sexual behaviour in male rats. *Comp. Biochem. Physiol., A* 134, 545– 550.
- Rahman, M. A., Haque, S., & Aktar, M. M. (2014). Developmental stage and assessment of embryonic growth of *Gallus gallus domesticus*. *Univ. j. zool. Rajshahi Univ*, 33, 9-18.
- Rojas-Suarez, J., & Miranda, J. (2022). COVID-19 in Pregnancy. *Clinics in Chest Medicine*.9
- World Health Organization (2019). World Health Organization model list of essential medicines: 21st list 2019. Geneva: World Health Organization. hdl:10665/325771. WHO/MVP/EMP/IAU/2019.06. License: CC BY-NC-SA 3.0 IGO.
- Alchalabi. A.S, Aklilu. E, Aziz. A, Rahim. H, Roland.S.H. Malek. M.F, Khan.M.A.(2017). Impact of electromagnetic radiation exposure during embryonic skeletal development in rats.*Asian pacific journal of reproduction* .6(3):104-111.2017.
- Dillasamolla .D,Almahdy,Adrul. F,Biomechy.o p,.Noverial(2016)."The effect of Bluetooth of smart phone against radiation teratogenicity in mice fetuses research journal of pharmaceutical,biological&chemical science 2016,7(2)p:1493.



- Kacirova,I;Grundmann,M;Brozmanova,H.(2015).Serum levels of valproic acid during delivery in mothers and in umbilical cord –correlation with birth length and weight .Biomed pap Med Fac Univ Palacky Olouok Czech Repub,2015(159)4:569-575.
- Mohamed. R; Modeste. c; Beharry. K; kheju. j; Labadie. D and Suepaul . R. (2021).The effect of prenatal exposure of rabbit to valproic acid.International journal of veterinary Science.11(1):1-6. Chateauvieux. S; Morceau. F; Dicato. M; Diederich. M. (2010). Molecular and therapeutic potential and Toxicity of valproic acid. J Biotechnol,2010:479-364.
- Mohamed.R;Modeste.c;Beharry.K;kheju.j;Labadie.D and Suepaul .R.(2021).The effect of prenatal exposure of rabbit to valproic acid.International journal of veterinary Science.11(1):1-6.
- Omrani,A.(2013),L'effet protecteur Des vitamines E,C,Et Des extraits Butanolique Des Deux plantes chrysanthemum fontanesii et Rhantherium Suaveolens vis d'une Toxicite Provoquee Par Valproate de Sodium Chez Les Souris en Gestation . Etude In Vivo et In Vitro .PhD Thesis.college of Biology,Department of zoolgy,University of qusntina, algeria
- Saeed.M;Saleem.U;Anwar,F;Ahmed.B; and Anwar,A.(2020).inhibition of valproic acid – Induced prenatal developmental abnormalities with antioxidants in Rats .American chemical society 5:4953-4961.
- Shona,S.I, Rizk,A.A, Elsadik,A.o, Emam, H.Y, Ali,E.N.(2018).Effect of valproic acid administration during pregnancy .folia morphol .77,2:200-210
- Siddiqi.N&Al nazwani.N.(2019).effect of electromagnetic field on the development of chick embryo :An in vivo study .Electromagnetic fields waves .2019.
- Hamid HH, Taha AM. Anatomical and histological structure of the cornea in sparrow hawk *Accipiter nisus*. Iraqi J Vet Sci. 2021;35(3):437-442. DOI: 10.33899/ijvs.2020.126976.1424 16. .
- Wenger.C;Nau.H.(1992).Alteration of embryonic folate metabolism by valproic acid during organogenesis :Implication for mechanism of teratogenesis .Neurology .1992:42:17-24.
- الحاج، حميد أحمد (2015). "التحضيرات المجهرية الضوئية، النظرية والتطبيق". دار المسيرة للنشر والتوزيع والطباعة. الطبعة الأولى، عمان – الأردن، ص 238.







# MINAR 12

CONGRESS

Rimar Academy  
أكاديمية ريمار

Minar Journal  
مجلة مينار

**RIMAR ACADEMY**  
PUBLISHING HOUSE

